EFFECTIVE AND TOTAL STRESS STRENGTH INTERPRETATION FOR SILTS

by:

Bonifacio I. dela Pena

Thesis submitted to the Faculty of
Virginia Polytechnic Institute and State University
in partial fulfillment of the requirements for the degree
of
Master of Science
In
Civil Engineering

Approved:

Thomas L Brandon

Prof. T.L. Brandon, Chairman

Prof. G.W. Clough

Prof. J.M. Duncan

April 24, 1991
Blacksburg, Virginia
U. S. A.

c.2

LD
5655
V855
1991
P462
C.2

TABLE OF CONTENTS

ACKNOWLEDGEMENTS

The author wishes to express his sincere appreciation to his academic advisor and committee chairman, Professor Thomas L. Brandon, for his guidance, suggestions, encouragement, and support throughout the preparation of this report. The privelege and honor of working with Professor Brandon has enhanced the author's professional life and this is truly appreciated.

Appreciation is also extended to the other members of the author's committee, Professor G.W. Clough and Professor J.M. Duncan, for their support, encouragement, and patience.

The author also extends his appreciation to Professor Alice Kinder for the assistance she rendered in writing this report.

And finally, the author expresses his gratitude to his wife, Karina G. dela Pena, and daughter, Camille Angela G. dela Pena, for their love and support during the preparation of this thesis.

LIST OF TABLES

LIST OF FIGURES

CHAPTER 1

INTRODUCTION

The purpose of this study is to investigate the primary factors which control the engineering behavior of silts. Although extensive expertise exists in dealing with the engineering behavior of sands and clays, relatively little experience exists in assessing the behavior of silts.

Silts may be classified in several ways. The ASTM classification states that silts are soils with grain sizes that ranges from 0.002 mm to 0.074 mm. According to the Unified Soil Classification System, silts are fine-grained soils with plasticity characteristics that plot below the A-line using Casagrande's plasticity chart. Terzaghi and Peck (1967) suggested that if silts are plastic, they can be treated like clays, and if non-plastic, they can be treated like sands.

These classifications currently used do not provide much basis to infer how silts will behave in the field for design purposes. Furthermore, basing the behavior of silts to either sands or clays does not help in assessing the engineering behavior.

One reason offered to explain why silts are among the least studied soil deposits concerns the unfavorable

effects of disturbance during sampling. Nacci et al. (1976) proposed using remolded samples of Rhode Island silt because tube and block sampling produced inferior results. The samples densified during transit to the laboratory. The decrease in void ratio due to the densification gives the undisturbed specimens higher strengths than that present in situ. Schultze et al.(1965) also tested reconstituted samples because of the same problem encountered in using undisturbed samples. Others have employed in-situ testing techniques to determine the shear strength of silt, but have encountered difficulties. Field vane shear tests were used by Ladd et al.(1985), but produced relatively high strengths attributed to partial drainage during shear. Kondrad et al.(1984) utilized the standard penetration test to estimate silt properties, and concluded that the results were not reliable because correlations for silts are not available.

Sands and clays differ from silts because they have methods of sampling or remolding that are well accepted for classification and determination of strength parameters. Undisturbed samples of clays can be readily obtained by thin walled sampling and block sampling. The effective stress induced by the negative pore pressure in the sample provides enough strength for samples to be

trimmed and tested in a triaxial apparatus. In-situ testing, such as the cone penetration test, proves to be useful because existing correlations are available to determine the field strength parameters. Correlations of index test results to field behavior also exist for clay. The undrained shear strength for normally consolidated clays can be evaluated by Skempton's correlation to undrained strength ratio, expressed as:

$$S_u/p = 0.11 + 0.0037(PI), \qquad (1)$$

where PI is the plasticity index of the soil.

For sands, it is well accepted that thin walled samples or block samples are not possible to obtain in the field. Sands are very susceptible to vibrations, thus densification occurs due to handling of sand samples. The negative pore pressure present in the samples upon extrusion may not be sufficient for the samples to be trimmed for triaxial testing. For these reasons, reconstituted samples are used to determine the strength parameters of sands. In-situ tests, such as standard penetration tests and cone penetration tests, have proven to be useful in obtaining reliable estimates of friction angles and densities.

Due to the difficulties in assessing the engineering behavior of silts using convention correlations used for sands and clays, a literature review was undertaken to compare the documented behavior of silts to those of sands and clays.

In the course of this research study, series of UU and CU triaxial test results of different silt samples were gathered to investigate the factors that control the strength parameters of silts. Undrained strength parameters measured both from CU and UU triaxial tests are compared.

Silt samples which exhibit dilative behavior during undrained shear make it difficult to define failure. Because of this behavior, the test results were interpreted using different failure criteria to assess the effective stress friction angle and the undrained shear strength of the samples.

CHAPTER 2

PROBLEMS WITH TRIAXIAL TESTING ON SILTS

Brandon et al. (1990) pointed out several problems in determining the shear strength properties of silts using conventional triaxial testing. The problems cited are:

1. UU triaxial tests provide erratic results.
2. The dilative tendencies of low-plasticity silts make it difficult to define failure in undrained triaxial tests.
3. Loss of saturation may occur when triaxial specimens of silts are sheared in CU tests.

Conventional UU triaxial tests are useful in determining the undrained shear strength of cohesive soils, but some problems are encountered for using them with silts.

Golder and Skempton (1948) conducted a series of UU triaxial tests on saturated silts and clays. All saturated clay samples behaved as ϕ_u=0 materials, but for the silt samples, the angle of shearing resistance varied between 18° and 38°. The reason given by the authors was that dilatancy could have caused this type of behavior

for silts, but no further explanation was offered. Bishop and Edlin (1950) cited that the deviation from the ϕ_u=0 results were due to primarily to the departure from the constant-volume condition normally assumed in undrained tests on fully saturated samples. They stated that the departure from the constant-volume condition may be caused by:

1. Compressibility of water
2. Incomplete saturation or entrapped air
3. Negative pressure set up in the pore water

during shear of sufficient magnitude to cause cavitation.

Penman (1953) stated that if an undrained test is conducted on highly dilatent materials, cavitation occurs when pore pressures fall to about -14.7 psi.

Bishop and Edlin (1950) stated that ϕ_u=0 behavior should exist in UU triaxial test on saturated specimens having the same void ratio as long as the pore pressure is greater than the vapor pressure of water, which is equal to -14.7 psi. In cases where pore pressures decreases to -14.7 psi, the sample is no longer saturated and the sample behaves as $\phi_u > 0$ material. The ϕ measured from the UU triaxial tests would then be approximately equal to the effective stress friction angle of the sample when cavitation occurs.

If it is assumed that cavitation occurs at -14.7 psi, the maximum value of S_u which can be measured in UU tests can be calculated as a function of ϕ'. Brandon et al.(1990) determined the contours of the maximum undrained shear strength, S_u, for the different values of effective stress friction angle ϕ'. These are shown in Figure 1. If UU triaxial tests are conducted on saturated soil samples, the value of the undrained shear strength, which corresponds to a certain cell pressure, can be measured. If the relationship of the undrained shear strength, S_u, and cell pressure plots on the line corresponding to the effective friction angle measured for the samples, then it may be assumed that the samples cavitated. Figure 2 shows this condition by using the data measured by Golder and Skempton (1948) from UU tests on Estuary silts. It is believed that cavitation occured because the data plot close to the $\phi' = 24^{o}$ line, which is the same undrained friction angle measured for the test.

The deviator stress-strain relationship for silts may be somewhat different as compared to other types of soil. Shown in Figure 3 is the deviator stress-strain relationship measured using the CU triaxial test results for Cape Canaveral silt performed by Newhouse (1990). The deviator stress showed a rapid increase at small range of

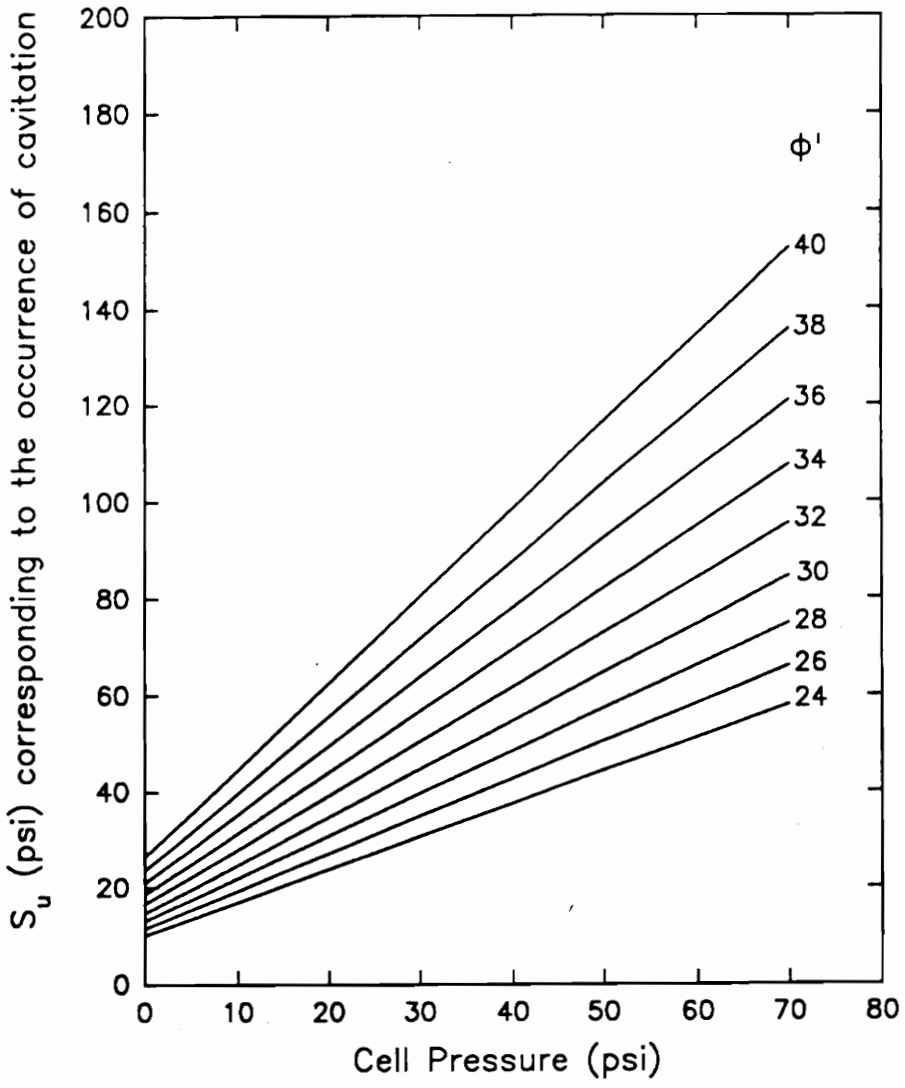

Figure 1 Maximum Undrained Shear Strength Measured In UU Trixial Test If Cavitation Occurs (Brandon et al., 1990)

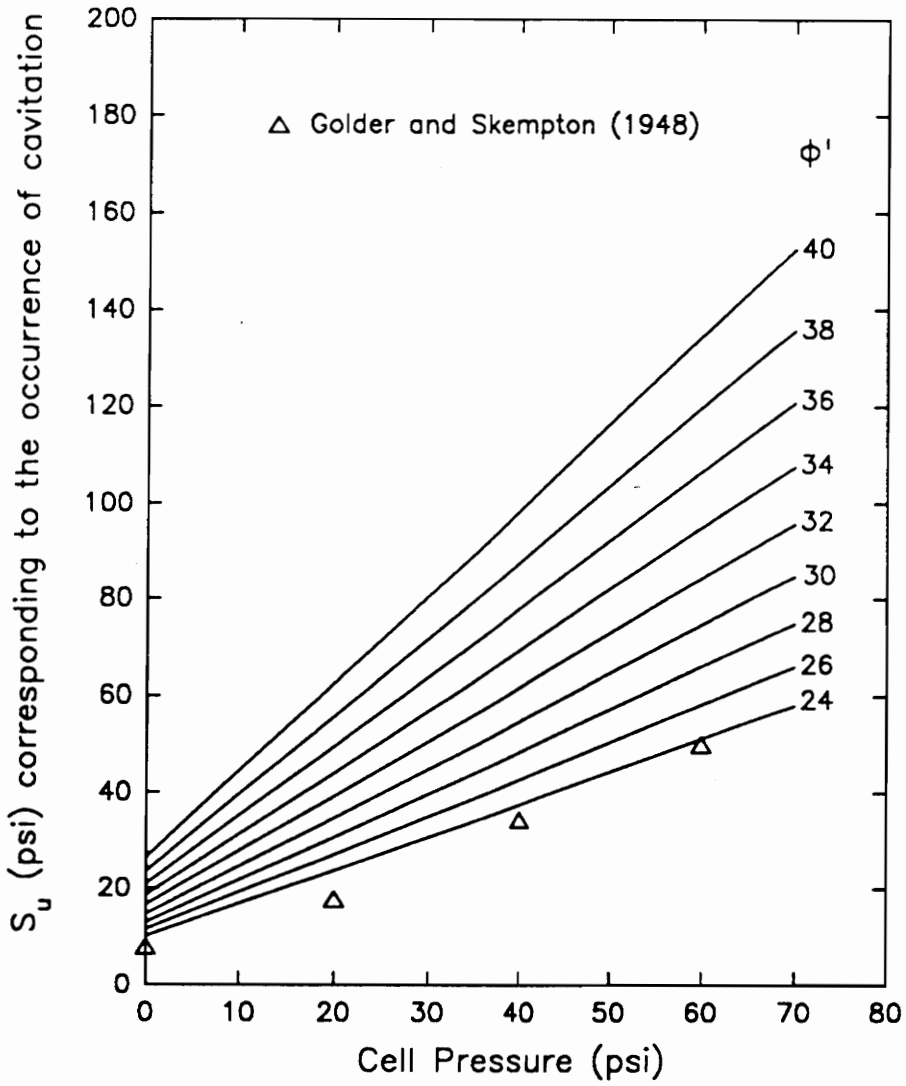

Figure 2 Golder and Skempton's (1948) Data For UU Triaxial Test On Clyde Estuary Silt Presented On Cavitation Plot (Brandon et al., 1990)

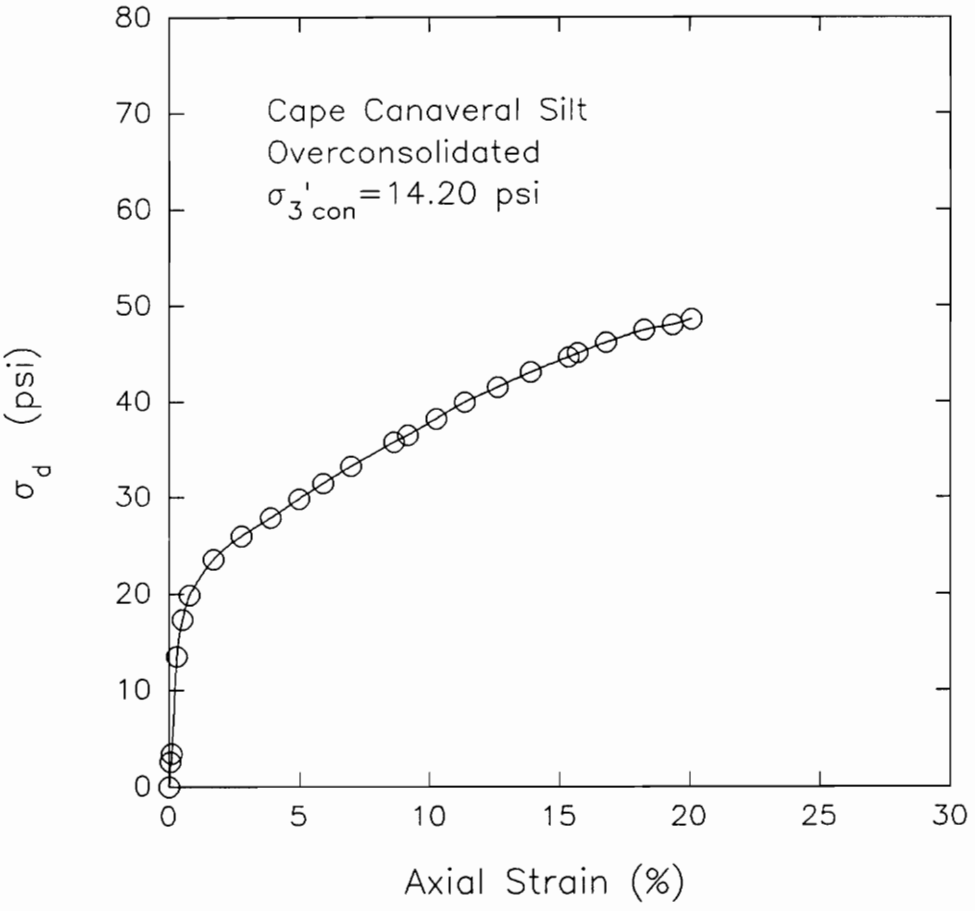

Figure 3 Deviator Stress-Strain Relationship Measured For CU Triaxial Test On Cape Canaveral Silt (Newhouse, 1990)

strains. The deviator stress continued to increase following a flatter slope, and did not peak throughout the duration of the test. This condition makes it difficult to define failure. The corresponding effective stress path for this sample is shown in Figure 4. The general trend of the stress path is to approach the K_f line at small strains, then continue to follow the K_f line as strains increase. A similar stress-strain behavior is shown in Figure 5, which was measured for a CU triaxial test on LMVD silt (Brandon et al., 1990). It can be seen that the stress-strain diagram followed a flatter slope but never reached a maximum deviator stress. Figure 6 illustrates the stress-strain curve for the reconstituted Braehead silt (Penman, 1953). Although the sample showed a peak in the stress-strain diagram, the maximum deviator stress did not occur until about 28% axial strain.

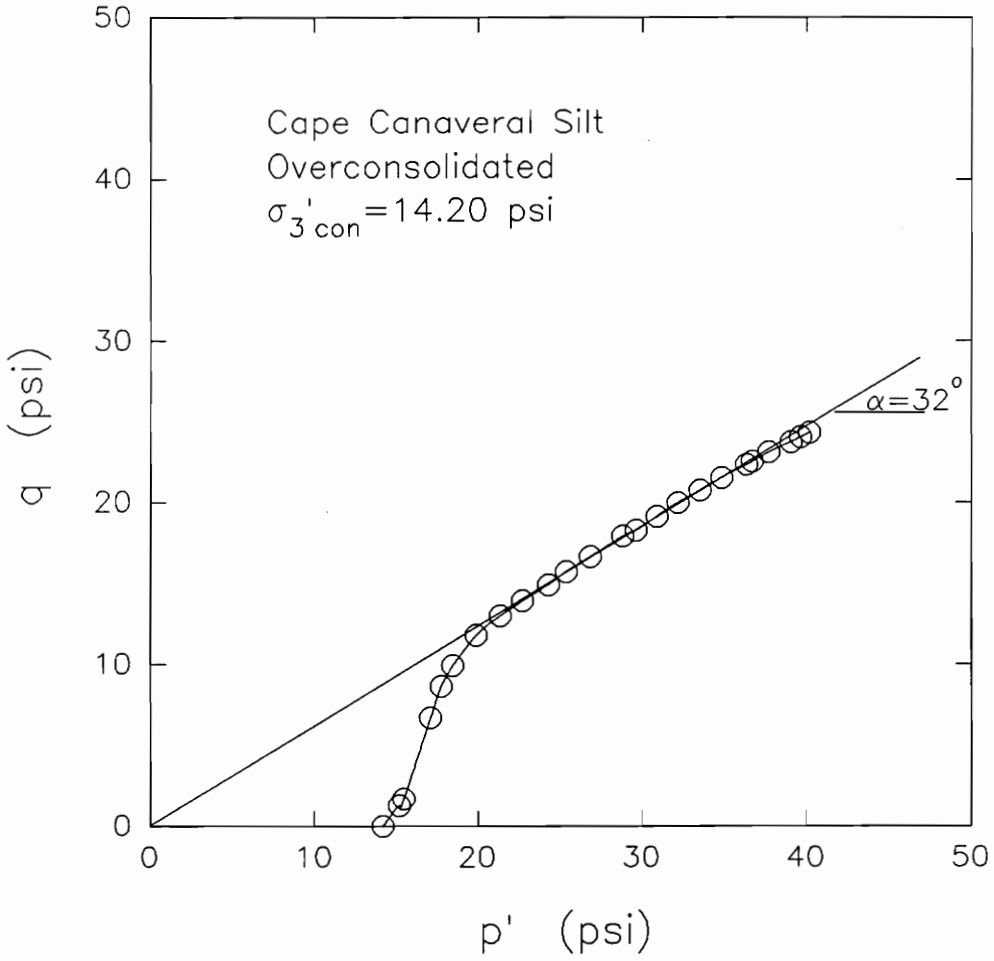

Figure 4 Effective Stress Path Measured For CU Triaxial Test On Overconsolidated Indisturbed Sample of Cape Canaveral Silt

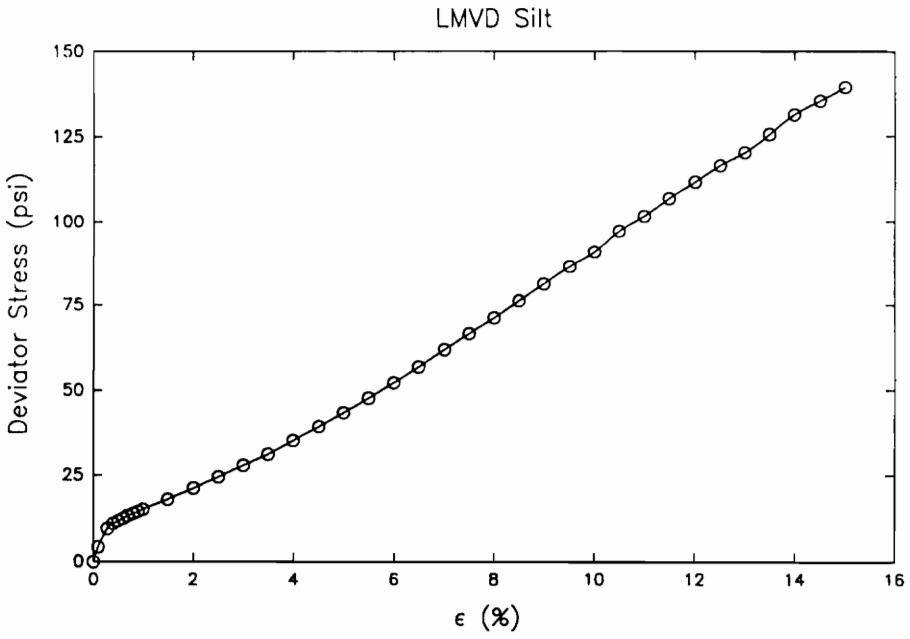

Figure 5 Deviator Stress-Strain Relationship Measured For Sample Number 1 of LMVD Silt (Brandon et al., 1990)

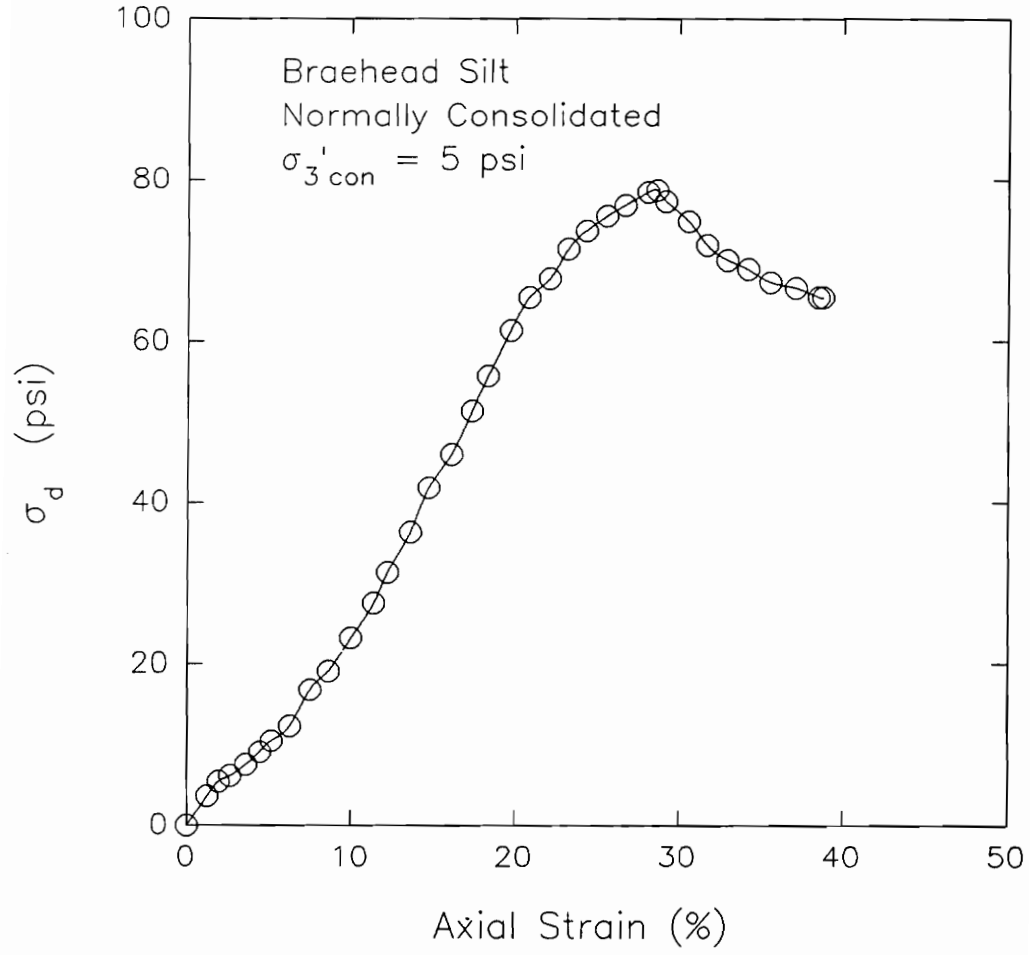

Figure 6 Deviator Stress-Strain Relationship Measured For CU Triaxial Test On Braehead Silt (Penman, 1953)

CHAPTER 3

FAILURE CRITERIA

The relationship of the deviator stress and strain measured from undrained triaxial tests on dilative silts usually does not show peak behavior. The deviator stress may continue to increase to strains up to about 30% without showing any strain softening. This makes it difficult to define failure for determining engineering design parameters.

The different failure criteria presented in geotechnical literature include the following:

1. Maximum deviator stress, $(\sigma_1-\sigma_3)_{max}$
2. Maximum principal stress ratio, $(\sigma_1'/\sigma_3')_{max}$
3. Maximum pore pressure, u_{max}, (Nacci et al, 1970)
4. A-bar = 0, (Torrey, 1982)
5. 10% limiting strain (Borgesson, 1981)
6. 15% limiting strain (Duncan and Fleming, 1990)
7. $Tan(\rho)/Tan(\phi')$ (Senneset, 1990)
8. Reaching the K_f line.

Figure 7 illustrates the different failure criteria, except limiting strain, plotted on an effective stress path for dilative silts. The selection of the failure criteria depends on the following: a.) the type of test

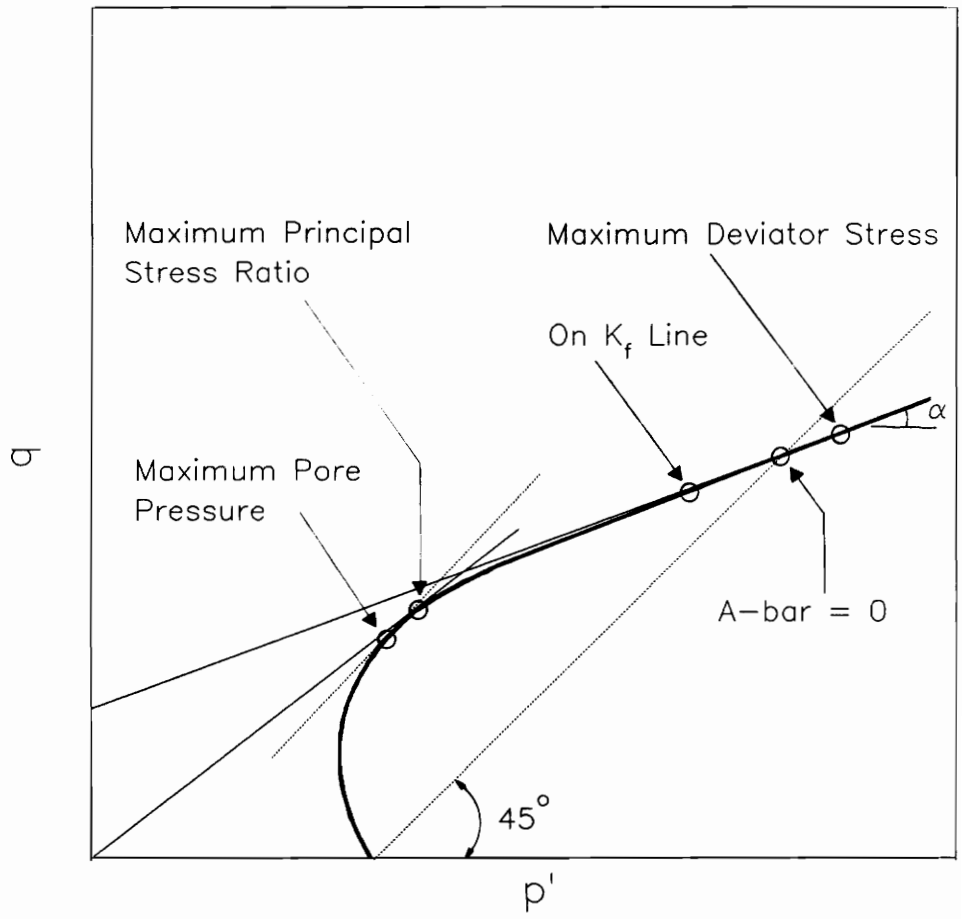

Figure 7 Effective Stress Path For A Dilative Silt Showing The Points Corresponding To The Different Failure Criteria

(drained vs. undrained), b.) the type of soil, and c.) the type of project.

Maximum Deviator Stress

The maximum deviator stress is one of the most common failure criterion applied to triaxial test results. It is applicable to UU, CU, and CD triaxial tests. Difficulties may be encountered when applying this failure criterion to soils possesing dilative properties. When dilative soils are tested in undrained tests, the samples have a tendency to expand, resulting in a decrease in pore pressure. This in turn makes the sample stronger as the strain increases. Because of this behavior, the relationship between the deviator stress and strain may never show a peak at a reasonable range of strains. If it does, the maximum deviator stress occurs at high values of strains. An example of this case is the stress-strain diagram for Braehead silt, shown in Figure 6. Although the stress-strain diagram showed a peak value, the maximum deviator stress did not occur until about 28% axial strain. For samples which show peak behavior at strains greater than about 15%, the specimens are often too deformed for reliable strength determinations.

Maximum Principal Stress Ratio

Maximum principal stress ratio as failure criterion is commonly used for CU triaxial tests. It cannot be applied to UU triaxial tests because pore pressures are not monitored during shearing of the sample, thus there is no knowledge of effective stresses. In CD tests, the maximum pore pressure occurs at the same time as the maximum deviator stress.

Figure 7 illustrates the point on the effective stress path defined by the maximum principal stress ratio. It is represented by the point of tangency of a line drawn from the origin and the effective stress path. For dilative soils characterized by $\phi'>0$ and $c'>0$, the maximum principal stress ratio occurs before the stress path reaches the K_f line. For dilative soils with $c'=0$, the maximum principal stress ratio represents the point where the effective stress path approaches the K_f line.

Maximum Pore Pressure

D'Andrea (1970) proposed the shear stress at maximum pore pressure as a failure criterion for Rhode Island silt because it provided a unique relationship between shear strength and effective consolidation pressure.

Maximum pore pressure as failure criterion can only be applied to CU triaxial tests. In UU tests, pore

pressures are not known, and in CD tests, change in pore pressure due to application of deviator stress is zero throughout the test. Figure 7 illustrates the point on the effective stress path represented by maximum pore pressure. It can be defined as the point of tangency between the stress path and the tangent line to the stress path oriented at 45° counterclockwise.

A-bar = 0

Torrey (1982) proposed A-bar = 0 as a failure criterion to define failure of dilative silts and sands. This failure criterion is applicable to CU tests where pore pressures fall to zero or negative values. It cannot be applied to UU and CD tests. The point of intersection of the line drawn from the effective consolidation pressure oriented at 45° counterclockwise and the effective stress path defines the point at A-bar = 0. This is shown in Figure 7.

If failure is defined by A-bar = 0, the effective stresses at failure are equal to total stresses. The undrained shear strength, S_u, could be defined by the equation:

$$S_u = \frac{(\sigma_1 - \sigma_3)_f}{2} \qquad (2)$$

For soils having a value of cohesion intercept, c', equal to zero, the undrained strength ratio, S_u/p, can be determined from the effective stress friction angle, ϕ', by the equation:

$$\frac{S_u}{p} = \frac{\sin \phi'}{1 - \sin\phi'} \qquad (3)$$

Limiting Strains

Limiting strains as failure criteria are applied to triaxial tests were the relationship between the deviator stress and strain does not show a peak behavior or the maximum deviator stress occurs at high strains. This failure criterion is applicable to CU, UU, and CD triaxial tests. The choice of a limiting strain has varied from author to author. Wang et al. (1982) used 5% limiting strain during the investigation of the geotechnical properties of Alaskan silts. Borgesson (1981) used 10% limiting strain to verify the shear strength of inorganic silty soils. Duncan and Fleming

(1990) used 15% limiting strain for the determination of shear strength for Alaskan silts.

Tan(ρ)/Tan(ϕ')

Prof. Kaare Senneset of the University of Trondheim proposed the use of Tan(ρ)/Tan(ϕ') as a failure criterion. ρ is defined as the effective stress friction angle measured from the Mohr's circle defined by the effective stresses at any point during the test. For soils with the effective cohesion intercept equal to zero, the maximum value of ρ would be the same as the effective stress friction angle if failure is defined by maximum principal stress ratio. Therefore, using Tan(ρ)/Tan(ϕ') as a failure criterion would give the same ϕ' as $(\sigma_1'/\sigma_3')_{max}$.

Reaching The K_f Line

The point where the effective stress path reaches the K_f line is shown in Figure 7. For dilatent materials with an effective cohesion intercept and effective stress friction angle greater than zero, the point where the stress path approaches the K_f line usually occurs after the point defined by maximum principal stress ratio. For soils whose effective cohesion intercepts are equal to

zero, the failure criteria defined by K_f line is approximately the same as the maximum principal stress ratio.

CHAPTER 4

TRIAXIAL TESTS ON DIFFERENT SILT SAMPLES

ALASKAN SILT

Fleming (1985) tested Alaskan silt from the Beaufort Sea. Both undisturbed and reconstituted samples were tested. The undisturbed samples were taken using 2.8 inches diameter Shelby tubes. The remolded or reconstituted samples were prepared by slurry consolidation. The soil was dried and pulverized and passed through the #16 sieve. The dried soil was mixed with water to a water content of approximately 40%. The slurry was then consolidated one-dimensionally using the consolidometer shown in Figure 8. A typical consolidation curve obtained for a reconstituted sample is shown in Figure 9. The coefficient of consolidation, c_v, determined from the consolidation tests of the reconstituted samples ranged from 270 ft^2/year to 780 ft^2/year. These values are close to those determined for undisturbed specimens (170 ft^2/year to 850 ft^2/year).

Index Properties of Alaskan Silt

Figure 10 shows the natural water contents and dry densities for the silt samples obtained from an offshore site in the Beaufort Sea. Grain size analyses were performed on undisturbed samples and reconstituted

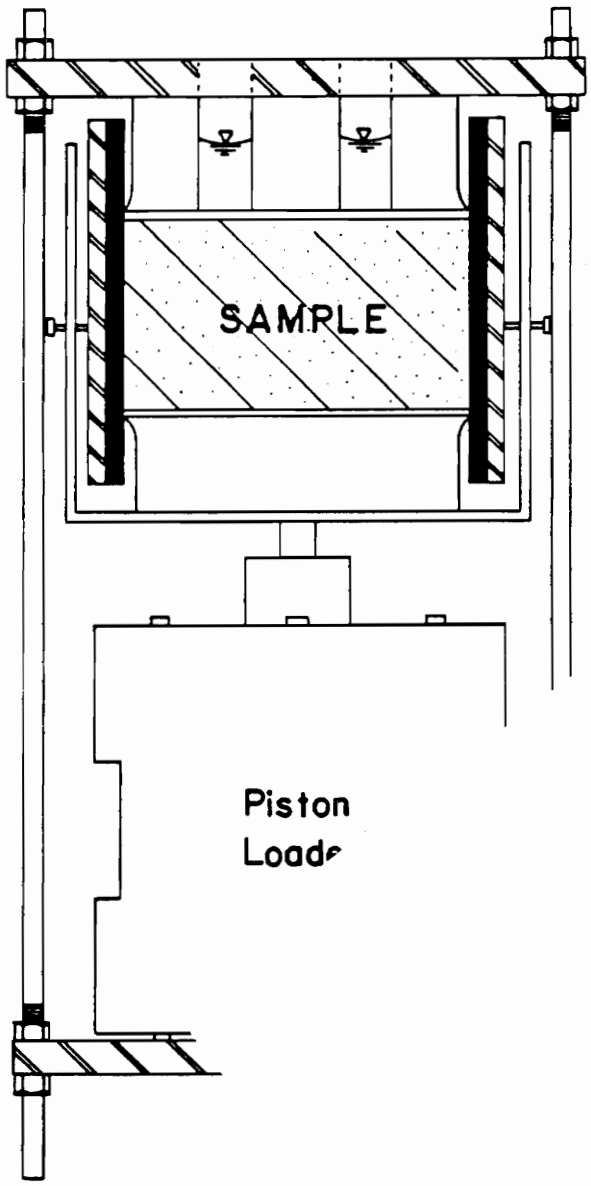

Figure 8 Consolidometer Used To Prepare The Reconstituted Samples of Alaskan Silt (Fleming, L.N., 1985)

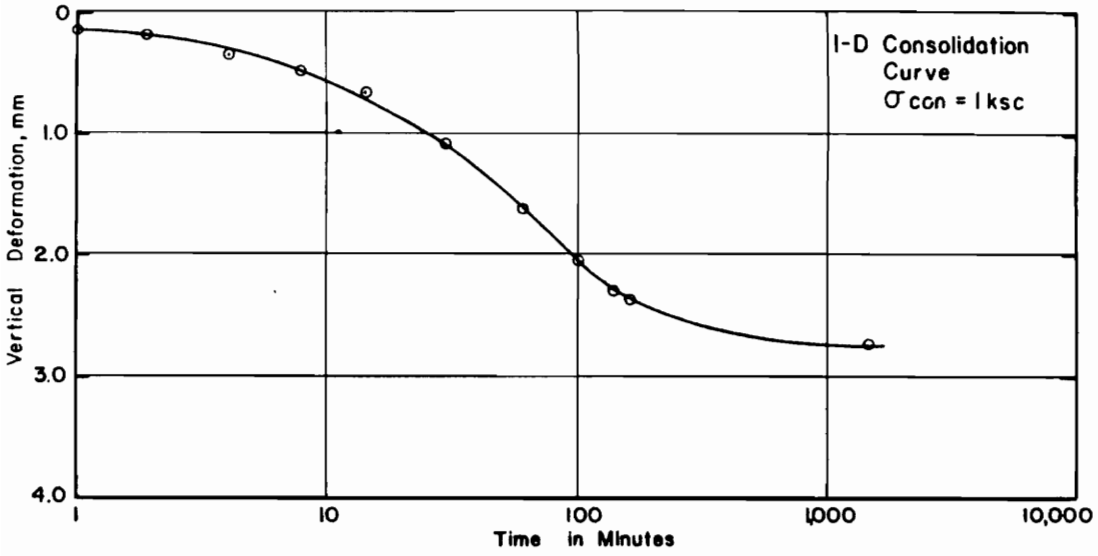

Figure 9 Consolidation Curve Measured For The Reconstituted Samples of Alaskan Silt (Fleming, 1985)

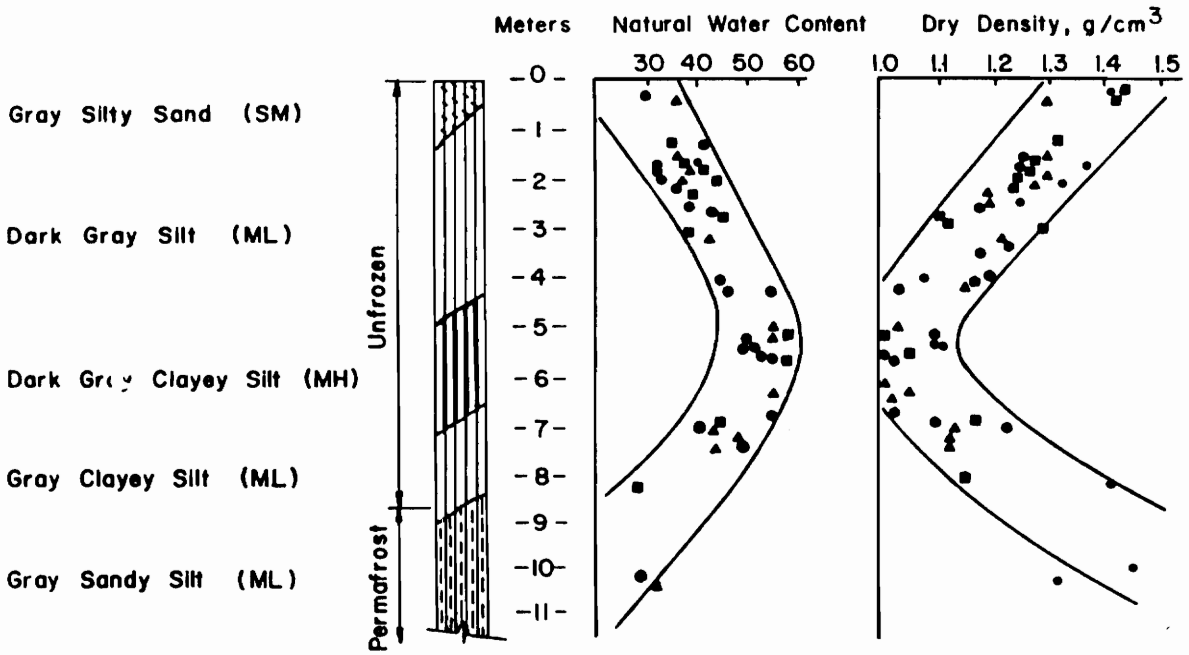

Figure 10 Generalized Subsurface Profile For Offshore Site In Beaufort Sea (Fleming, 1985)

samples. As shown in Figure 11, the average grain size distribution curve for the reconstituted samples plots well within the range of grain size distribution curves for the unmixed samples. The grain size components are given in Table 1. Shown in Figure 12 is a plasticity chart for the Alaskan silt. Most samples plot close to the A-line, with the majority of the samples classifying as ML according to ASTM D-2487-85.

Isotropically Consolidated Undrained Triaxial Tests On Reconstituted Alaskan Silt

A series of isotropically consolidated undrained triaxial tests were performed on reconstituted Alaskan silt. The samples tested had diameters of 1.40 inches and heights of 3.0 inches. All specimens were initially consolidated in the batch consolidometer to a vertical stress of 14.20 psi. The specimens were then reconsolidated in triaxial cells to isotropic effective consolidation stresses of 14.20, 21.30, and 28.40 psi. Conventional procedures of back pressure saturation were performed to give B values from 0.988 to 0.998. The initial specimen properties are given in Table 2.

The stress-strain curves for the Alaskan silt are shown in Figure 13. Only the specimen consolidated to

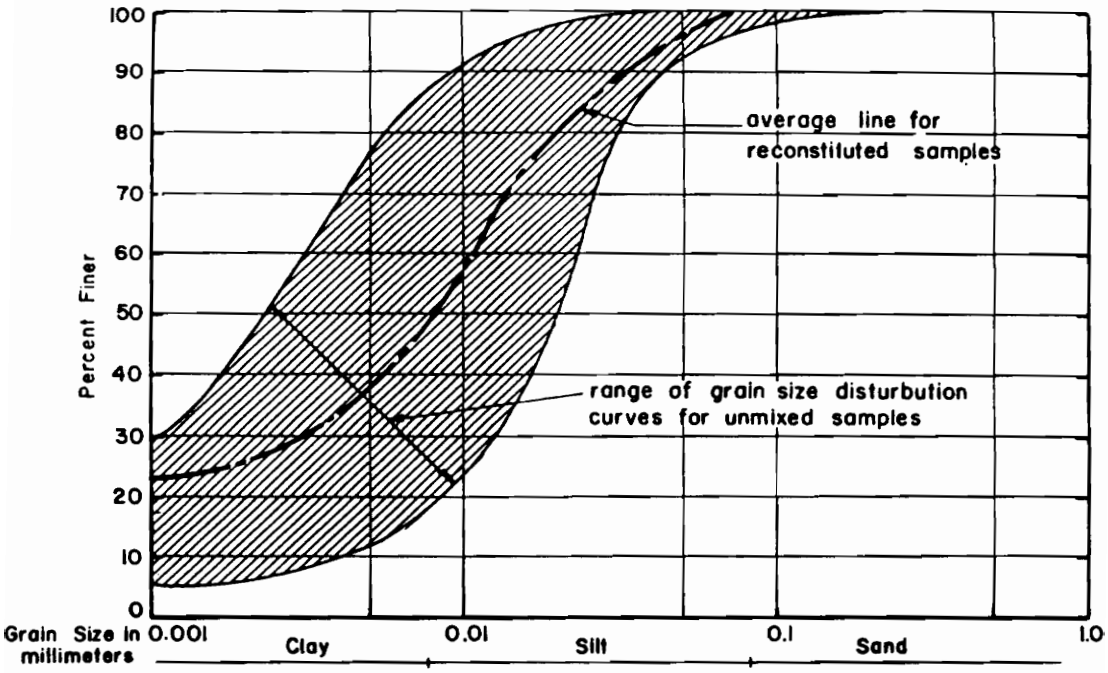

Figure 11 Range of Grain Size Distribution Curve For Samples Before Mixing Along With The Average Line For The Reconstituted Samples (Fleming, 1985)

Table 1 Components of Alaskan Silt

Component	Amount
% Sand	5%
% Silt	70%
% Clay	15%

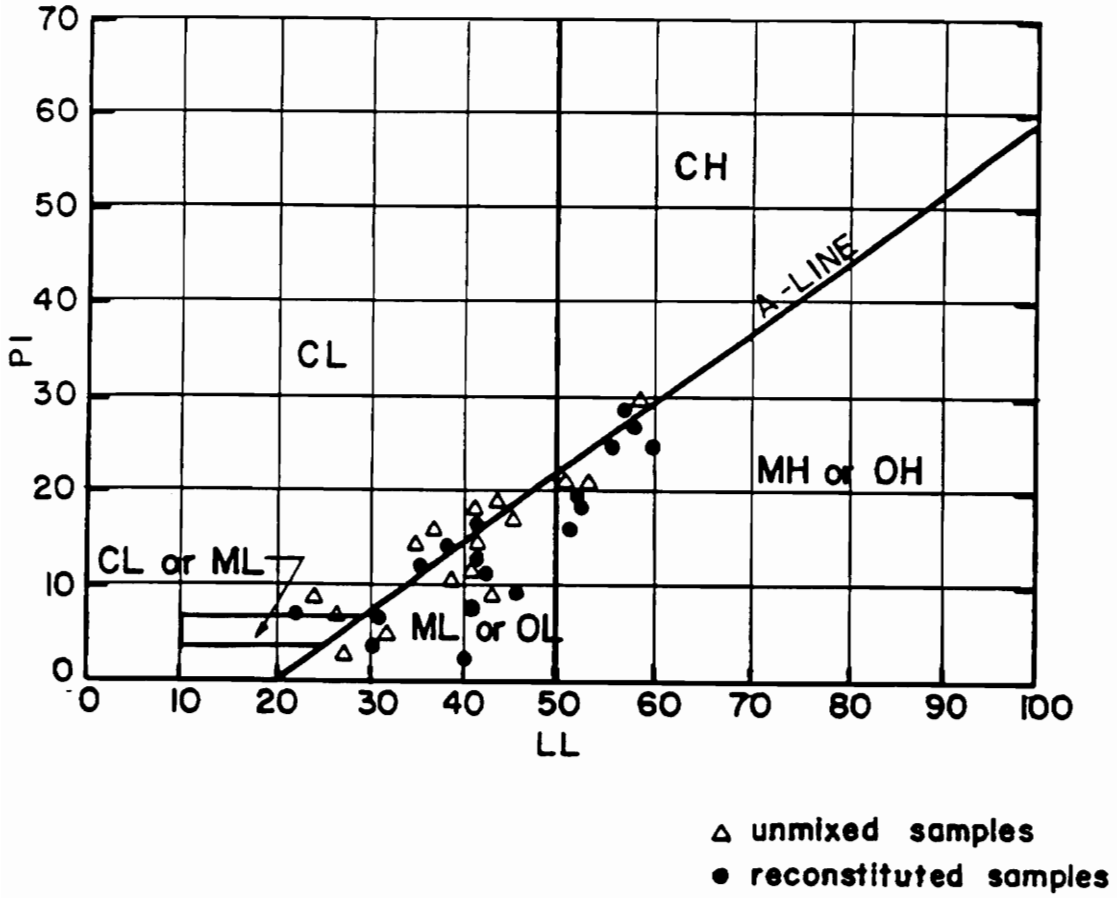

Figure 12 Plasticity Chart For The Original Unmixed Samples and Reconstituted Samples of Alaskan Silt (Fleming, 1985)

Table 2 Properties of the Normally Consolidated ICU Test Specimens For Alaskan Silts

Test Number	Natural Water Content (%)	Dry Unit Weight (Pcf)
1	31.40	88.50
2	31.70	87.20
3	31.80	87.20
4	31.30	87.80

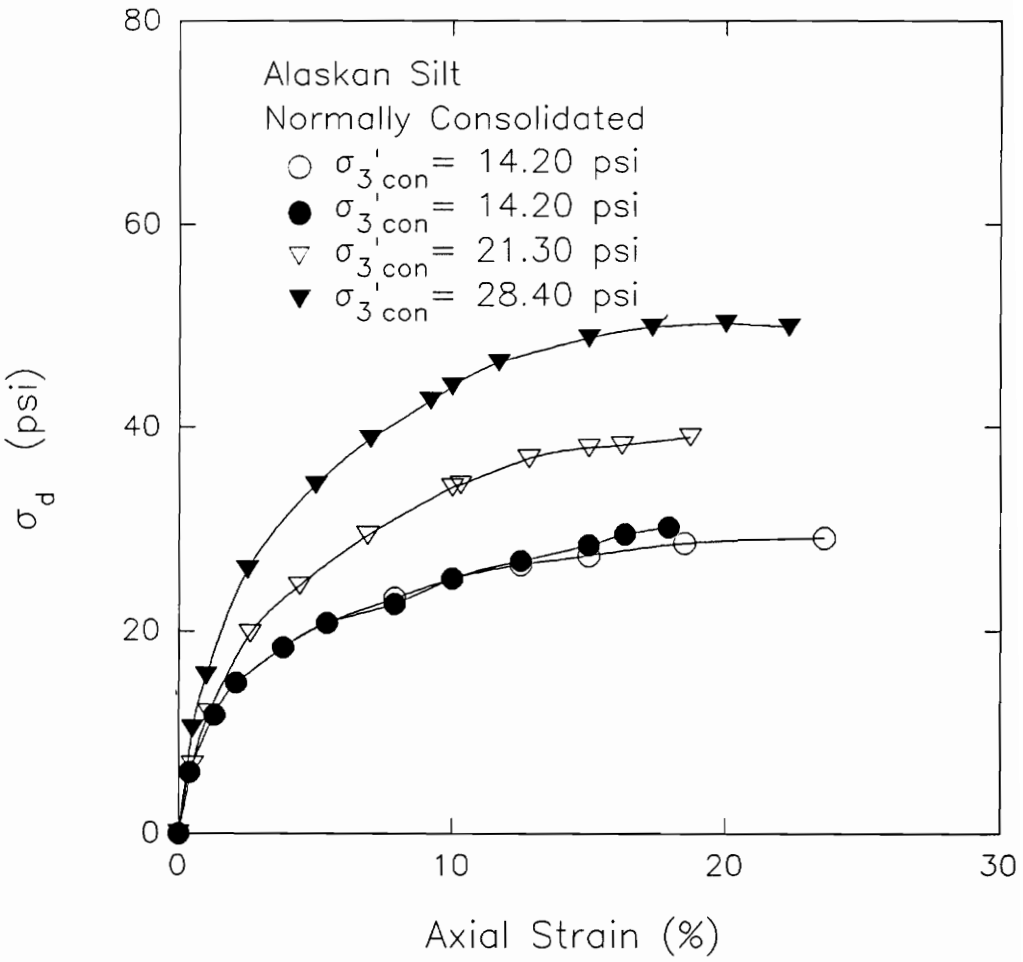

Figure 13 Deviator Stress-Strain Relationship Measured For The ICU Triaxial Tests On Normally Consolidated Alaskan Silt

28.40 psi exibited a peak deviator stress at a strain of about 20%.

Figures 14 and 15 illustrate the minor effective stress-strain and principal stress ratio-strain relationships for the Alaskan Silt. The principal stress ratio-strain relationship showed small variations with regards to the effective consolidation pressure. Maximum principal stress ratios were attained at strains ranging from 9.60% to 10.50%.

The relationships between A-bar-Strain and pore pressure-strain are plotted on Figure 16 and 17 respectively. All samples showed a peak in their pore pressure-strain behavior and then pore pressure decreased as shearing continued. Maximum pore pressures occured at axial strains ranging from 3% to 4%.

Figure 18 shows the effective stress paths for the Alaskan silt. The stress paths clearly delineate the K_f line, with an α value equal to 31°. This corresponds to an effective stress friction angle, ϕ', equal to 37°.

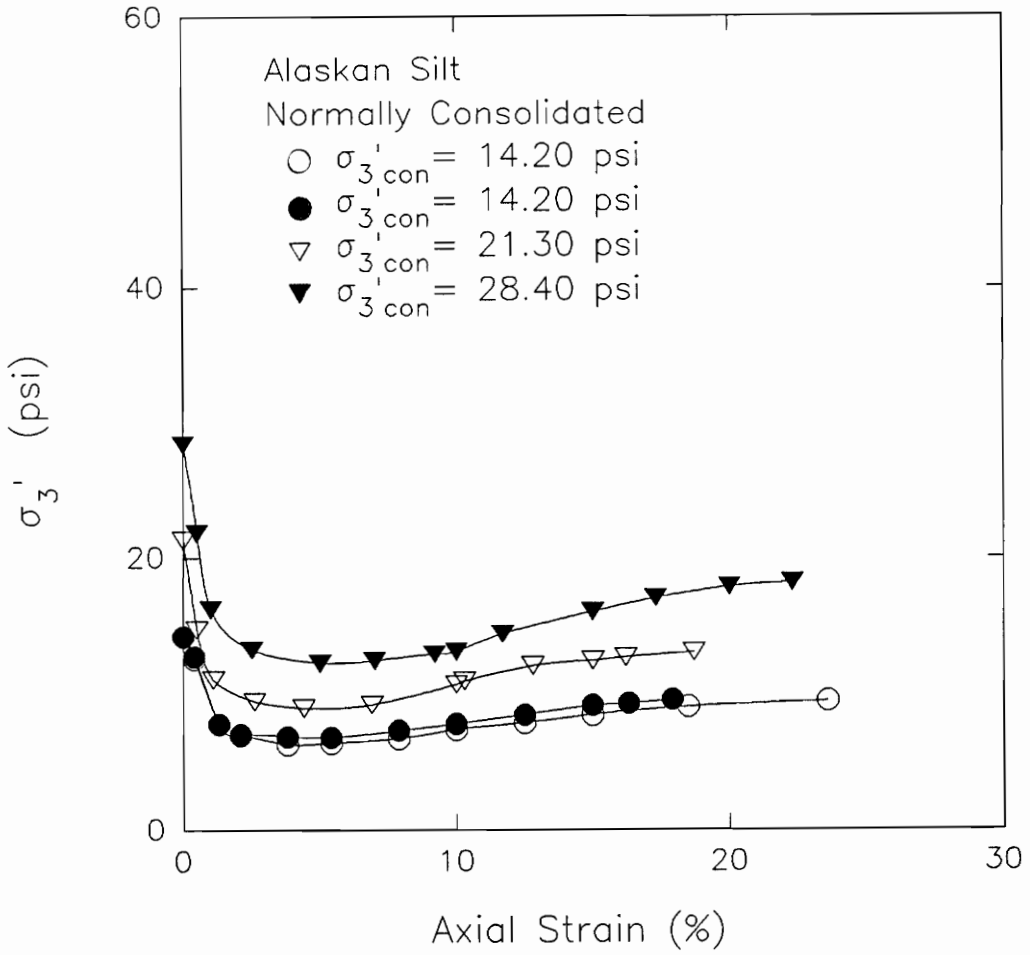

Figure 14 Minor Effective Stress-Strain Relationship Measured For The ICU Triaxial Tests On Normally Consolidated Alaskan Silt

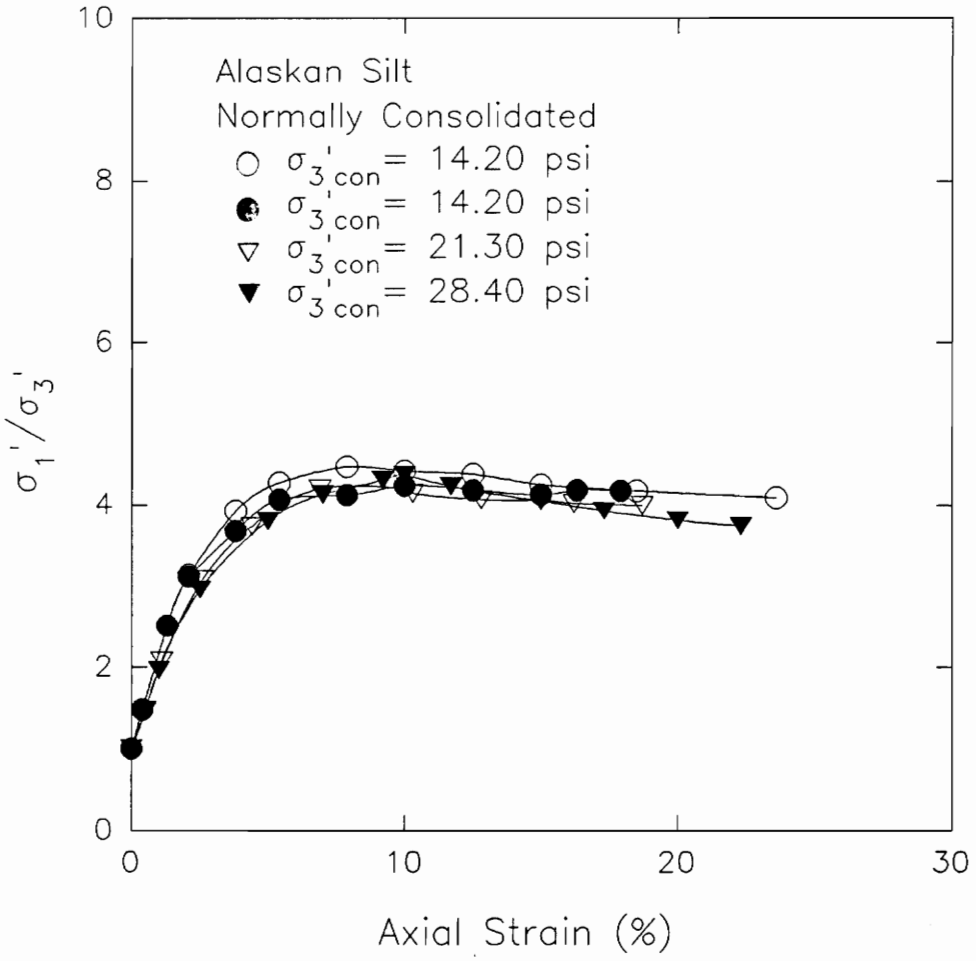

Figure 15 Principal StressRatio-Strain Relationship Measured For The ICU Triaxial Tests On Normally Consolidated Alaskan Silt

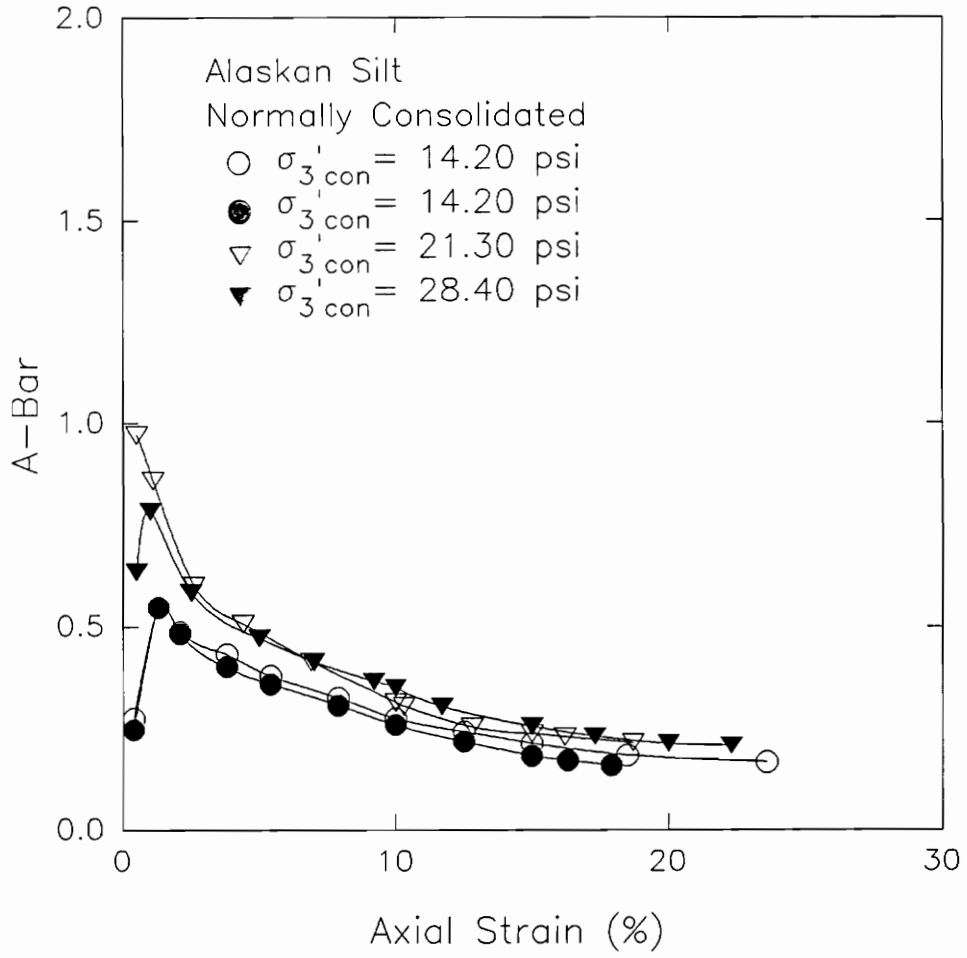

Figure 16 A-bar-Strain Relationship Measured For The ICU Triaxial Tests On Normally Consolidated Alaskan Silt

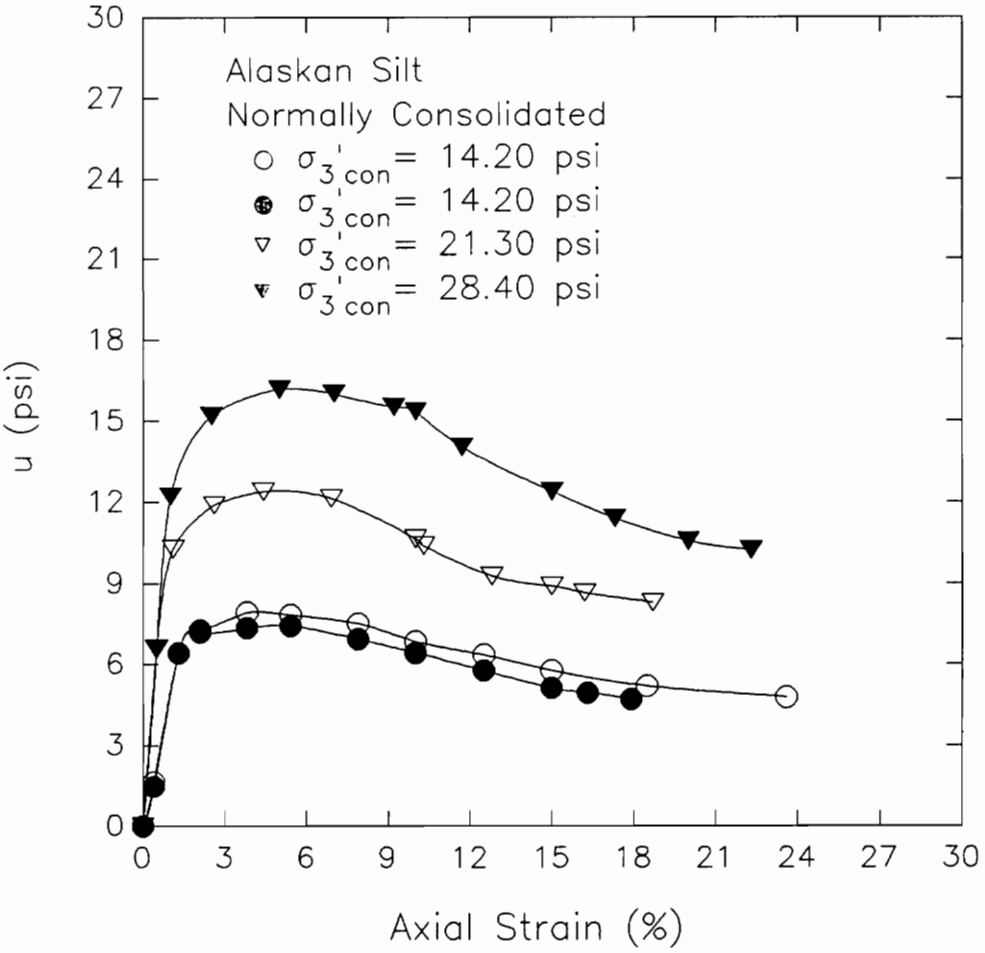

Figure 17 Pore Pressure-Strain Relationship Measured For ICU Triaxial Tests On Normally Consolidated Alaskan Silt

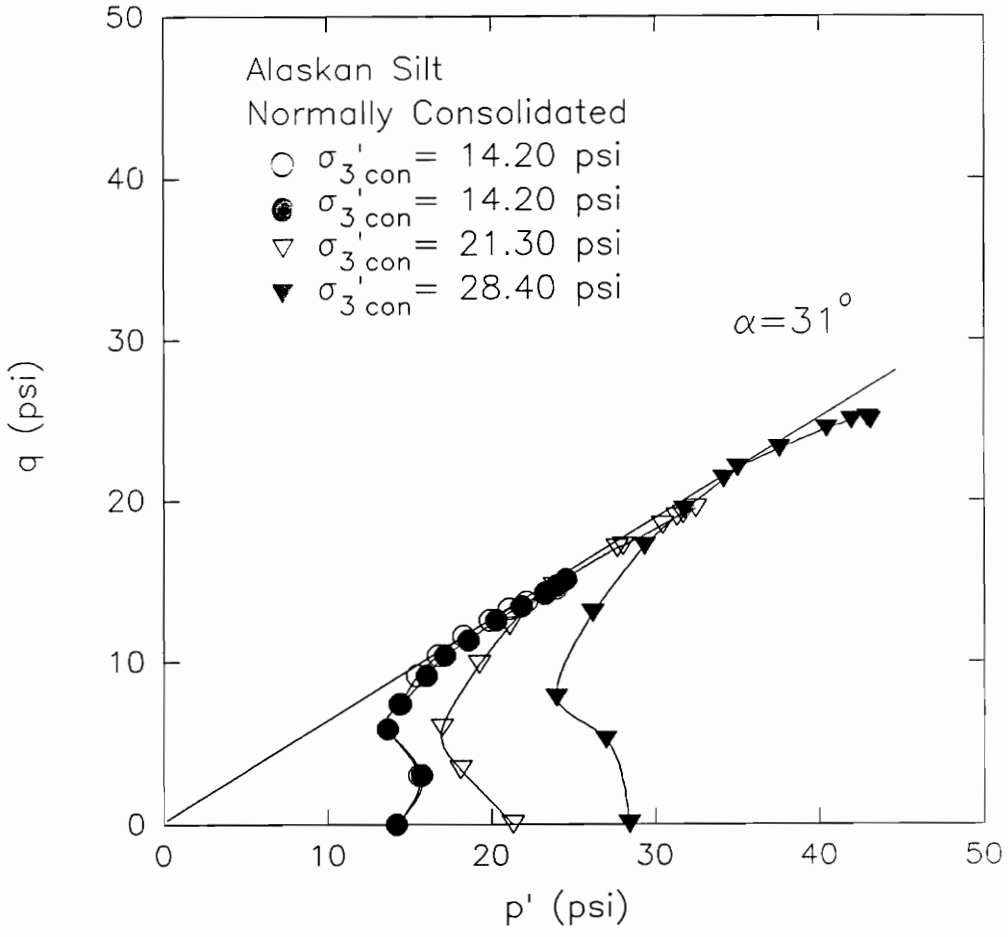

Figure 18 Effective Stress Paths Measured For The ICU Triaxial Tests On Normally Consolidated Alaskan Silt

Effective Stress Interpretation of ICU Tests On Reconstituted Alaskan Silt

All the specimens reached maximum pore pressures at strains from 3% to 4%. Effective Mohr's circles, based on maximum pore pressure as a failure criterion, are plotted in Figure 19. Constraining the effectice cohesion, c', intercept to zero, an effective stress friction angle, ϕ', of 35° was calculated.

Only the specimen consolidated to 28.40 psi reached a maximum deviator stress during the test and this was attained at strain of 20%. The Mohr's circle for this test is shown in Figure 20, with an effective stress friction angle, ϕ', of 36°.

Using the maximum principal stress ratio as failure criterion, the Mohr's circles are plotted on Figure 21. The samples reached maximum principal stress ratio at strains of 9.60% to 10.50%. Again, constraining the effective cohesion intercept to zero, the envelope gives an effective stress friction angle of 38°.

Limiting strains as failure criteria can also be applied to this test data. Mohr's circles for 10% limiting strain are shown in Figure 22. The envelope gives an effective stress friction angle of 38°. Based on 15% limiting strain, as shown in Figure 23, the resulting friction angle is 38°.

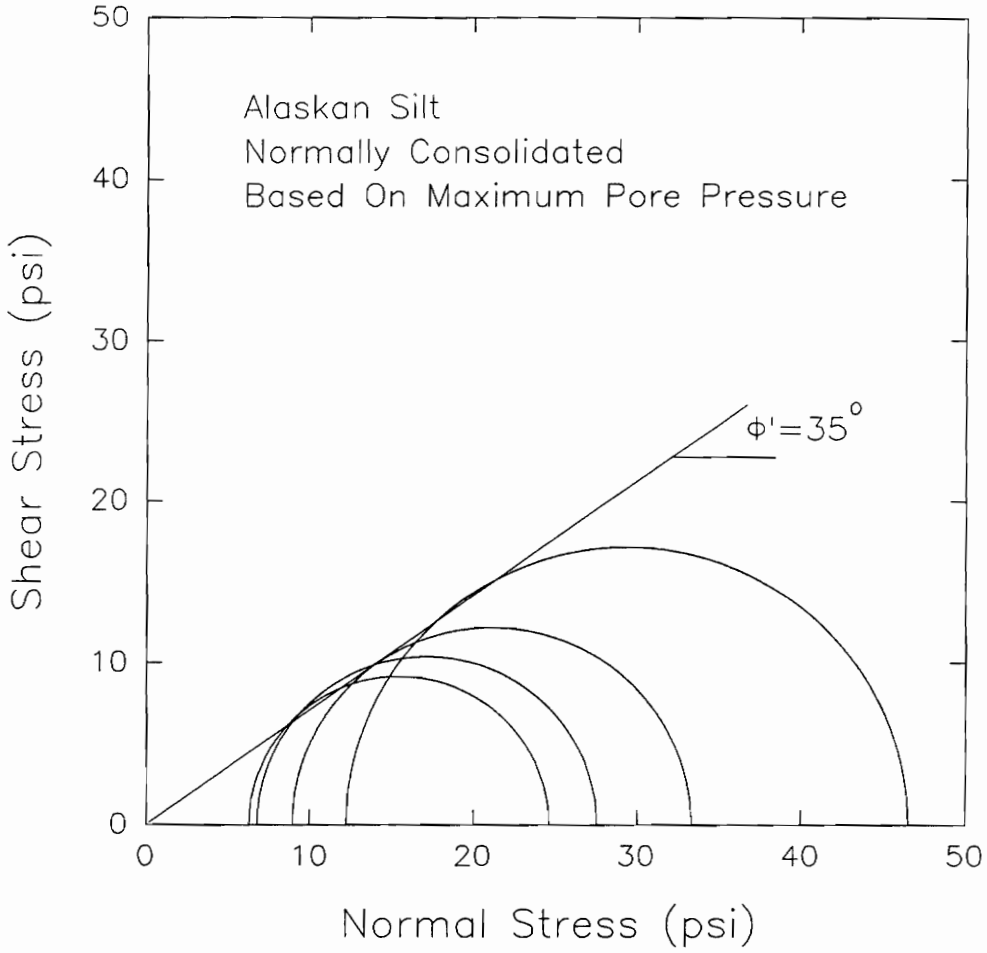

Figure 19 Effective Stress Mohr's Circles Measured For The ICU Triaxial Tests On Normally Consolidated Alaskan Silt For Failure Based On Maximum Pore Pressure

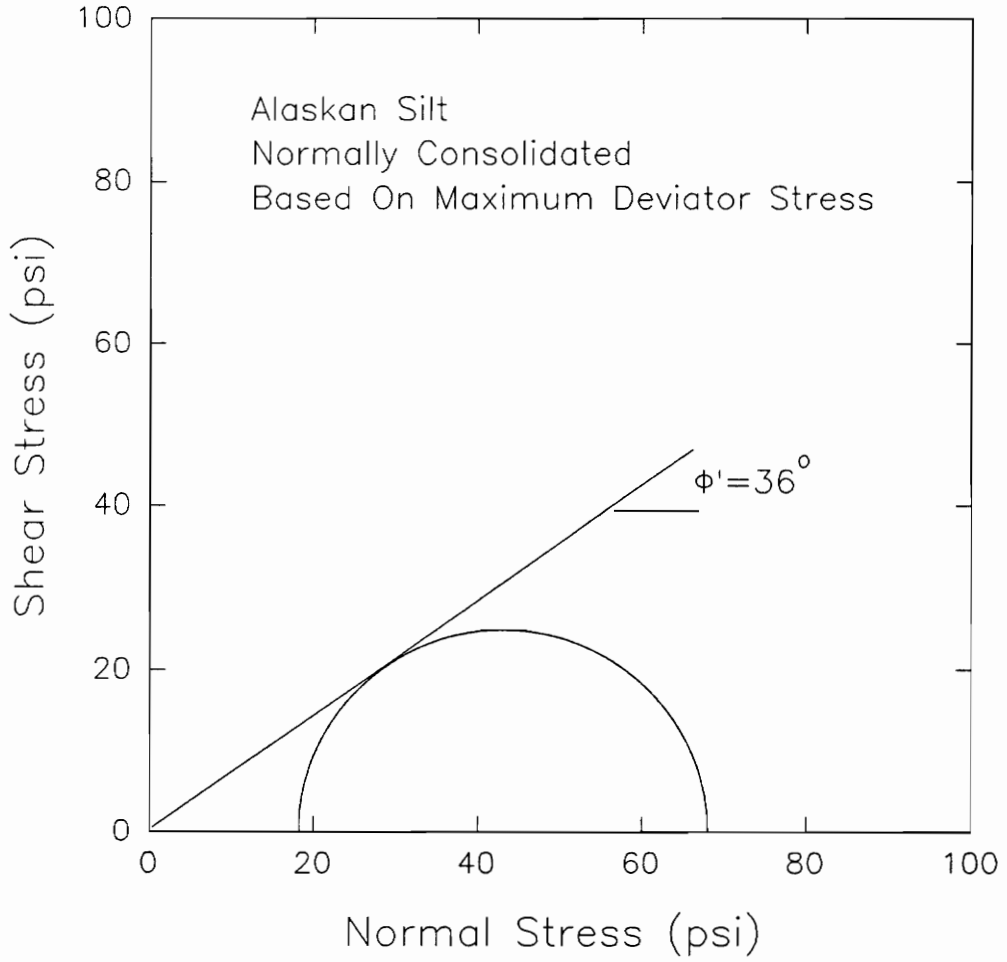

Figure 20 Effective Stress Mohr's Circles Measured For The ICU Triaxial Tests On Normally Consolidated Alaskan Silt For Failure Based On Maximum Deviator Stress

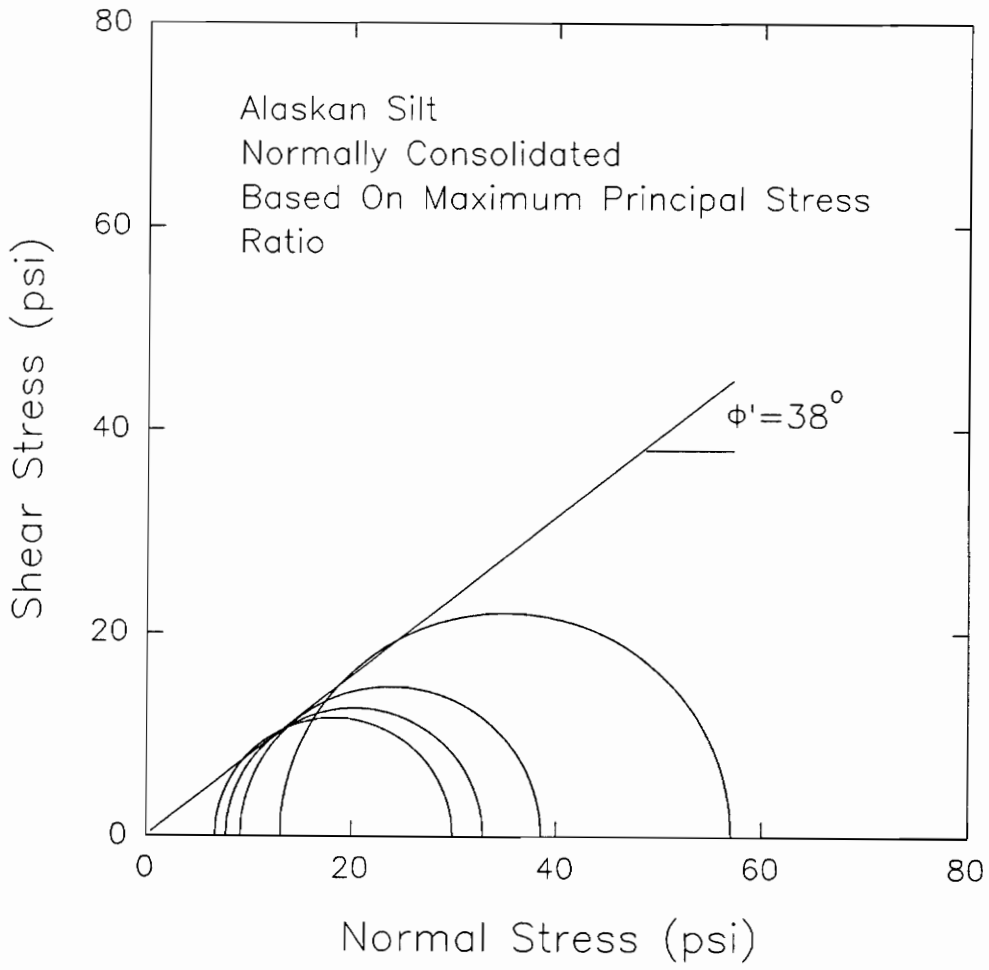

Figure 21 Effective Stress Mohr's Circles Measured For The ICU Triaxial Tests On Normally Consolidated Alaskan Silt For Failure Based On Maximum Principal Stress Ratio

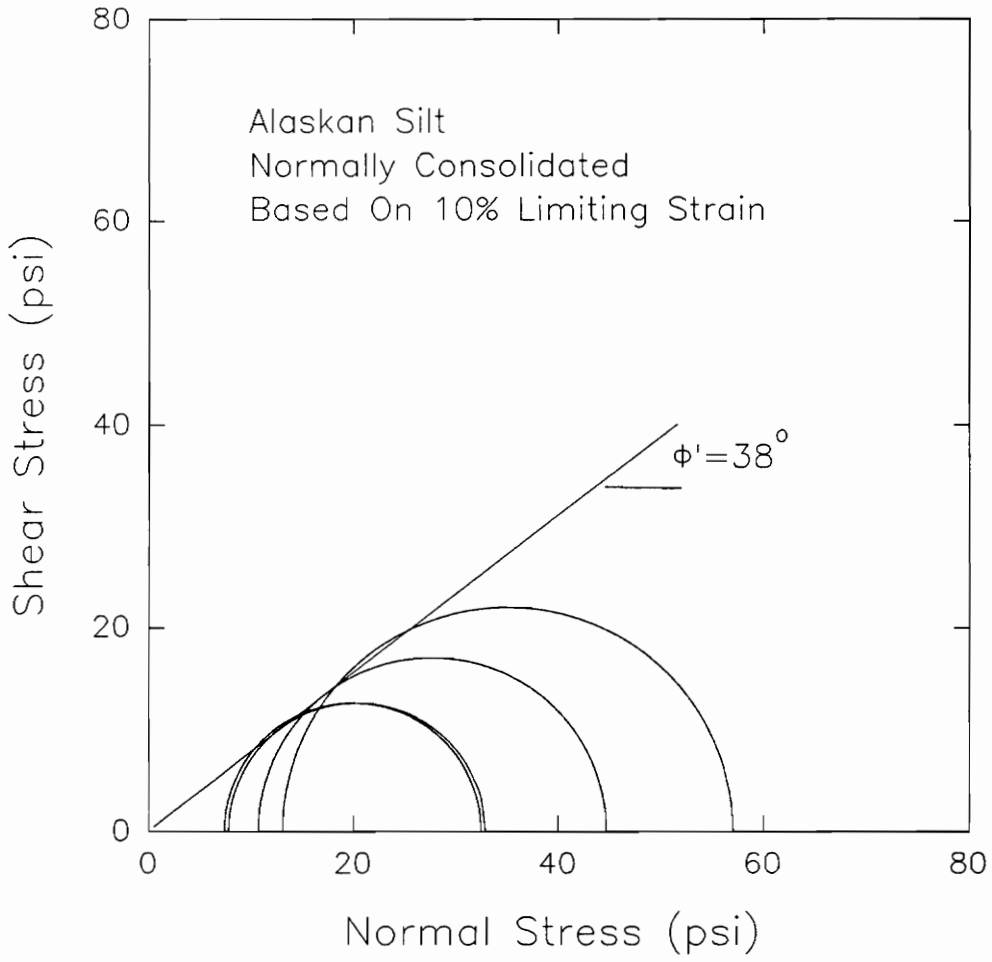

Figure 22 Effective Stress Mohr's Circles Measured For The ICU Triaxial Tests On Normally Consolidated Alaskan Silt For Failure Based On 10% Limiting Strain

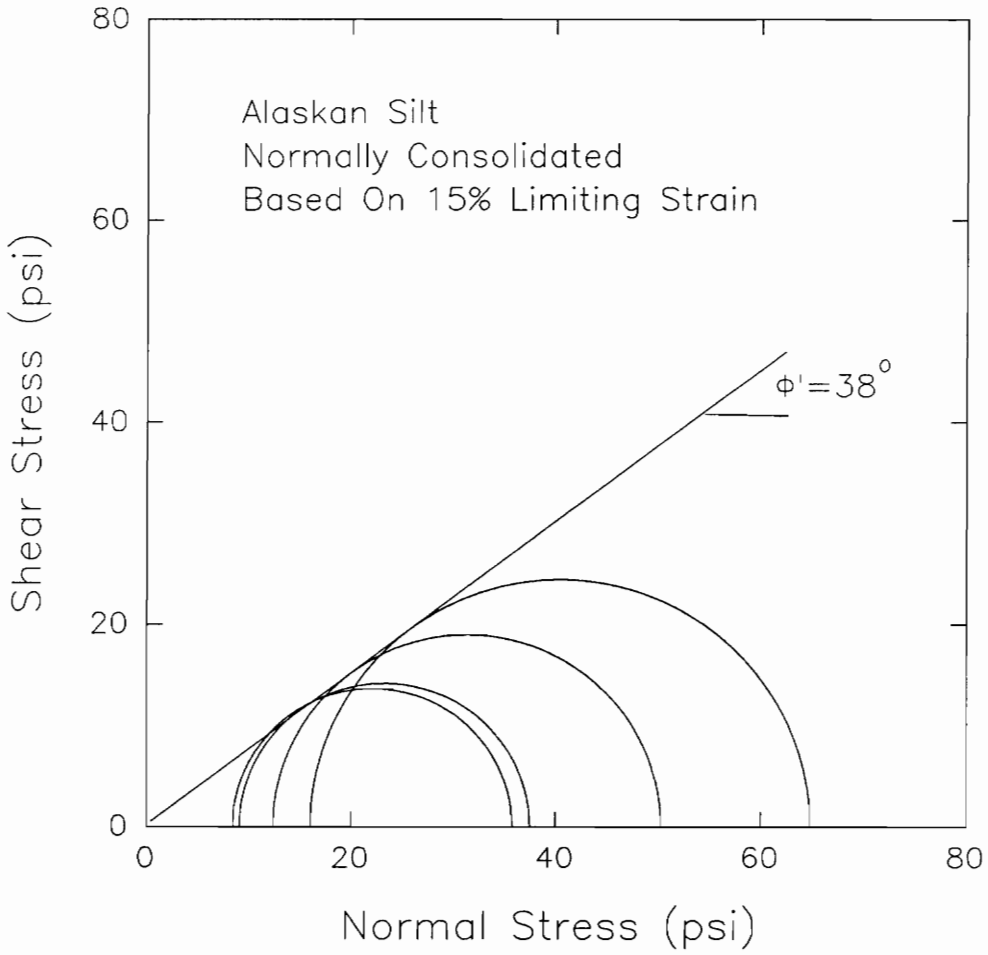

Figure 23 Effective Stress Mohr's Circles Measured For The ICU Triaxial Tests On Normally Consolidated Alaskan Silt For Failure Based On 15% Limiting Strain

Since all specimens had positive pore pressures throughout the tests, A-bar equal to zero as a failure criterion could not be applied.

A summary of effective stress friction angle based on different failure criteria is given in Table 3. The resulting values of the effective stress friction angles for the samples ranged from 36° to 38°.

Total Stress Interpretation of ICU Tests On Reconstituted Alaskan Silt

Shown in Figure 24 is the undrained strength and effective consolidation pressure relationship based on maximum pore pressure. The undrained strength ratio, S_u/p, can be defined by determining the slope of the line drawn from the origin through the data points. The value of S_u/p derived based on maximum pore pressure is equal to 0.62. Note that this value is a good estimate due to little scatter in the results.

Using maximum deviator stress as failure criterion to define the undrained strength ratio for this test gave a biased estimate because only one sample was represented. The undrained strength-consolidation

Table 3 Effective Stress Friction Angle For Reconstituted Samples of Alaskan Silt At Different Failure Criteria

Failure Criteria	ϕ' (Degrees)	Average Strain To Failure (%)
U_{max}	35	4.0
Max $(\sigma_1 - \sigma_3)$	36	20.0
Max σ_1'/σ_3'	38	10.0
10% Limiting Strain	38	10.0
15% Limiting Strain	38	15.0
$\bar{A} = 0$	N/A	N/A

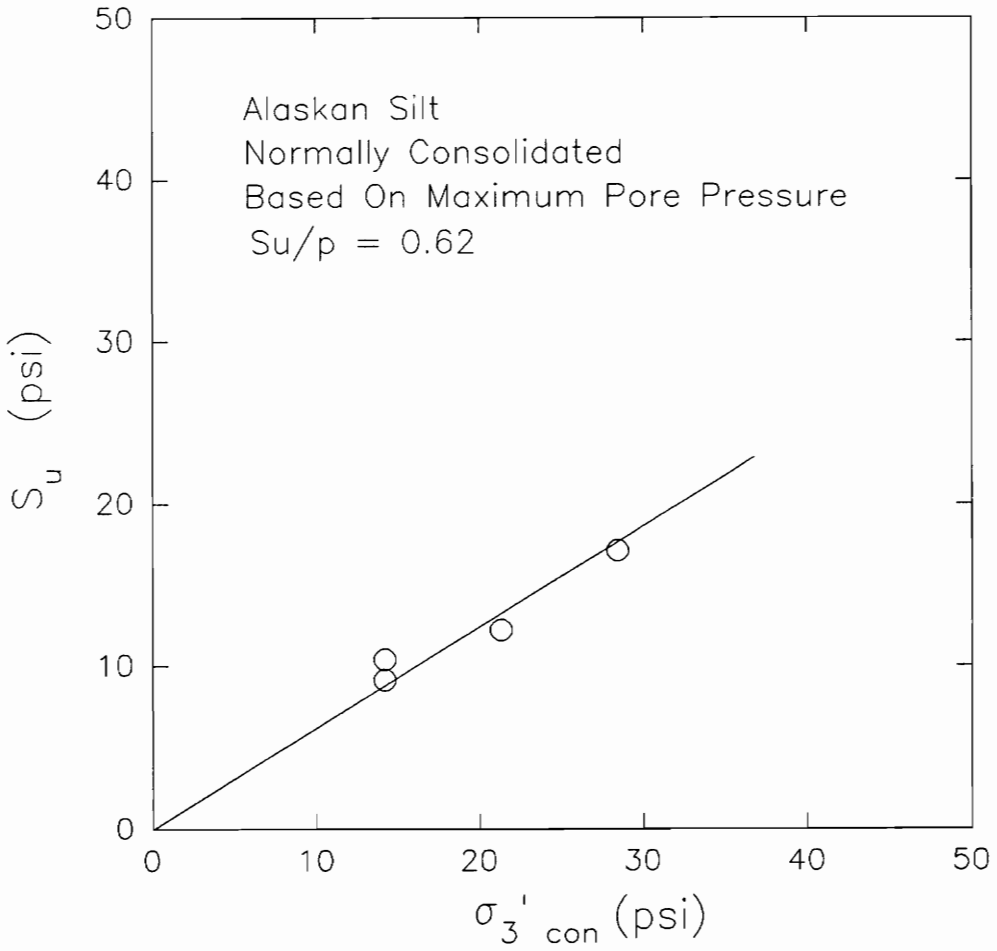

Figure 24 Undrained Shear Strength-Effective Consolidation Pressure Relationship Measured For The ICU Triaxial Test On Normally Consolidated Alaskan Silt For Failure Based On Maximum Pore Pressure

pressure relationship is shown in Figure 25 which gives a value of S_u/p of 0.9.

Figure 26 shows the undrained shear strength and consolidation pressure relationship based on maximum principal stress ratio. The data exhibit little scatter, and the undrained strength ratio, S_u/p, is approximately equal to 0.81.

Figures 27 and 28 show the undrained strength ratio based on 10% and 15% limiting strains, respectively. The estimated S_u/p for the 10% limiting strain is 0.81 and 0.88 for 15% limiting strain.

As discussed in the effective stress analysis, A-bar equal to zero cannot be applied because the pore pressures remained positive during the test.

A summary of the undrained strength ratios determined for the samples is given in Table 4. The range of S_u/p for the different failure criteria is 0.81 to 0.90, except for S_u/p based on maximum pore pressure which gave the lowest value of 0.62. Using Skempton's correlation of S_u/p, expressed as, $S_u/p = 0.11 + 0.0037\ (PI)$, the undrained shear strength can be estimated based on the plasticity index. This correlation gives an S_u/p equal to 0.13.

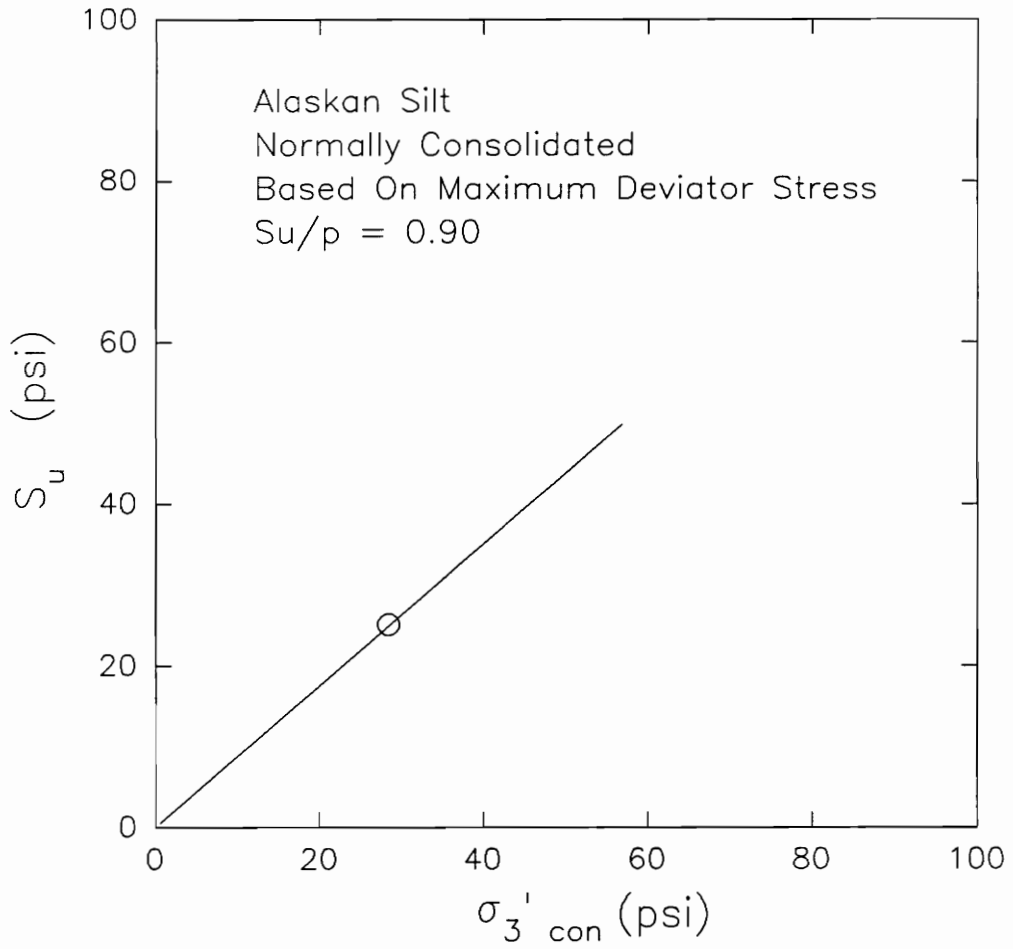

Figure 25 Undrained Shear Strength-Effective Consolidation Pressure Relationship Measured For The ICU Triaxial Test On Normally Consolidated Alaskan Silt For Failure Based On Maximum Deviator Stress

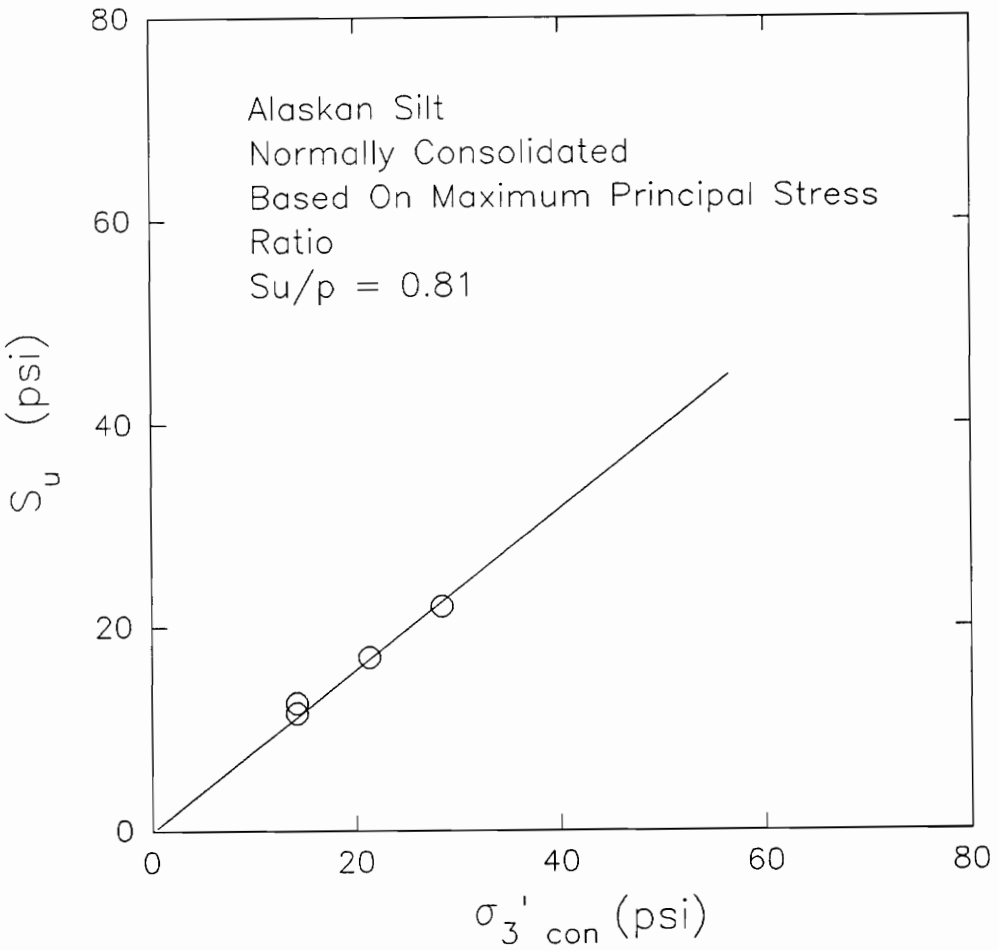

Figure 26 Undrained Shear Strength-Effective Consolidation Pressure Relationship Measured For The ICU Triaxial Test On Normally Consolidated Alaskan Silt For Failure Based On Maximum Principal Stress Ratio

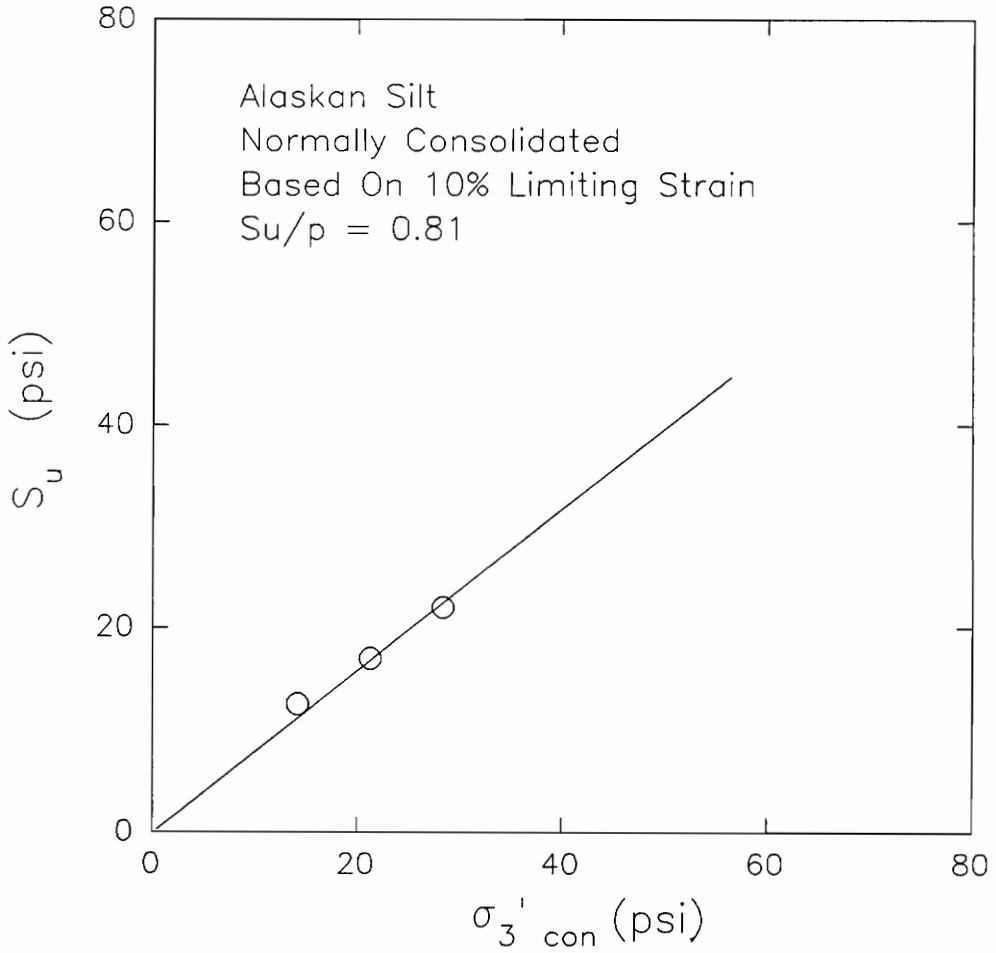

Figure 27 Undrained Shear Strength-Effective Consolidation Pressure Relationship Measured For The ICU Triaxial Test On Normally Consolidated Alaskan Silt For Failure Based On 10% Limiting Strain

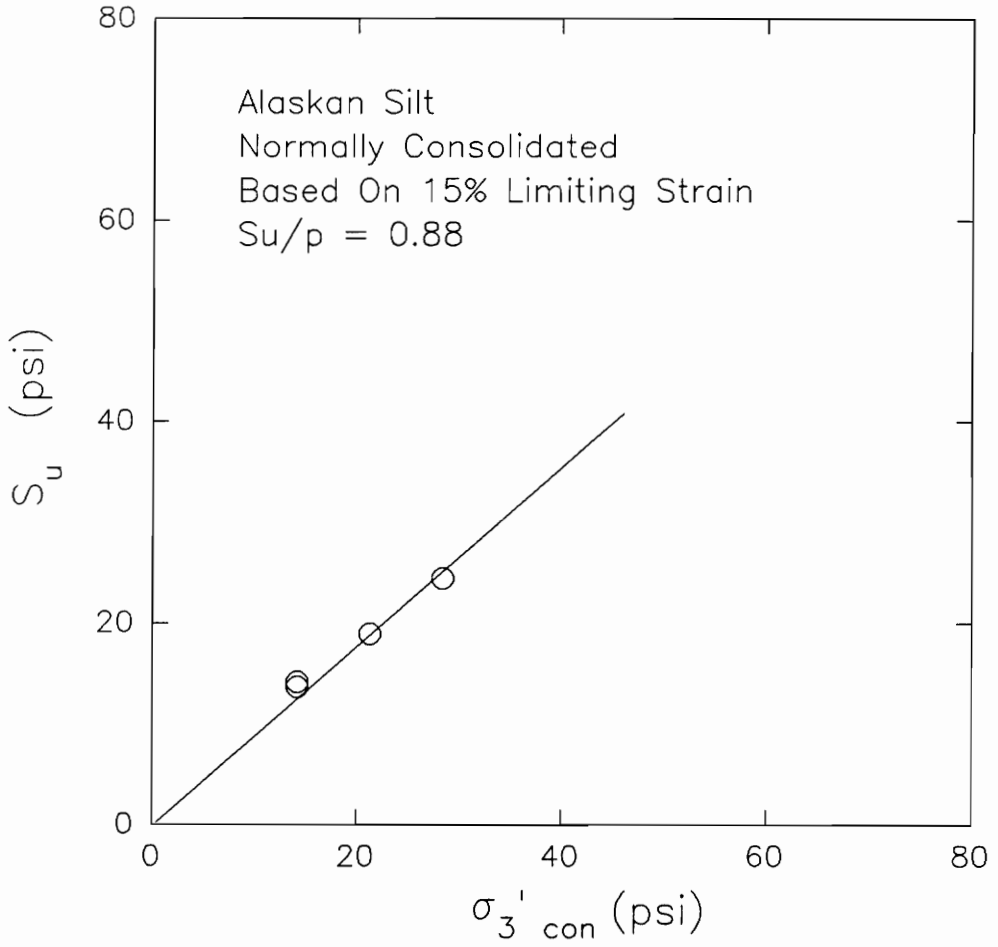

Figure 28 Undrained Shear Strength-Effective Consolidation Pressure Relationship Measured For The ICU Triaxial Test On Normally Consolidated Alaskan Silt For Failure Based On 15% Limiting Strain

Table 4 **S_u/p Ratios Determined For Reconstituted Samples of Alaskan Silt At Different Failure Criteria**

Failure Criteria	S_u/p	Average Strain To Failure (%)
U_{max}	0.62	4.0
Max $(\sigma_1 - \sigma_3)$	0.90	20.0
Max σ_1'/σ_3'	0.81	10.0
10% Limiting Strain	0.81	10.0
15% Limiting Strain	0.88	15.0
$\bar{A} = 0$	N/A	N/A

Unconsolidated Undrained Triaxial Tests On Reconstituted Alaskan Silt.

Four UU Triaxial tests were performed on reconstituted samples of Alaskan silt. The sample preparation procedure was identical to the one used for the ICU tests. Table 5 shows the properties of the UU test specimens of the reconstituted Alaskan silt. The cell pressures applied were 7.10 psi, 14.20 psi, 21.30 psi, and 28.40 psi. The loading rate during the test was 0.55 lb/minute.

Figure 29 shows the deviator stress-strain relationship measured during the test. None of the samples exhibited a peak deviator stress in the range of the strains used, thus precluding the use of maximum deviator stress as a failure criterion. In this case, failure could be defined by limiting strains.

The Mohr's circles using 10% limiting strain as failure criterion are plotted in Figure 30. Using a ϕ_u=0 interpretation, the undrained strength, Su, is about 3.20 psi. This gives an undrained strength ratio, S_u/p, of 0.23 since the samples were initially consolidated to 14.20 psi.

Another failure criteria proposed by Fleming (1985) is 15% limiting strain. Based on this failure criteria,

Table 5 Properties of UU Tests Samples Of Reconstituted Alaskan Silt

Test Number	Water Content (%)	Cell Pressure (psi)	Dry Density (pcf)	OCR
1	7.10	33.60	86.60	1
2	14.20	33.20	84.70	1
3	21.30	33.20	85.30	1
4	28.40	34.20	85.30	1

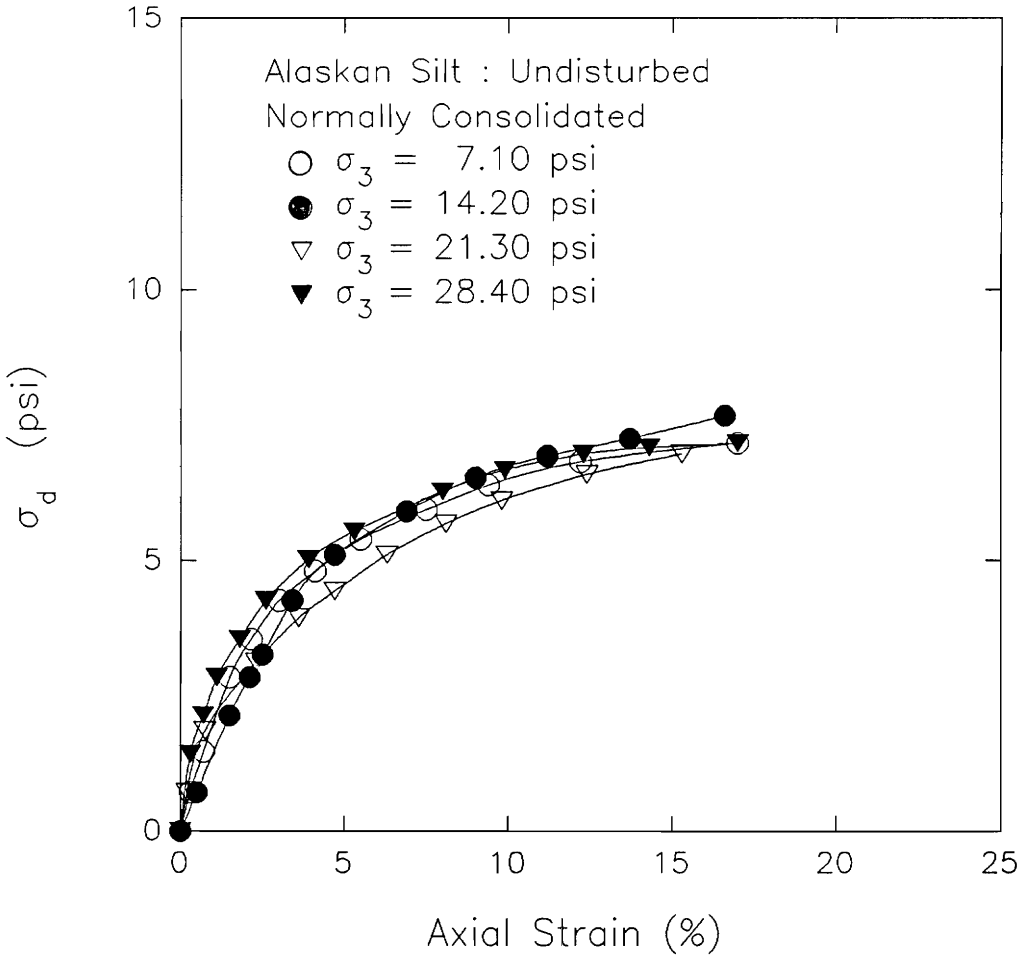

Figure 29 Deviator Stress-Strain Relationship Measured For UU Triaxial Tests On Reconstituted Alaskan Silt

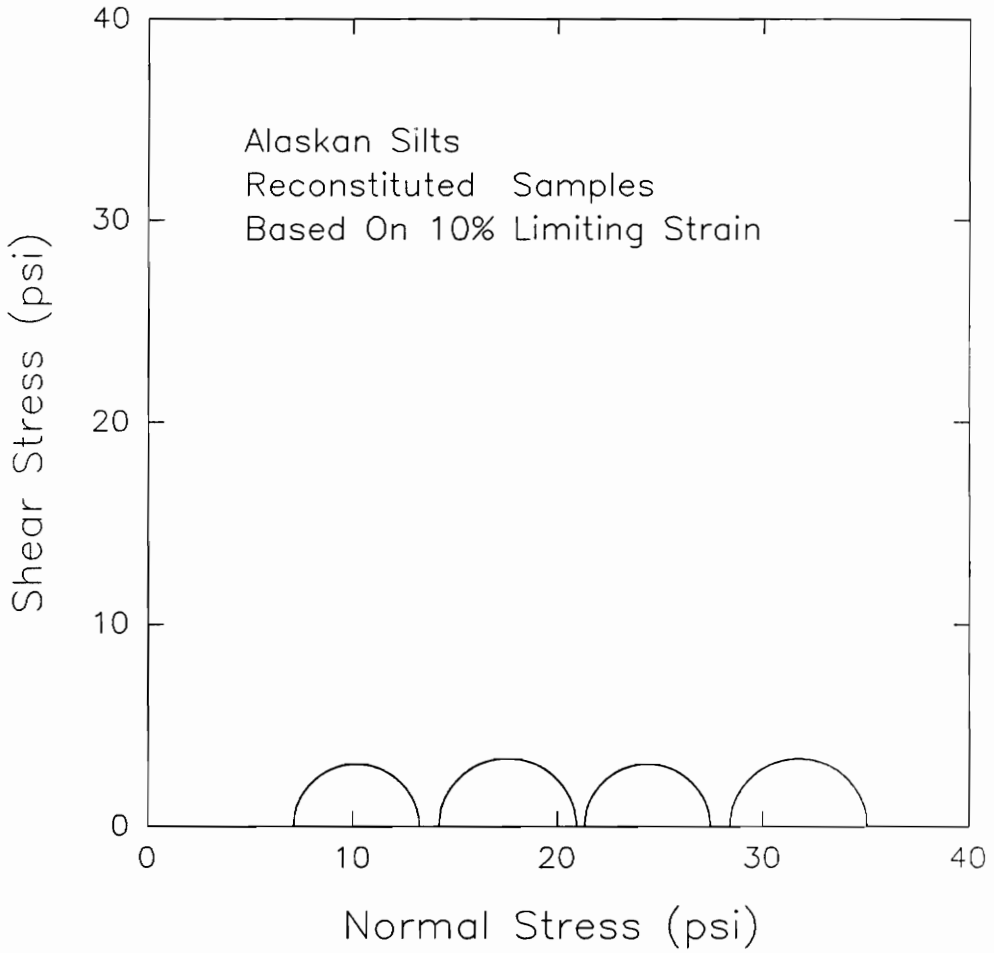

Figure 30 Mohr's Circles Measured For UU Triaxial Tests On Reconstituted Alaskan Silt For Failure Based On 10% Limiting Strain

the Mohr's circles are plotted in Figure 31. Using $\phi_u = 0$ method, the resulting undrained shear strength is 3.60 psi. This gives an undrained strength ratio, S_u/p, of 0.25.

Table 6 summarizes the values of S_u/p ratios for different failure criteria measured for the UU triaxial tests for the samples.

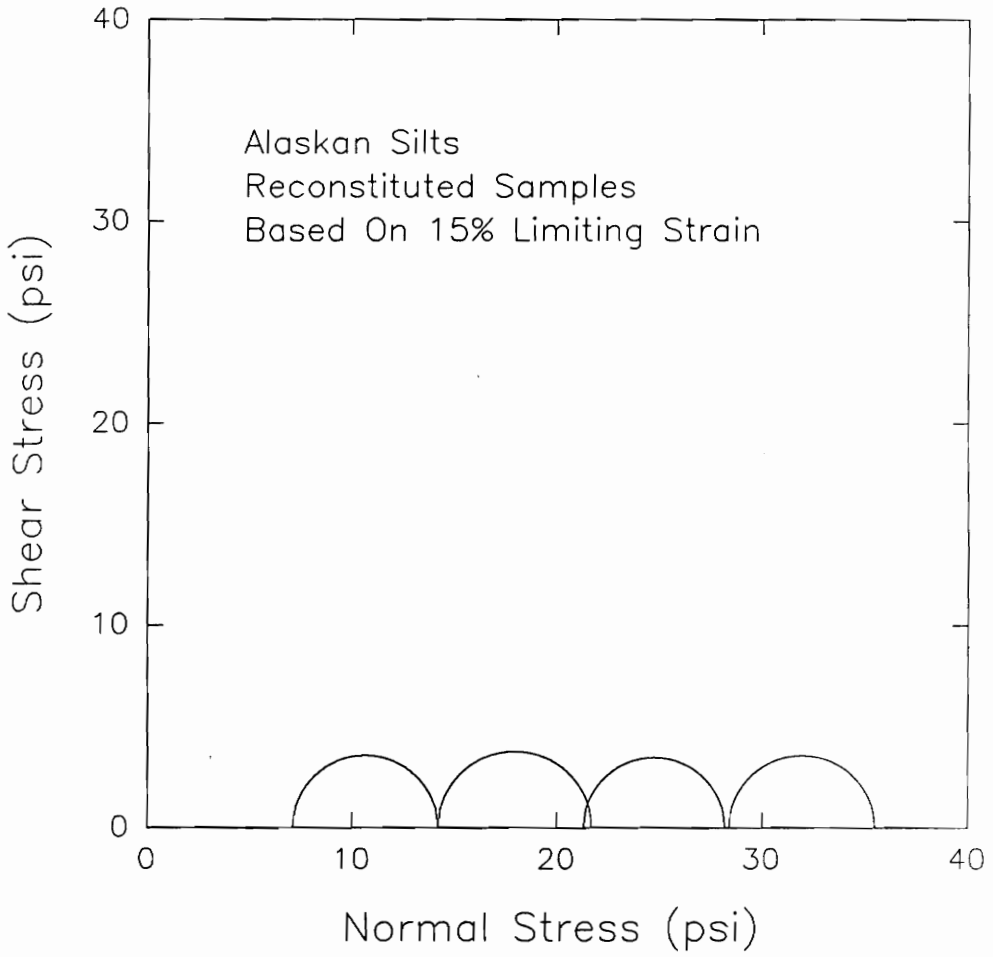

Figure 31 Mohr's Circles Measured For UU Triaxial Tests On Reconstituted Alaskan Silt For Failure Based On 15% Limiting Strain

Table 6 Su/p Ratios at Different Failure Criteria Measured For UU Triaxial Test On Alaskan Silt

Failure Criteria	S_u/p
$(\sigma_1-\sigma_3)_{max}$	N/A
10% Limiting Strain	0.23
15% Limiting Strain	0.25

Braehead Silt

Penman (1953) performed triaxial tests on saturated silt specimens from Braehead Power Station, Scotland. The samples used were reconstituted from dry samples obtained from borings on the site. De-aired water was added to the dry silt to form a slurry. A more detailed material and sample preparation are discussed in reference (11).

Index Properties of Braehead Silt

Figure 32 shows the grain size distribution curve for Braehead silt. The grain size components are given in Table 7. The sample consists mostly of silt particles with grain size diameter less than 0.074 mm and greater than 0.003 mm. No clay size components are present in the sample. The specific gravity of the specimen is 2.71 and the liquid limit is 24.6%.

Consolidated Undrained Triaxial Test On Normally Consolidated Sample of Reconstituted Braehead Silt.

One CU triaxial test was conducted on a reconstituted sample of Braehead silt. The sample had a diameter of 1.50 inches and was 3.50 inches long. The displacement rate used in the test was 0.025 inch per minute which corresponds to about 1% strain per minute.

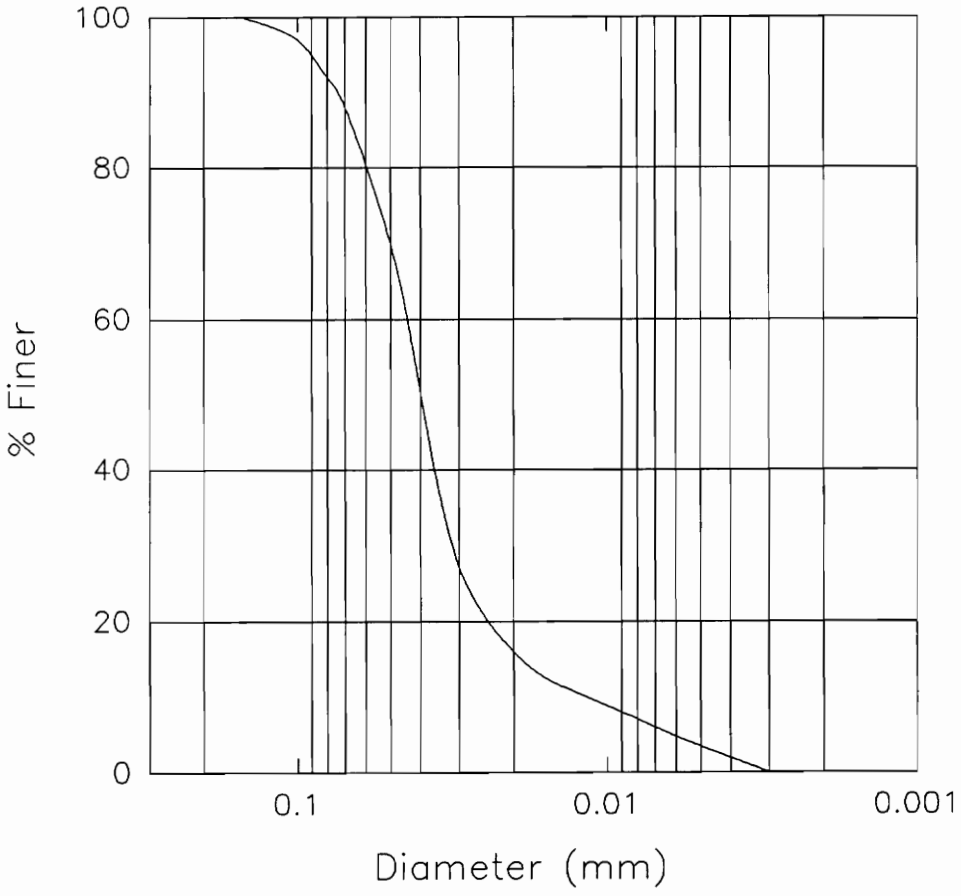

Figure 32 Grain Size Distribution Curve For Braehead Silt

Table 7 Grain Size Components of Braehead Silt

Component	Amount
% Sand	18.0%
% Silt	82.0%
% Clay	0 %

The sample was fully saturated prior to shearing. The effective consolidation pressure used during the test was 5 psi.

Shown in Figures 33 and 34 are the deviator stress-strain and minor effective stress-strain relationships. Even though the stress-strain diagram reached a maximum value, the peak does not occur until a strain of about 28%. The maximum value of the minor effective stress occured at the same strain as the maximum deviator stress.

Figure 35 illustrates the principal stress ratio-strain relationship for this test. The principal stress ratio had a maximum value of 3.90 at a strain of 7.50%.

Figures 36 and 37 show the A-bar-strain and pore pressure-strain relationships. The pore pressure during straining reached a maximum value of 2.30 psi at a strain of about 2%.

The behavior of the pore pressure is reflected in the effective stress path shown in Figure 38. When pore pressure started decreasing, the stress path approached the K_f line and continued to climb the K_f line up to a strain of 28%. When the pore pressure started increasing again, the stress path reversed direction where p' and q both decreased. The measured angle α for the K_f line is

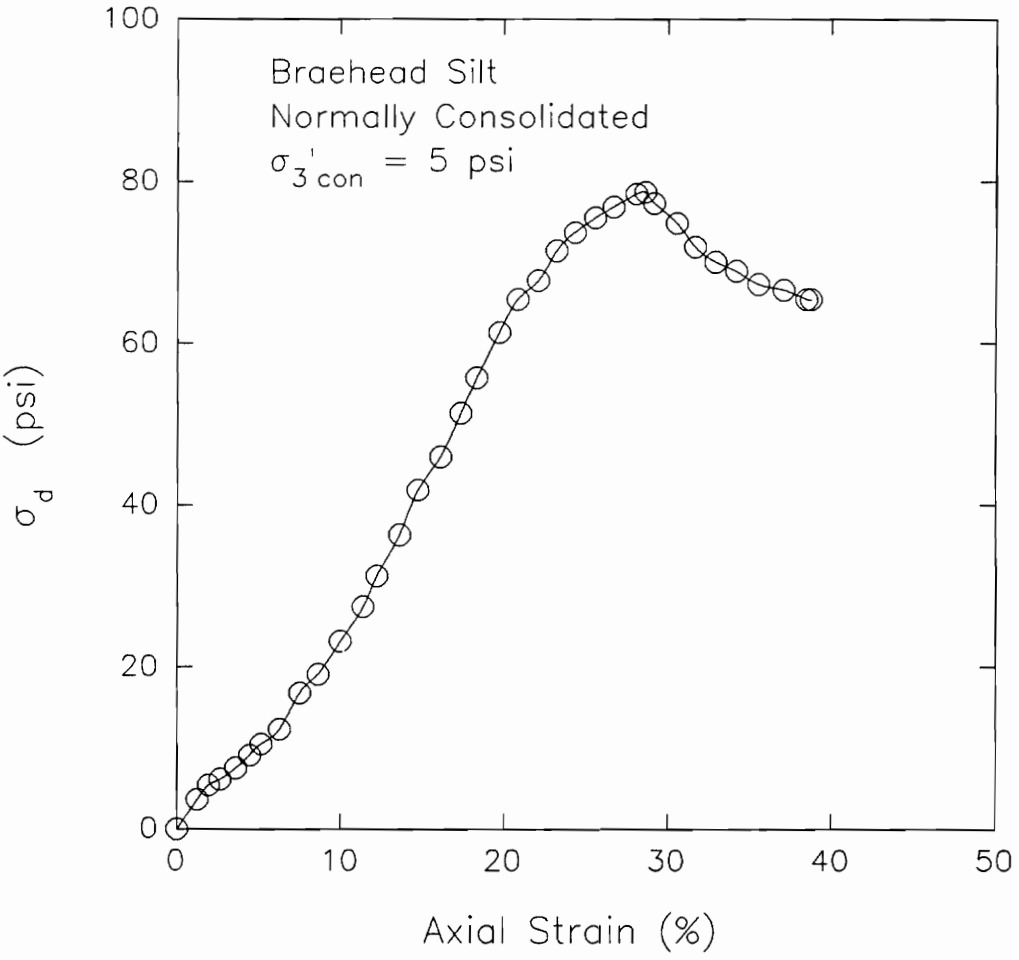

Figure 33 Deviator Stress-Strain Relationship Measured For CU Triaxial Test On Reconstituted Sample of Braehead Silt

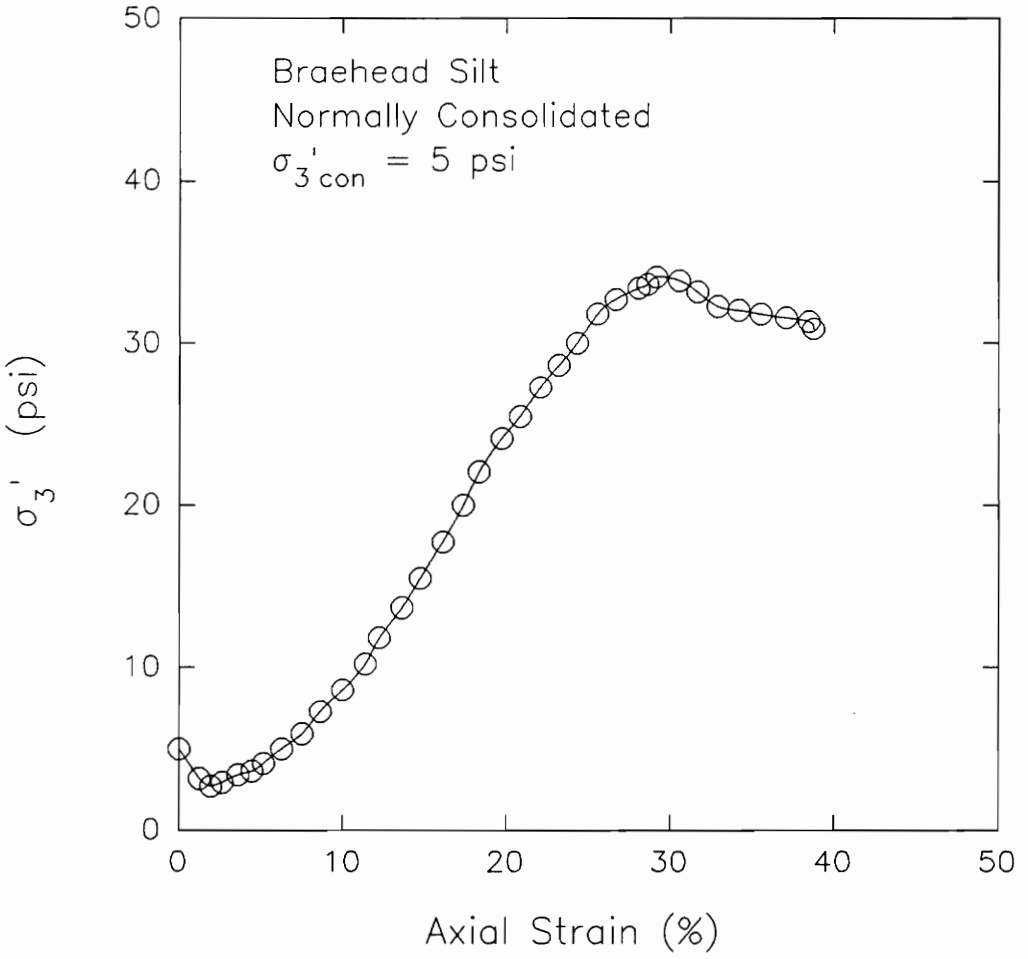

Figure 34 Minor Effective Stress-Strain Relationship Measured For CU Triaxial Test On Reconstituted Sample of Braehead Silt

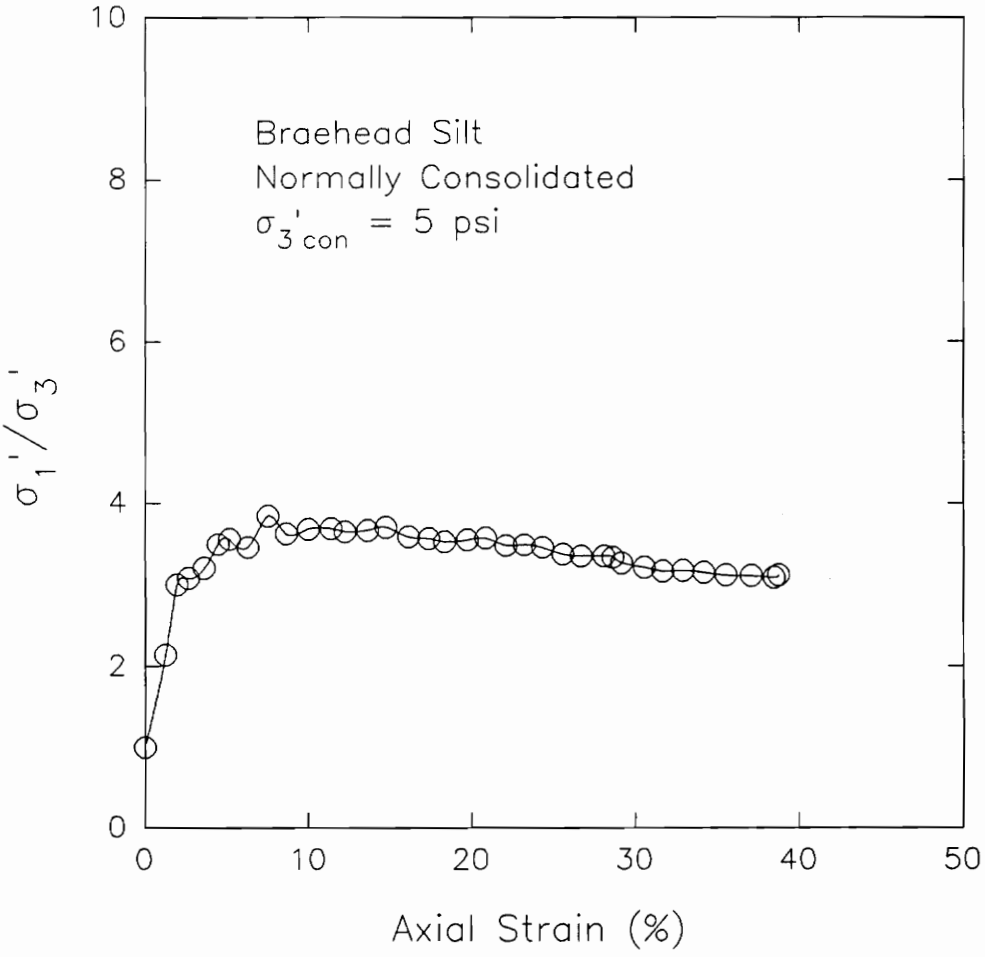

Figure 35 Principal Stress Ratio-Strain Relationship Measured For CU Triaxial Test On Reconstituted Sample of Braehead Silt

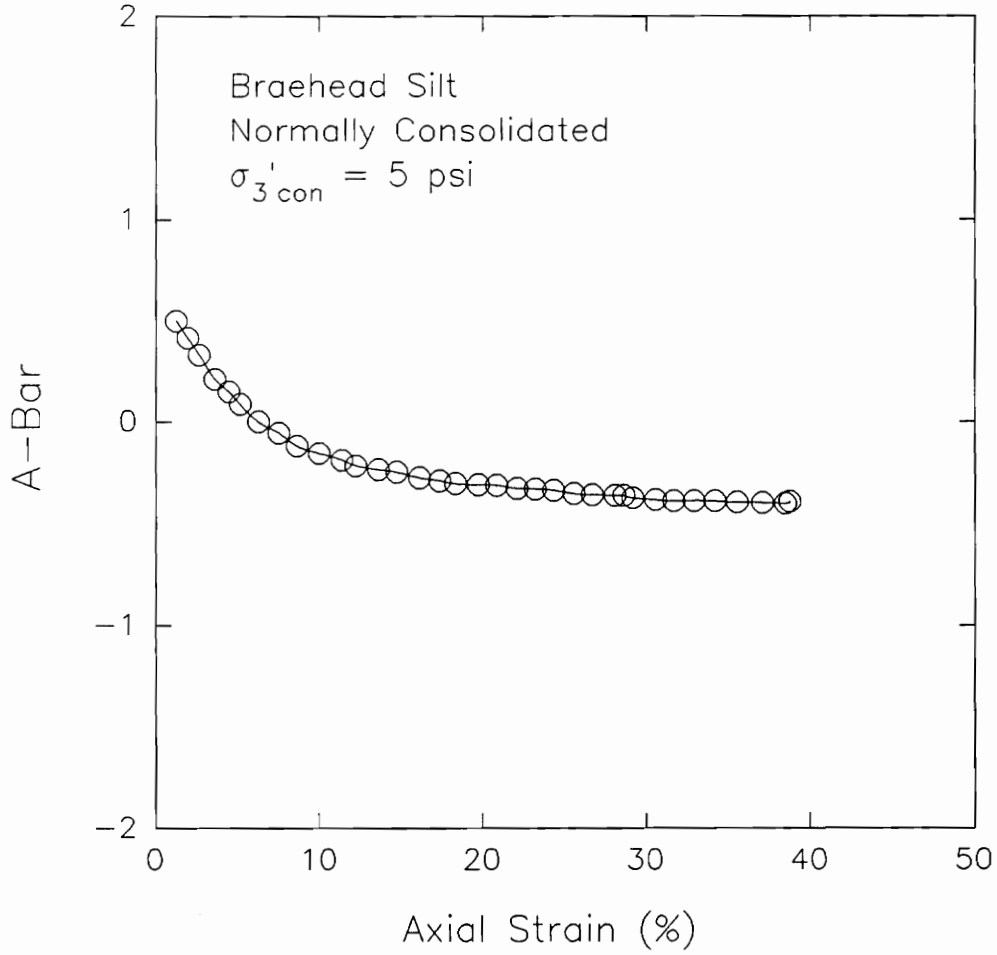

Figure 36 A-bar-Strain Relationship Measured For CU Triaxial Test On Reconstituted Sample of Braehead Silt

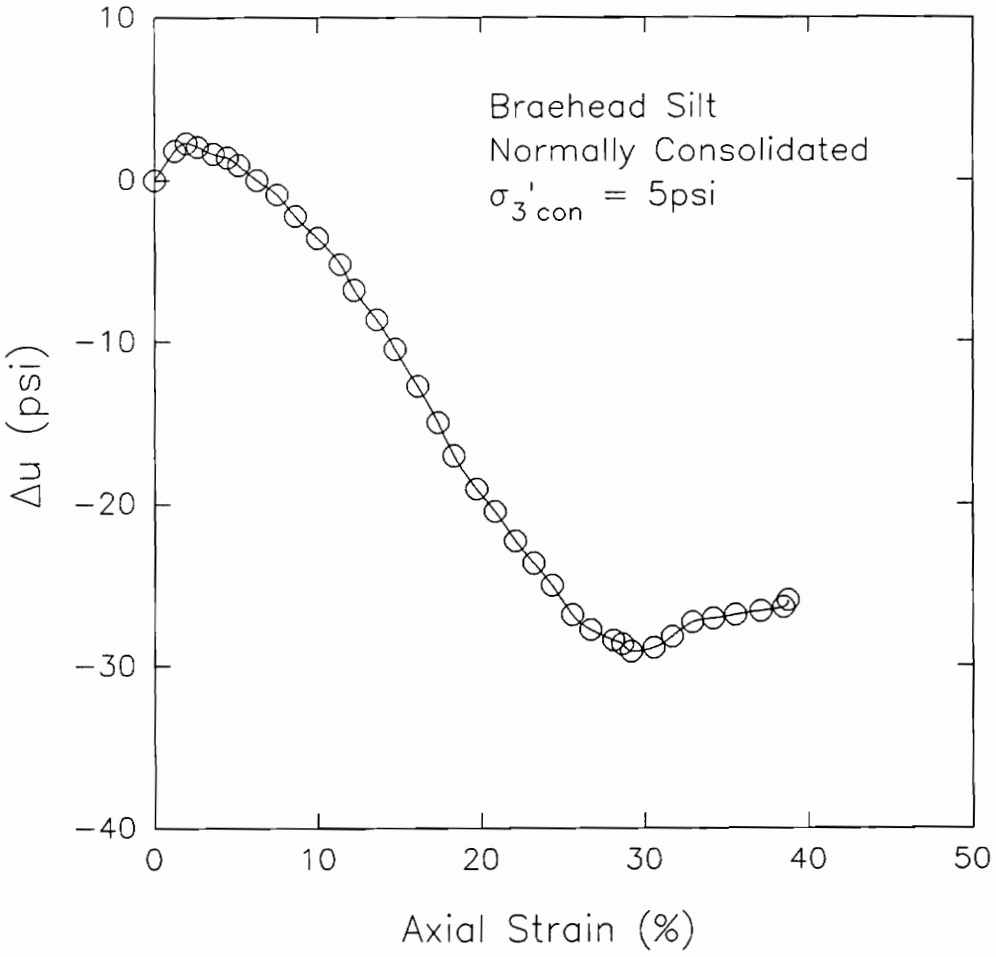

Figure 37 Pore Pressure-Strain Relationship Measured For CU Triaxial Test On Reconstituted Sample of Braehead Silt

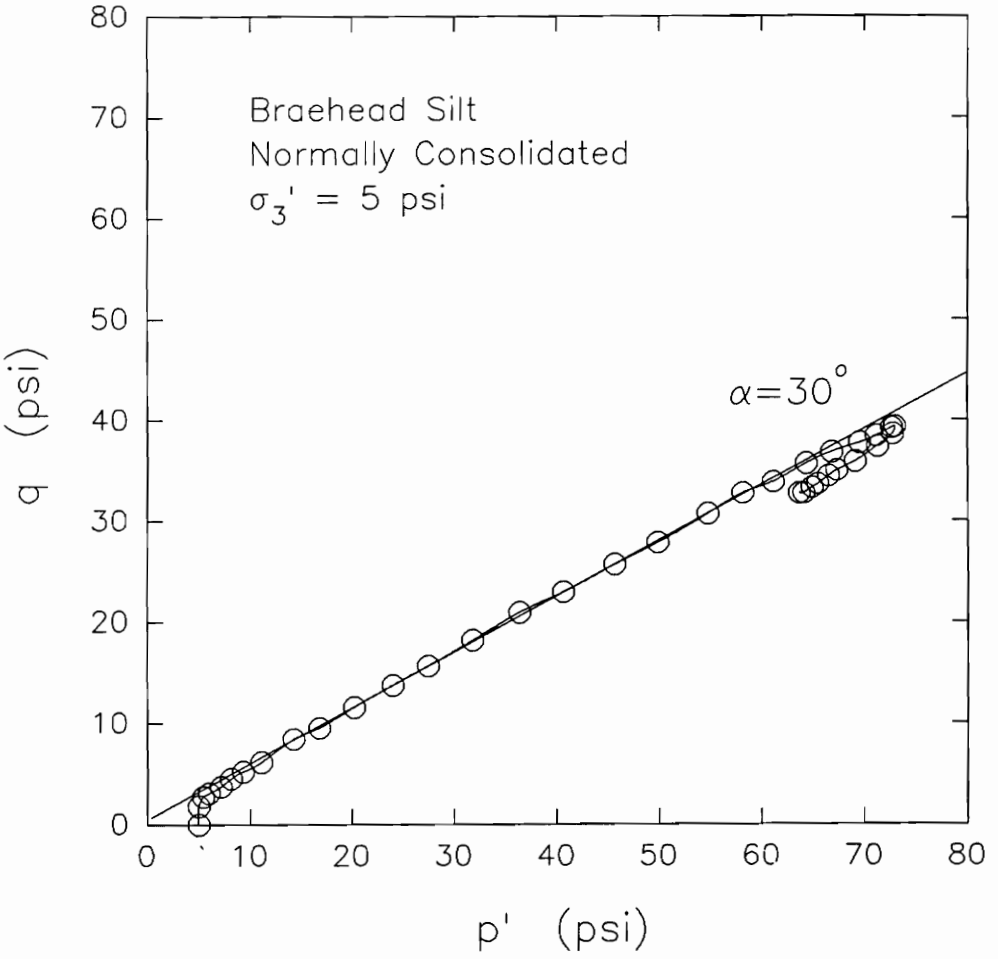

Figure 38 Effective Stress Path Measured For CU Triaxial Test On Reconstituted Sample of Braehead Silt

30°, which corresponds to an effective stress friction angle, ϕ', equal to 35°.

Effective Stress Interpretation of The CU Triaxial Test On Reconstituted Sample of Braehead Silt.

The effective stress interpretation for Braehead silt is done in the same manner as the previous silt samples.

Figure 39 shows the Mohr's circles based on maximum pore pressure as failure criterion. Constraining the effective cohesion intercept to zero, the value of ϕ' calculated is equal to 31°.

Figure 40 illustrates the Mohr's circle for failure based on maximum deviator stress. A ϕ' of 37° is calculated for this failure criterion.

Shown in Figure 41 is the Mohr's circle based on maximum principal stress ratio. The value of the effective stress friction angle calculated is 36°.

Figures 42 and 43 illustrate the Mohr's circles for failure based on 10% and 15% limiting strains. These failure criteria gave values of effective stress friction angles equal to 35° for 10% limiting strain and 36° for 15% limiting strain.

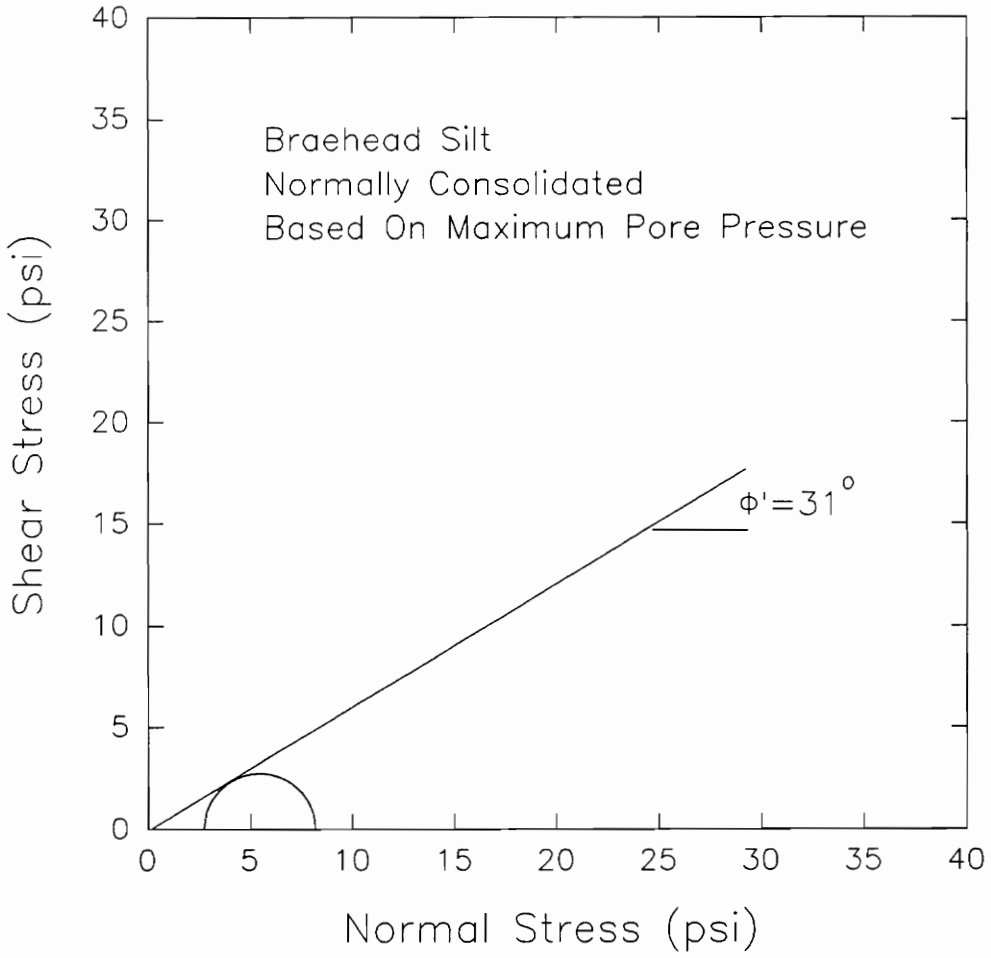

Figure 39 Effective Stress Mohr's Circle Measured For CU Triaxial Test On Reconstituted Sample of Braehead Silt For Failure Based On Maximum Pore Pressure

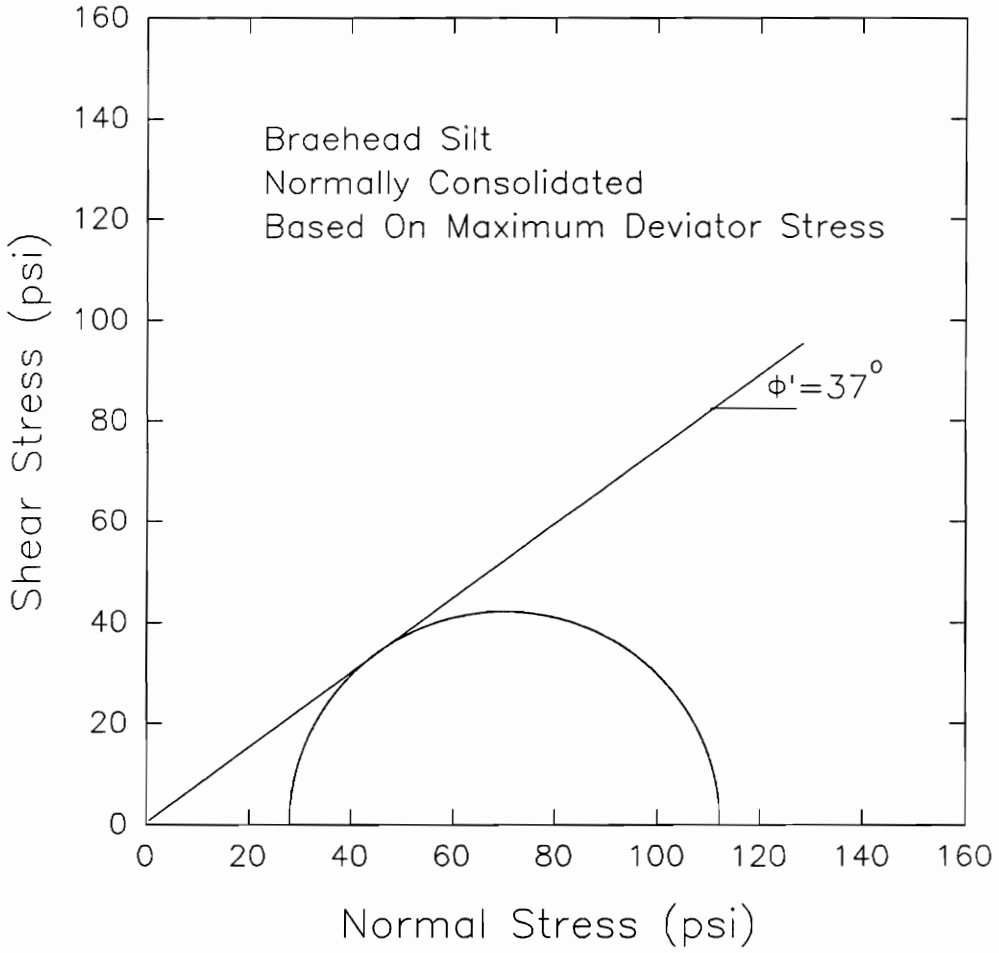

Figure 40 Effective Stress Mohr's Circle Measured For CU Triaxial Test On Reconstituted Sample of Braehead Silt For Failure Based On Maximum Deviator Stress

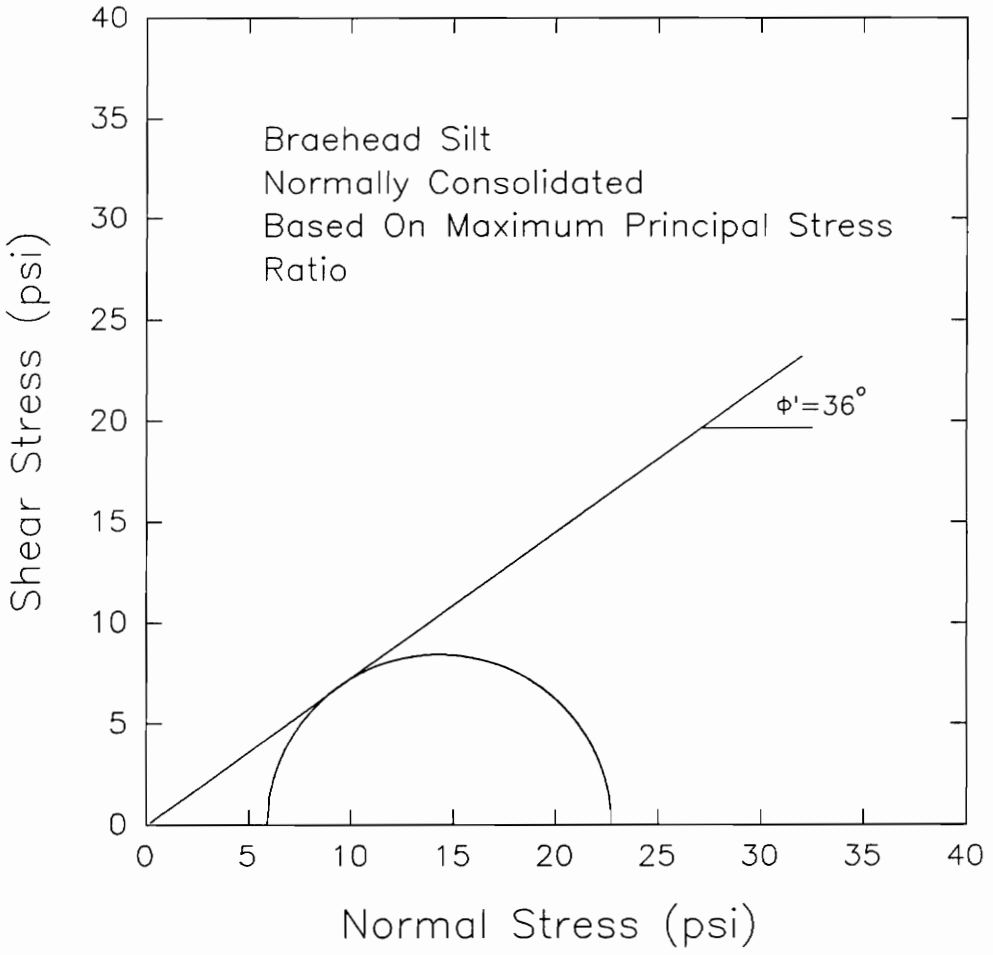

Figure 41 Effective Stress Mohr's Circle Measured For CU Triaxial Test On Reconstituted Sample of Braehead Silt For Failure Based On Maximum Principal Stress Ratio

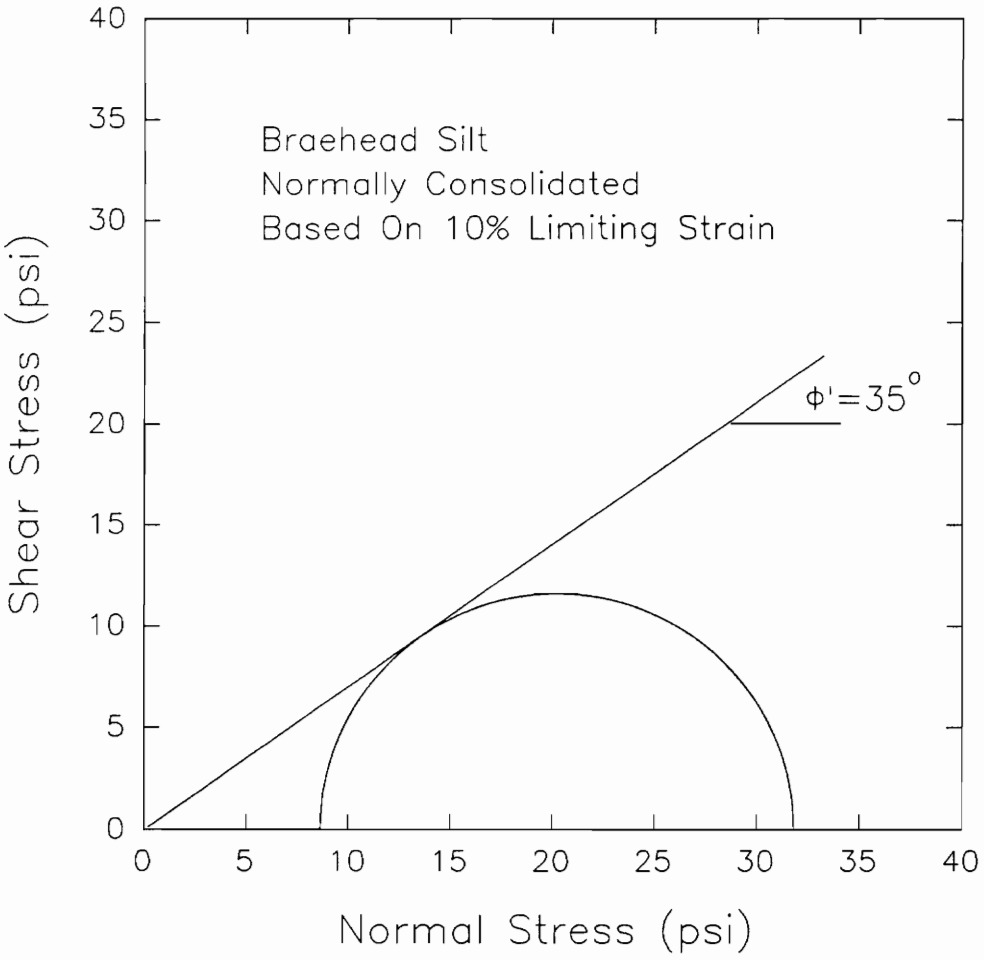

Figure 42 Effective Stress Mohr's Circle Measured For CU Triaxial Test On Reconstituted Sample of Braehead Silt For Failure Based On 10% Limiting Strain

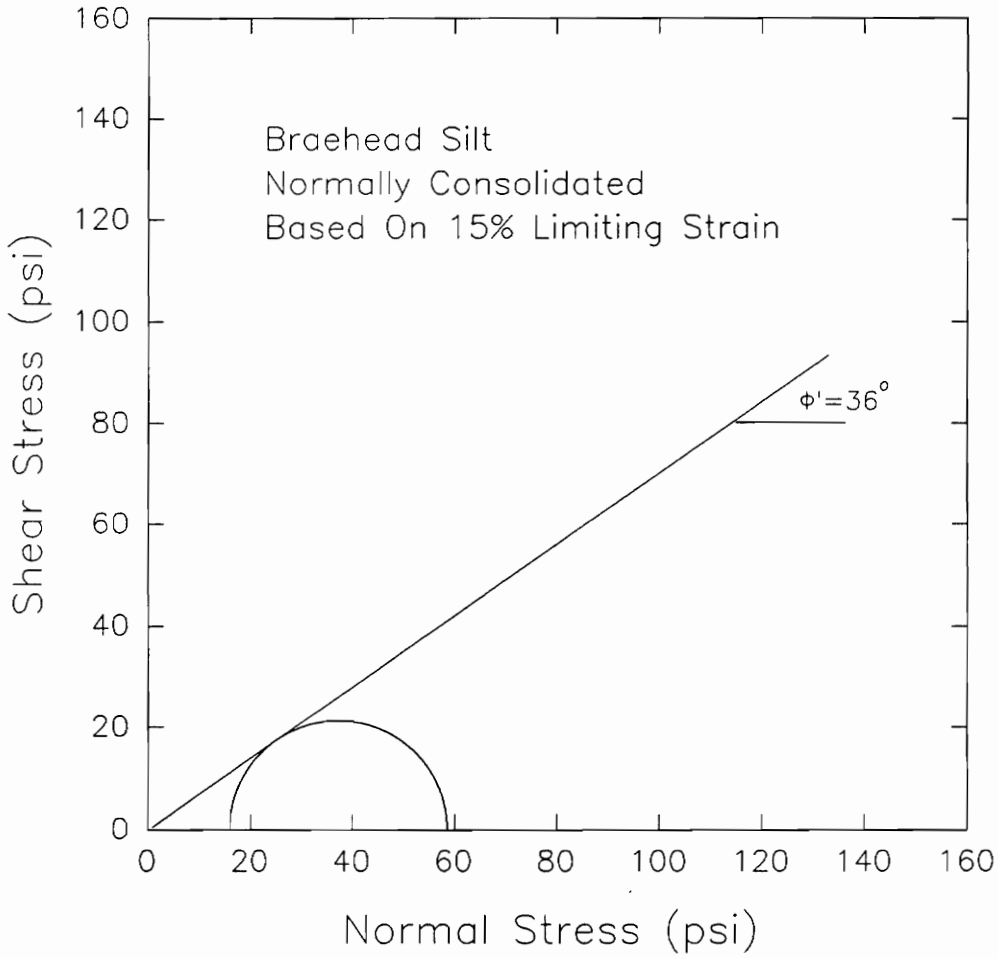

Figure 43 Effective Stress Mohr's Circle Measured For CU Triaxial Test On Reconstituted Sample of Braehead Silt For Failure Based On 15% Limiting Strain

The Mohr's circle using A-bar equal to zero failure criterion is shown in Figure 44. The effective stress friction angle calculated is 34°.

A summary of the values of the effective stress friction angles for different failure criteria are given in Table 8. The lowest value of ϕ' was obtained using maximum pore pressure as failure criterion. The average ϕ' from the different failure criteria, except u_{max}, is equal to 35° which is the same ϕ' calculated from the effective stress path.

Total Stress Interpretation For CU Triaxial Test On Reconstituted Sample of Braehead Silt

The values of the undrained strength ratios could be evaluated using the CU test results for the reconstituted Braehead silt.

Figure 45 shows the relationship between the undrained strength and effective consolidation pressure for failure based on maximum pore pressure. Defining S_u/p as the slope of the line drawn from the origin to the data point, the undrained strength ratio calculated is equal to 0.55.

Shown in Figure 46 is the S_u/p ratio determined using maximum deviator stress as failure criterion. The value of S_u/p calculated is 7.80.

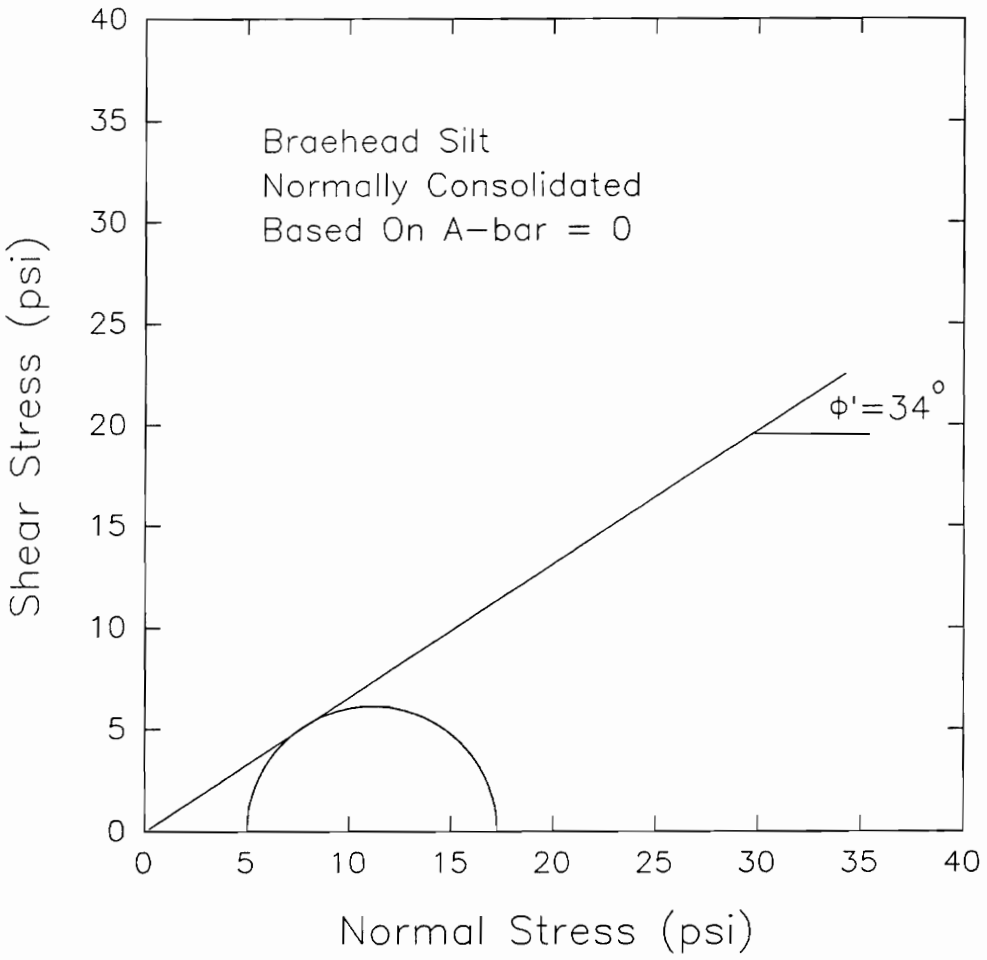

Figure 44 Effective Stress Mohr's Circle Measured For CU Triaxial Test On Reconstituted Sample of Braehead Silt For Failure Based On A-bar=0

Table 8 Effective Stress Friction Angle At Different Failure Criteria For Braehead Silt

Failure Criteria	ϕ' (Degrees)	Average Strain To Failure (%)
u_{max}	31	2%
Max$(\sigma_1-\sigma_3)$	37	28%
Max(σ_1'/σ_3')	36	7.5%
10% Limiting Strain	35	10%
15% Limiting Strain	36	15%
A-bar = 0	34	7.5%

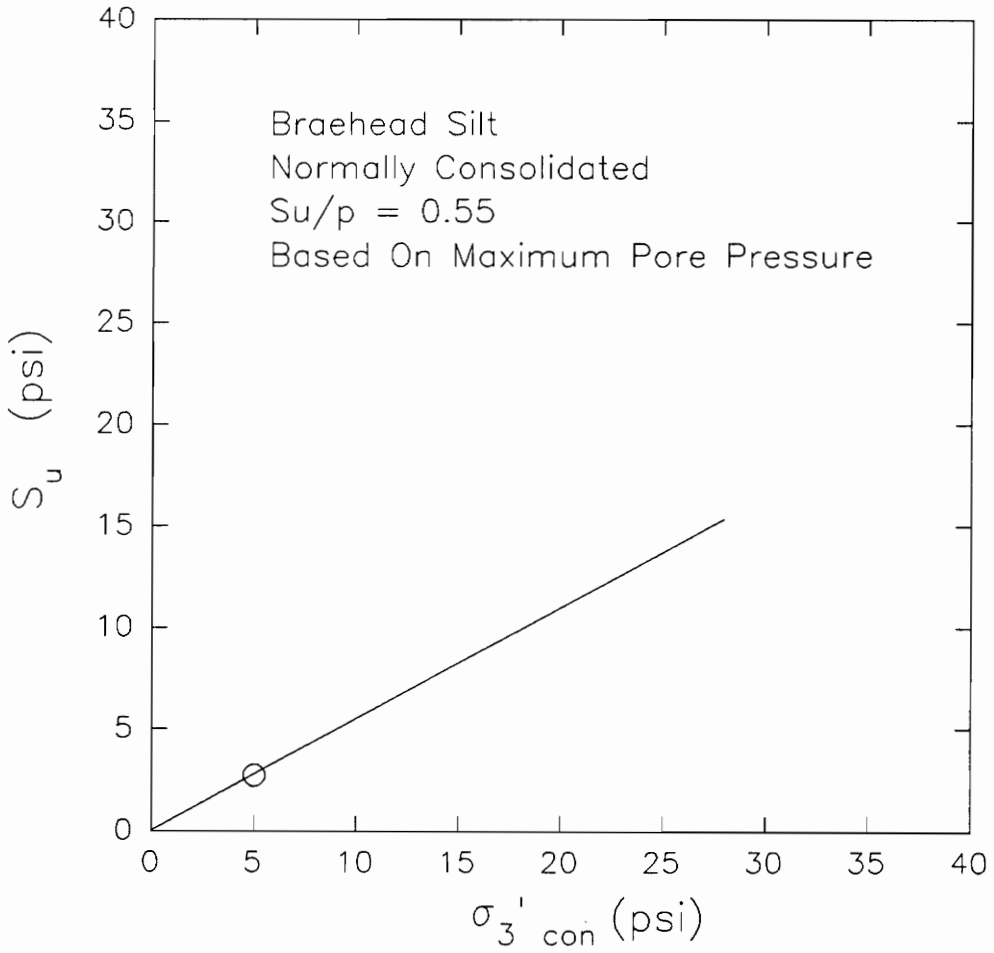

Figure 45 Undrained Shear Strength-Effective Consolidation Pressure Relationship Measured For CU Triaxial Test On Reconstituted Sample of Braehead Silt For Failure Based On Maximum Pore Pressure

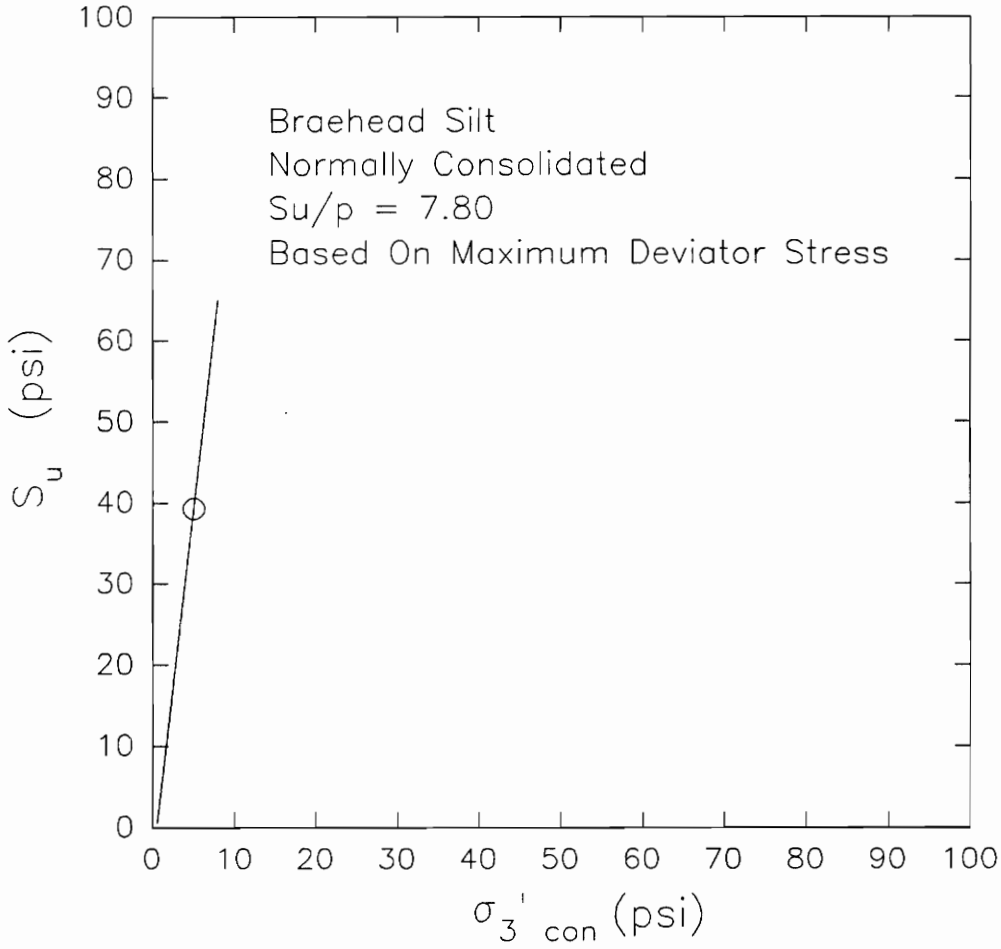

Figure 46 Undrained Shear Strength-Effective Consolidation Pressure Relationship Measured For CU Triaxial Test On Reconstituted Sample of Braehead Silt For Failure Based On Maximum Deviator Stress

Values of the undrained strength ratios based on 10% and 15% limiting strains are shown in Figures 48 and 49 respectively. S_u/p ratios calculated are 2.30 for 10% limiting strain and 4.20 for 15% limiting strain.

Figure 50 shows the S_u/p based on A-bar equal to zero. An S_u/p of 1.20 was determined using this failure criterion.

Table 9 summarizes the S_u/p ratios measured for different failure criteria. Similar with the previous silt samples analysed, the maximum pore pressure failure criterion gave the lowest value of S_u/p. Skempton's correlation of S_u/p cannot be applied to this test because a plastic limit test was not performed on the sample.

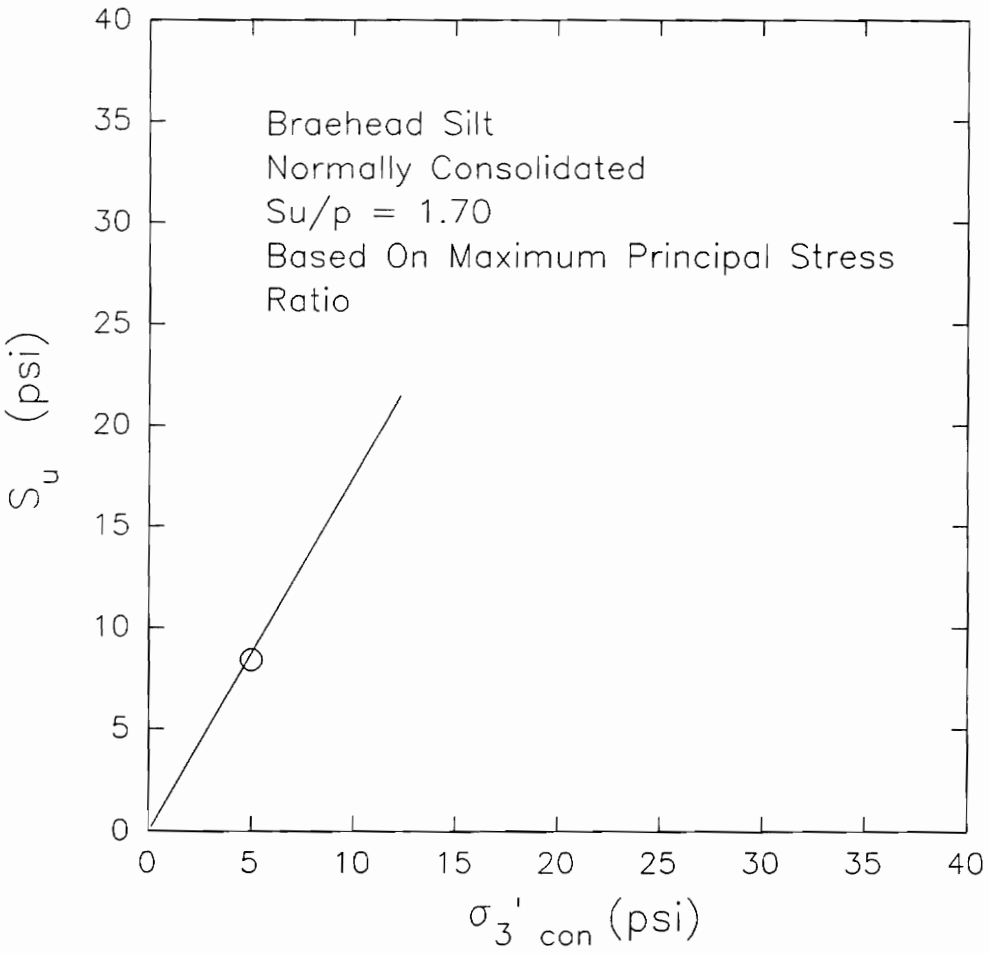

Figure 47 Undrained Shear Strength-Effective Consolidation Pressure Relationship Measured For CU Triaxial Test On Reconstituted Sample of Braehead Silt For Failure Based On Maximum Principal Stress Ratio

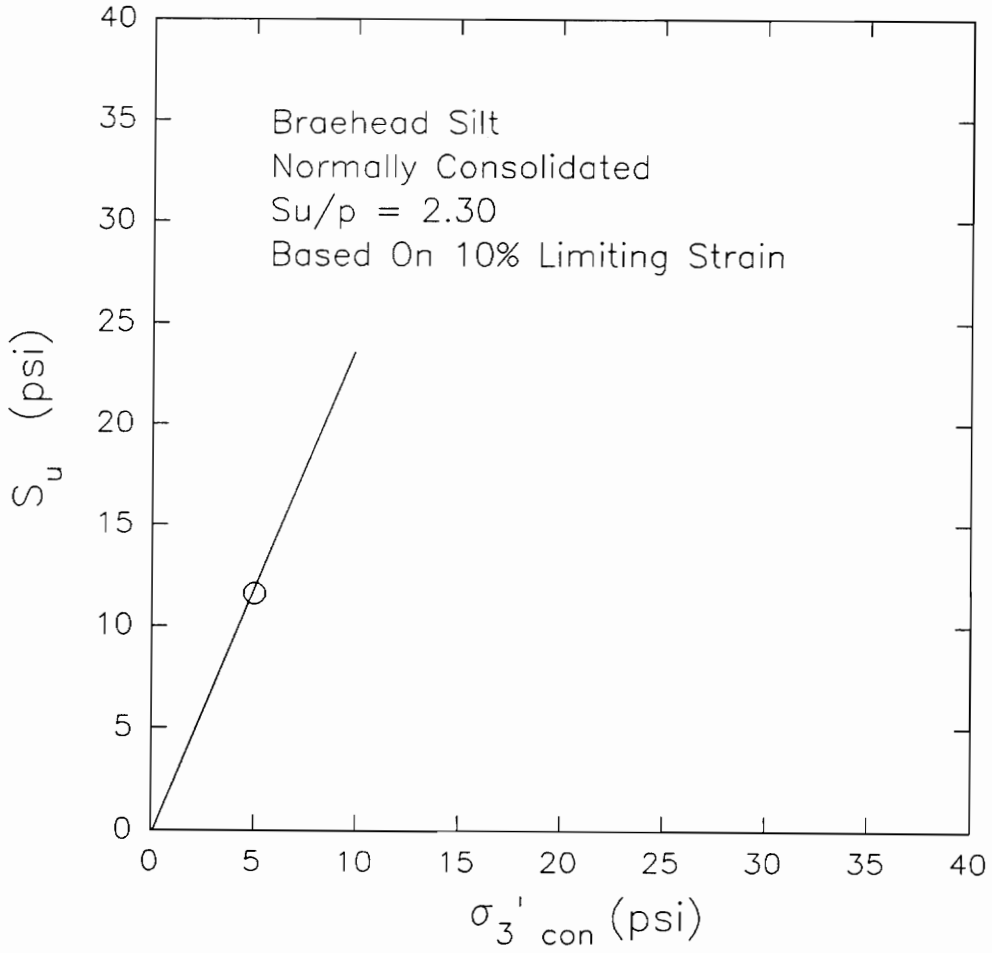

Figure 48 Undrained Shear Strength-Effective Consolidation Pressure Relationship Measured For CU Triaxial Test On Reconstituted Sample of Braehead Silt For Failure Based On 10% Limiting Strain

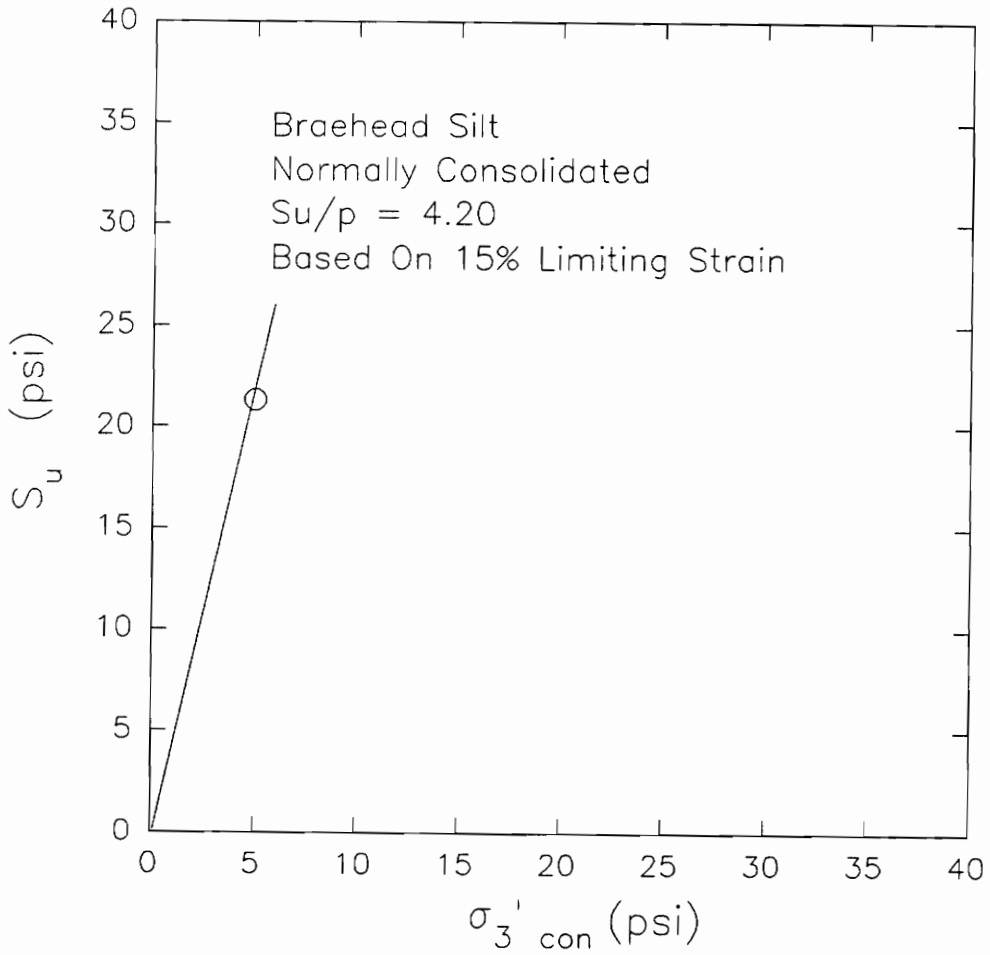

Figure 49 Undrained Shear Strength-Effective Consolidation Pressure Relationship Measured For CU Triaxial Test On Reconstituted Sample of Braehead Silt For Failure Based On 15% Limiting Strain

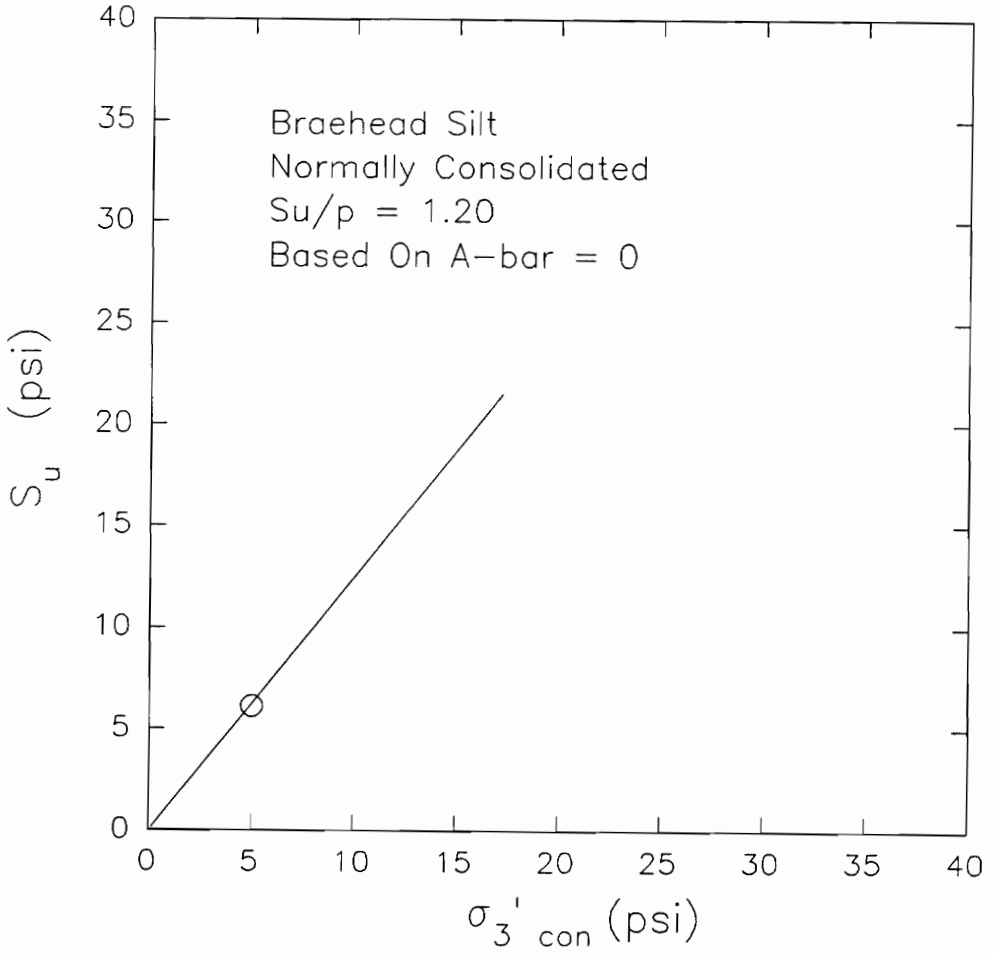

Figure 50 Undrained Shear Strength-Effective Consolidation Pressure Relationship Measured For CU Triaxial Test On Reconstituted Sample of Braehead Silt For Failure Based On A-bar = 0

Table 9 S_u/p Ratios Measured For CU Triaxial Test At Different Failure Criteria For Braehead Silt

Failure Criteria	Su/p
u_{max}	0.55
Max($\sigma_1-\sigma_3$)	7.8
Max(σ_1'/σ_3')	1.7
10% Limiting Strain	2.3
15% Limiting Strain	4.2
A-bar = 0	1.2

Cape Canaveral Silt

Newhouse (1990) tested silt specimens from Cape Canaveral, Florida. Undisturbed samples of silts were obtained from the site at depths of 47 feet to 49 feet below ground surface. The initial properties of the specimens are given in Table 10. The specimens were described as non-plastic gray sandy silts, which classify as ML according to the Unified Soil Classification System.

Consolidated Undrained Triaxial Test On Overconsolidated Undisturbed Sample of Cape Canaveral Silt

One CU test was performed on an undisturbed sample of Cape Canaveral silt. The initial properties of the sample for CU test are given in Table 11. The effective consolidation pressure used for the triaxial test was 14.20 psi. A consolidation test was also performed on a specimen from the same sampling tube. From the consolidation curve shown in Figure 51, the sample had a C_r of 0.008 and a C_c equal to 0.10. The past consolidation pressure of the material ranges from 60 psi to 90 psi. This corresponds to an overconsolidation ratio that ranges from 4.2 to 6.3. The strain rate used for the

Table 10 Initial Properties of Cape Canaveral Silt

Water Content	40.9 %
Degree of Saturation	100.0 %
Dry Density	82.9 pcf
Void Ratio	0.995

Table 11 Properties of CU Triaxial Specimens for Cape Canaveral Silt

Water Content	36.0 %
Dry Density	84.6 pcf
Void Ratio	0.959
Degree of Saturation	99.8 %

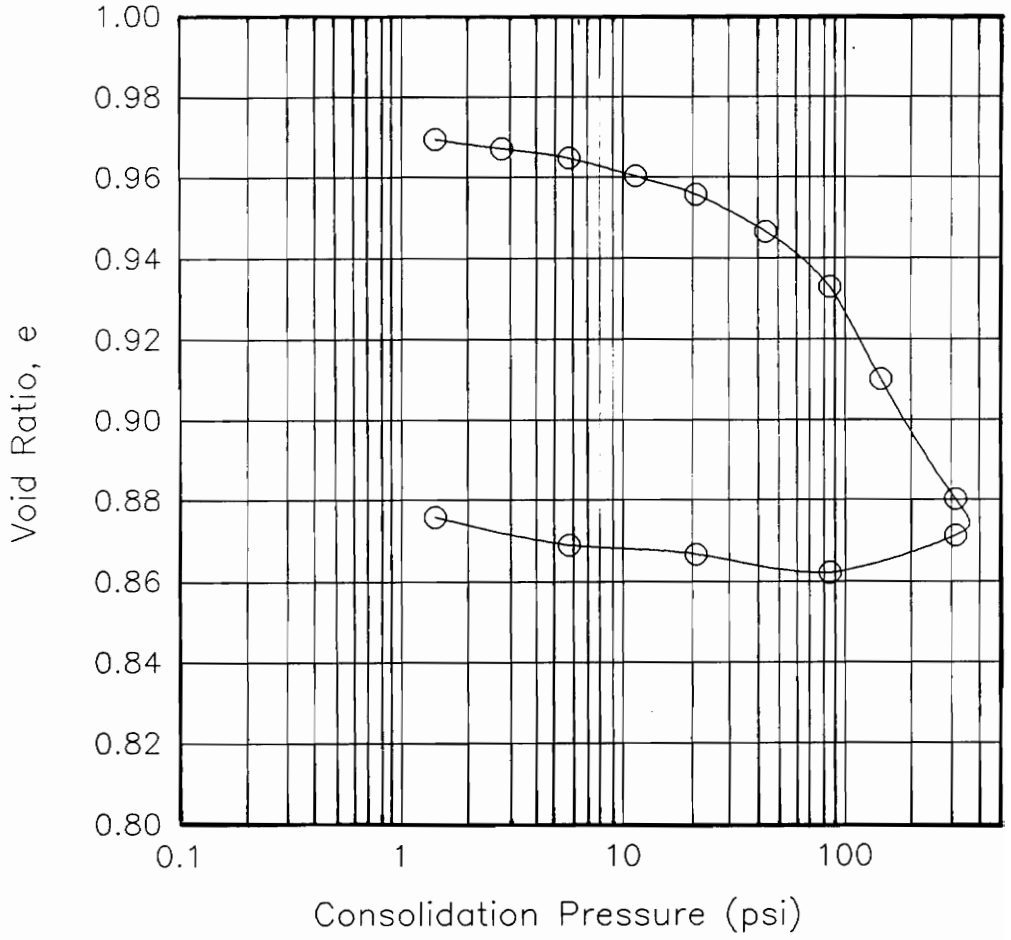

Figure 51 Consolidation Curve For Cape Canaveral Silt (Newhouse, 1990)

test was 1.10% per hour. Normal procedures of back pressure saturation were done to insure that the sample was saturated prior to shearing.

Figure 52 illustrates the deviator stress-strain relationship for the specimen. The deviator stress increased rapidly at small strains. The stress-strain diagram exhibited a distinct break at a strain of about 1%. After a steep portion, the stress-strain diagram followed a flatter slope but never peaked throughout the test. This stress-strain behavior is due to the dilative properties of the soil sample.

Figures 53 and 54 illustrate the minor effective stress-strain and principal stress ratio-strain relationships. The sample had a maximum principal stress ratio of 4.3 at a strain of about 8.5%.

Shown in Figures 55 and 56 are the A-bar-strain and pore pressure-strain relationships. The maximum pore pressure (minimum σ_3') was reached at a strain of about 1.7%. After reaching a peak value, it then continued to decrease until a strain of about 20%.

Figure 57 illustrates the effective stress path for the sample. The stress path clearly defines the K_f line with an α value equal to 32°. This corresponds to an effective stress friction angle, ϕ', equal to 38.5°.

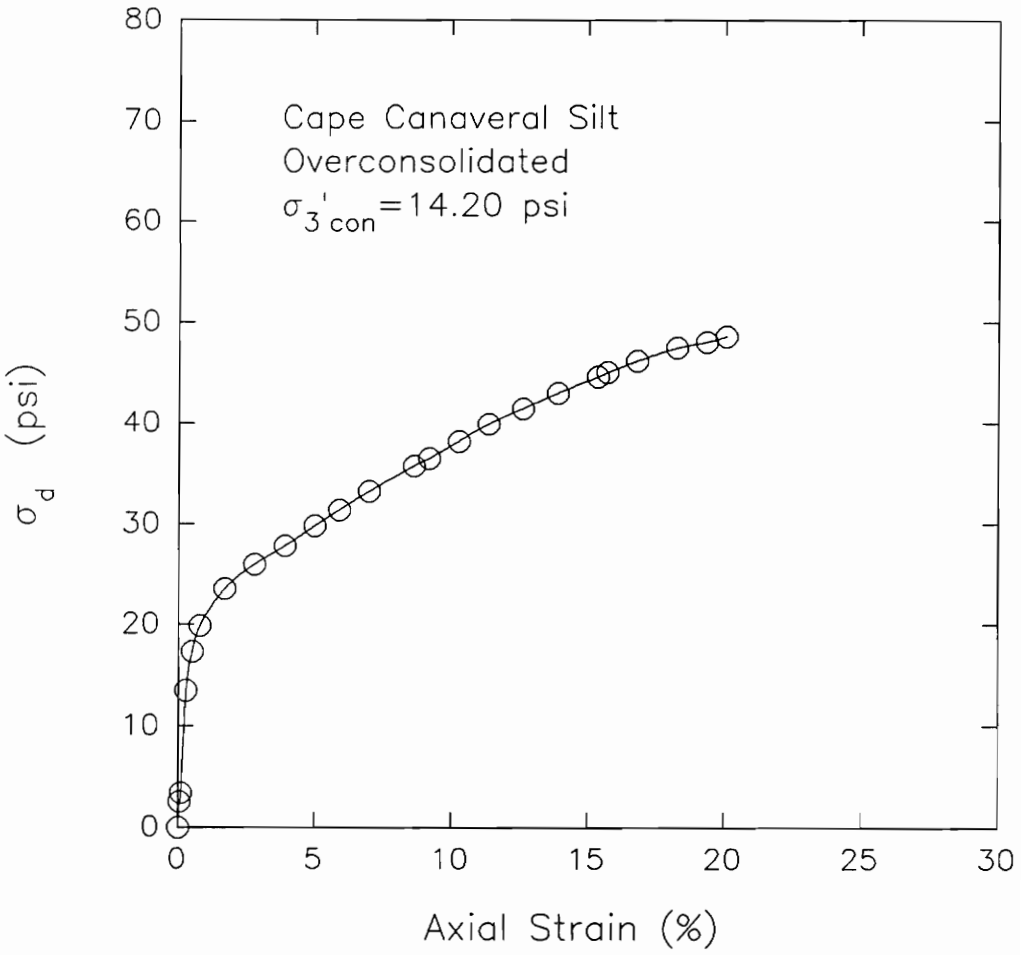

Figure 52 Deviator Stress-Strain Relationship Measured For CU Triaxial Test On Overconsolidated Undisturbed Sample of Cape Canaveral Silt

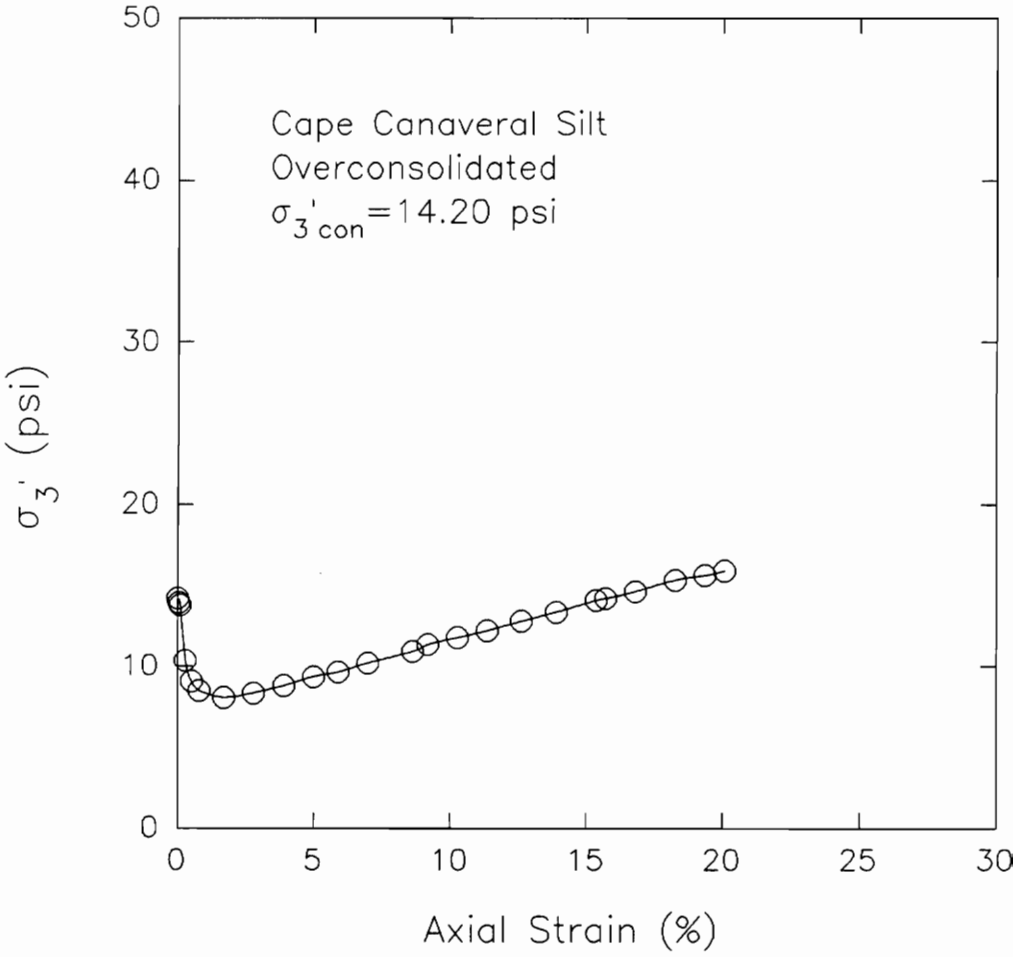

Figure 53 Minor Effective Stress-Strain Relationship Measured For CU Triaxial Test On Overconsolidated Undisturbed Sample Of Cape Canaveral Silt

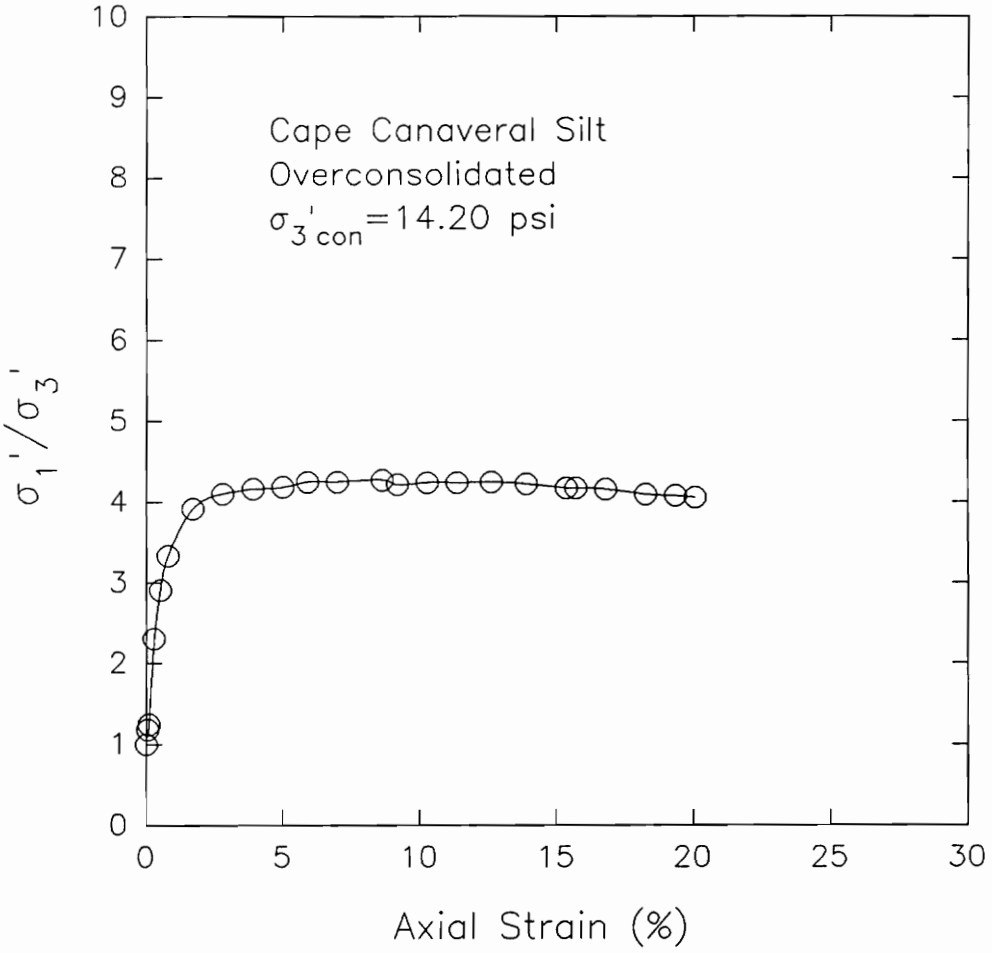

Figure 54 Principal Stress Ratio-Strain Relationship Measured For CU Triaxial Test On Overconsolidated Undisturbed Sample Of Cape Canaveral Silt

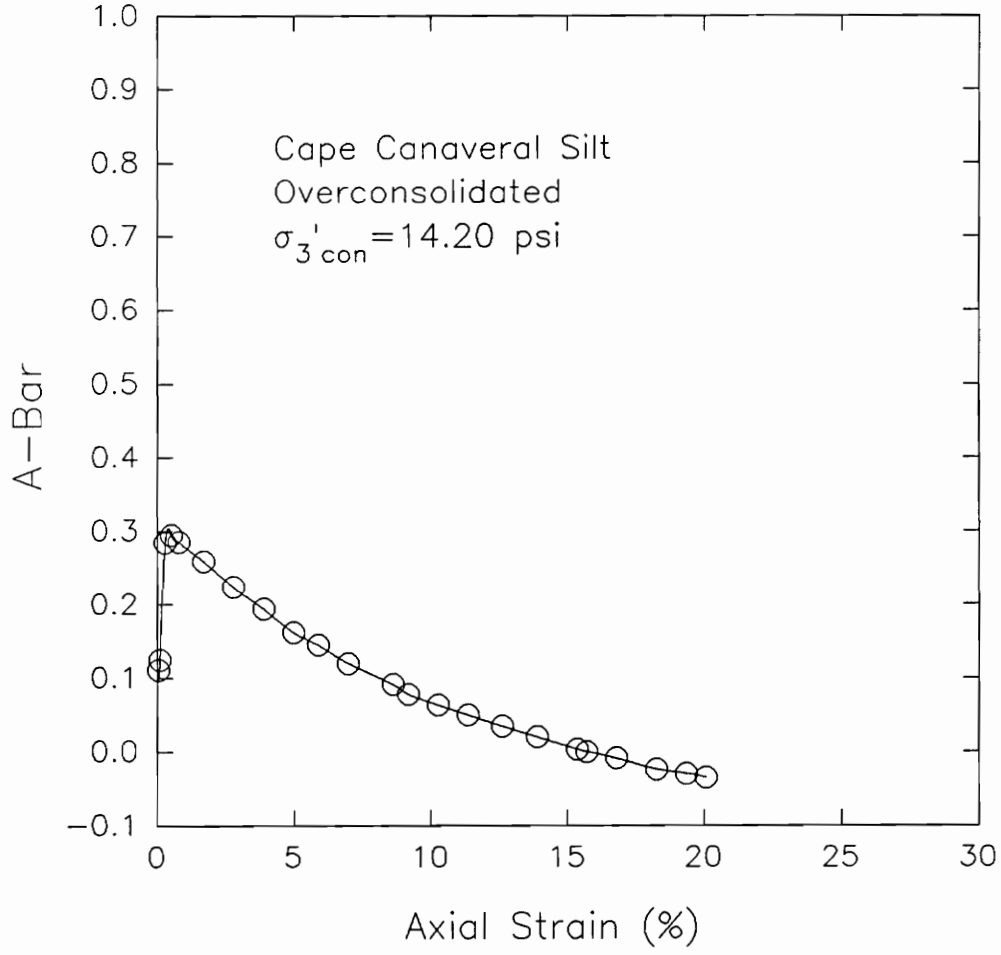

Figure 55 A-bar-Strain Relationship Measured For CU Triaxial Test On Overconsolidated Undisturbed Sample Of Cape Canaveral Silt

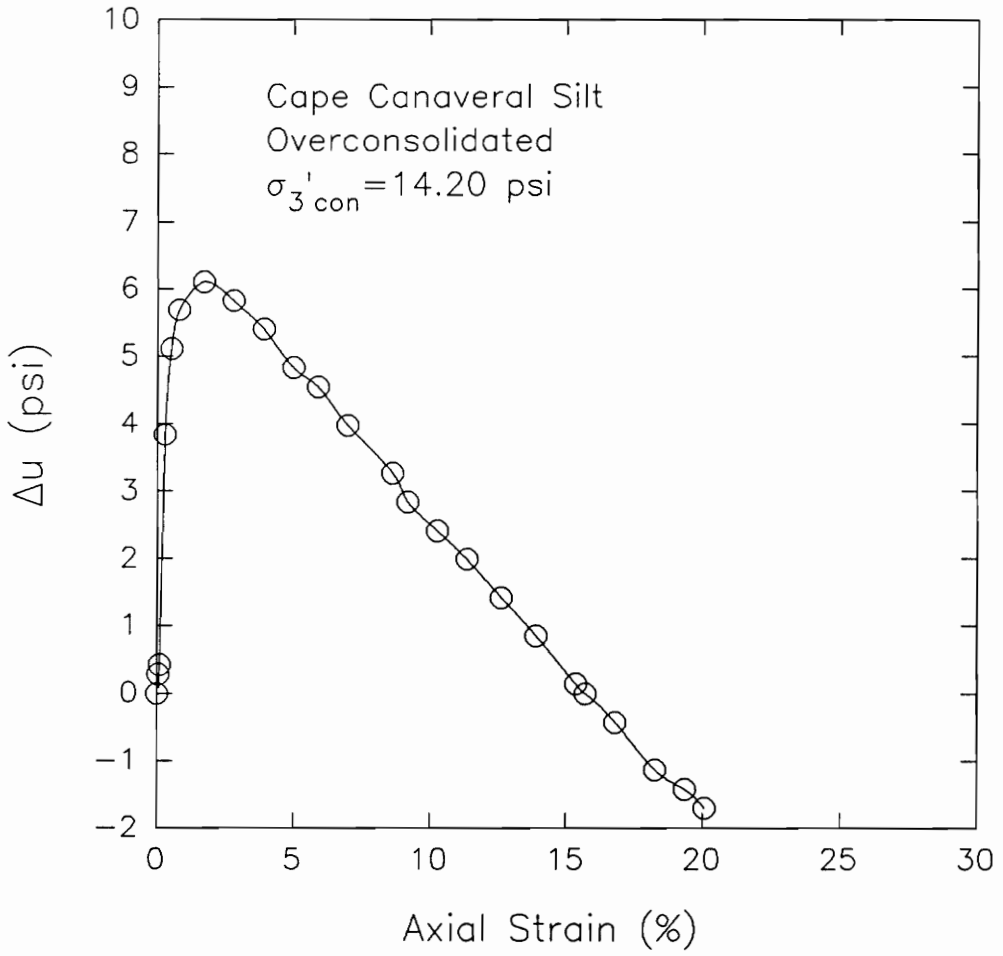

Figure 56 Pore Pressure-Strain Relationship Measured For CU Triaxial Test On Overconsolidated Undisturbed Sample Of Cape Canaveral Silt

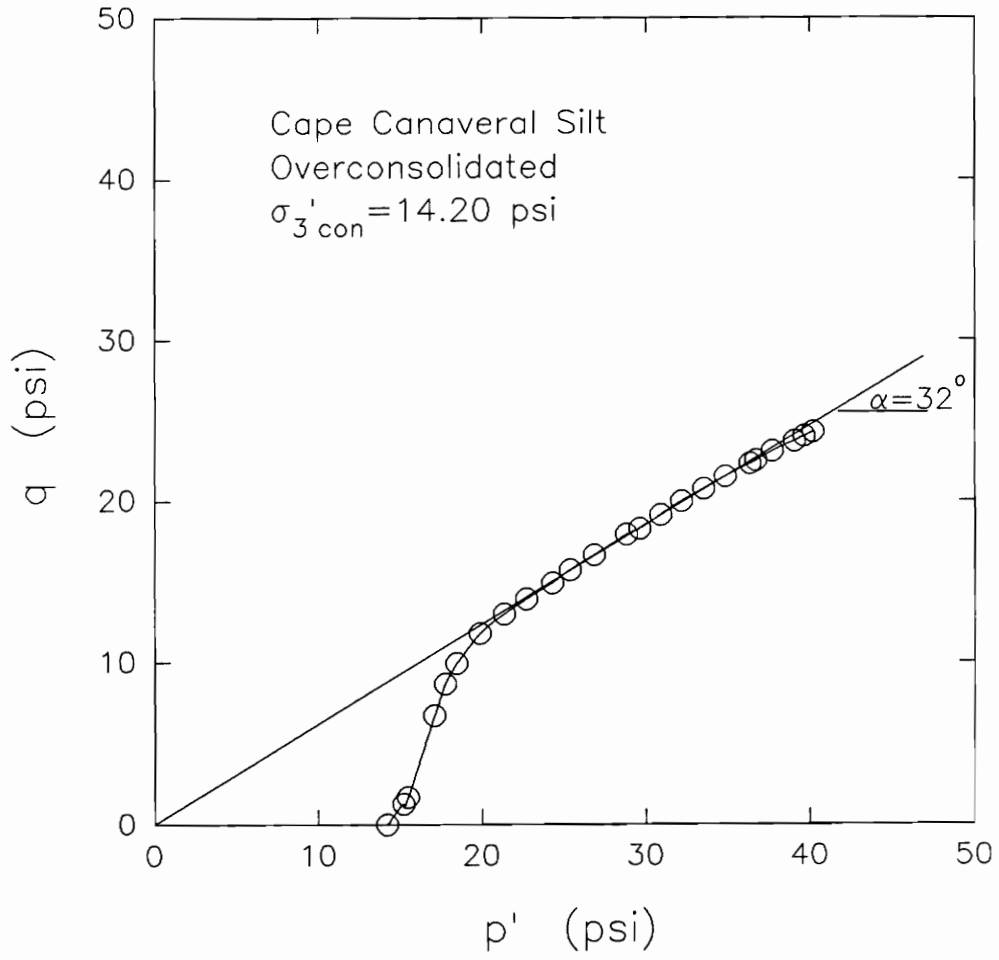

Figure 57 Effective Stress Path Measured For CU Triaxial Test On Overconsolidated Undisturbed Sample Of Cape Canaveral Silt

Effective Stress Interpretation of The CU Triaxial Test On Overconsolidated Undisturbed Sample of Cape Canaveral Silt

All failure criteria could be applied to the CU test results on the sample, except that based on maximum deviator stress.

Figure 58 shows the Mohr's circle based on maximum pore pressure as failure criterion. With the effective cohesion intercept constrained to zero, the envelope gives an effective stress friction angle equal to 35°.

For failure based on maximum principal stress ratio, the Mohr's circle for the sample is shown in Figure 59. An effective stress friction angle of 38° was computed using this failure criterion.

Figure 60 illustrates the Mohr's circle using 10% limiting strain as failure criterion. The value of ϕ' calculated is equal to 38°.

Figure 61 shows the Mohr's circle for failure based on 15% limiting strain. The effective stress friction angle computed is equal to 38°.

For A-bar=0, the Mohr's circle is shown in Figure 62. The value of ϕ' calculated using this failure criterion is equal to 38°.

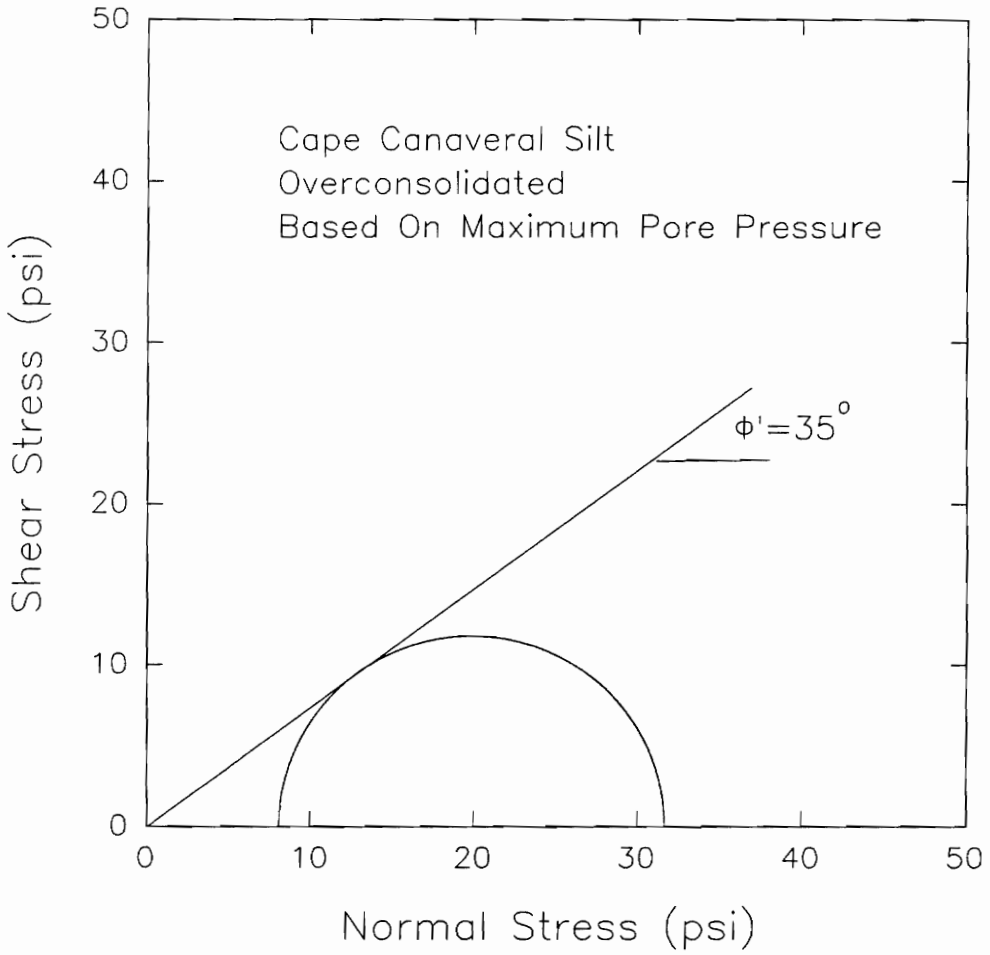

Figure 58 **Effective Stress Mohr's Circle Measured For CU Triaxial Test On Overconsolidated Undisturbed Sample of Cape Canaveral Silt For Failure Based On Maximum Pore Pressure**

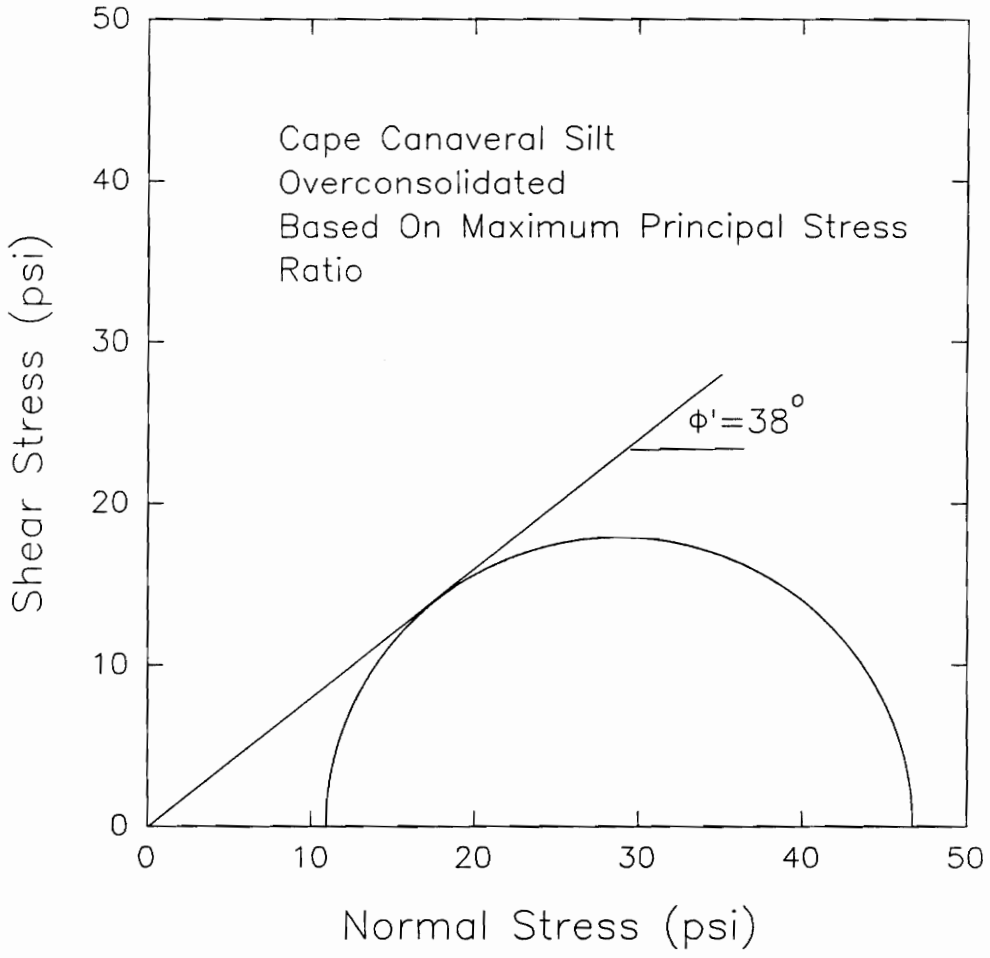

Figure 59 Effective Stress Mohr's Circle Measured For CU Triaxial Test On Overconsolidated Undisturbed Sample of Cape Canaveral Silt For Failure Based On Maximum Principal Stress Ratio

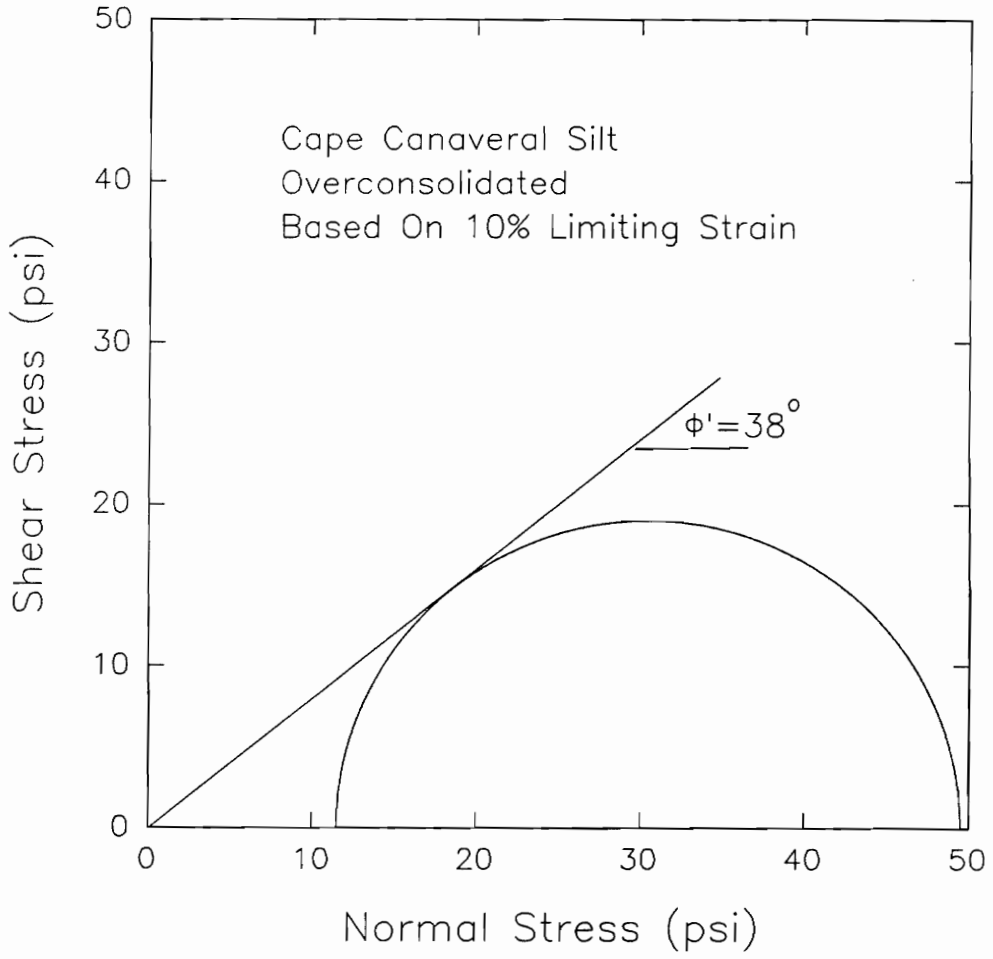

Figure 60 Effective Stress Mohr's Circle Measured For CU Triaxial Test On Overconsolidated Undisturbed Sample of Cape Canaveral Silt For Failure Based On 10% Limiting Strain

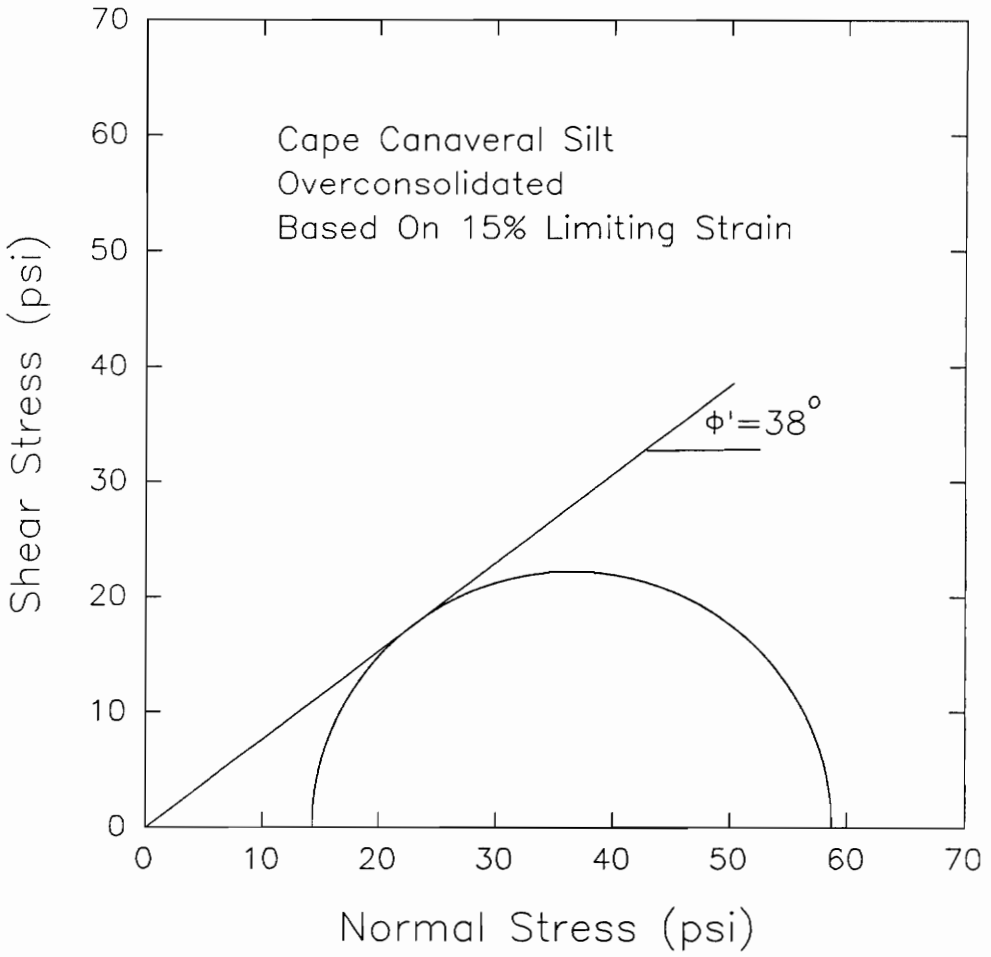

Figure 61 Effective Stress Mohr's Circle Measured For CU Triaxial Test On Overconsolidated Undisturbed Sample of Cape Canaveral Silt For Failure Based On 15% Limiting Strain

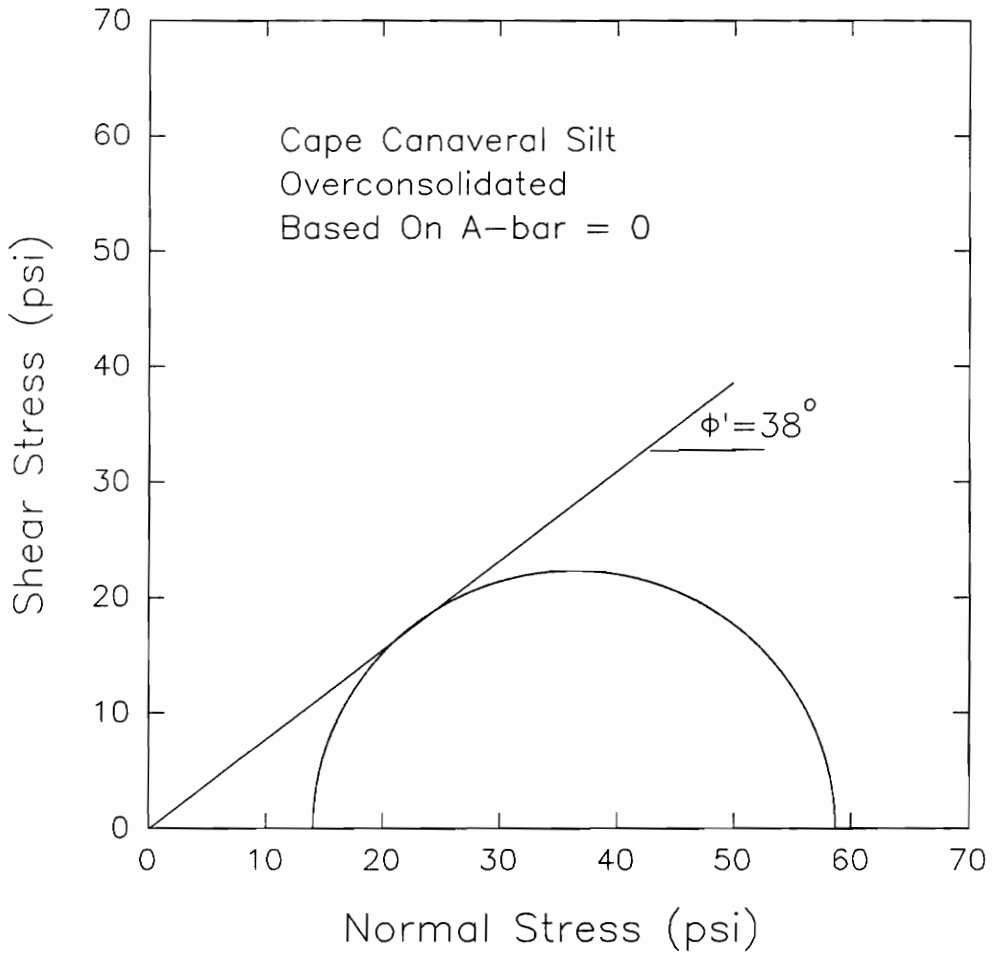

Figure 62 Effective Stress Mohr's Circle Measured For CU Triaxial Test On Overconsolidated Undisturbed Sample of Cape Canaveral Silt For Failure Based On A-bar = 0

A summary of the effective stress friction angles measured for different failure criteria are given in Table 12. Again, the maximum pore pressure failure criterion gave the lowest value of the effective stress friction angle. For the different failure criteria, except σ_{dmax} and u_{max}, the values of ϕ' are all equal to 38°. This can be well compared to ϕ' obtained from the effective stress path which gave a value equal to 38.5°.

Total Stress Interpretation of CU Test On Overconsolidated Undisturbed Samples of Cape Canaveral Silt

The undrained strength ratio of Cape Canaveral silt was calculated in the same manner as the previous silt samples.

Similar to the effective stress interpretation of the test results, maximum deviator stress as failure criterion could not be applied because the sample never exhibited a peak deviator stress throughout the test.

Figure 63 shows the undrained strength and effective consolidation pressure relationship for failure based on maximum pore pressure. The S_u/p calculated is equal to 0.83.

Table 12 Values of the Effective Stress Friction Angles Determined For Different Failure Criteria For CU Test On Cape Canaveral Silt

Failure Criteria	ϕ' (Degrees)	Average Strain To Failure (%)
u_{max}	35	1.7
Max($\sigma_1-\sigma_3$)	N/A	N/A
Max(σ_1'/σ_3')	38	8.5
10% Limiting Strain	38	10
15% limiting Strain	38	15
A-bar = 0	38	16

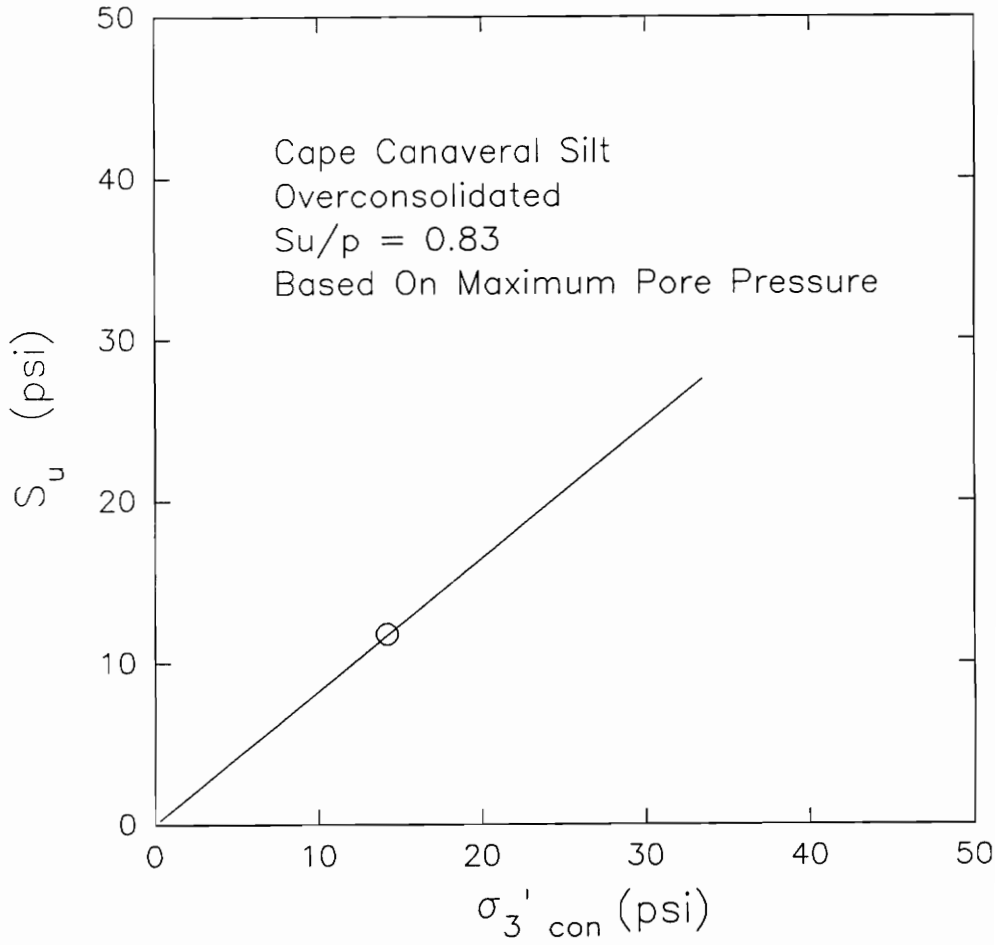

Figure 63 Undrained Shear Strength-Effective Consolidation Pressure Relationship Measured For CU Triaxial Test On Overconsolidated Undisturbed Sample of Cape Canaveral Silt For Based On Maximum Pore Pressure

Figure 64 illustrates the data for failure based on maximum principal stress ratio. The S_u/p measured is equal to 1.26.

For failure based on 10% and 15% limiting strains, the relationships between S_u and $\sigma_3'_{con}$, are shown in Figures 65 and 66 respectively. The S_u/p ratios calculated are 1.34 for 10% limiting strain, and 1.6 for 15% limiting strain.

Figure 67 illustrates the data for failure based on A-bar equal to zero. The S_u/p measured is equal to 1.60.

Table 13 summarizes the S_u/p ratios determined for the different failure criteria. Maximum pore pressure as failure criterion gave the lowest undrained strength ratio equal to 0.83. The other failure criteria, except σ_{dmax}, gave S_u/p ratios that range from 1.30 to 1.60.

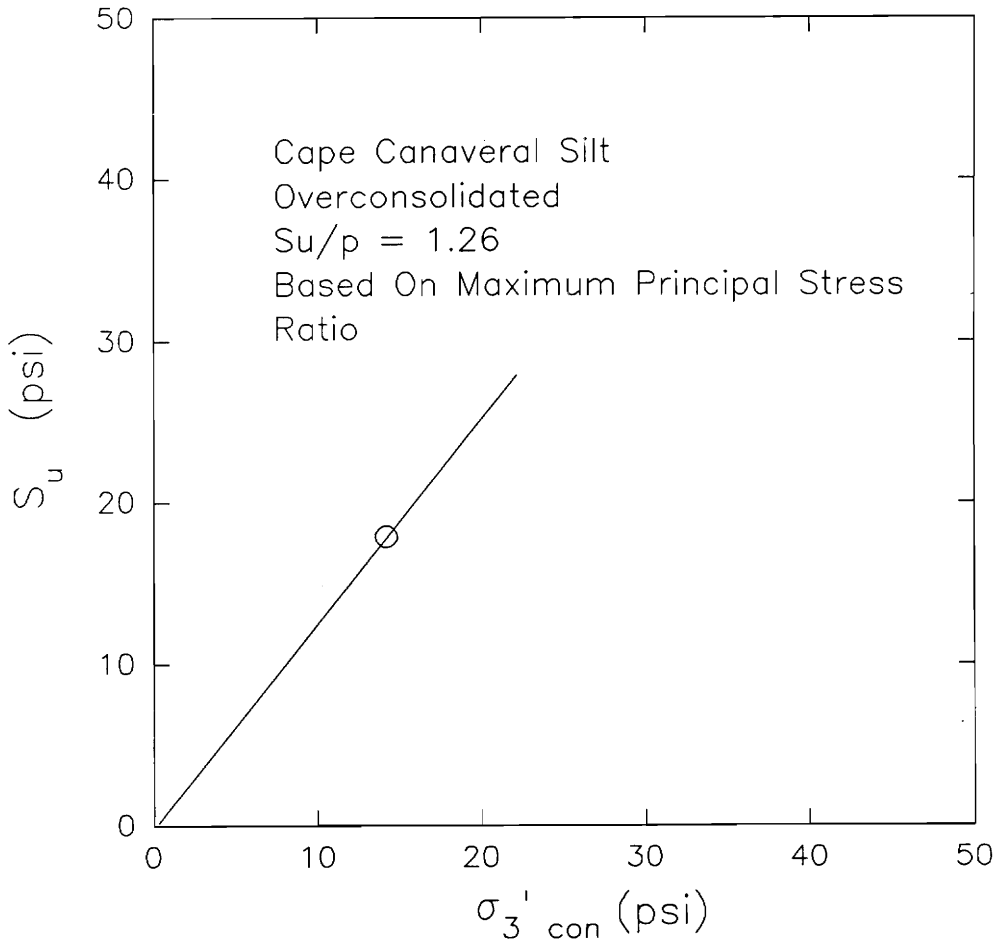

Figure 64 Undrained Shear Strength-Effective Consolidation Pressure Relationship Measured For CU Triaxial Test On Overconsolidated Undisturbed Sample of Cape Canaveral Silt For Based On Maximum Principal Stress Ratio

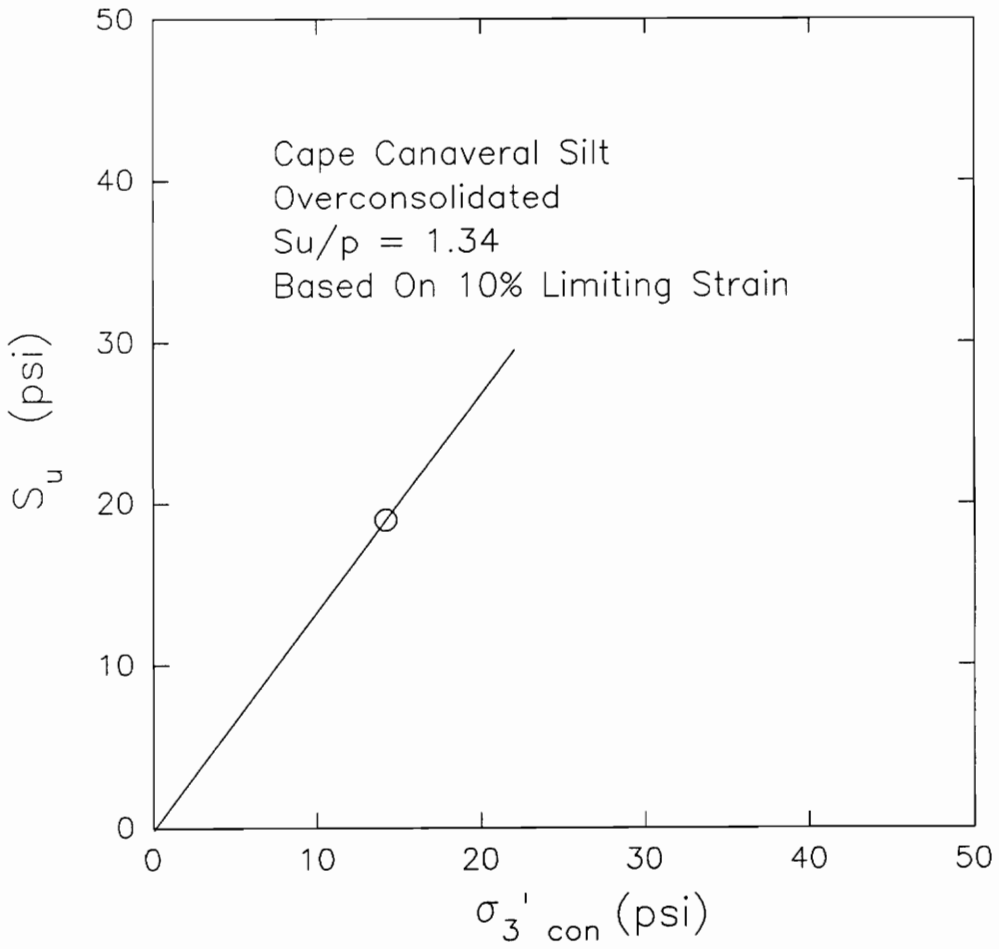

Figure 65 Undrained Shear Strength-Effective Consolidation Pressure Relationship Measured For CU Triaxial Test On Overconsolidated Undisturbed Sample of Cape Canaveral Silt For Based On 10% Limiting Strain

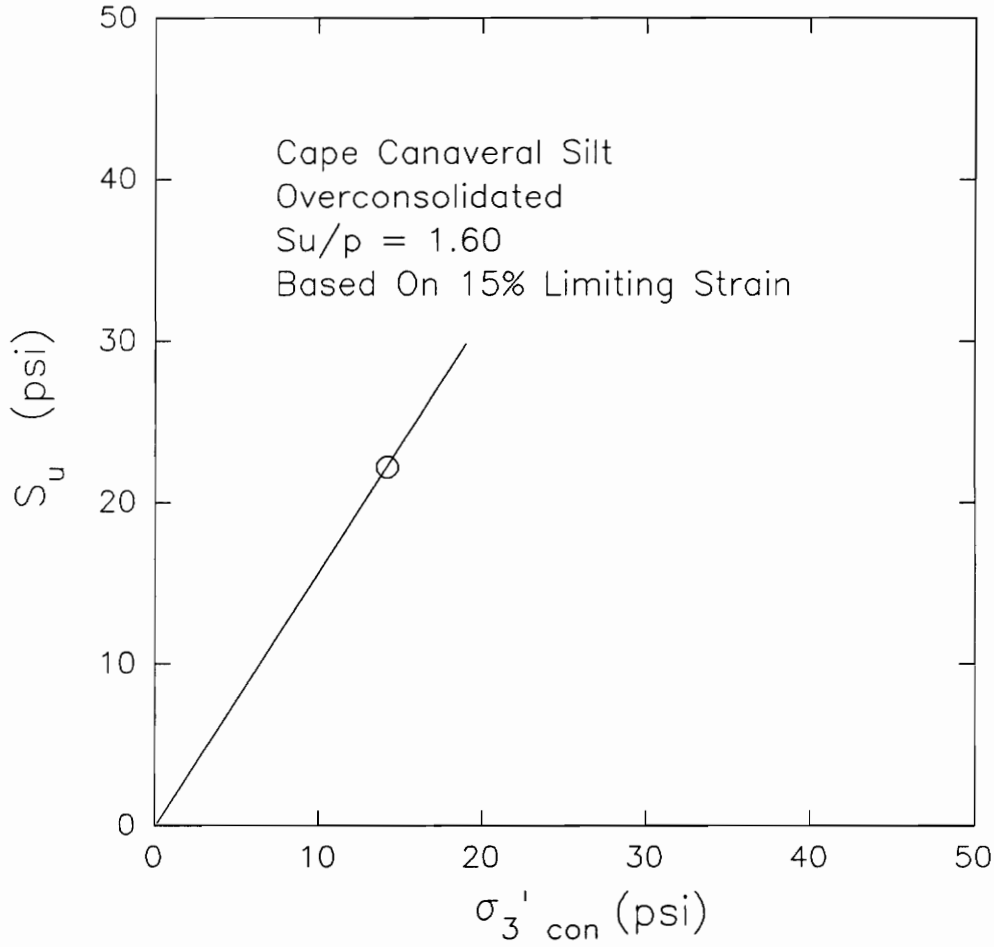

Figure 66 Undrained Shear Strength-Effective Consolidation Pressure Relationship Measured For CU Triaxial Test On Overconsolidated Undisturbed Sample of Cape Canaveral Silt For Based On 15% Limiting Strain

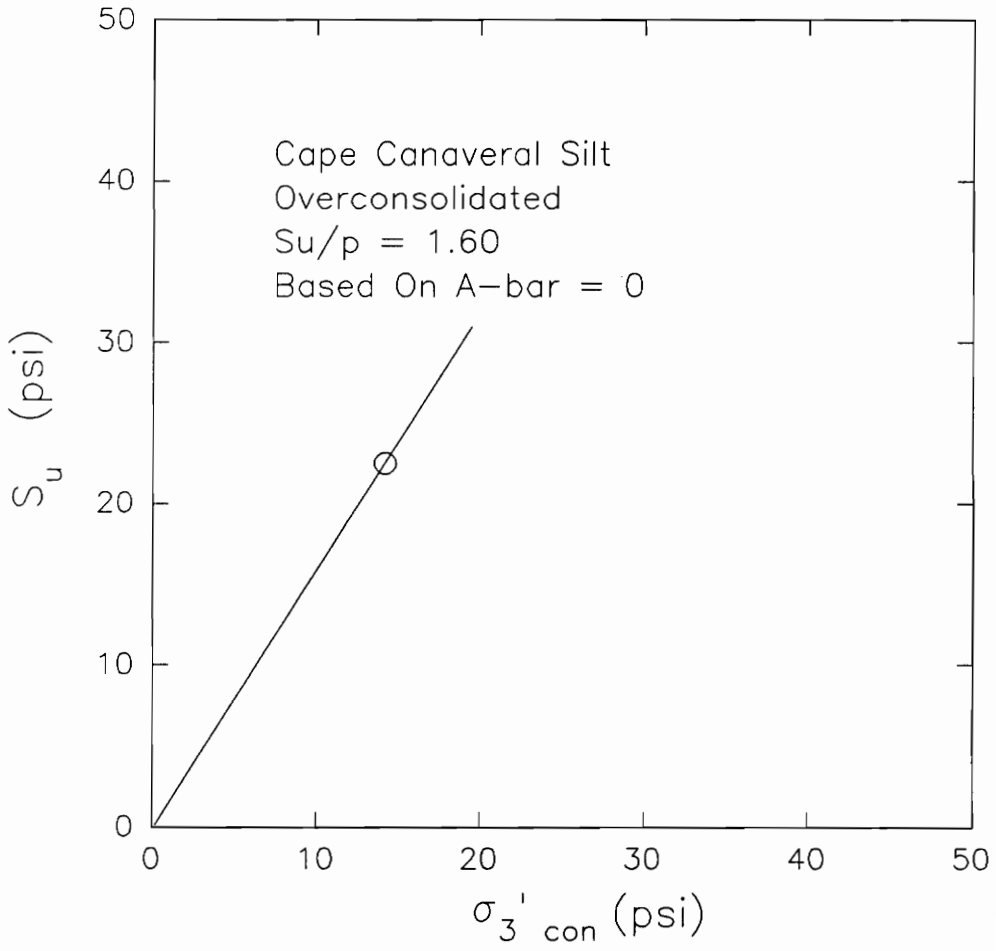

Figure 67 Undrained Shear Strength-Effective Consolidation Pressure Relationship Measured For CU Triaxial Test On Overconsolidated Undisturbed Sample of Cape Canaveral Silt For Based On A-bar = 0

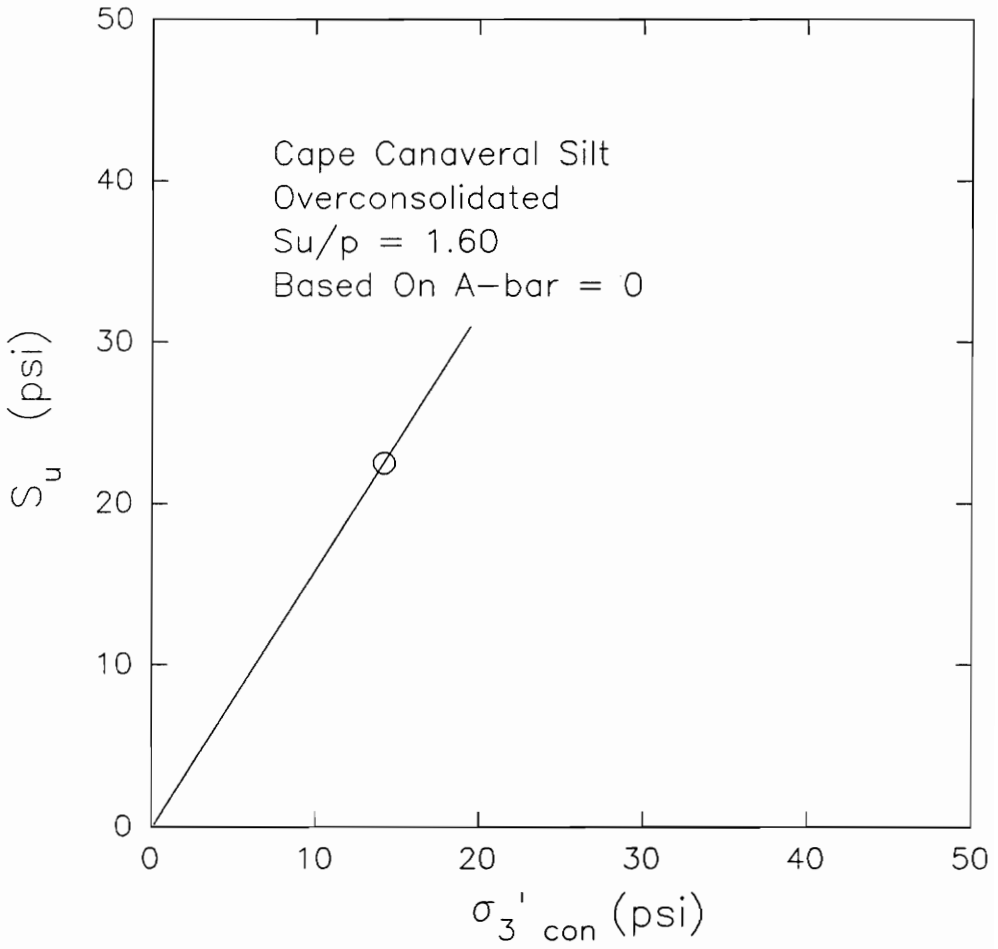

Figure 67 Undrained Shear Strength-Effective Consolidation Pressure Relationship Measured For CU Triaxial Test On Overconsolidated Undisturbed Sample of Cape Canaveral Silt For Based On A-bar = 0

Table 13 S_u/p Ratios Determined For Different Failure Criteria For CU Test On Cape Canaveral Silt

Failure Criteria	S_u/p	Average Strain To Failure (%)
u_{max}	0.83	1.7
Max($\sigma_1-\sigma_3$)	N/A	N/A
Max(σ_1'/σ_3')	1.26	8.5
10% Limiting Strain	1.34	10
15% limiting Strain	1.6	15
A-bar = 0	1.6	16

GRAY SILT AND BROWN SILT

West Williamson L.P.P. Pump Station

Duncan and Sehn (1987) tested silt specimens from a Pumping Station in West Williamson, West Virginia. The silts obtained from the site were named Gray silt and Brown silt. The study conducted by Duncan and Sehn was performed to determine the cause of settlements that occurred at the site which resulted in a culvert failure. The series of triaxial tests were conducted in two phases. The first phase was done in Ohio River Division Laboratory, and the second phase was conducted in the Virginia Tech Geotechnical Laboratory. The longitudinal cross-section of the site is shown in Figure 68.

Index Properties of Gray Silt And Brown Silt, West Williamson L.P.P. Pump Station

The plasticity, water content, and consistency of brown silt and gray silt are summarized in Table 14 and 15 for Phase I and Phase II, respectively. It can be seen that the properties of the silts obtained from both phases are similar. The plasticity charts for the specimens are shown in Figures 69 and 70. Most of the

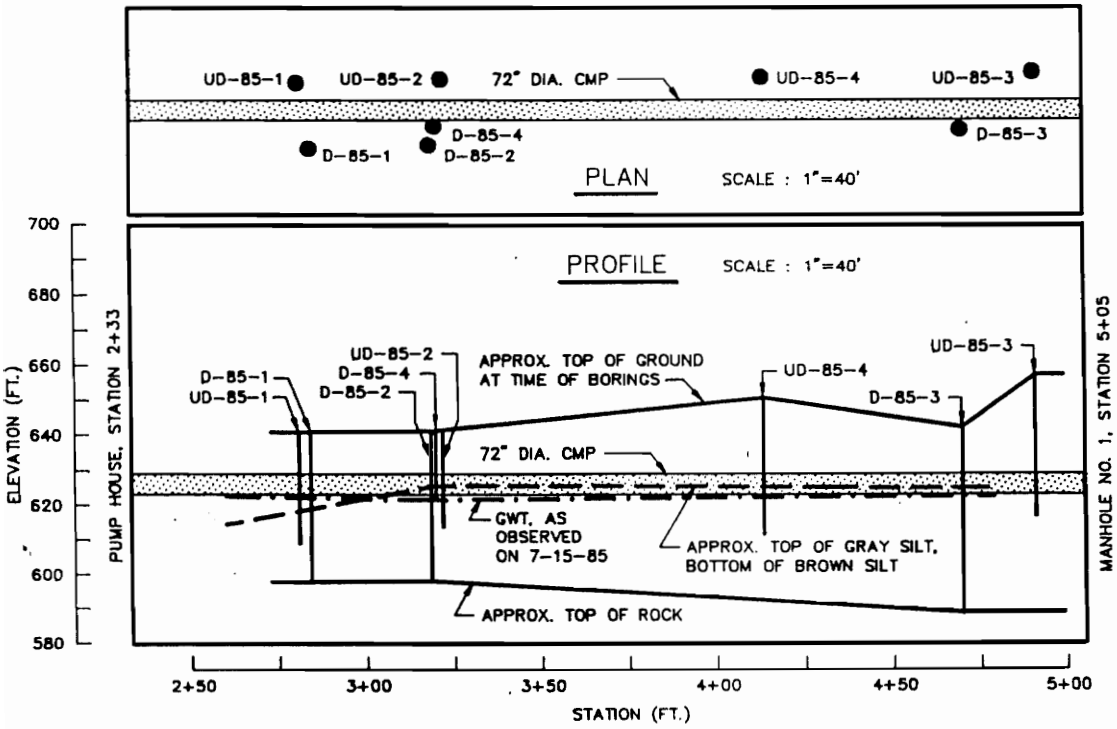

Figure 68 Longitudinal Cross-Section, West Williamson L.P.P. Pump Sation (Duncan and Sehn, 1985)

Table 14 Plasticity, Water Content, and Consistency of Brown and Gray Silt, West Williamson L.P.P. Pumping Plant ORD Laboratory (Duncan & Sehn, 1985)

Samples of Plastic Brown Silt

	Minimum	Maximum	Average
Liquid Limit (%)	37	44	35
Plastic Limit (%)	17	25	22
Plasticity Index (%)	10	19	13
Water Content (%)	18.2	37.5	28.3
Consistency - Very Soft to Medium			

Samples of Non-Plastic Brown Silt

	Minimum	Maximum	Average
Water Content (%)	18.2	27.4	23.9
All of these Samples were Non-Plastic			

Samples of Plastic Gray Silt

	Minimum	Maximum	Average
Liquid Limit (%)	26	42	32
Plastic Limit (%)	17	28	21
Plasticity Index (%)	7	14	11
Water Content (%)	23.8	43.2	29.1
Consistency - Very Soft to Medium			

Table 15 Plasticity, Water Content and Consistency of Brown and Gray Silt From West Williamson L.P.P.Pump Station Tested At VPI (Duncan & Sehn, 1985)

Sample	Unif. Class	Description	Gs	LL (%)	PL (%)	PI (%)	w_n (%)
UD-100-S1	ML	Brown Silt	2.76	46	29	17	32
UD-100-S2	ML	Brown Silt	2.71	42	27	15	33
UD-100-S3	CL-ML	Brown Sand-Silty Clay	2.68	25	20	5	26
UD-100-S4	ML	Gray Sandy Silt	2.66	21	18	3	21
UD-100-S5	ML	Gray Sandy Silt	2.71	21	18	3	20
UD-101-S1	ML	Brown Sandy Silt	2.70	28	24	4	25
UD-101-S2	ML	Gray Sandy Silt	2.70	21	18	3	21

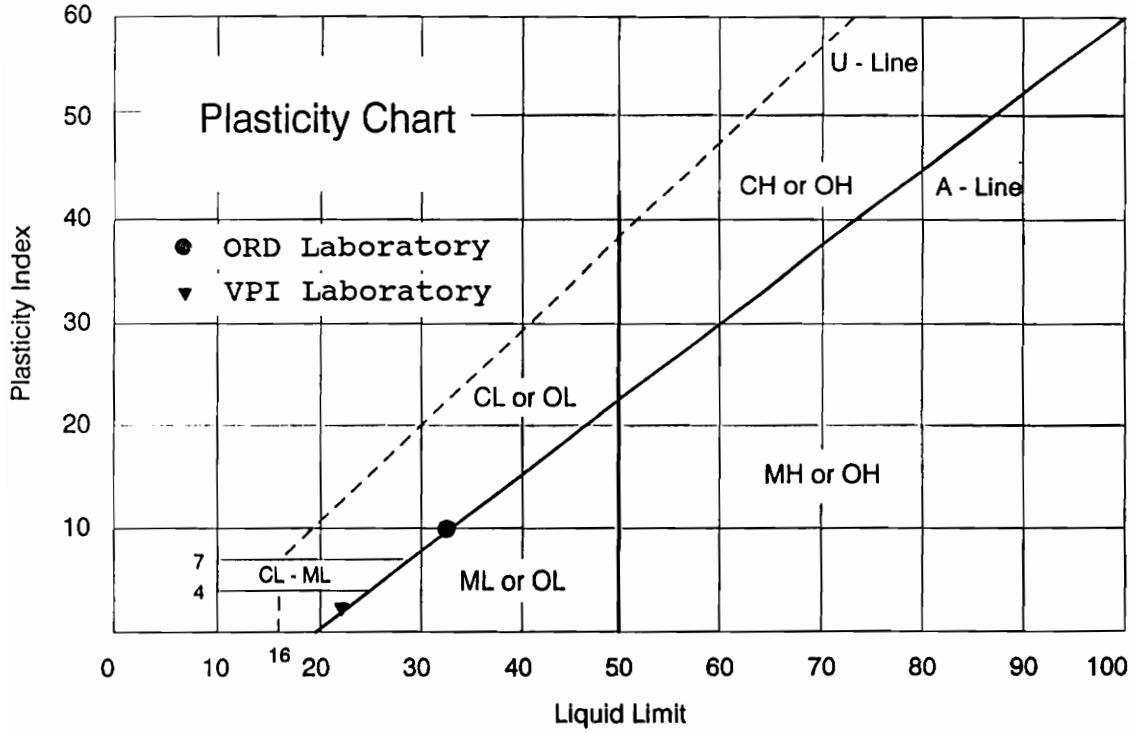

Figure 69 Plasticity Chart For Gray Silt

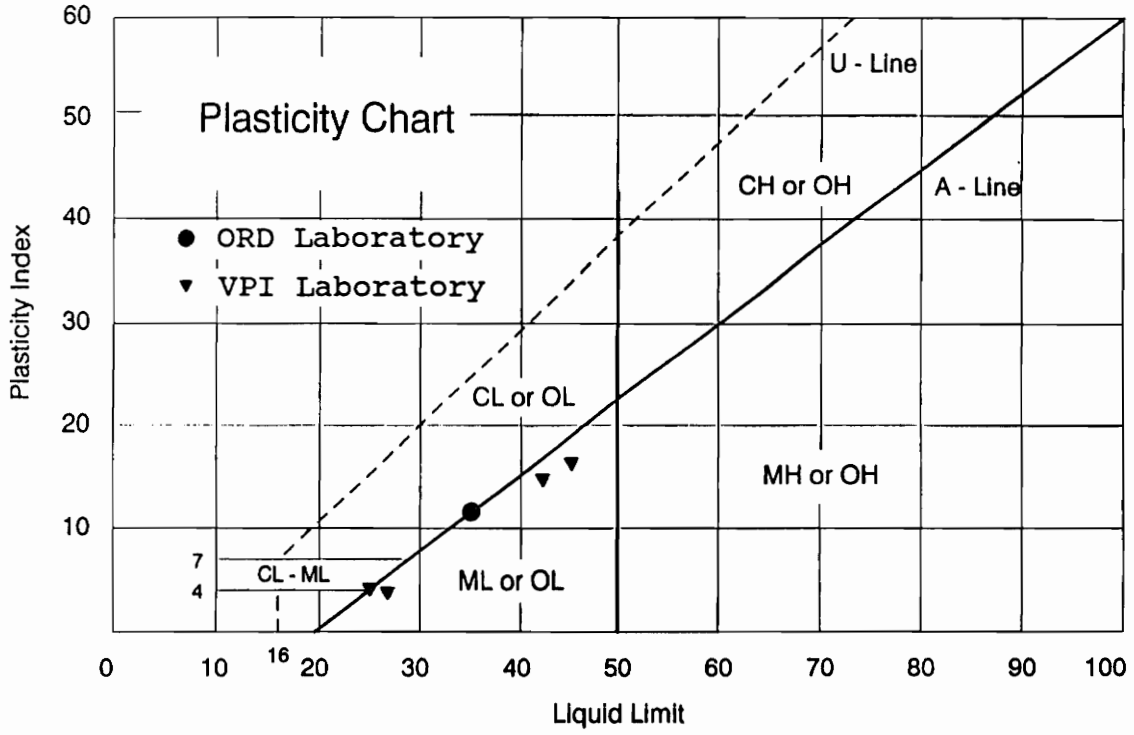

Figure 70 Plasticity Chart For Brown Silt

samples obtained from the site are classified as ML based on the Unified Classification System. The natural soil deposit comprises of dark brown sandy silt with low to medium plasticity underlain by low plasticity gray to dark gray silt. The average specific gravity for the gray silt is 2.67 and 2.70 for the brown silt. The gradation curves are shown in Figures 71, 72, and 73 and the grain size components are summarized in Table 16. Consolidation tests results for gray silt and brown silt are shown in Figures 74 and 75 respectively.

Consolidated Undrained Triaxial Tests On Overconsolidated Undisturbed Samples of Gray Silt

CU Triaxial tests were conducted on three samples of gray silt. The specimens were obtained from boring number UD-85-2 at depths of 23 feet to 25.2 feet. Table 17 gives the initial properties of gray silt for CU triaxial tests and the Atterberg limits are given in Table 18. Normal procedures of back pressure saturation were done on the samples to insure that they were fully saturated before shearing. Based on the consolidation curve shown in Figure 74, the past consolidation pressure for gray

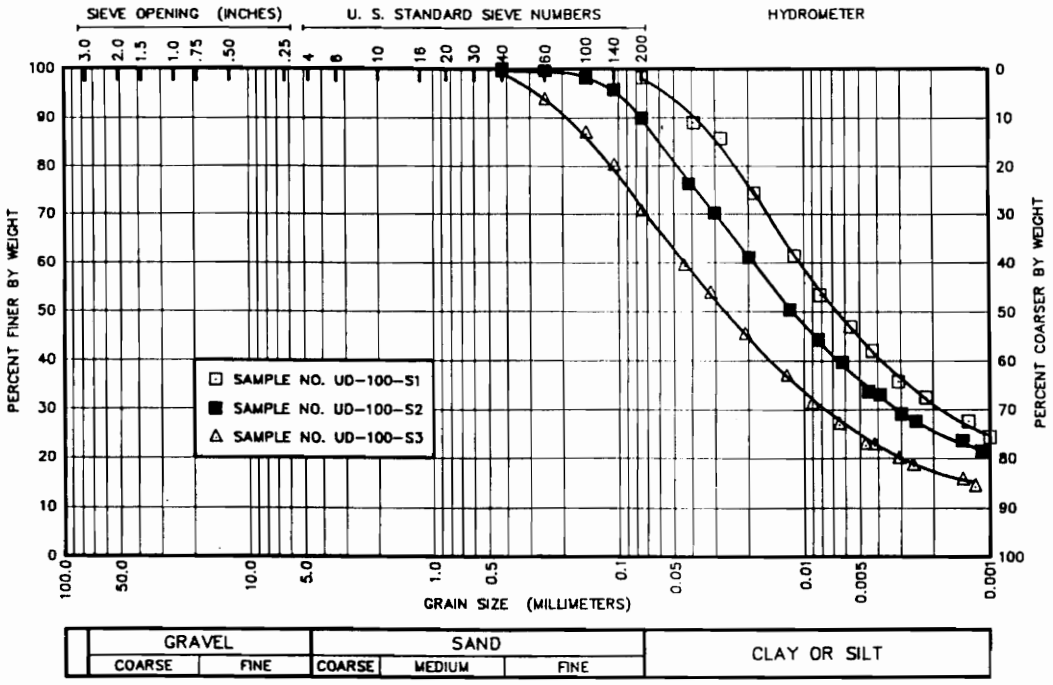

Figure 71 Grain Size Distribution Curves For Silts From West Williamson L.P.P. Pump Station Site (Duncan and Sehn, 1985)

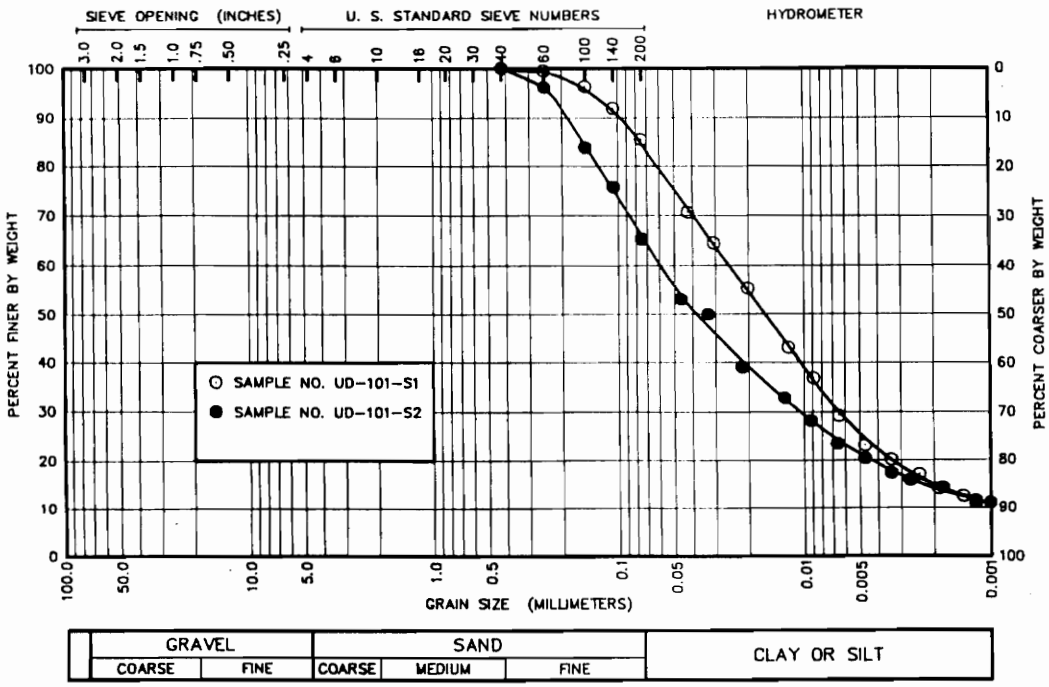

Figure 72 Grain Size Distribution Curves For Silts From West Williamson L.P.P. Pump Station Site (Duncan and Sehn, 1985)

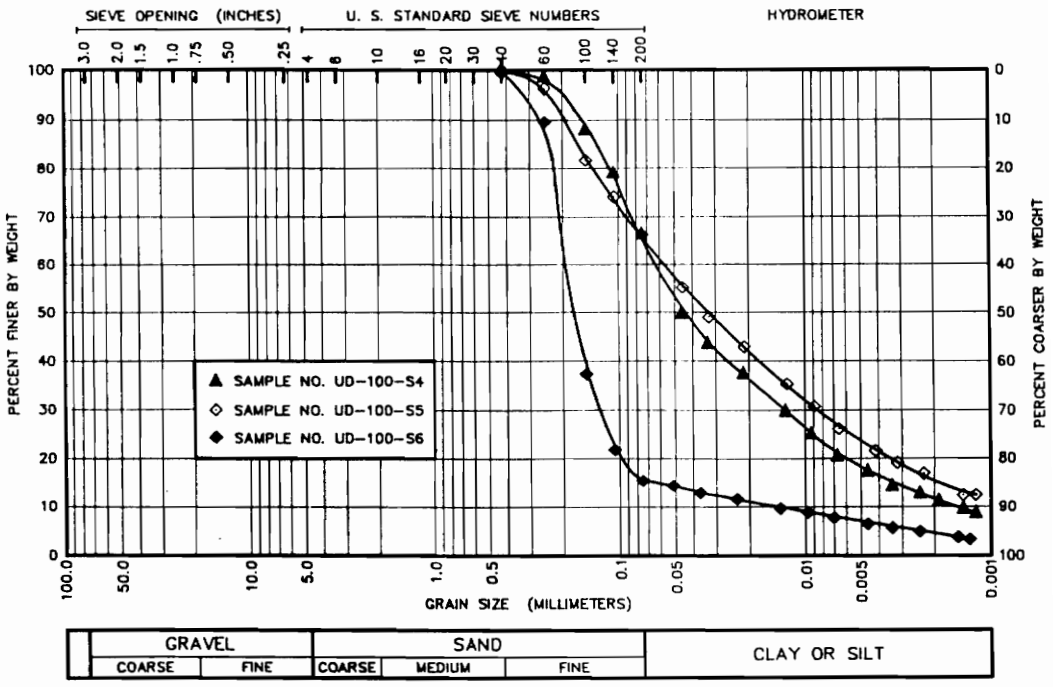

Figure 73 Grain Size Distribution Curves For Silts From West Williamson L.P.P. Pump Station Site (Duncan and Sehn, 1985)

Table 16 Components of Brown Silt and Gray Silt

Brown Silt Components

Sample	%Sand	%Silt	%Clay
UD-100-S1	2.4	67.6	30.0
UD-100-S2	12.0	63.0	25.0
UD-100-S3	30.0	54.0	16.0
UD-101-S1	17.0	68.0	15.0

Gray Silt Components

Sample	%Sand	%Silt	%Clay
UD-100-S4	37.0	52.0	11.0
UD-100-S5	35.0	50.0	15.0
UD-101-S2	35.0	51.0	14.0

Table 17 Properties of Undisturbed CU Triaxial Specimens of Gray Silt

Initial Properties

Sample Number	1	2	3
Water Content (%)	30.0	30.329	
Dry Density (pcf)	90.7	92.0	94.5
Degree of Sat.(%)	96.1	100.0	100.0
Void Ratio	0.837	0.812	0.763

Properties Before Shear

Sample Number	1	2	3
Water Content (%)	33.4	30.4	28.3
Dry Density (pcf)	91.3	94.0	95.9
Degree of Sat.(%)	100.0	100.0	100.0
Void Ratio	0.825	0.773	0.737

Dimensions

Sample Number	1	2	3
Initial Diameter(in.)	1.44	1.43	1.41
Initial Height(in)	2.927	2.935	2.964

Table 18 Atterberg Limits of CU Triaxial Specimens of Gray Silt

Liquid Limit	38 %
Plastic Limit	22 %
Plasticity Index	16 %
Specific Gravity, G_s	2.67

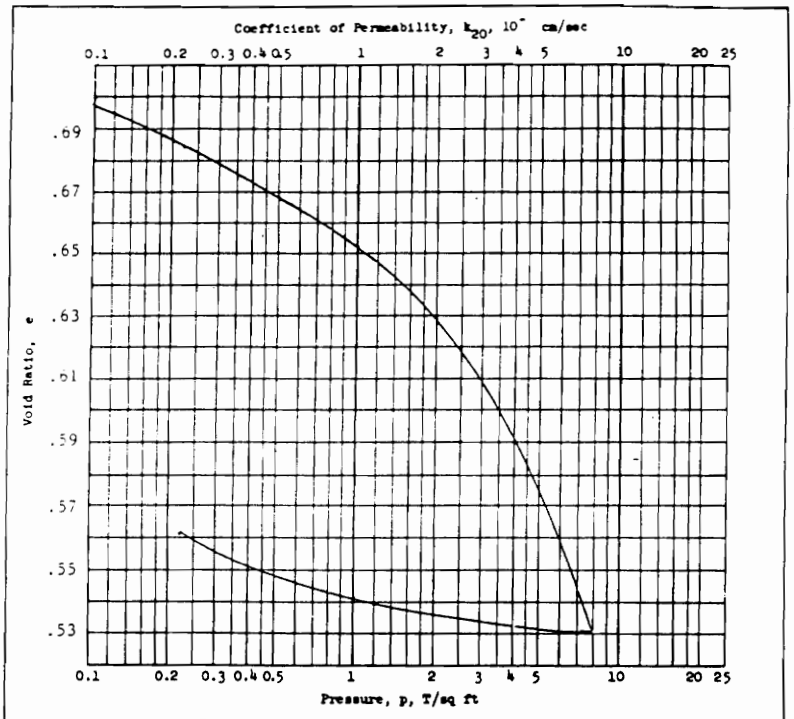

Type of Specimen Undisturbed		Before Test		After Test	
Diam 2.50 in.	Ht 0.814 in.	Water Content, w_o	25.5 %	w_f	21.9 %
Overburden Pressure, p_o 1.48 T/sq ft		Void Ratio, e_o	0.6972	e_f	0.5309
Preconsol. Pressure, p_c T/sq ft		Saturation, S_o	97.5 %	S_f	100+ %
Compression Index, C_c 0.22		Dry Density, γ_d	98.2 lb/ft^3		
Classification Sandy CLAY (CL)		k_{20} at e_o =	$\times 10^{-}$ cm/sec		
LL 38	G_s 2.67	Project West Williamson LPP Pump Station			
PL 22	D_{10}				
Remarks Test specimen was taken from a tube depth of 23.76 to 25.2 of a total depth of 23.0-25.2.		Area			
		Boring No. UD-85-2		Sample No. 7-B	
		Depth El 23.0-25.2		Date Dec 85	
		CONSOLIDATION TEST REPORT			

ENG FORM 1 MAY 63 2090 PREVIOUS EDITIONS ARE OBSOLETE.

Figure 74 Consolidation Test On Gray Silt, West Williamson L.P.P. Pump Station (Duncan and Sehn, 1985)

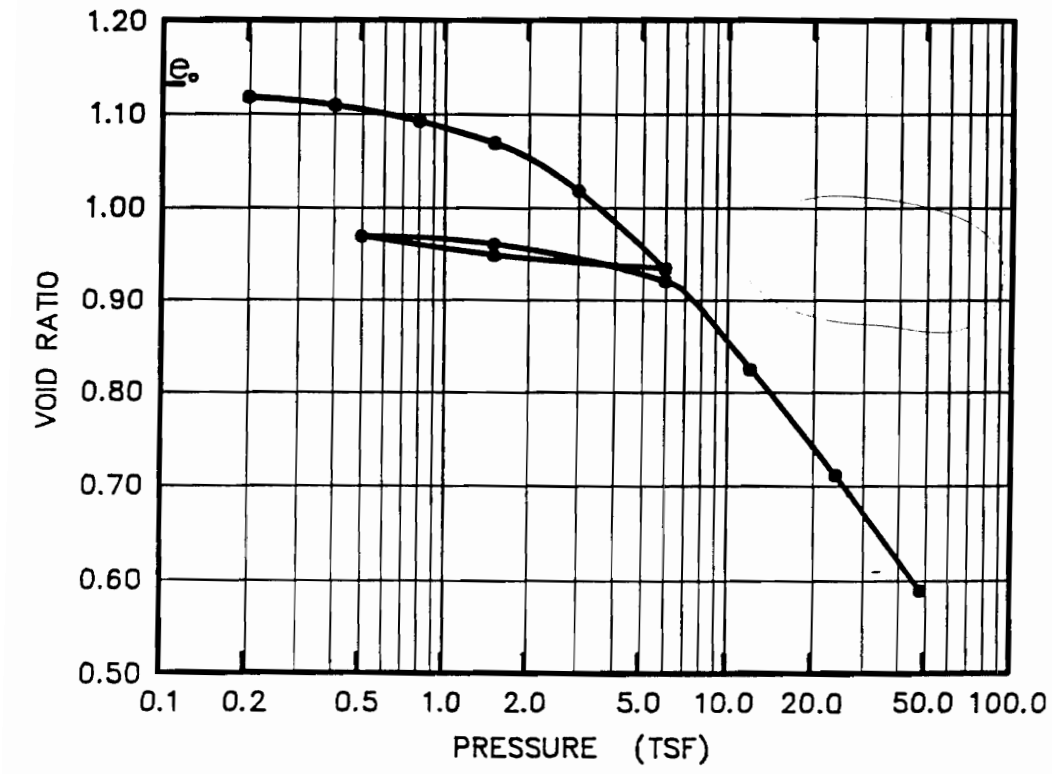

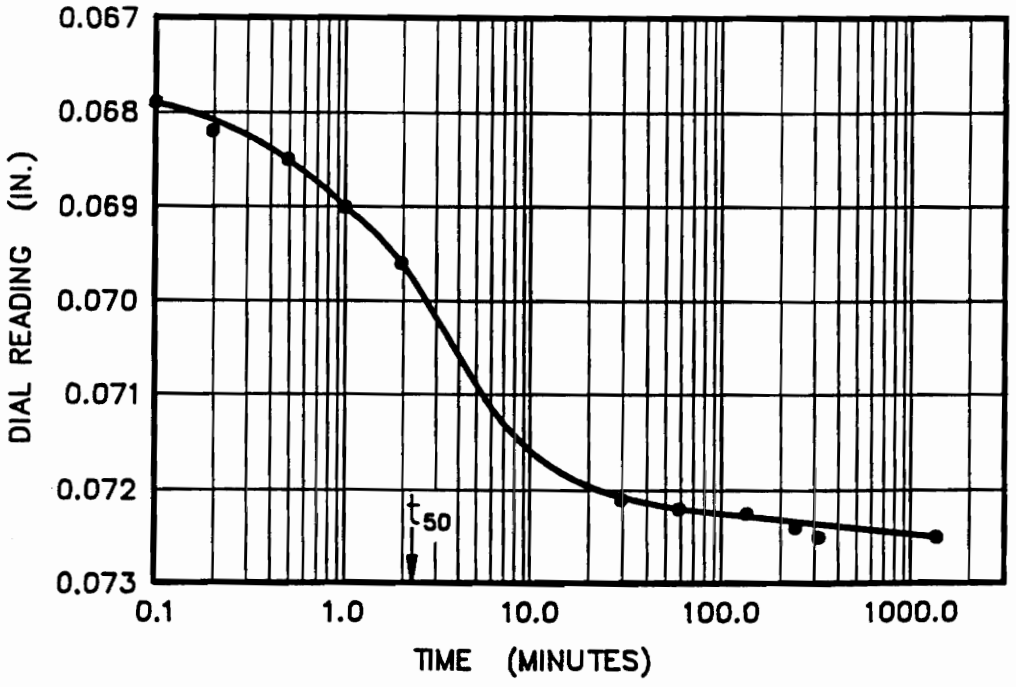

Figure 75 Consolidation Test Results For Brown Silt West Williamson L.P.P. Pumping Plant (Duncan and Sehn, 1985)

silt ranges from 35 psi to 42 psi determined by the Casagrande method. The effective consolidation pressure applied during the CU tests are 4.9 psi, 10.6 psi, and 21.0 psi. These effective consolidation pressures correspond to overconsolidation ratios of 7.8, 3.6, and 1.8.

Shown in Figure 76 are the stress-strain diagrams for the samples. All samples showed a peak in stress-strain curve. The sample consolidated to the highest $\sigma_3'_{con}$, 21 psi, had a very pronounced peak at strain of about 8%. The samples consolidated at 4.9 psi and 10.6 psi reached their maximum deviator stresses at strains of approximately 14% and 18%, respectively.

Shown in Figures 77 and 78 are the minor effective stress-strain and principal stress ratio-strain relationships. The average principal stress ratio calculated from the tests is 4.40 at an average strain of 5.5%.

Figures 79 and 80 illustrate the A-bar-strain and pore pressure-strain relationships. Pore pressures reached their maximum values at strains ranging from 0.5% to 5.2% in the order of increasing consolidation pressures. For the sample consolidated to the highest consolidation pressure, the pore pressure behaved differently compared with the other two samples. After

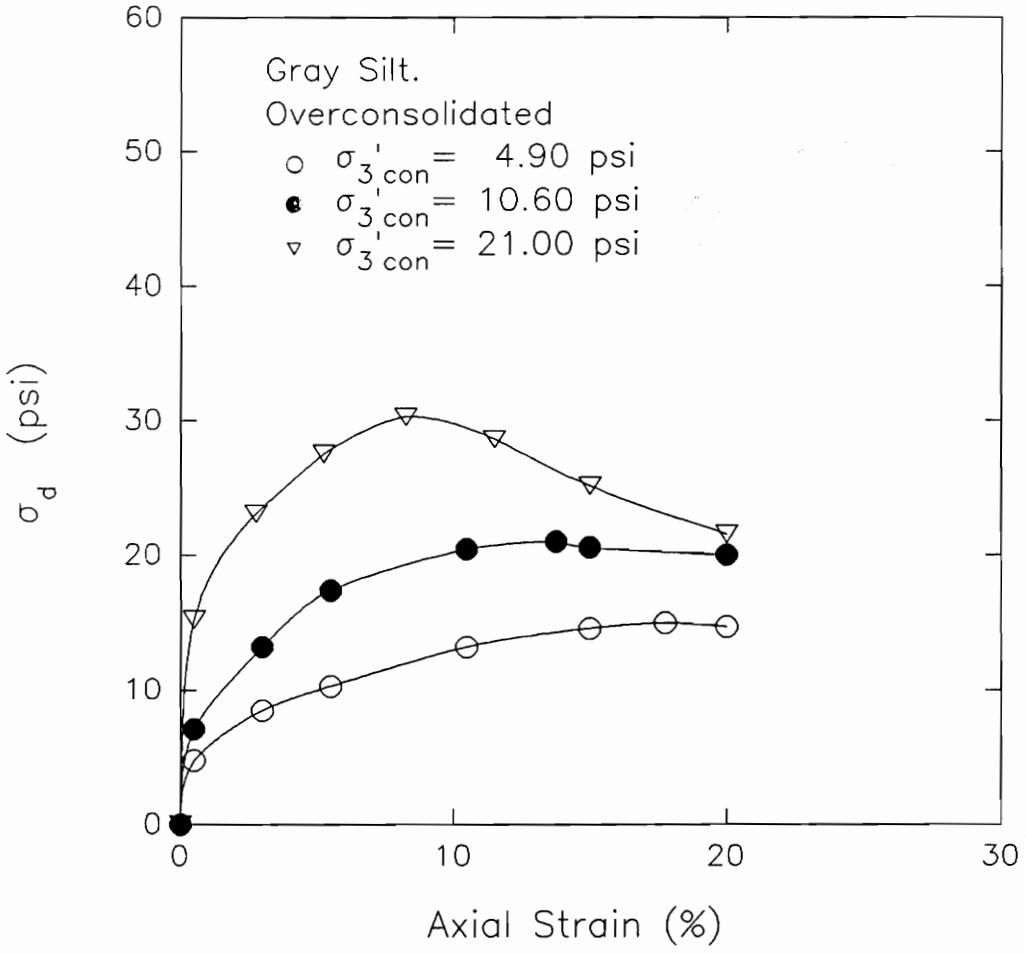

Figure 76 Deviator Stress-Strain Relationship Measured For CU Triaxial Tests On Overconsolidated Undisturbed Samples Of Gray Silt, West Williamson L.P.P. Pump Station (Ud-85-2-7B)

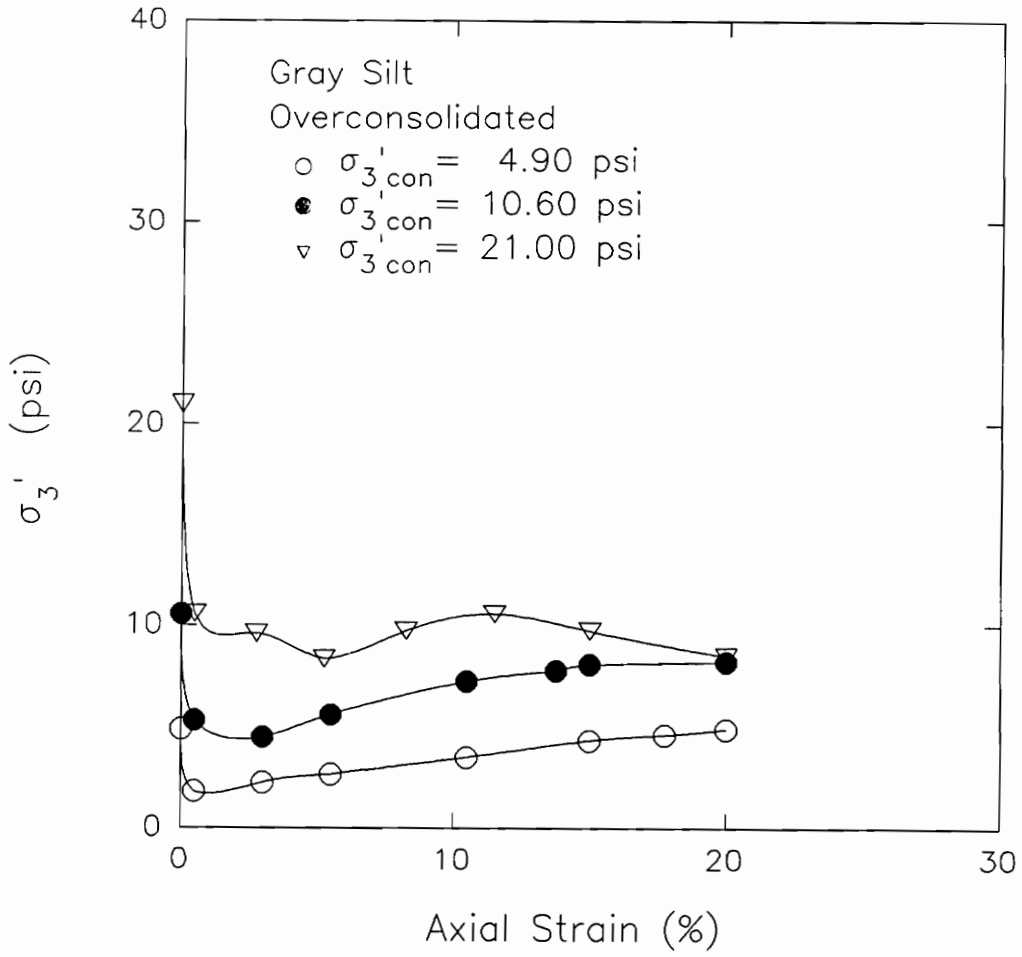

Figure 77 Minor Effective Stress-Strain Relationship Measured For CU Triaxial Tests On Overconsolidated Undisturbed Samples Of Gray Silt, West Williamson L.P.P. Pump Station (Ud-85-2-7B)

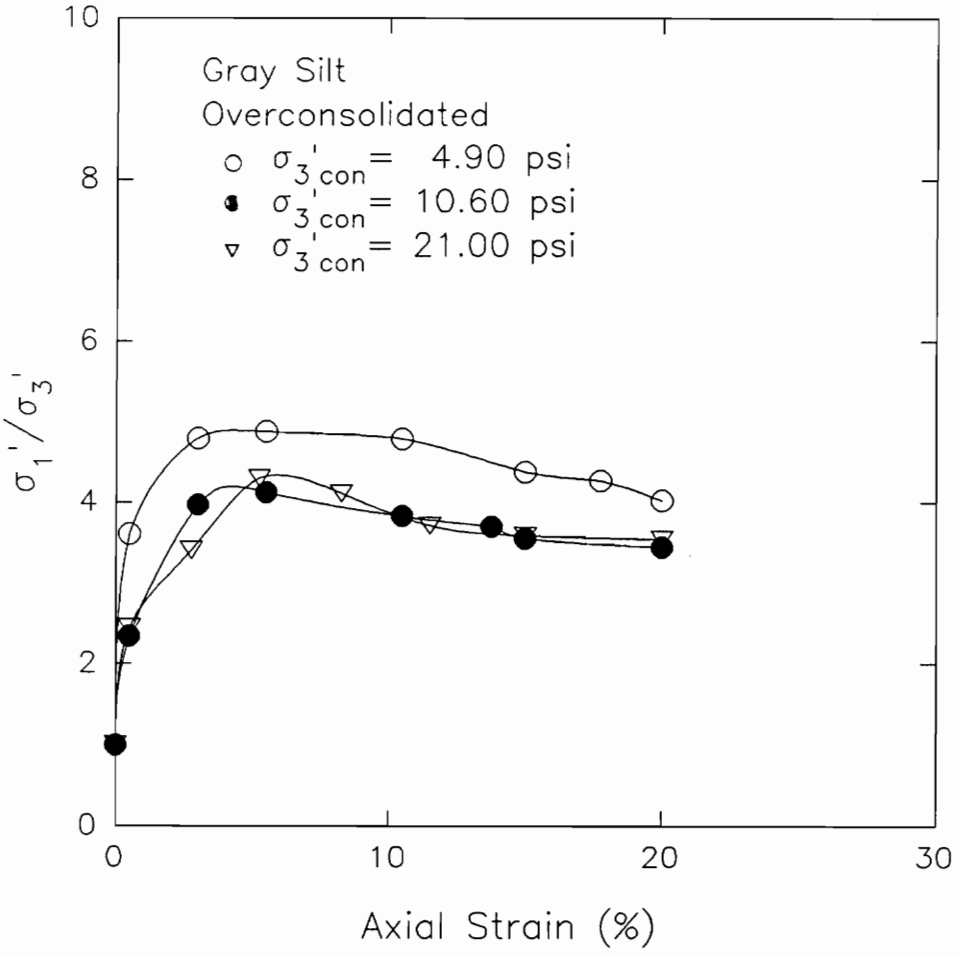

Figure 78 Principal Stress Ratio-Strain Relationship Measured For CU Triaxial Tests On Overconsolidated Undisturbed Samples Of Gray Silt, West Williamson L.P.P. Pump Station (Ud-85-2-7B)

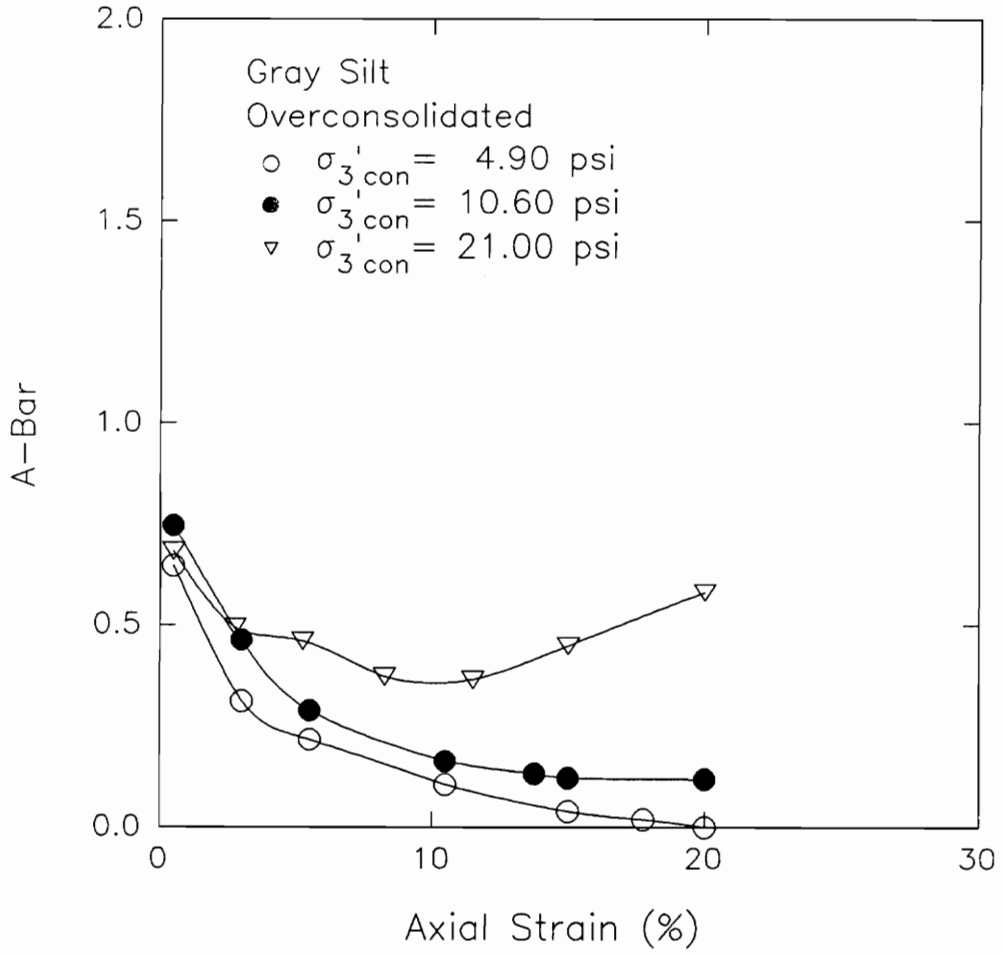

Figure 79 A-bar-Strain Relationship Measured For CU Triaxial Tests On Overconsolidated Undisturbed Samples Of Gray Silt, West Williamson L.P.P. Pump Station (Ud-85-2-7B)

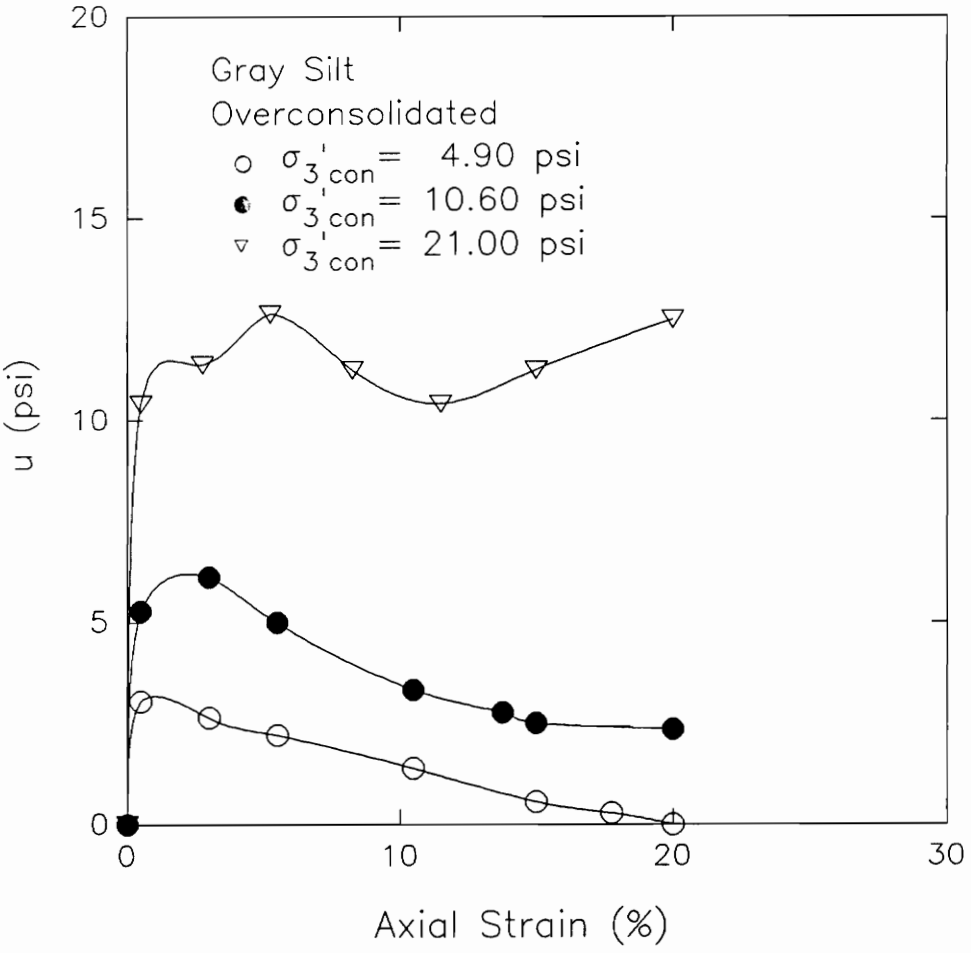

Figure 80 Pore Pressure-Strain Relationship Measured For CU Triaxial Tests On Overconsolidated Undisturbed Samples Of Gray Silt, West Williamson L.P.P. Pump Station (Ud-85-2-7B)

reaching a maximum value at 5% strain, it decreased to about 10.4 psi at 11.5% strain, and then increased to a value of about 12.5 psi at 20% strain. The behavior of the pore pressure for this sample is reflected in the effective stress paths shown in Figure 81. The point where the pore pressure started to increase, the effective stress path started to reverse direction where both p' and q decreased. Based on the stress paths measured for these tests, one unique K_f line cannot be fitted because of scatter in the results. Plotting the K_f line for each stress path would give values of α equal to 32°, 33°, and 34°. These give an average value of α equal to 33° which corresponds to an effective stress friction angle, ϕ', equal to 40°.

Effective Stress Interpretation of CU Tests On Overconsolidated Undisturbed Samples of Gray Silt

All failure criteria could be applied to the CU tests results on gray silt, except that based on A-bar = 0.

Shown in Figure 82 are the Mohr's circles for the samples based on maximum pore pressure. Constraining the effective cohesion intercept to zero, the effective

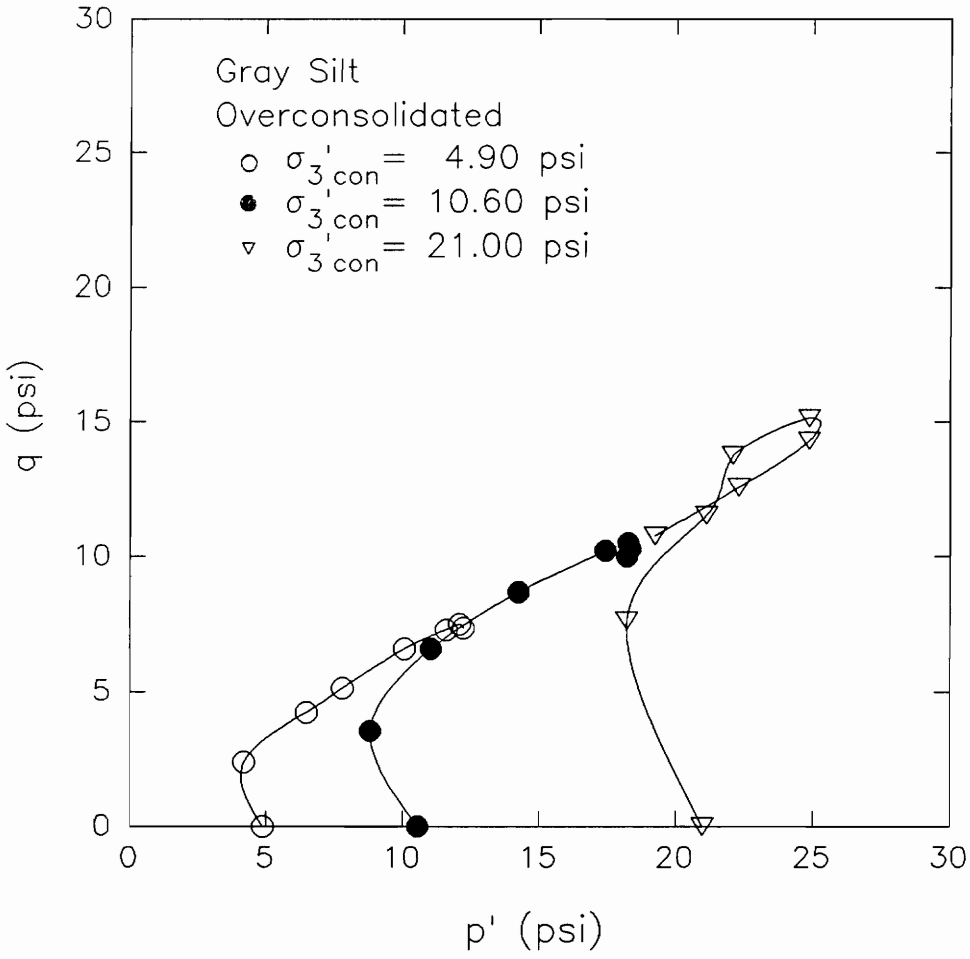

Figure 81 **Effective Stress Paths Measured For CU Triaxial Tests On Overconsolidated Undisturbed Samples Of Gray Silt, West Williamson L.P.P. Pump Station (Ud-85-2-7B)**

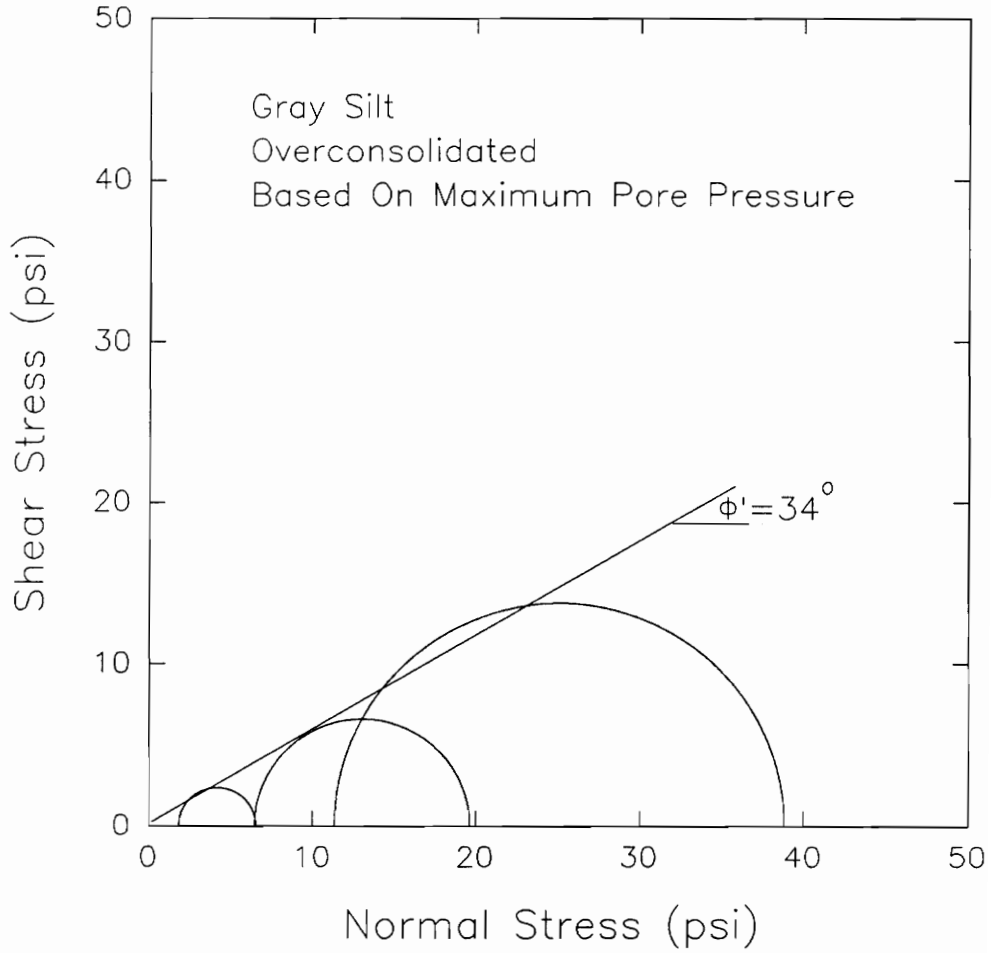

Figure 82 Effective Stress Mohr's Circles Measured For CU Triaxial Tests On Overconsolidated Undisturbed Gray Silt For Failure Based On Maximum Pore Pressure (UD-101-S1-A)

stress friction angle measured is 34°. This represents the best estimate due to scatter in the results.

The Mohr's circles based on maximum deviator stress are plotted in Figure 83. The effective stress friction angle computed is 38°.

Figure 84 shows the Mohr's circles based on maximum principal stress ratio. The effective stress friction angle computed is equal to 38°. This also represents the best estimate due to some scatter in the results.

Shown in Figures 85 and 86 are the Mohr's circles using 10% and 15% limiting strains as failure criteria. Constraining the effective cohesion intercept to zero, the envelopes give values of effective friction angle equal to 37° for both 10% and 15% limiting strains.

Only one sample is represented for the envelope drawn based on A-bar = 0. The Mohr's circle for this failure criterion is shown in Figure 87. The computed effective stress friction angle is 37°.

The values of the effective stress friction angles based on different failure criteria are summarized in Table 19. The lowest effective stress friction angle was derived from the maximum pore pressure as a failure criterion and the other failure criteria gave values that range from 37° to 38°.

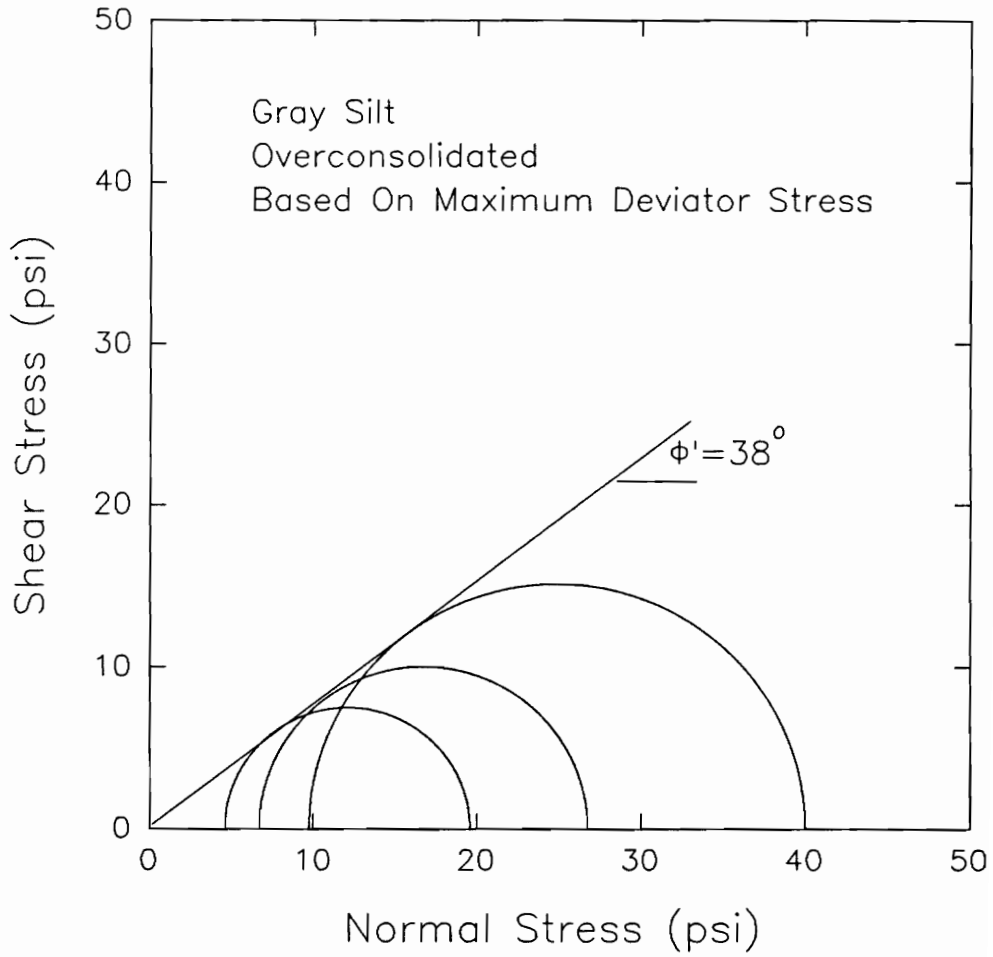

Figure 83 Effective Stress Mohr's Circles Measured For CU Triaxial Tests On Overconsolidated Undisturbed Gray Silt For Failure Based On Maximum Deviator Stress (UD-101-S1-A)

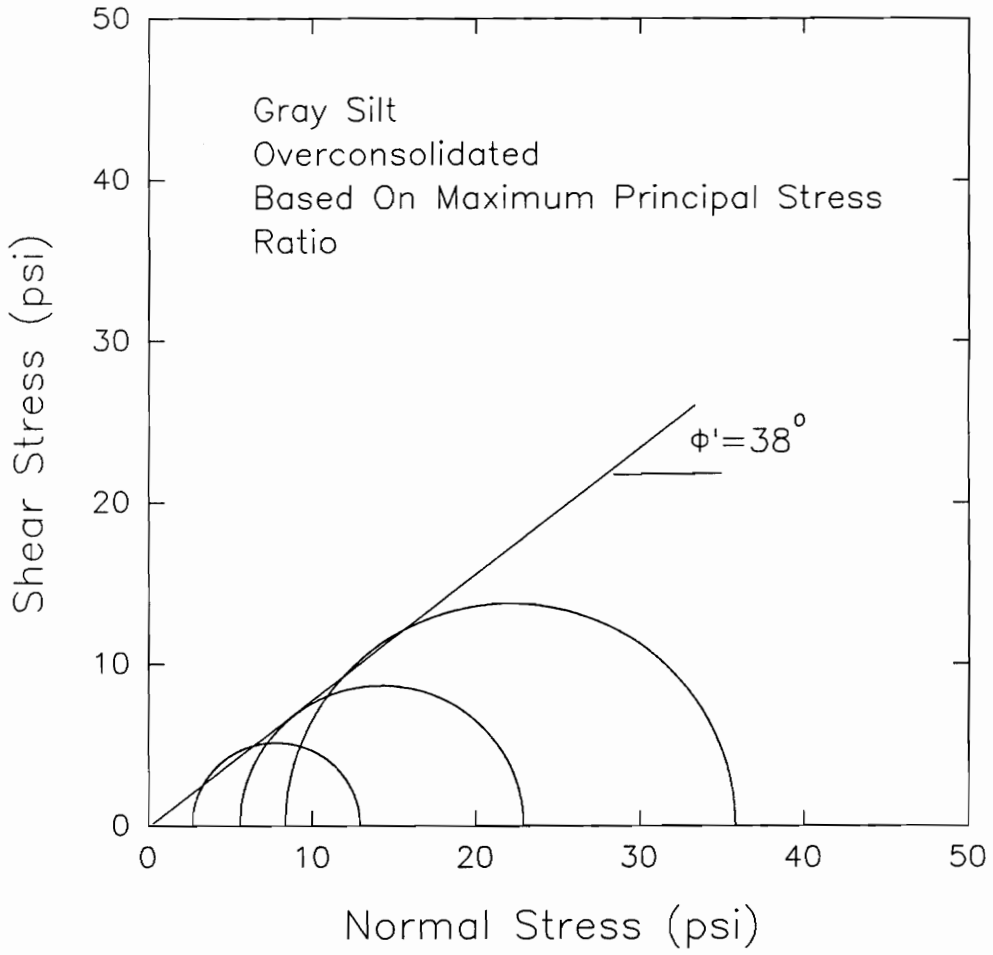

Figure 84 Effective Stress Mohr's Circles Measured For CU Triaxial Tests On Overconsolidated Undisturbed Gray Silt For Failure Based On Maximum Principal Stress Ratio (UD-101-S1-A)

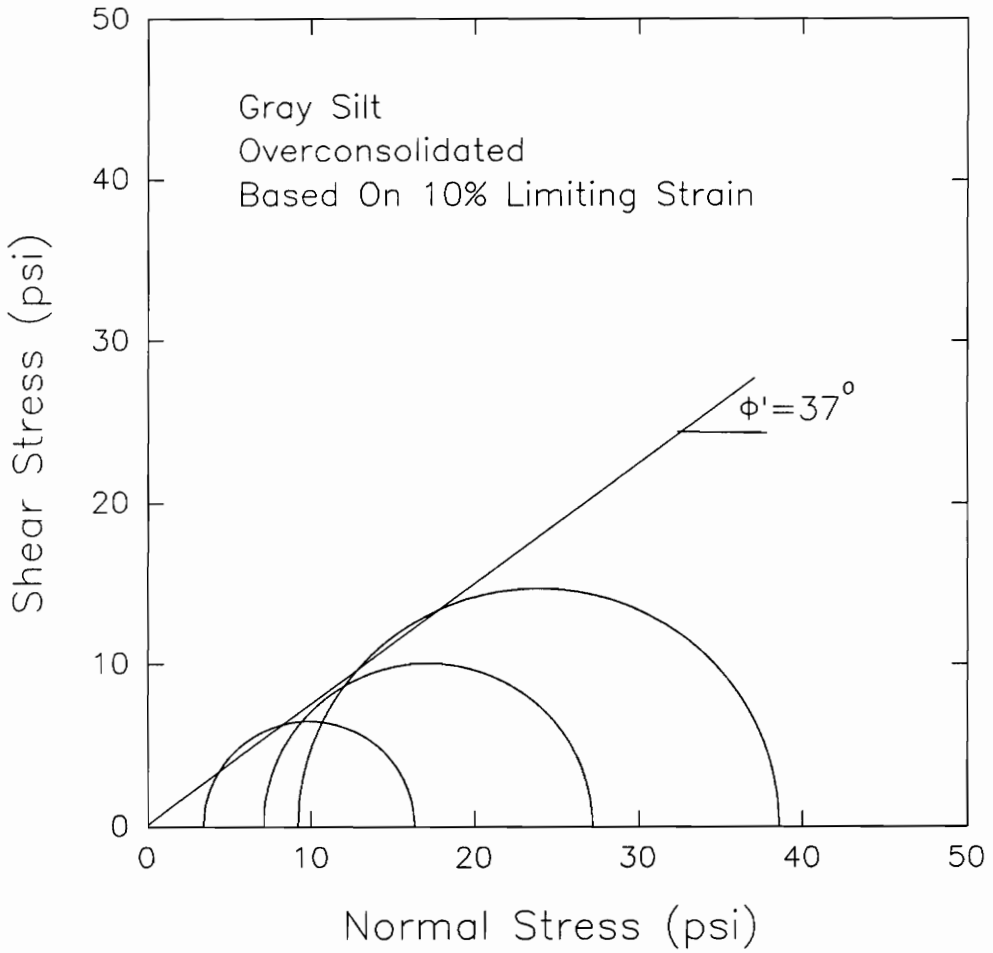

Figure 85 Effective Stress Mohr's Circles Measured For CU Triaxial Tests On Overconsolidated Undisturbed Gray Silt For Failure Based On 10% Limiting Strain (UD-101-S1-A)

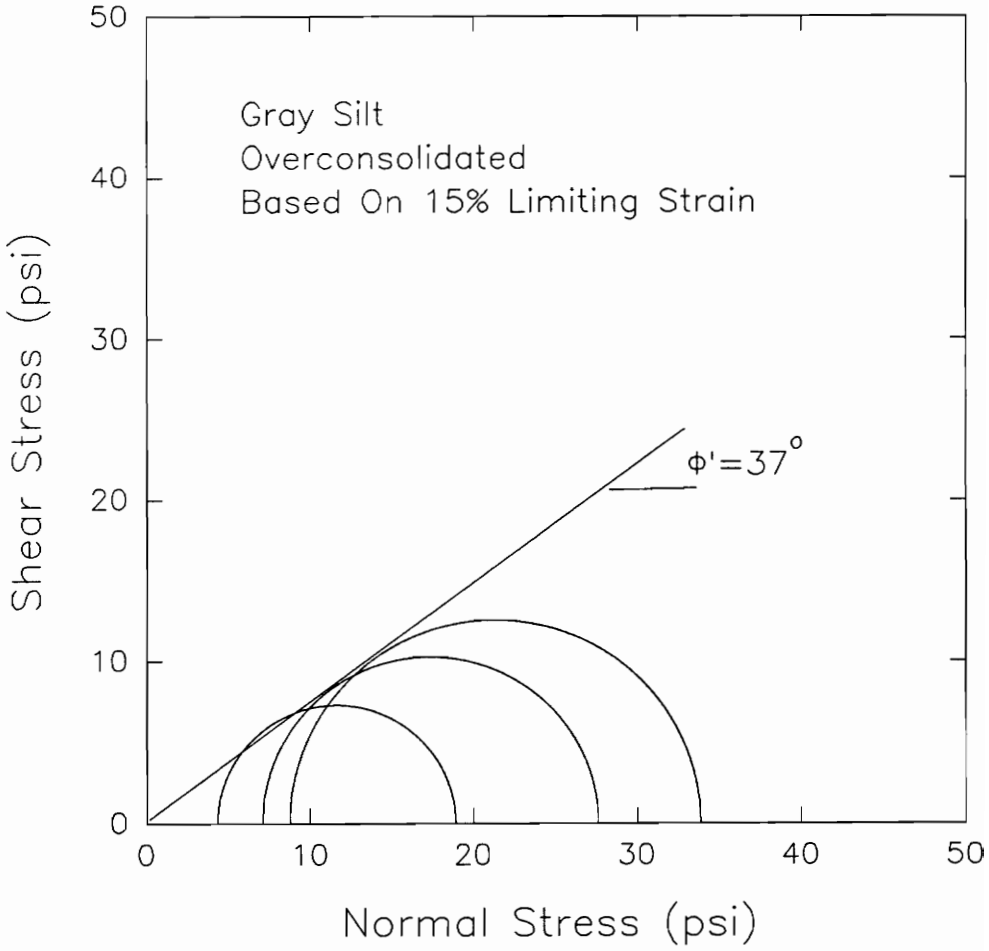

Figure 86 Effective Stress Mohr's Circles Measured For CU Triaxial Tests On Overconsolidated Undisturbed Gray Silt For Failure Based On 15% Limiting Strain (UD-101-S1-A)

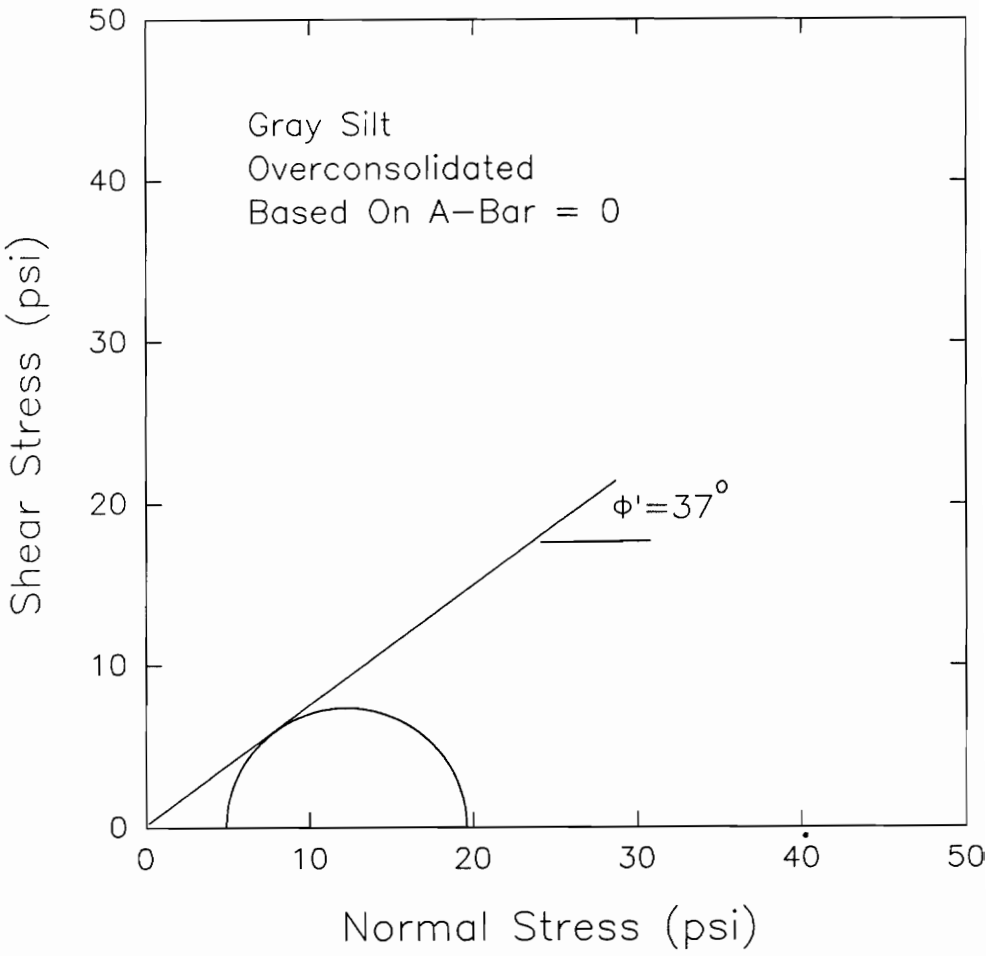

Figure 87 Effective Stress Mohr's Circles Measured For CU Triaxial Tests On Overconsolidated Undisturbed Gray Silt For Failure Based On A-bar = 0 (UD-101-S1-A)

Table 19 Effective Stress Friction Angle At Different Failure Criteria For Gray Silt

Failure Criteria	ϕ'	Average Strain To Failure (%)
u_{max}	34	3
Max $(\sigma_1 - \sigma_3)$	38	15
Max σ_1/σ_3	38	5.5
10% Limiting Strain	37	10
15% Limiting Strain	37	15
A-bar=0	37	20

Total Stress Interpretation of CU Triaxial Tests On Overconsolidated Undisturbed Samples of Gray Silt.

Using the CU triaxial tests on overconsolidated samples of undisturbed gray silt, the undrained strength ratios can be evaluated using different failure criteria.

Shown in Figure 88 is the relationship between undrained shear strength and effective consolidation pressure for failure based on maximum pore pressure. An S_u/p of 0.65 was calculated from this failure criterion.

Figure 89 shows the undrained strength ratio based on maximum deviator stress. It can be seen that for varying degrees of consolidation, the S_u/p ratio is not constant.

For failure based on maximum principal stress ratio, the value of the undrained strength ratio is shown in Figure 90. The calculated value of S_u/p is 0.80.

Using 10% and 15% limiting strains as failure criteria, as shown in Figures 91 and 92, calculation of S_u/p ratio using the previous method is not possible because of the non-linear relationship between undrained strength and effective consolidation pressure.

Figure 93 shows the value of S_u/p based on A-bar = 0 as failure criterion. An S_u/p of 1.5 was calculated based

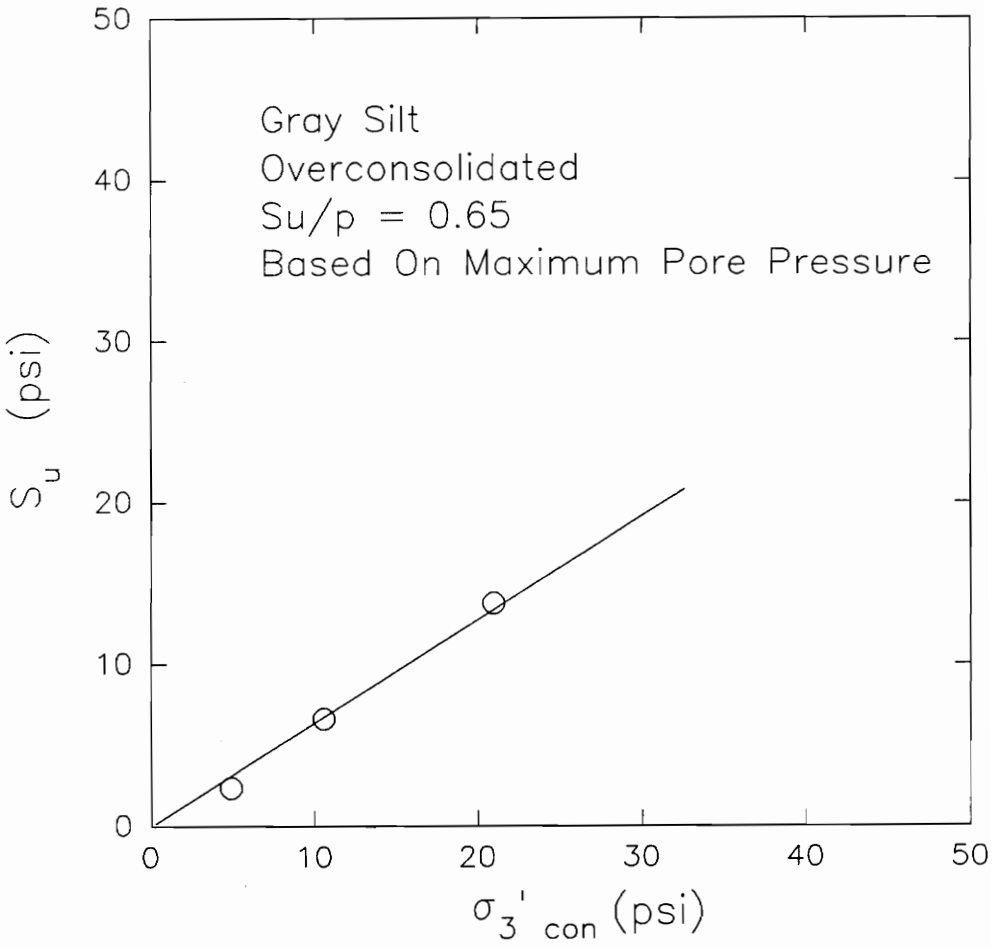

Figure 88 Undrained Shear Strength-Effective Consolidation Pressure Relationship Measured For CU Triaxial Tests On Overconsolidated Undisturbed Gray Silt For Failure Based On Maximum Pore Pressure (UD-101-S1-A)

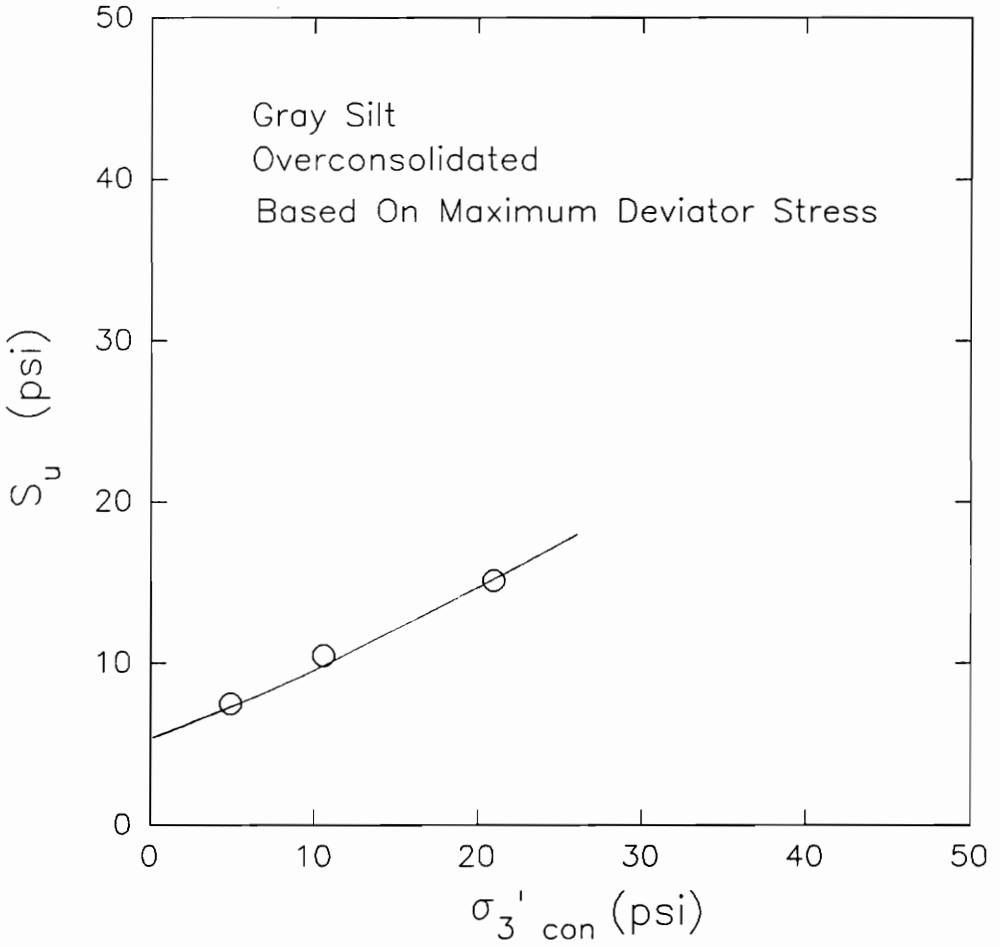

Figure 89 Undrained Shear Strength-Effective Consolidation Pressure Relationship Measured For CU Triaxial Tests On Overconsolidated Undisturbed Gray Silt For Failure Based On Maximum Deviator Stress (UD-101-S1-A)

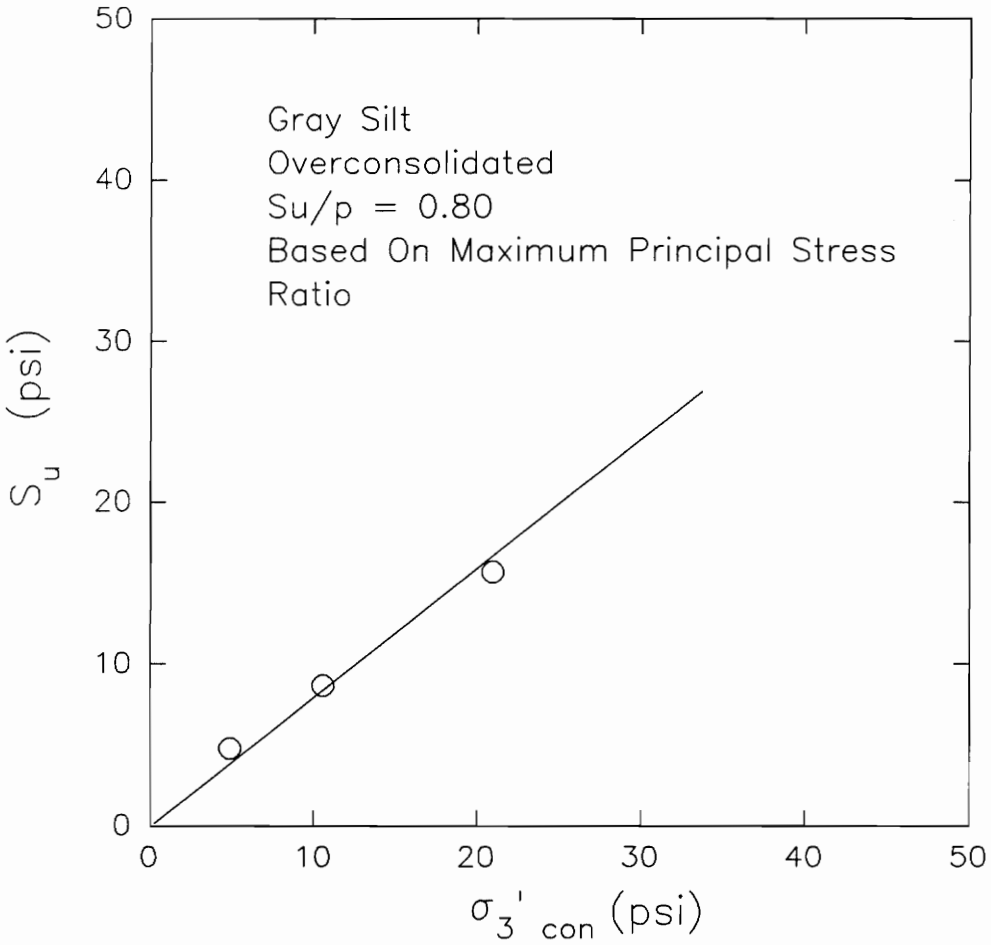

Figure 90 Undrained Shear Strength-Effective Consolidation Pressure Relationship Measured For CU Triaxial Tests On Overconsolidated Undisturbed Gray Silt For Failure Based On Maximum Principal Stress Ratio (UD-101-S1-A)

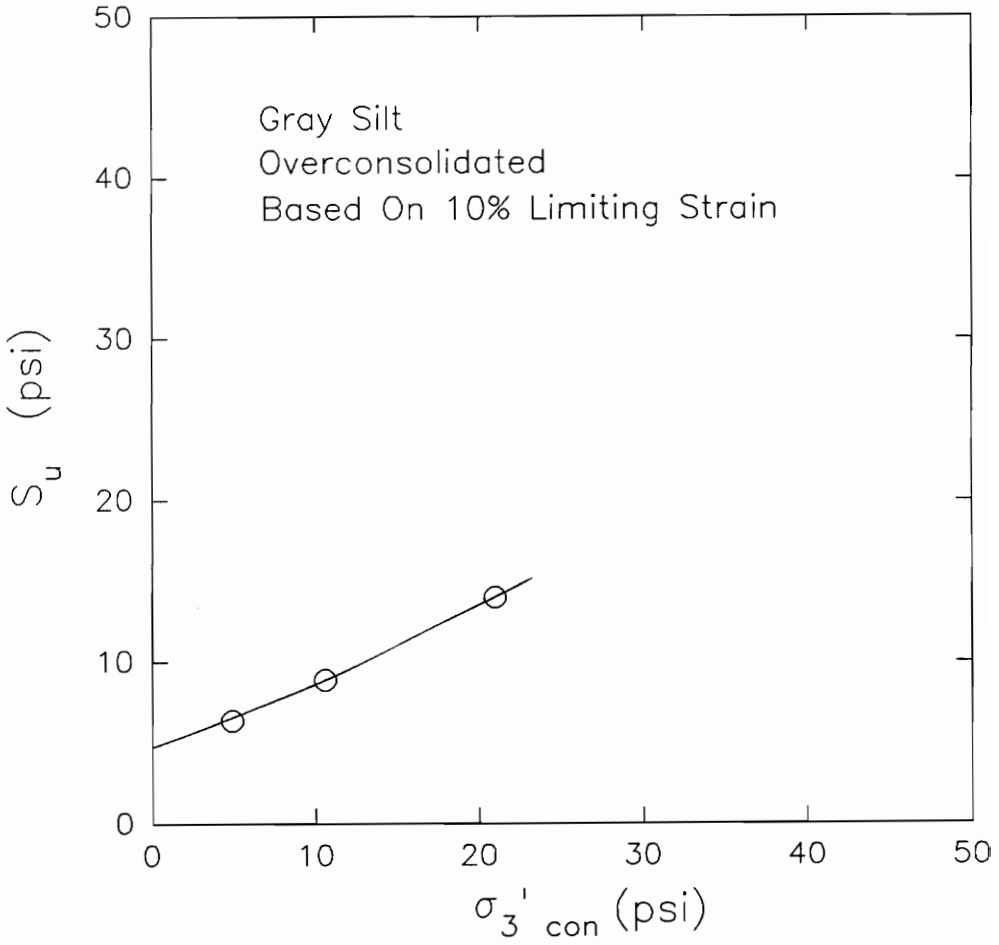

Figure 91 Undrained Shear Strength-Effective Consolidation Pressure Relationship Measured For CU Triaxial Tests On Overconsolidated Undisturbed Gray Silt For Failure Based On 10% Limiting Strain (UD-101-S1-A)

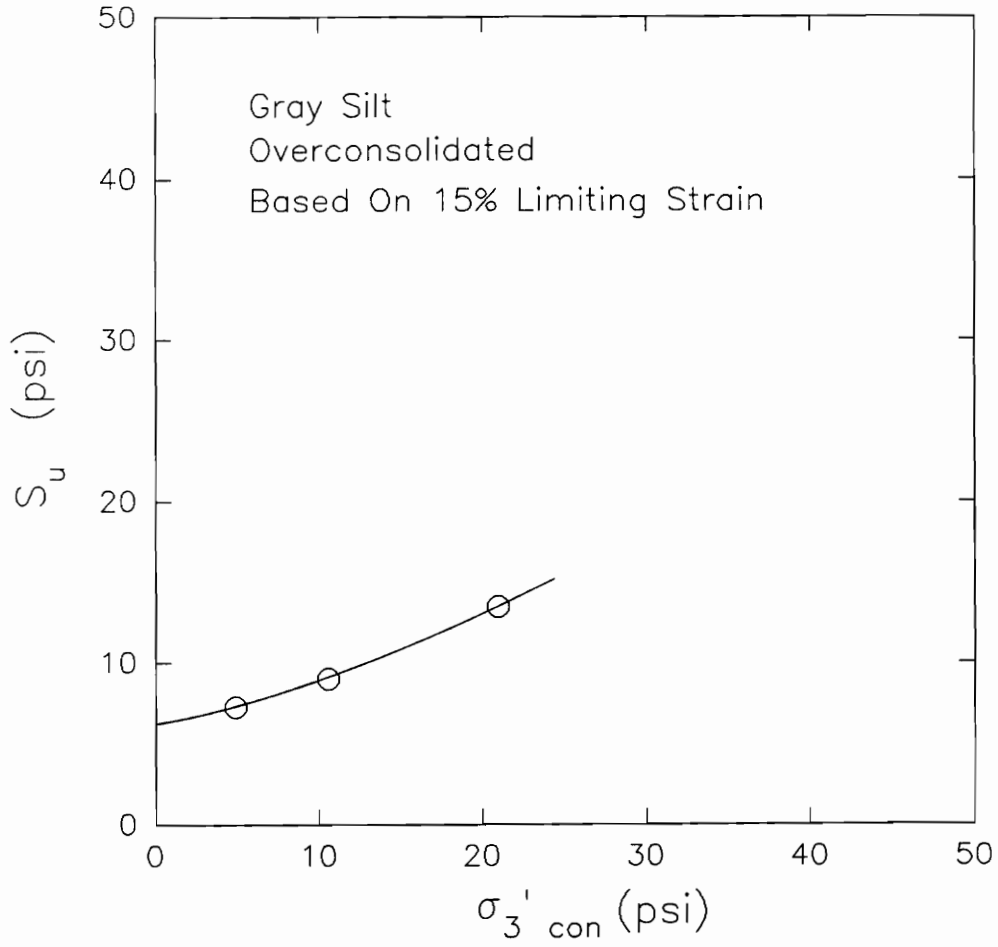

Figure 92 **Undrained Shear Strength-Effective Consolidation Pressure Relationship Measured For CU Triaxial Tests On Overconsolidated Undisturbed Gray Silt For Failure Based On 15% Limiting Strain (UD-101-S1-A)**

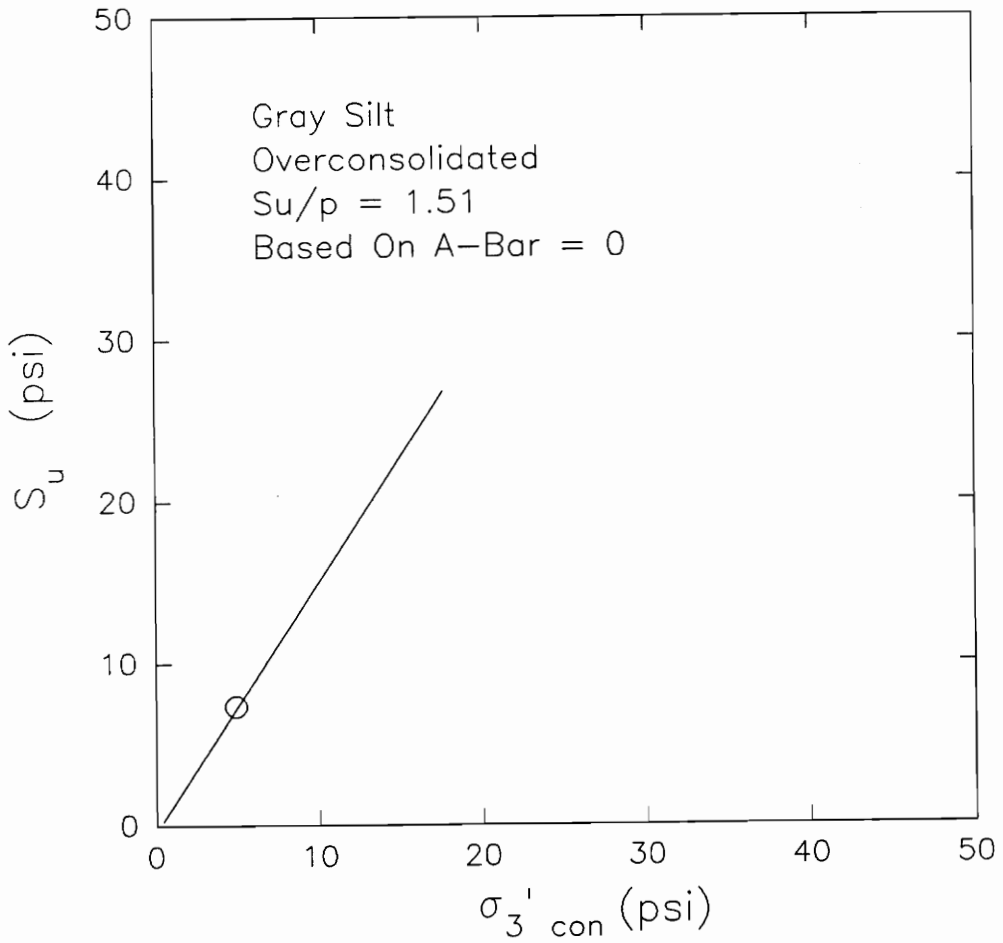

Figure 93 Undrained Shear Strength-Effective Consolidation Pressure Relationship Measured For CU Triaxial Tests On Overconsolidated Undisturbed Gray Silt For Failure Based On A-bar = 0 (UD-101-S1-A)

on this failure criterion. This does not represent a reliable estimate since it is a representative of only one sample.

Table 20 summarizes the values of S_u/p determined for different failure criteria for gray silt. As with the previous effective stress analysis, the lowest value of the undrained strength ratio was obtained from failure based on maximum pore pressure. Skempton's correlation of S_u/p with plasticity index cannot be applied to these tests results because the samples were overconsolidated.

Table 20 S_u/p Ratios Determined For Different Failure Criteria for CU Test On Gray Silt

Failure Criteria	S_u/p	Average Strain To Failure (%)
u_{max}	0.65	3
Max $(\sigma_1 - \sigma_3)$	N/A	15
Max σ_1/σ_3	0.8	5.5
10% Limiting Strain	N/A	10
15% Limiting Strain	N/A	15
A-bar=0	1.5	20

Unconsolidated Undrained Tests On Overconsolidated Undisturbed Samples of Gray Silt, West Williamson L.P.P. Pumping Plant

Six UU triaxial tests were performed on different samples of gray silt. Four UU triaxial tests were conducted on sample UD-101-S2-A, one on sample UD-100-S4-A1, and one on sample UD-101-S2-C2. The plots for sample UD-101-S2-A are shown in Figures 94, 95, 96, and 97. For the other gray silt samples, the results are shown in Appendix A.

The properties for UU triaxial tests of sample UD-101-S2-A are given in Table 21. The cell pressures used during the tests were 4.9 psi, 20.8 psi, 10.4 psi, and 34.7 psi. Shown in Figure 94 are the deviator stress-strain relationships. It can be seen that the stress-strain curves are independent of cell pressures, indicating that the samples have similar properties and were saturated prior to shearing. The stress-strain curve of the sample subjected to a cell pressure of 34.7 psi had a peak deviator stress at a strain of about 12%. The other three samples did not show any peak behavior in their stress-strain relationship.

Figure 95 illustrates the Mohr's circles based on maximum deviator stress as failure criterion. Using ϕ_u=0

Table 21 Properties of Overconsolidated Undisturbed Specimens For UU Triaxial Tests of Sample UD-101-S2-A, West Williamson L.P.P. Pumping Plant.

Liquid Limit	21.0%
Plastic Limit	18.0%
Plasticity Index	3.0%
Natural Water Content	21.0%
Specific Gravity	2.7

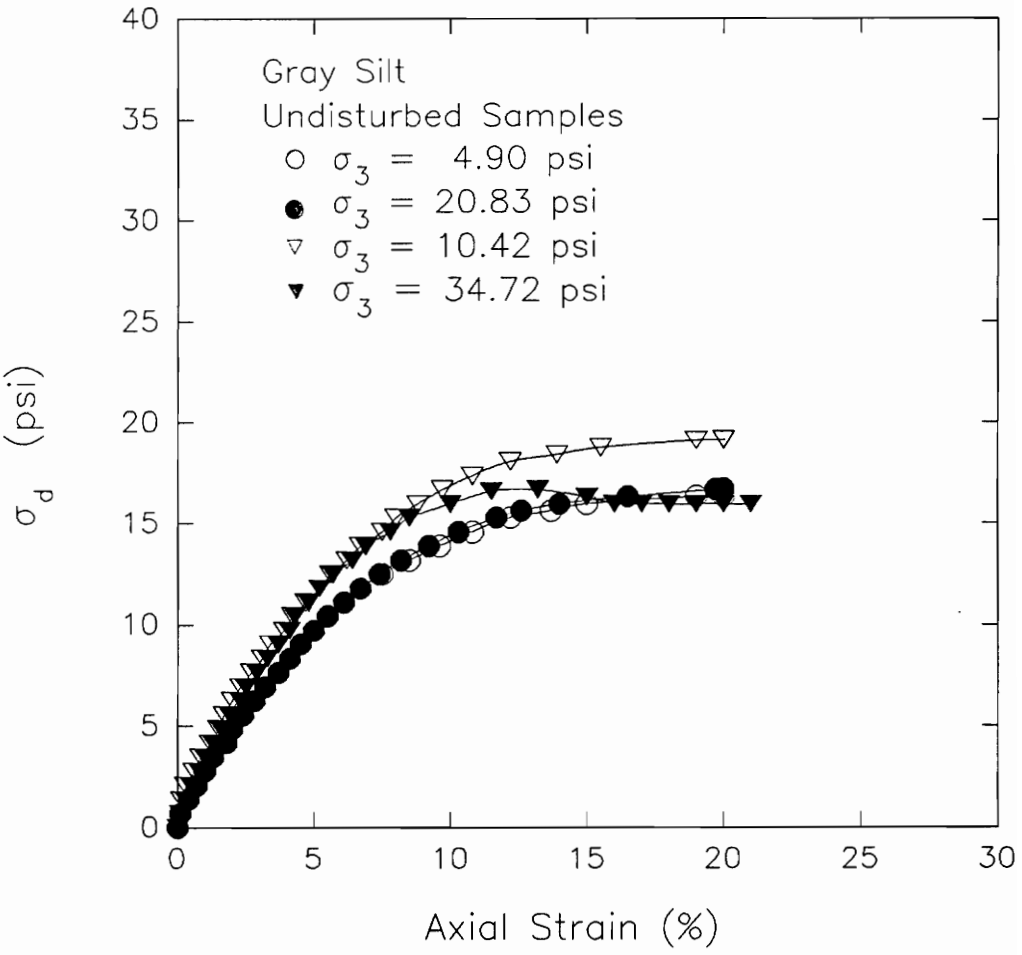

Figure 94 Deviator Stress-Strain Relationship Measured For UU Triaxial Tests On Undisturbed Samples of Gray silt, West Williamson L.P.P. Pump Station (Sample UD-101-S2-A)

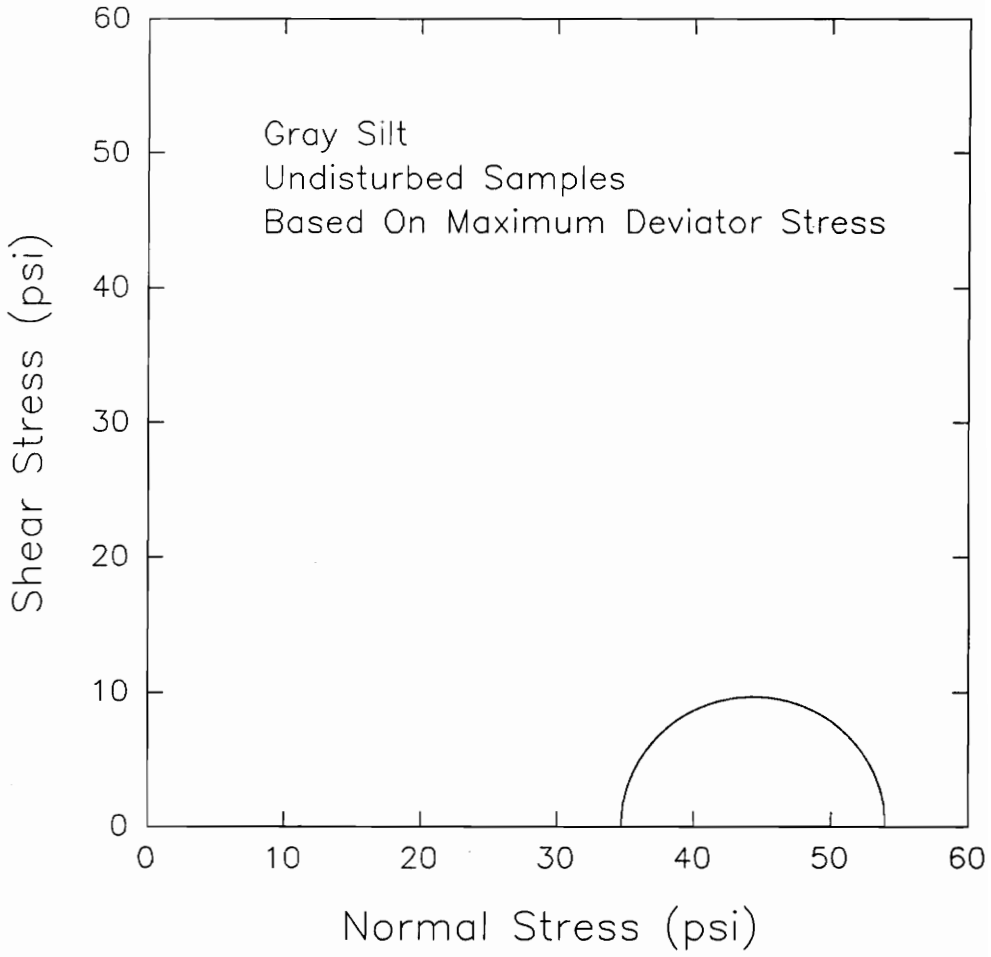

Figure 95 **Mohr's Circles Measured For UU Triaxial Tests On Undisturbed Samples of Gray Silt For Failure Based On Maximum Deviator Stress, West Williamson L.P.P. Pump Station (Sample UD-101-S2-A)**

interpretation, the undrained shear strength, S_u, computed is 8.30 psi. Using an effective overburden pressure of 21 psi, the S_u/p ratio would be 0.40.

Shown in Figure 96 are the Mohr's circles using 10% limiting strain failure criterion. The undrained strength, S_u, calculated is 8.70 psi, which gives an undrained strength ratio, S_u/p, of 0.41.

The Mohr's circles based on 15% limiting strain are shown in Figure 97. The undrained strength calculated is 8.8 psi. This gives an undrained strength ratio, S_u/p, equal to 0.42.

Table 22 summarizes the values of S_u/p for different failure criteria for sample UD-101-S2-A. The values of S_u/p based on different failure criteria have an average value equal to 0.41.

The plots measured for samples UD-100-S4-A1 and UD-101-S2-C2 are shown in Appendix A. Tables 23 and 24 summarize the values of S_u/p for these samples for different failure criteria.

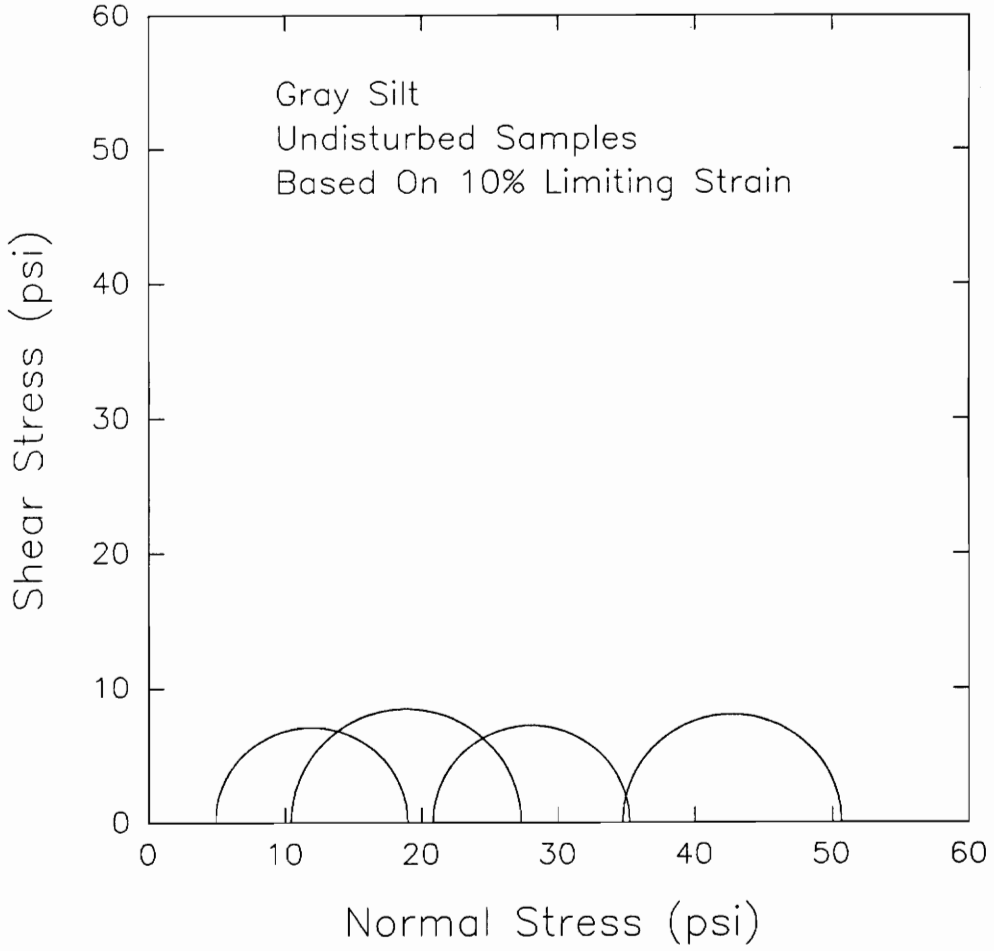

Figure 96 Mohr's Circles Measured For UU Triaxial Tests On Undisturbed Samples of Gray Silt For Failure Based On 10% Limiting Strain, West Williamson L.P.P. Pump Station (Sample UD-101-S2-A)

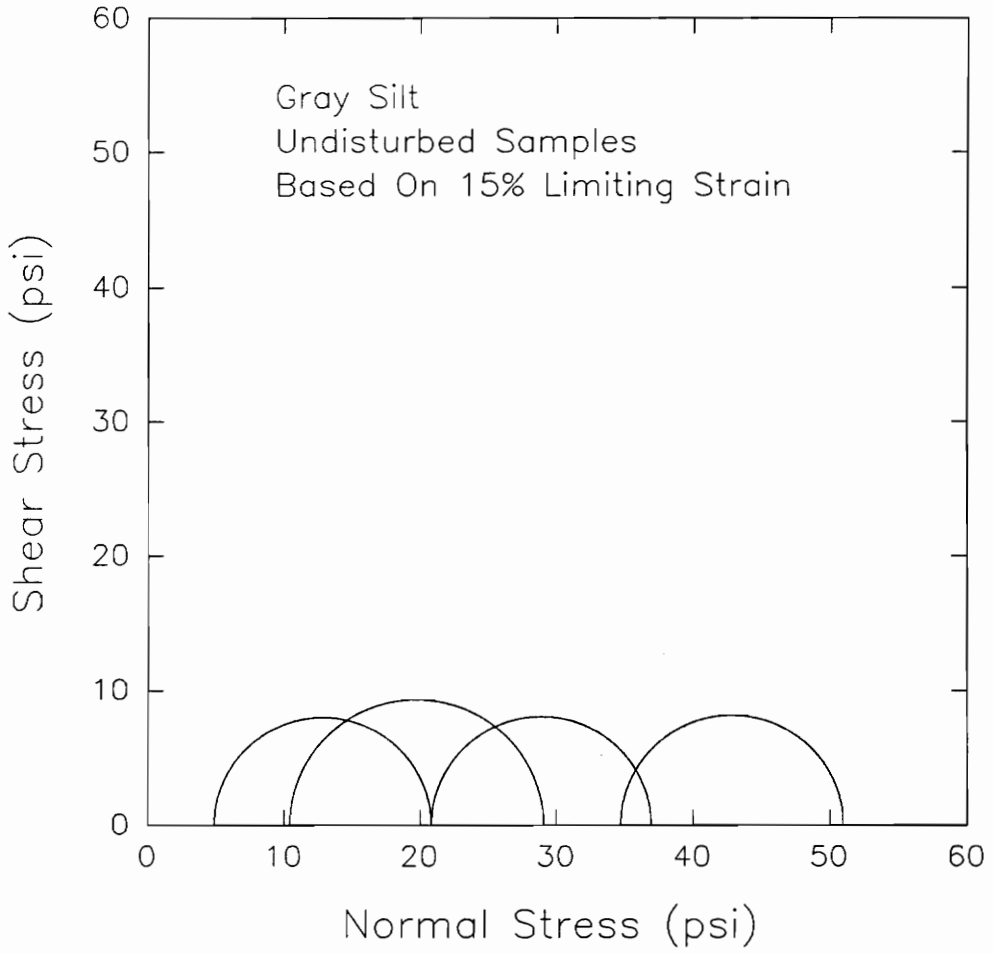

Figure 97 Mohr's Circles Measured For UU Triaxial Tests On Undisturbed Samples of Gray Silt For Failure Based On 15% Limiting Strain, West Williamson L.P.P. Pump Station (Sample UD-101-S2-A)

Table 22 S_u/p **Ratios Determined From UU Triaxial Tests On Overconsolidated Undisturbed Specimens of Gray Silt, Sample UD-101-S2-A, West Williamson L.P.P.Pumping Plant**

Failure Criteria	S_u/p
$(\sigma_1-\sigma_3)_{max}$	0.40
10% Limiting Strain	0.41
15% Limiting Strain	0.42

Table 23 **S_u/p Ratios Determined From UU Triaxial Tests On Overconsolidated Undisturbed Specimens of Gray Silt, Sample UD-100-S4-A1, West Williamson L.P.P. Pumping Plant**

Failure Criteria	S_u/p
$(\sigma_1-\sigma_3)_{max}$	N/A
10% Limiting Strain	0.48
15% Limiting Strain	0.51

Table 24 **S_u/p Ratios Determined From UU Triaxial Tests On Overconsolidated Undisturbed Specimens of Gray Silt, Sample UD-101-S2-C2, West Williamson L.P.P. Pumping Plant**

Failure Criteria	S_u/p
$(\sigma_1-\sigma_3)_{max}$	N/A
10% Limiting Strain	0.20
15% Limiting Strain	0.22

Unconsolidated Undrained Triaxial Tests On Overconsolidated Undisturbed Samples of Brown Silt

Eight UU triaxial tests were conducted on Brown silt at the Virginia Tech Laboratory and ten UU triaxial tests were conducted at ORD Laboratory. Results of UU tests for sample UD-85-4-9 are shown in Figures 98, 99, 100, and 101. The results of UU tests for the other samples of brown silt are shown in Appendix B.

For sample UD-85-4-9, four UU triaxial tests were performed. The properties of the specimens are given in Tables 25 and 26.

Figure 98 shows the deviator stress-strain relationship for the samples. All specimens exhibited similar behavior, wherein the deviator stress increased rapidly at small strains and showed a distinct break at a strain of about 1%. The deviator stress continued to increase with increasing strain, but did not show any strain softening for the duration of the tests.

Figure 99 shows the Mohr's circles for failure based on maximum deviator stress. Using ϕ_u=0 interpretation of the results, the undrained shear strength calculated is equal to 2.2 psi. These samples were obtained at a depth of approximately 21 feet. The effective overburden

Table 25 Properties of Overconsolidated Undisturbed Specimens of Brown Silt (Sample UD-85-4-9), West Williamson L.P.P. Pumping Plant

Test #	Cell Pressure (psi)	Water Content (%)	Initial Void Ratio	S (%)	Dry Density (pcf)
1	4.83	33.9	0.972	95.8	86.7
2	10.40	33.1	0.892	100.0	90.4
3	20.83	33.9	0.914	100.0	89.3
4	13.90	32.7	0.872	100.0	91.3

Table 26 Index Properties of Sample UD-85-4-9 For UU Triaxial Tests

Liquid Limit	44%
Plastic Limit	25%
Plasticity Index	19%
Specific Gravity	2.74

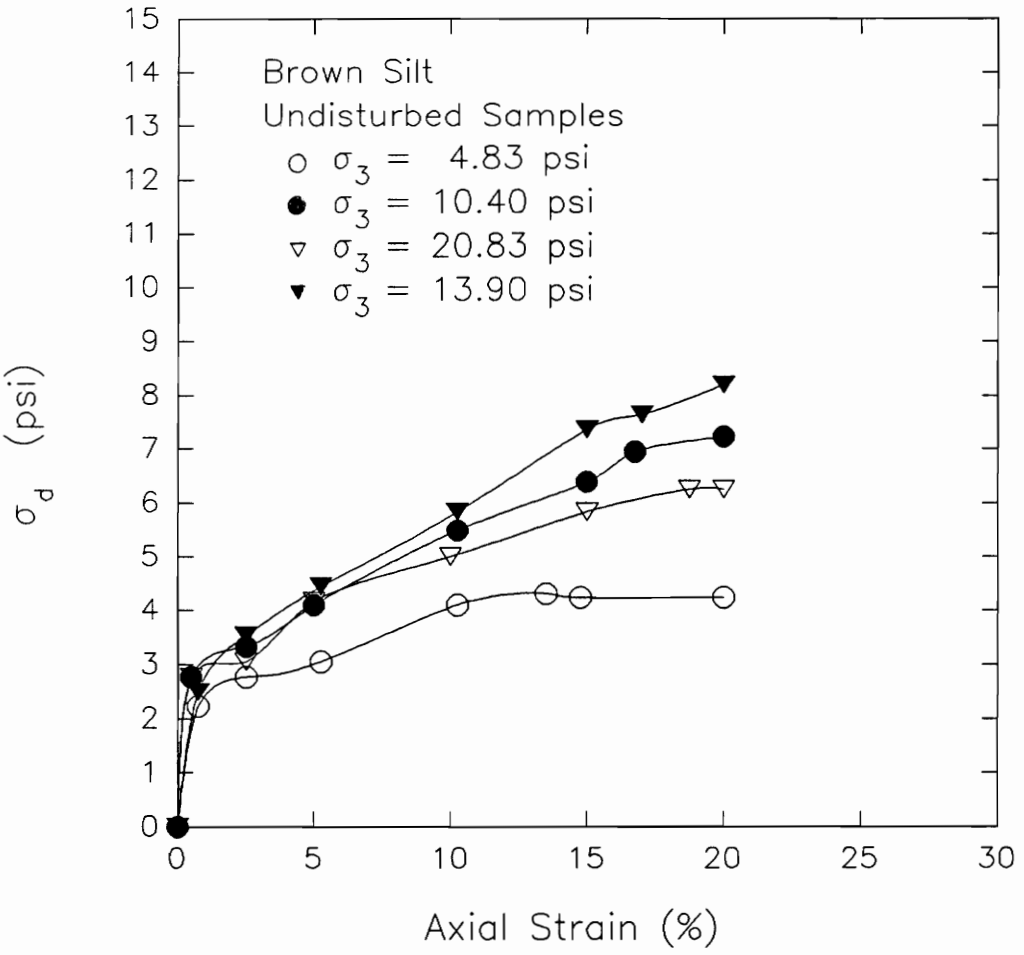

Figure 98 Deviator Stress-Strain Relationship Measured For UU Triaxial Tests On Undisturbed Samples Of Brown Silt, West Willliamson L.P.P. Pumping Plant (Sample UD-85-4-9)

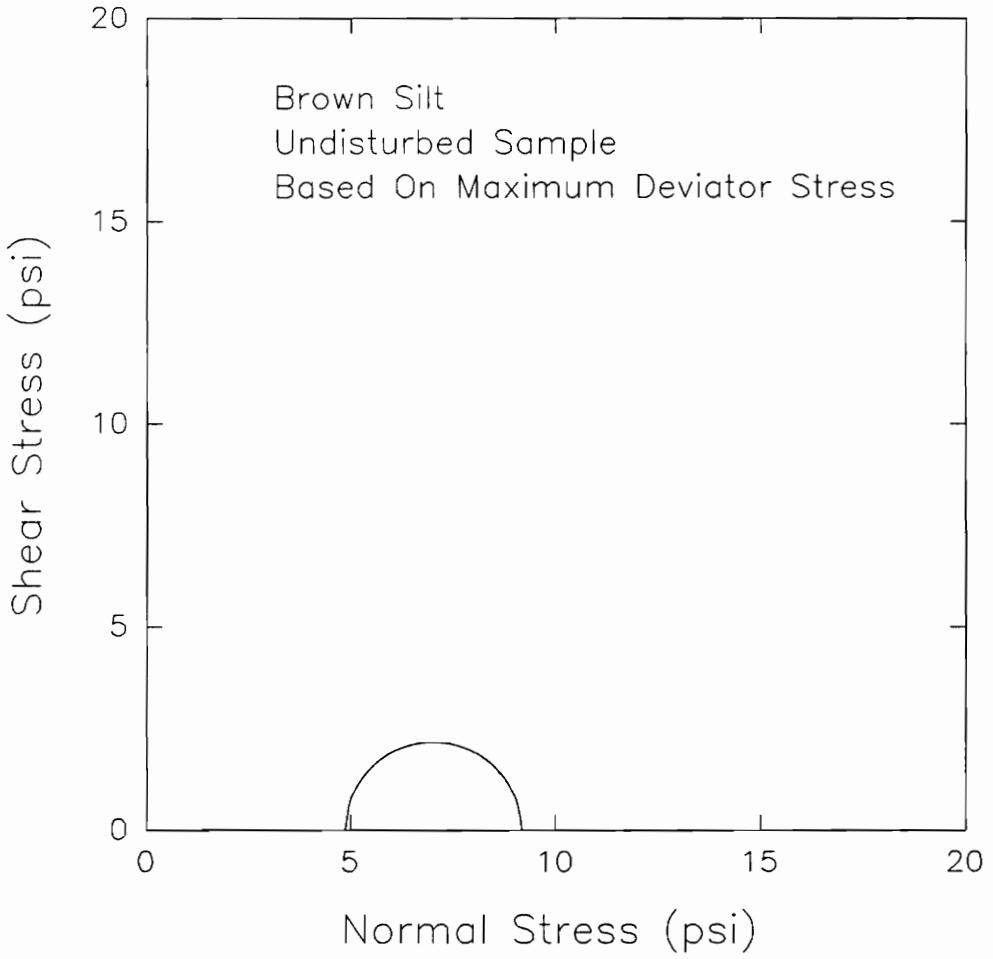

Figure 99 Mohr's Circles Measured For UU Triaxial Tests On Undisturbed Samples of Brown Silt For Failure Based On Maximum Deviator Stress, West Williamson L.P.P. Pumping Plant (Sample UD-85-4-9)

pressure at this depth is approximately 18 psi. For the failure criteria based on maximum deviator stress, the calculated S_u/p is equal to 0.12.

The Mohr's circles based on 10% limiting strain as failure criterion are shown in Figure 100. A small scatter in the results can be attributed to disturbance effects. The undrained shear strength, S_u, calculated from these results is 2.6 psi which gives an undrained strength ratio equal to 0.15.

Shown in Figure 101 are the Mohr's circles for failure based on 15% limiting strain. The best estimate of the undrained shear strength is 3.1 psi which gives a value of S_u/p equal to 0.17.

Table 27 summarizes the values of Su/p for UU triaxial tests on Sample UD-85-4-9 for different failure criteria. The Su/p ratios calculated would give an average value equal to 0.13.

The plots measured for UU triaxial tests on the other samples of Brown silt are shown in Appendix B. A summary of the values of undrained strength ratios for different failure criteria are given in Tables 28 and 29.

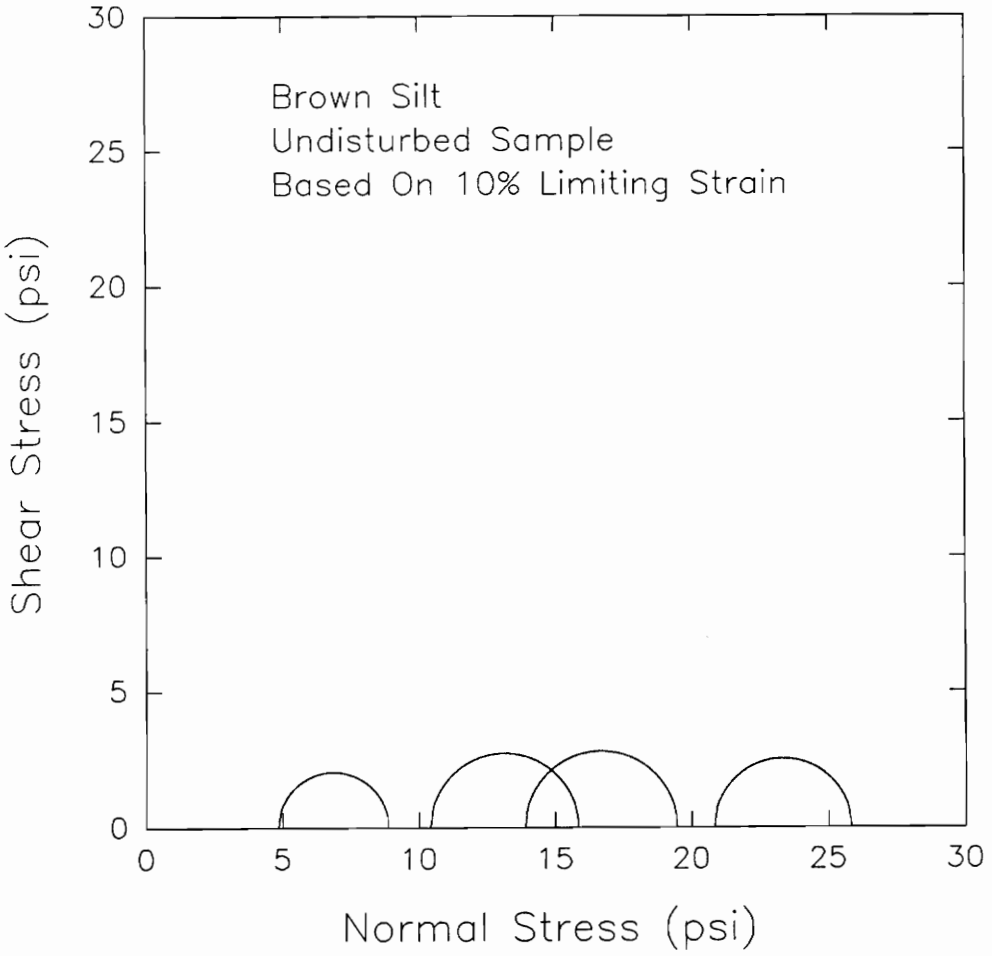

Figure 100 Mohr's Circles Measured For UU Triaxial Tests On Undisturbed Samples of Brown Silt For Failure Based On 10% Limiting Strain, West Williamson L.P.P. Pumping Plant (Sample UD-85-4-9)

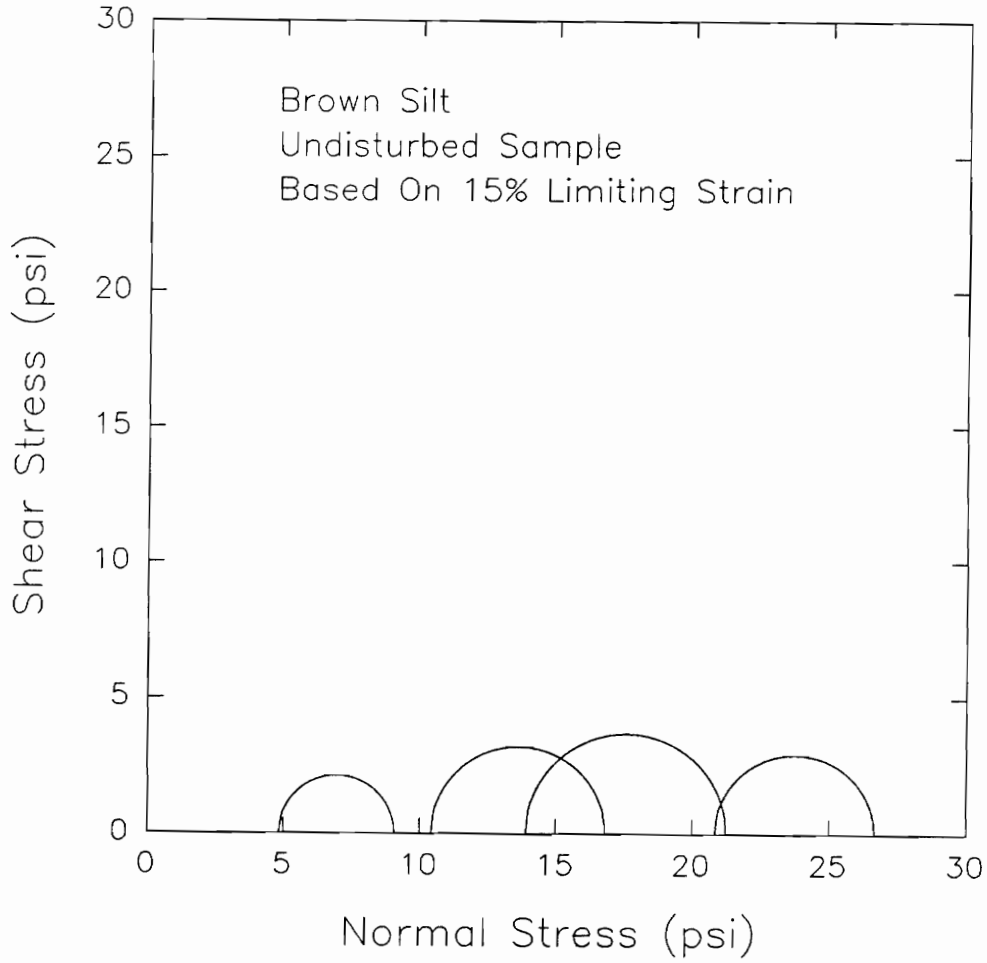

Figure 101 Mohr's Circles Measured For UU Triaxial Tests On Undisturbed Samples of Brown Silt For Failure Based On 15% Limiting Strain, West Williamson L.P.P. Pumping Plant (Sample UD-85-4-9)

Table 27 S_u/p Ratios for Different Failure Criteria Determined From UU Triaxial Test On Sample UD-85-4-9, West Williamson L.P.P. Pumping Plant

Failure Criteria	S_u/p
$(\sigma_1-\sigma_3)_{max}$	0.12
10% Limiting Strain	0.15
15% Limiting Strain	0.17

Table 28 S_u/p Ratios for Different Failure Criteria Determined From UU Triaxial Test On Sample UD-85-4-11B, West Williamson L.P.P. Pumping Plant

Failure Criteria	S_u/p
$(\sigma_1-\sigma_3)_{max}$	0.42
10% Limiting Strain	0.38
15% Limiting Strain	0.40

Table 29 S_u/p Ratios for Different Failure Criteria Determined From UU Triaxial Test On Sample UD-100-S1-A, West Williamson L.P.P. Pumping Plant

Failure Criteria	S_u/p
$(\sigma_1-\sigma_3)_{max}$	0.52
10% Limiting Strain	0.48
15% Limiting Strain	0.50

RHODE ISLAND SILT

Samples of remolded Rhode Island silt were tested by Nacci and D'Andrea (1976). Obtaining undisturbed samples by conventional sampling techniques, including thin-walled cylinder and block sampling, was not possible because the liquidity index of this silt was above 1.00. The silt liquefies at small amounts of disturbance and furthermore, it was assumed that the specimen densified during transit. To duplicate the natural fabric composition of the soil for laboratory testing, a unique sample preparation technique was devised as shown in Figure 102. Bulk samples were obtained from the site and these were mixed with distilled water to produce a slurry. Cylindrical triaxial specimens were obtained by slow sedimentation of this slurry. During sample preparation, the silt was consolidated under a pressure of approximately 7.10 psi.

Index Properties of Rhode Island Silt

Rhode Island Silt is a loose layered silt. The gradation curve for this silt is shown in Figure 103 and the grain size components are given in Table 30. The gradation curve shows that the sample consisted mostly of

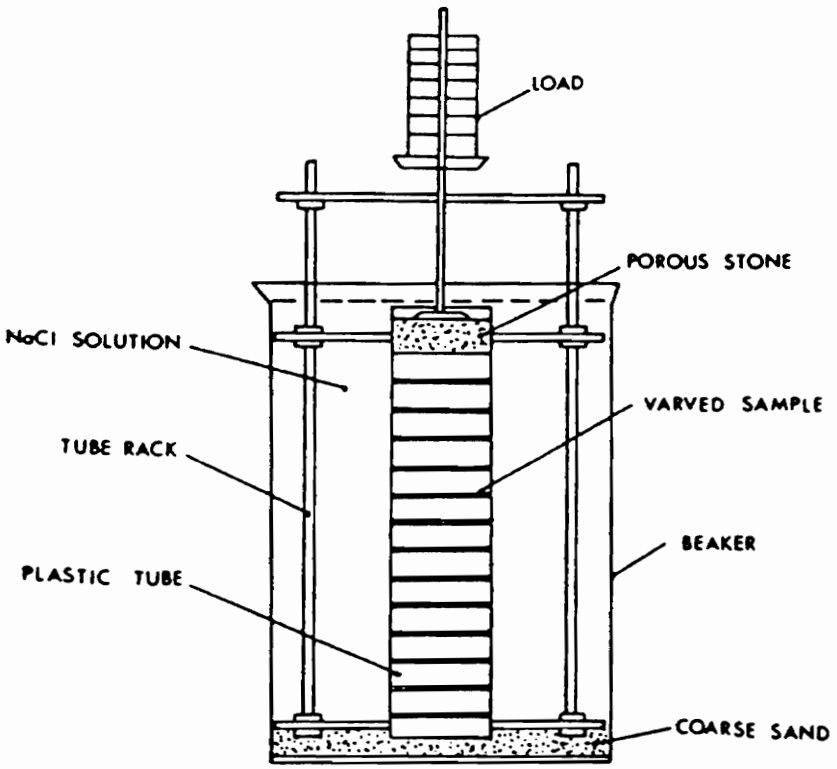

Figure 102 Sedimentation Apparatus For Rhode Island Silt

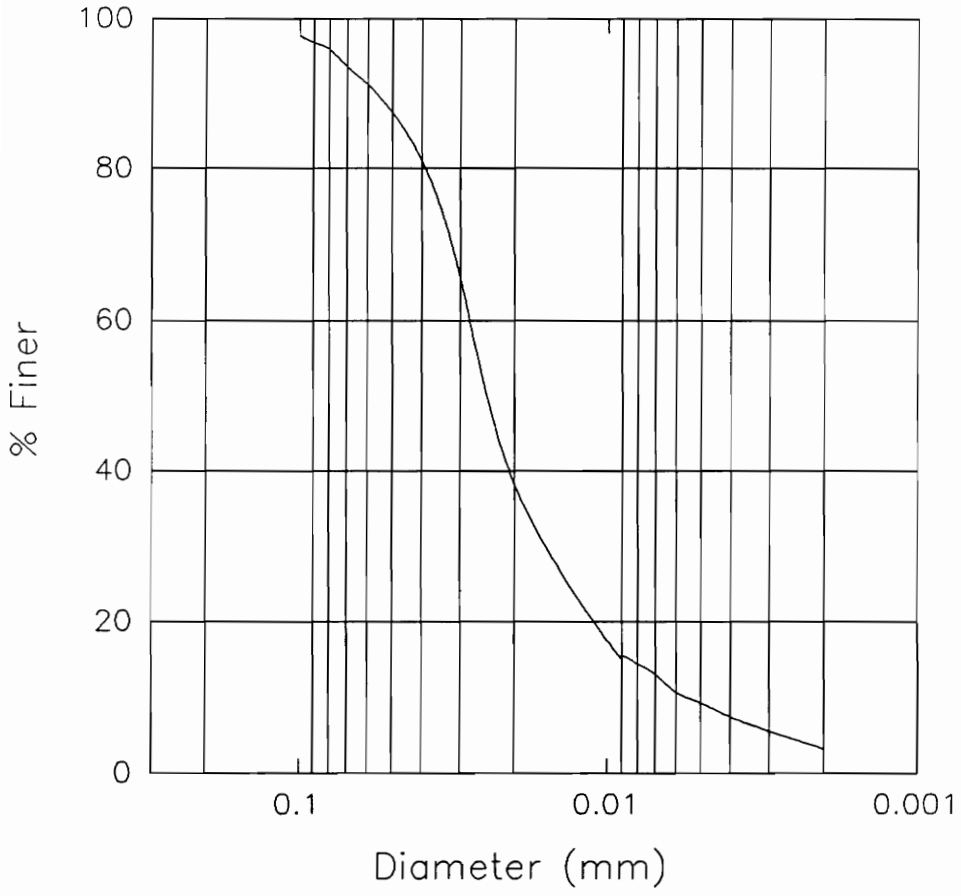

Figure 103 Grain Size Analysis Curve For Rhode Island Silt

Table 30 Grain Size Components of Rhode Island Silt

Components	Amount
% Sand	10%
% Silt	87%
% Clay	3%

silt particles with grain size diameter less than 0.074 mm and greater than 0.002 mm. The Atterberg limits are plotted on the plasticity chart in Figure 104 and summarized in Table 31. The sample plots just below the A-line. Rhode Island silt has specific gravity of 2.75, and has a high natural water content, ranging from 30% to 40%.

Consolidated Undrained Triaxial Test On Remolded Rhode Island Silt

CU Triaxial tests were conducted on remolded specimens of normally consolidated Rhode Island Silt using Geonor equipment. Conventional procedures of back pressure saturation were conducted prior to consolidation to give full saturation on the specimen. The specimen was sheared under a strain rate of 3 percent per hour. The slow rate of shearing the sample insured that the pore pressure measured at the base of the sample was the same pore pressure throughout the sample. Figure 105 shows the stress-strain curve for the specimen. A maximum deviator stress was not attained for the range of strains used. Shown in Figures 106 and 107 are the effective stress-strain and principal stress ratio-strain relationships. No peak behavior can be seen on the principal stress

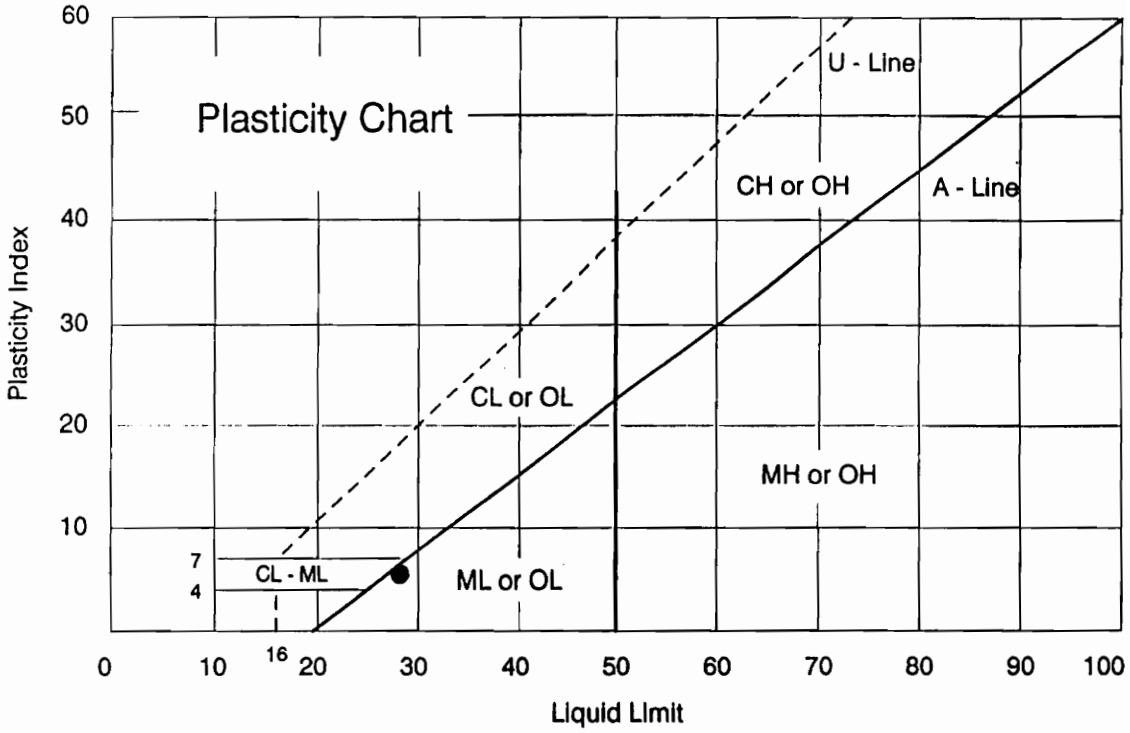

Figure 104 Plasticity Chart For Rhode Island Silt

Table 31 Properties of Rhode Island Silt (Nacci et al.)

Natural Water Content	30%-40%
Liquid Limit	28%
Plastic Limit	22%
Plasticity Index	6%
Liquidity Index	1.50-2.50
Moist Unit Weight	115-122 pcf
G_s	2.75

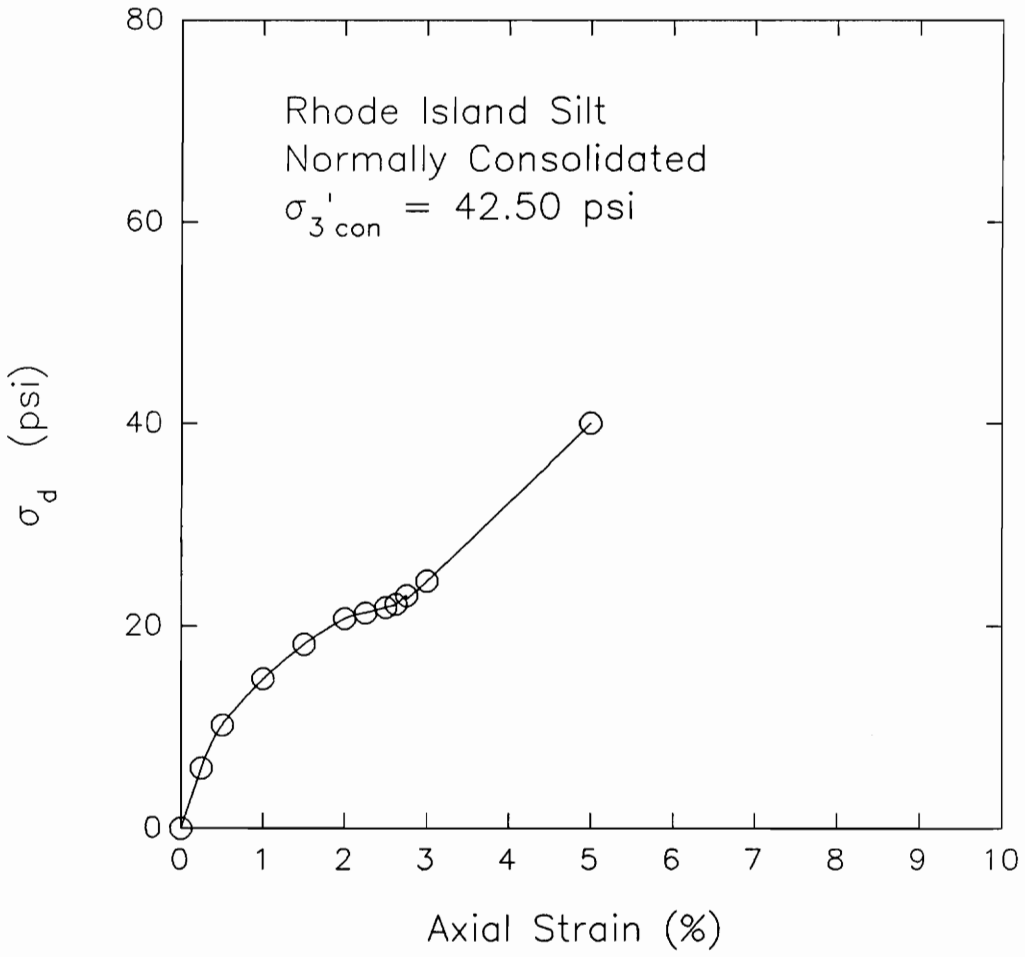

Figure 105 Deviator Stress-Strain Relationship Measured For CU Triaxial Test On Normally Consolidated Rhode Island Silt

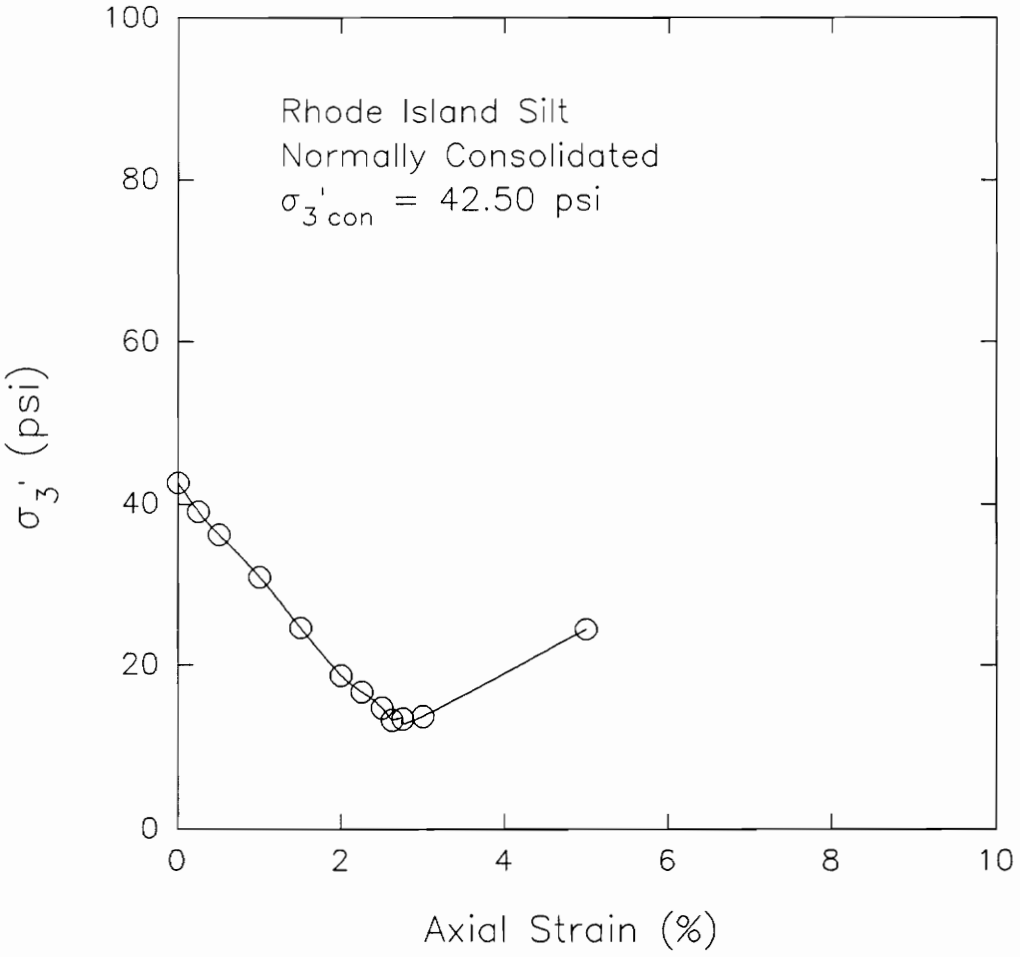

Figure 106 Minor Effective Stress-Strain Relationship Measured For CU Triaxial Test On Normally Consolidated Rhode Island Silt

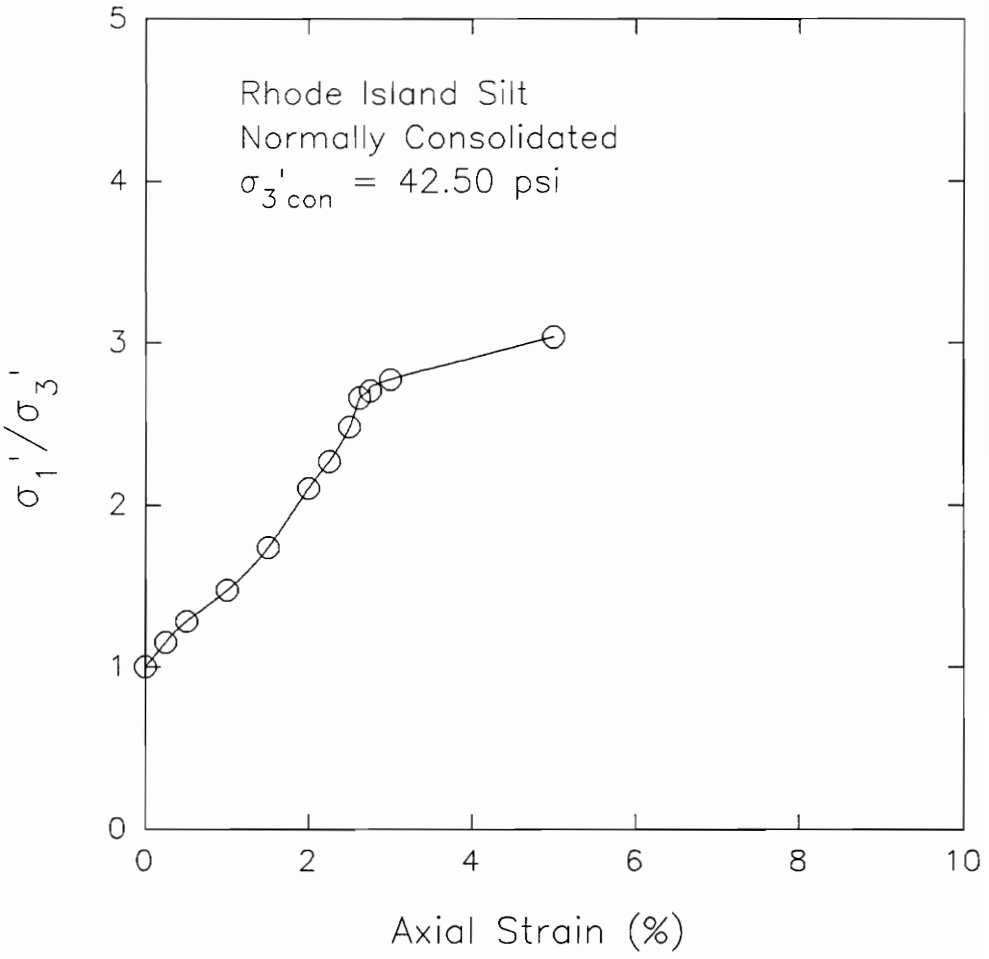

Figure 107 Principal Stress Ratio-Strain Relationship Measured For CU Triaxial Test On Normally Consolidated Rhode Island Silt

ratio-strain relationship. Figure 108 shows that the maximum pore pressure occurred at less than 3 percent strain. The same behavior can be seen from the A-bar-Strain relationship because of direct proportionality between A-bar and pore pressure, as shown in Figure 109.

Effective Stress Interpretation of CU Triaxial Test On Remolded Rhode Island Silt

The results clearly indicate that the maximum pore pressure is the only failure criteria that can be applied. The effective stress Mohr's circle is shown in Figure 110 which renders an effective stress friction angle equal to 27°. The envelope was determined by constraining the cohesion intercept c' to zero. Figure 111 shows the effective stress path for the Rhode Island silt. The K_f line defined gives a value of α equal to 25°. This corresponds to an effective friction angle equal to 28°.

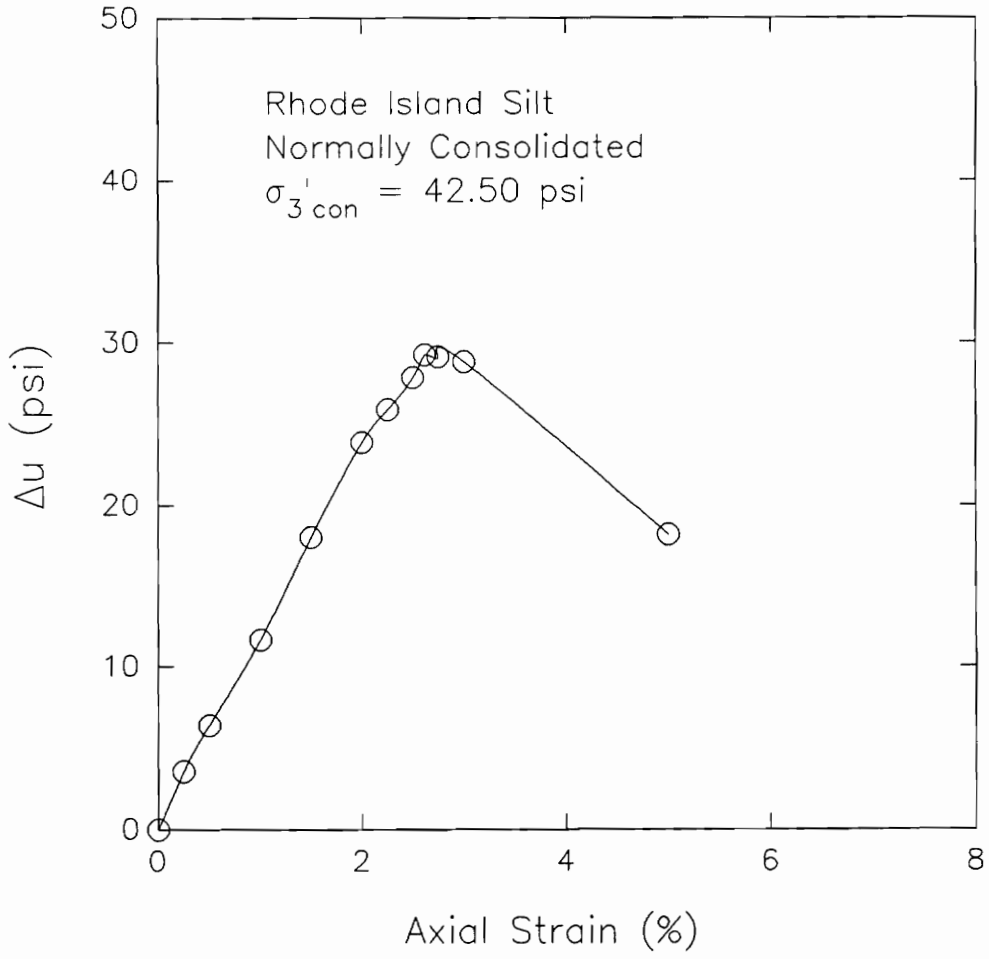

Figure 108 Pore Pressure-Strain Relationship Measured For CU Triaxial Test On Normally Consolidated Rhode Island Silt

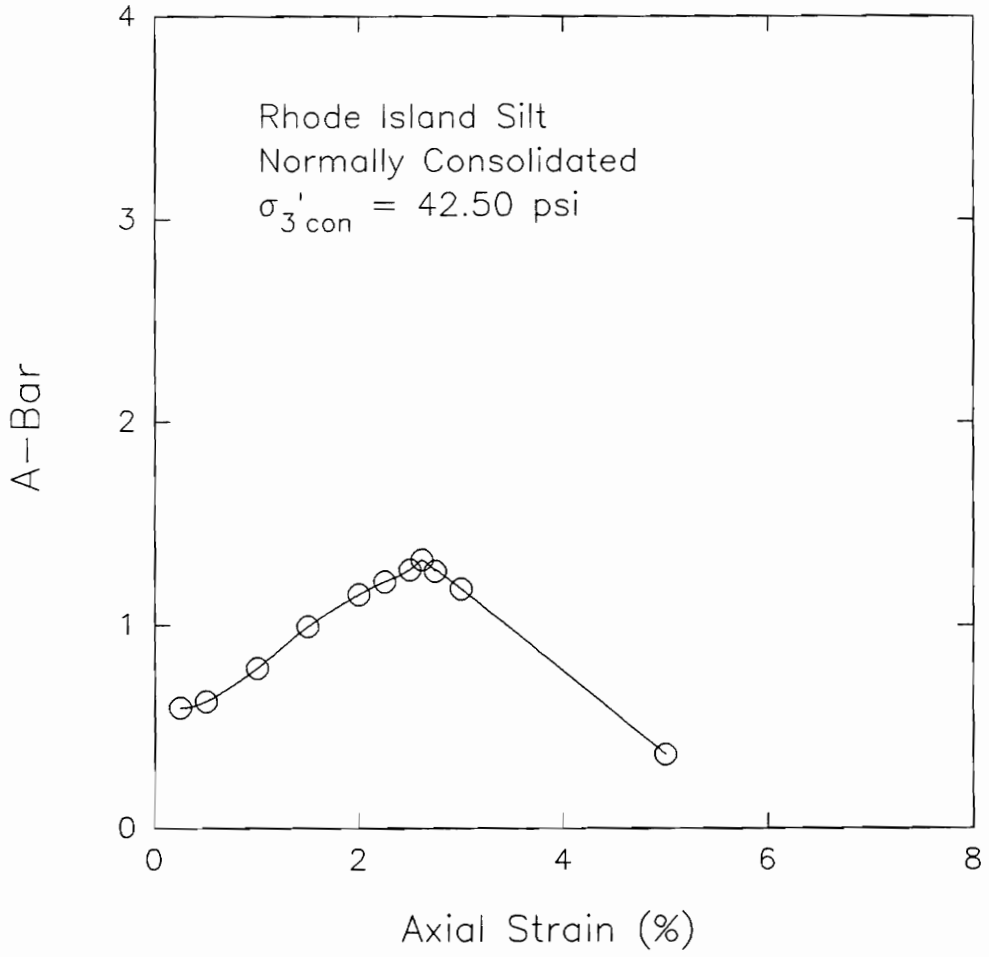

Figure 109 A-bar-Strain Relationship Measured For CU Triaxial Test On Normally Consolidated Rhode Island Silt

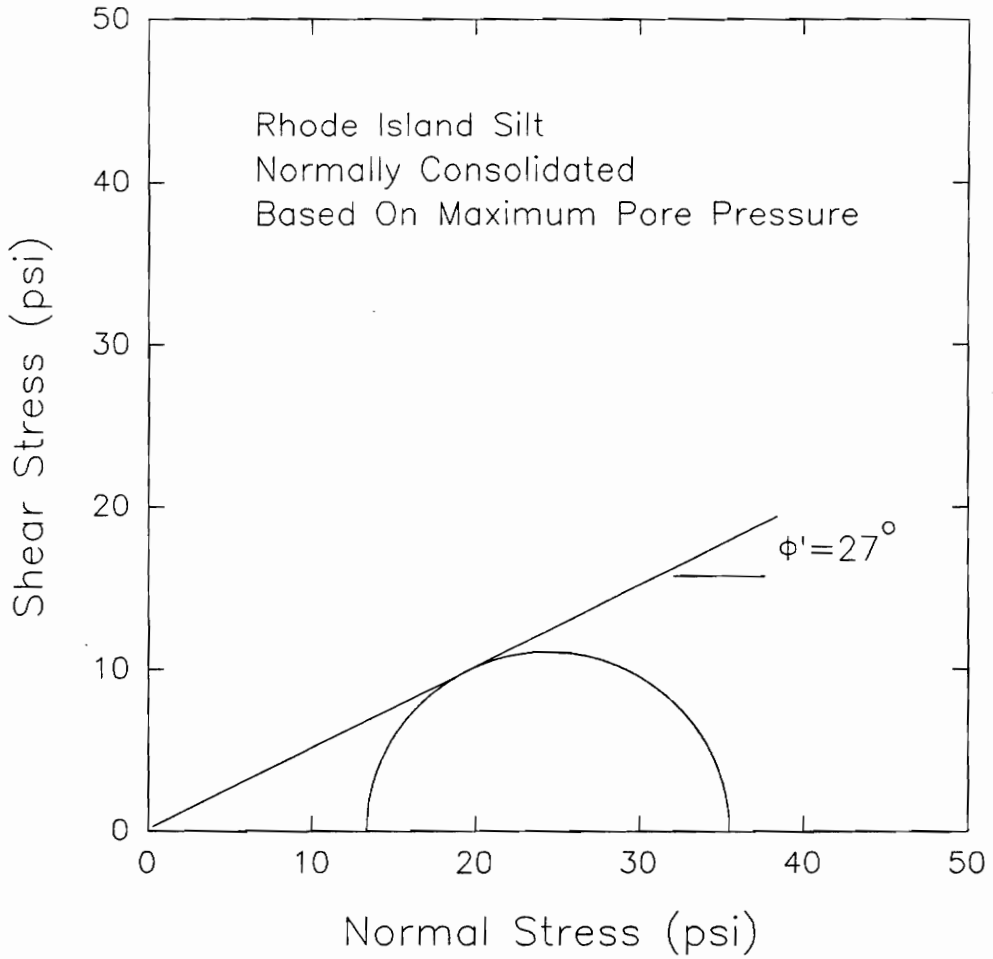

Figure 110 Effective Stress Mohr's Circle Measured For CU Triaxial Test On Normally Consolidated Rhode Island Silt For Failure Based On Maximum Pore Pressure

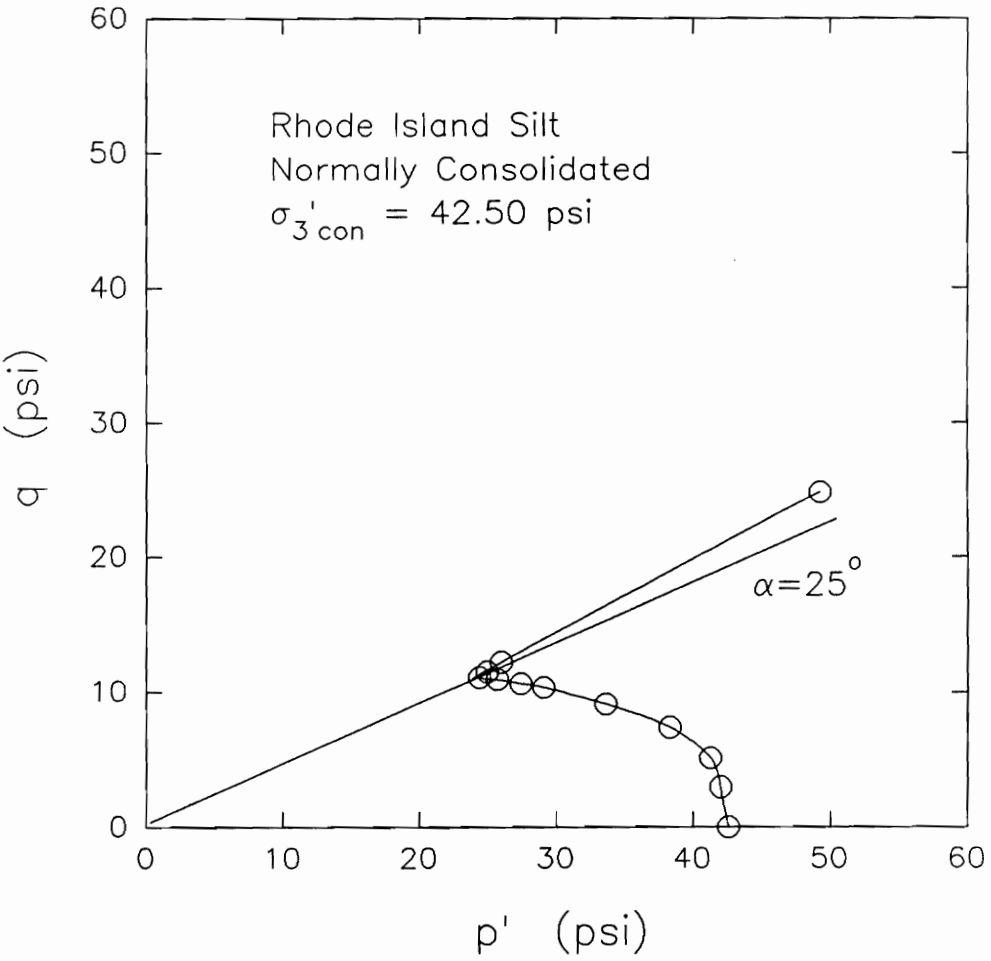

Figure 111 Effective Stress Path Measured For CU Triaxial Test On Normally Consolidated Rhode Island Silt

Total Stress Interpretation of CU Test On Remolded Rhode Island Silt

Undrained shear strength can also be determined using the consolidated undrained triaxial test. This is done by determining the relationship between the undrained shear strength, S_u, measured during the test and the effective consolidation pressure, $\sigma_3'_{con}$. For normally consolidated clays, the undrained strength ratio, S_u/p, is constant.

Shown in Figure 112 is the relationship between the undrained strength and effective consolidation pressure for the Rhode Island silt. This is based on maximum pore pressure. No other data can be compared to this relationship because there is only one failure criteria satisfied in this test. The slope of the line drawn from the origin through the data point represents the undrained strength ratio. The value of S_u/p derived from this test is 0.26. This can be compared to Skempton's correlation of S_u/p. Using a plasticity index equal to 6%, the correlation would give an S_u/p equal to 0.13.

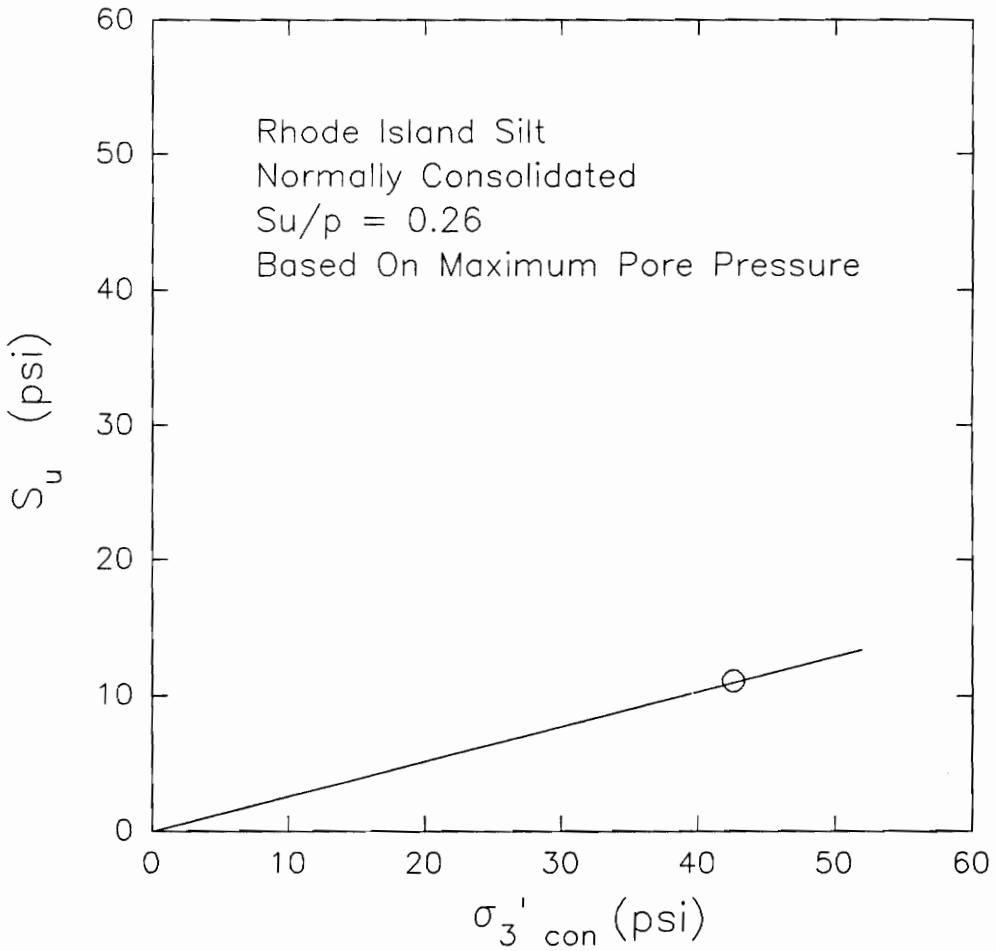

Figure 112 Undrained Shear Strength-Effective Consolidation Pressure Relationship Measured For CU Triaxial Test On Normally Consolidated Rhode Island Silt For Failure Based On Maximum Pore Pressure

Yukon Silt

Hampton (1981) summarized the triaxial tests results performed for Yukon silt. The samples were obtained from the western and central portion of the Yukon Prodelta in Norton Sound, Alaska. The specimens were tested at Cornell University in the summer of 1979.

Consolidated Undrained Test On Normally Consolidated Undisturbed Yukon Silt (Western Prodelta)

Undisturbed samples of Yukon silt obtained from the western prodelta were tested in CU triaxial tests. The effective consolidation pressure used in the test was 42.60 psi. This corresponds to an induced overconsolidation ratio equal to 1.

Figure 113 shows the deviator stress-strain relationship for the specimen. Similar to the previous silt samples, there was a rapid increase in deviator stress at small strains. After a steep portion, the deviator stress continued to increase with strain, following a flatter slope. No peak was observed on the stress-strain diagram. The test was generally terminated at 10% strain or when a failure plane was observed in the sample.

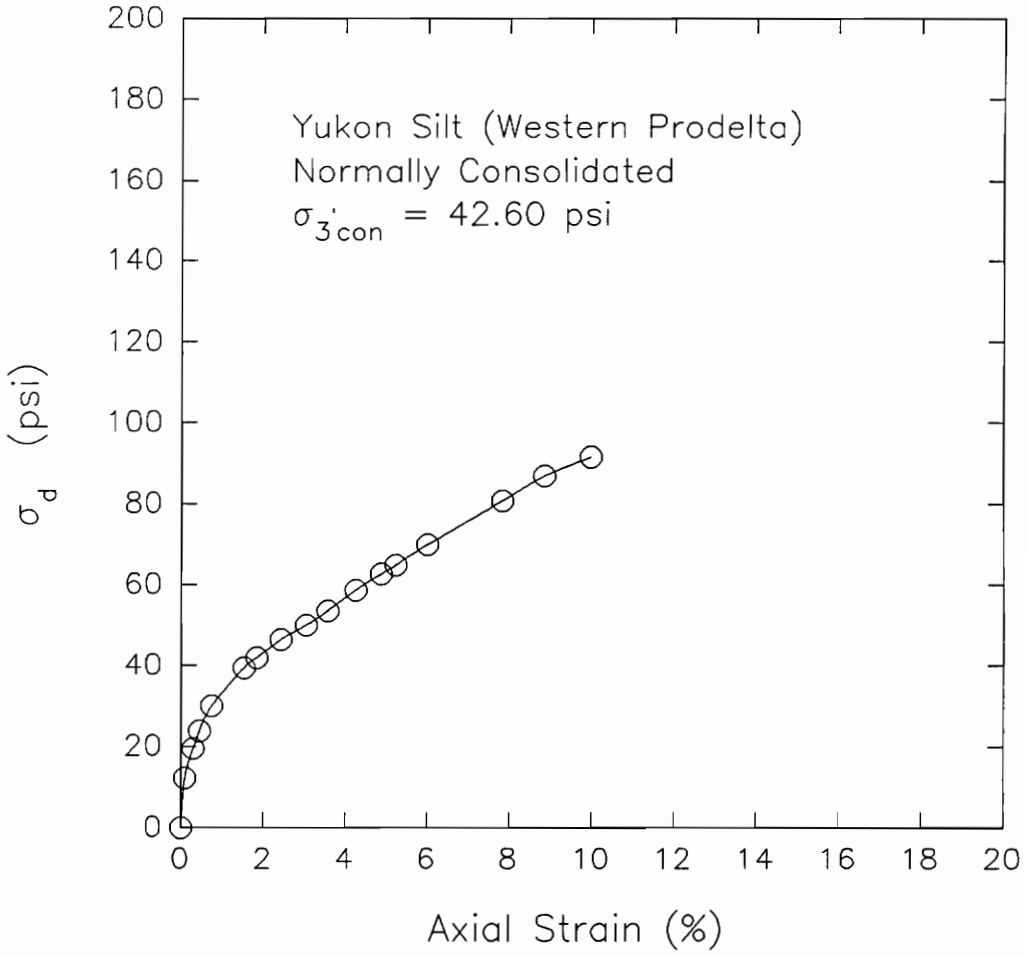

Figure 113 Deviator Stress-Strain Relationship Measured For CU Triaxial Test On Undisturbed Sample of Normally Consolidated Yukon Silt (Western Prodelta)

Figures 114 and 115 illustrate the minor effective stress-strain and principal stress ratio-strain relationships. The sample had a maximum principal stress ratio equal to 5.70 at a strain of about 5%.

Shown in Figures 116 and 117 are the A-bar-strain and pore pressure-strain relationships. The pore pressure increased rapidly at small strains and reached a peak at a strain of about 3.5%. Although the pore pressure decreased after reaching a maximum value, it remained positive throughout the test.

The effective stress path for the specimen is shown in Figure 118. The behavior exhibited by the stress path was to approach the K_f line at low strains and continue to climb the K_f line as strains increased. An α equal to 35° was measured, which corresponds to an effective stress friction angle equal to 44°.

Effective Stress Interpretation of The CU Triaxial Test On Normally Consolidated Undisturbed Yukon Silt (Western Prodelta)

Some of the failure criteria cannot be applied to the test results since the test was terminated at low strains.

Figure 119 illustrates the Mohr's circle for failure based on maximum pore pressure. Constraining the

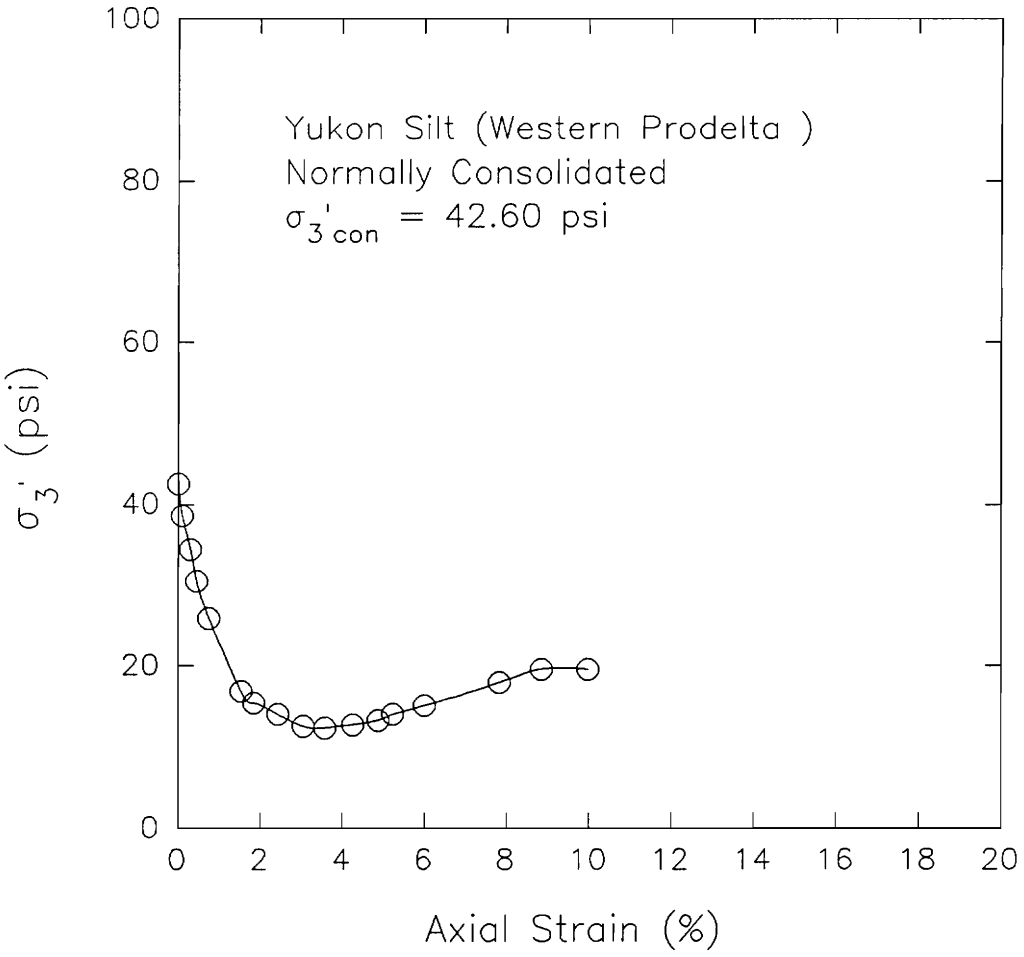

Figure 114 Minor Effective Stress-Strain Relationship Measured For CU Triaxial Test On Undisturbed Sample of Normally Consolidated Yukon Silt (Western Prodelta)

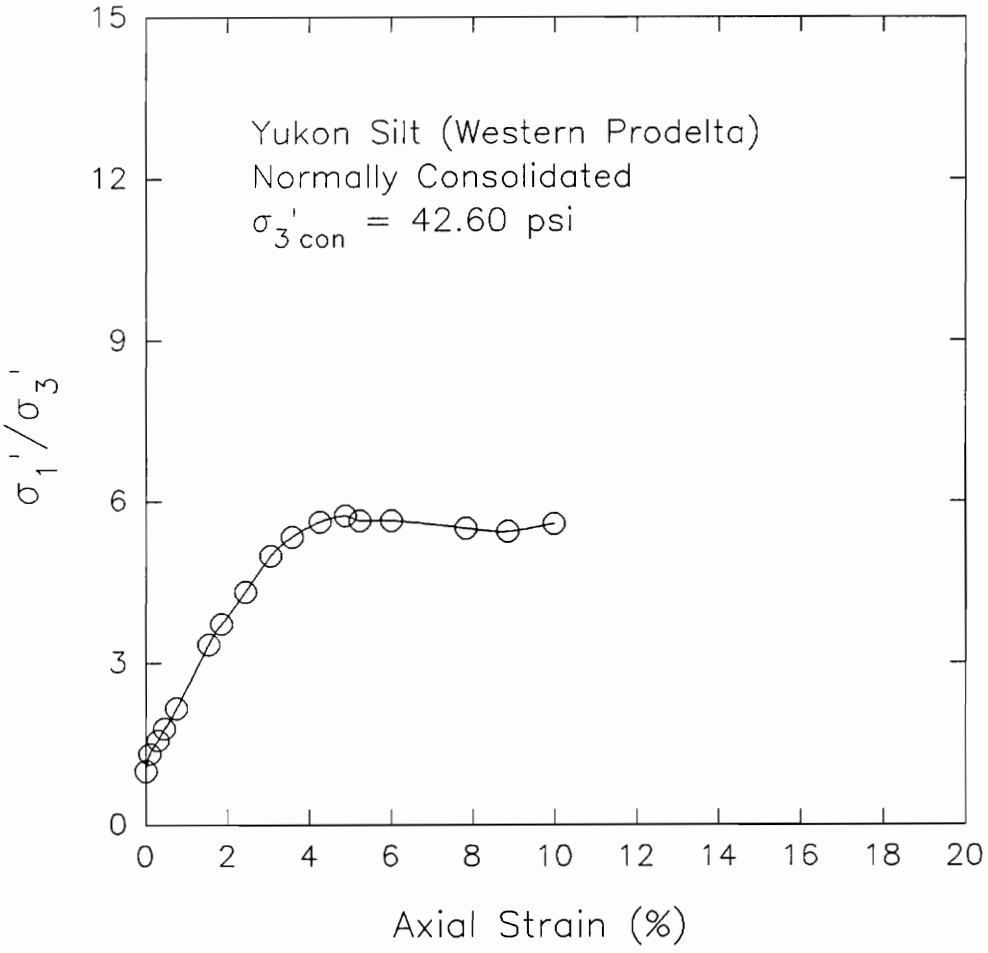

Figure 115 Principal Stress Ratio-Strain Relationship Measured For CU Triaxial Test On Undisturbed Sample of Normally Consolidated Yukon Silt (Western Prodelta)

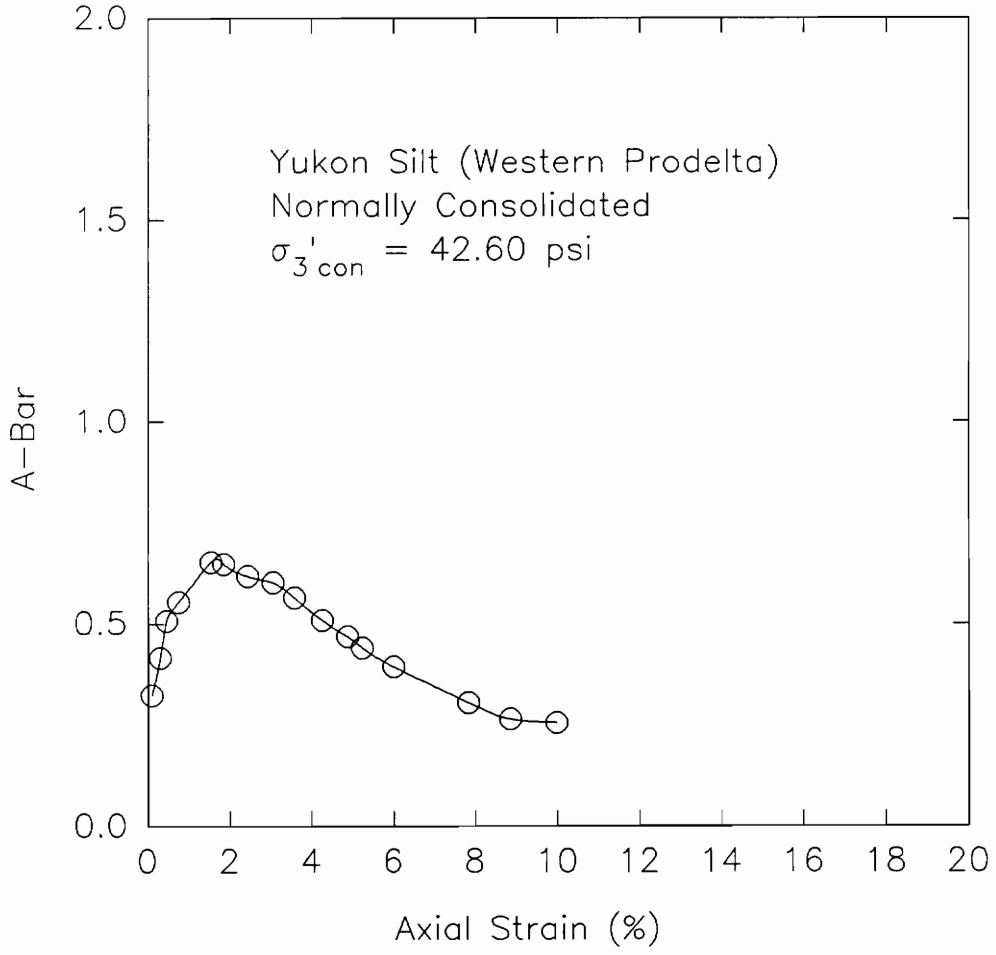

Figure 116 A-bar-Strain Relationship Measured For CU Triaxial Test On Undisturbed Sample of Normally Consolidated Yukon Silt (Western Prodelta)

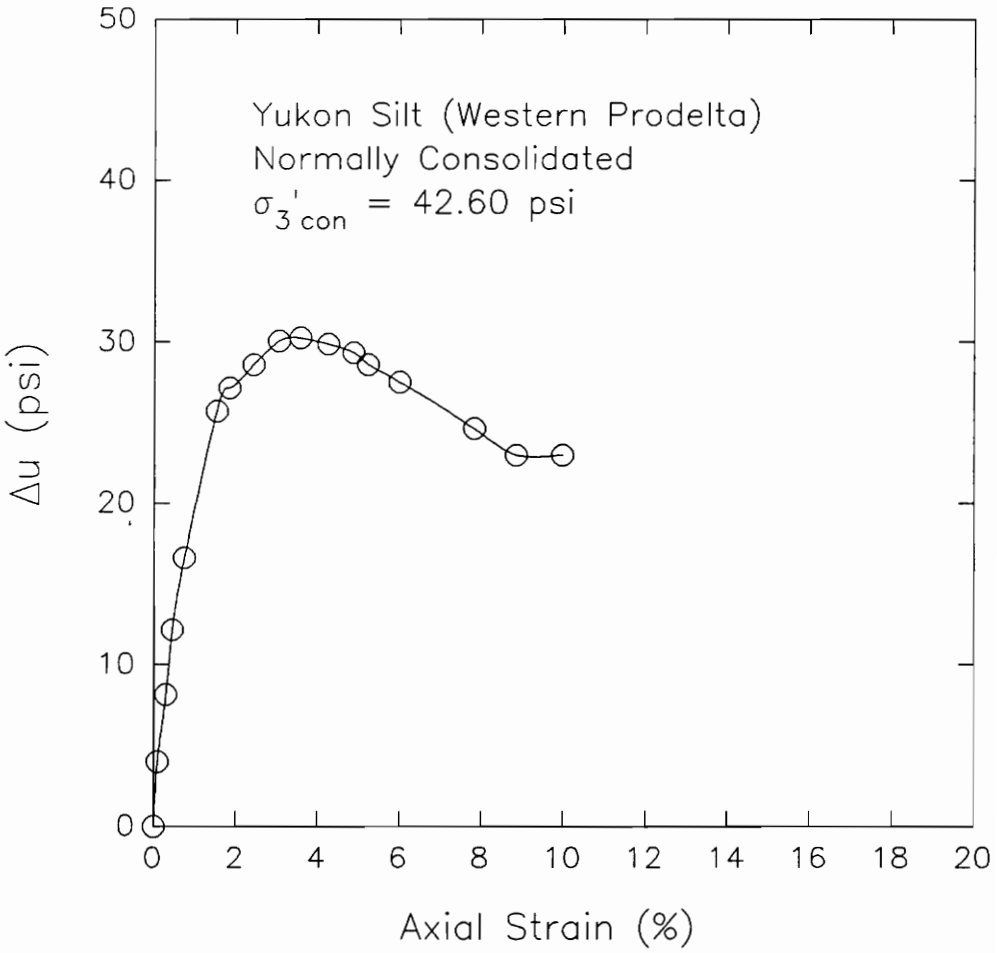

Figure 117 Pore Pressure-Strain Relationship Measured For CU Triaxial Test On Undisturbed Sample of Normally Consolidated Yukon Silt (Western Prodelta)

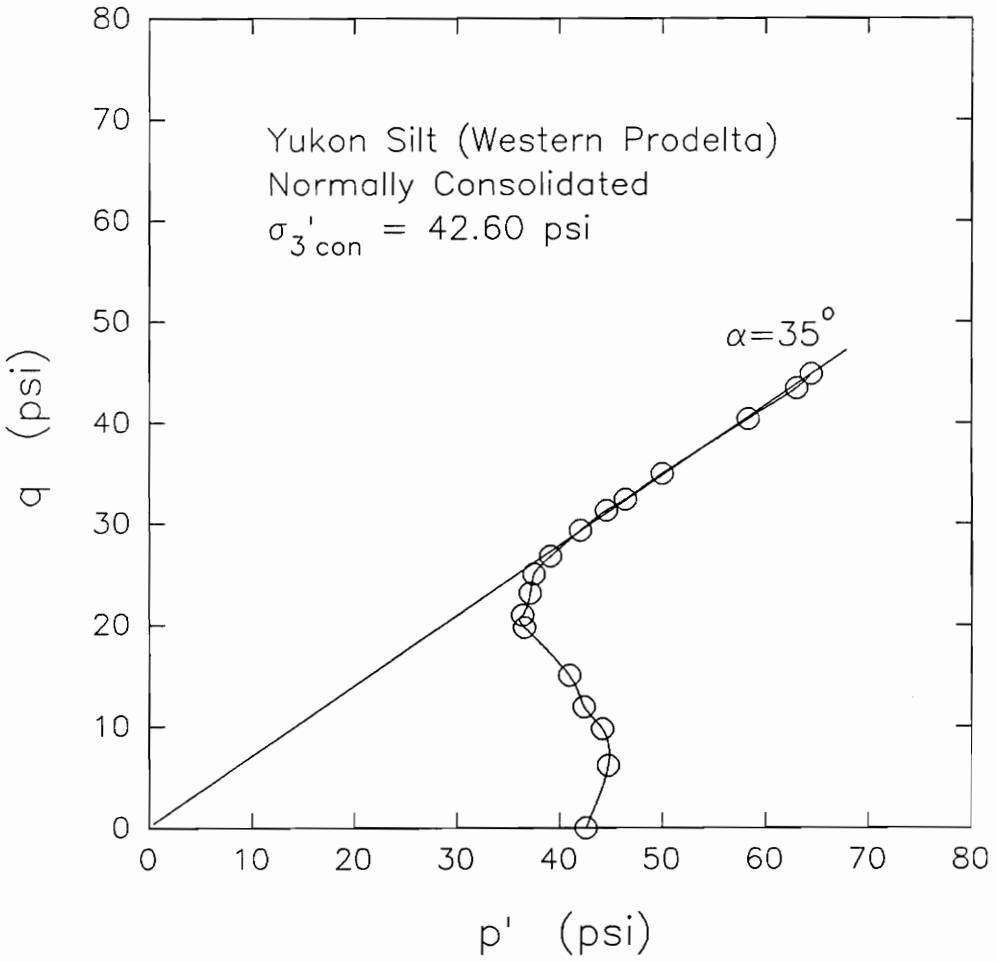

Figure 118 Effective Stress Path Measured For CU Triaxial Test On Undisturbed Sample of Normally Consolidated Yukon Silt (Western Prodelta)

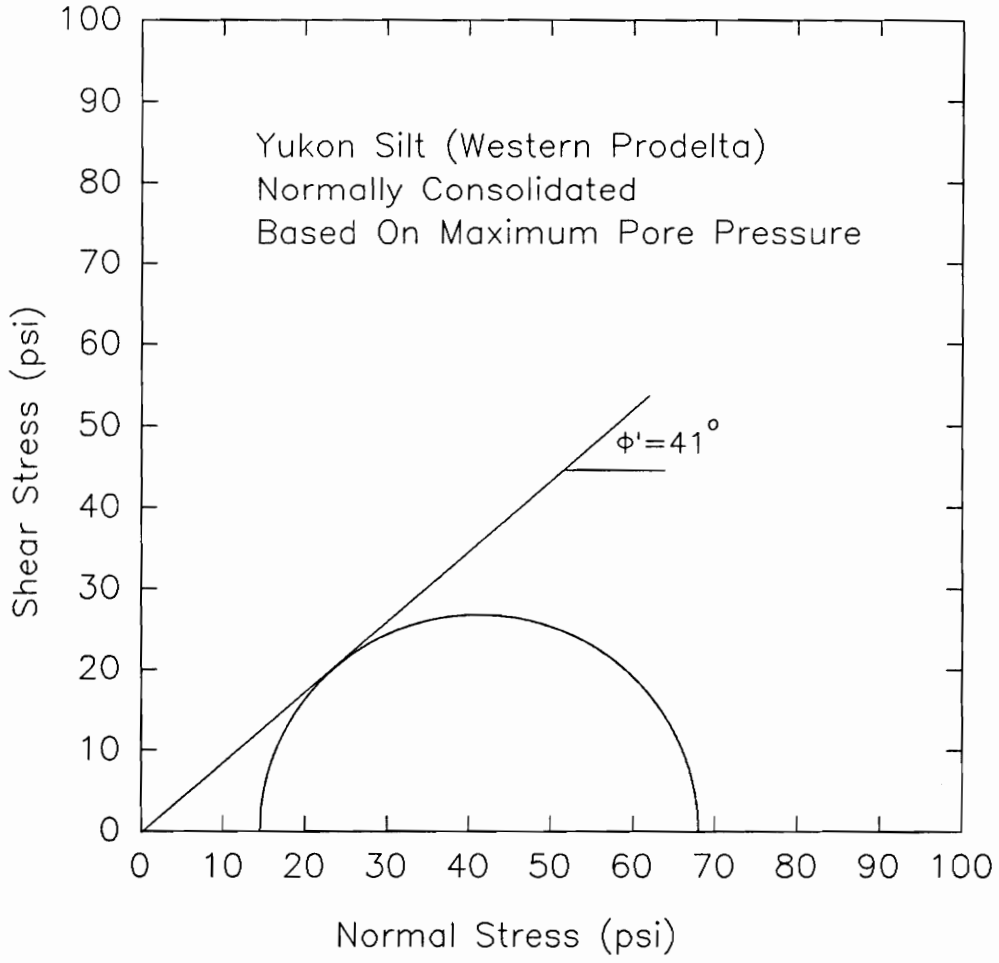

Figure 119 Effective Stress Mohr's Circle Measured For CU Triaxial Tests On Undisturbed Sample of Normally Consolidated Yukon Silt For Failure Based On Maximum Pore Pressure (Western Prodelta)

effective cohesion intercept to zero, the effective stress friction angle calculated is equal to 41°.

A ϕ' equal to 45° was measured based on maximum principal stress ratio. The Mohr's circle for this failure criterion is shown in Figure 120.

Shown in Figure 121 is the Mohr's circle based on 10% limiting strain. The value of the effective stress friction angle measured using this failure criterion is 45°.

A summary of the effective stress friction angles for the different failure criteria is given in Table 32. The value of ϕ' obtained using the different failure criteria applied, except maximum pore pressure, are all equal to 45°. This can be well compared with the ϕ' obtained from the effective stress path which gave a value equal to 44°.

Total Stress Interpretation Of The CU Triaxial Test On Undisturbed Sample of Normally Consolidated Yukon Silt (Western Prodelta)

The determination of the undrained strength ratio for these test results was done in the same manner as the previous silt samples.

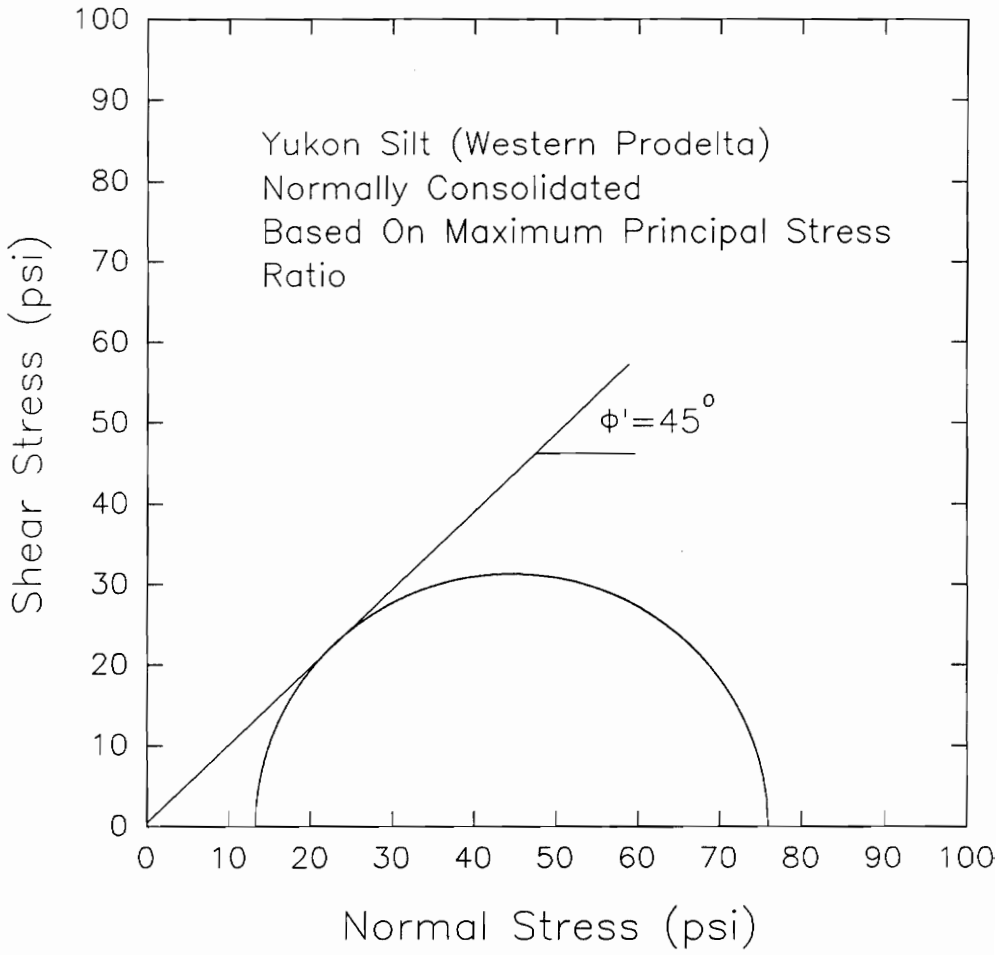

Figure 120 Effective Stress Mohr's Circle Measured For CU Triaxial Tests On Undisturbed Sample of Normally Consolidated Yukon Silt For Failure Based On Maximum Principal Stress Ratio (Western Prodelta)

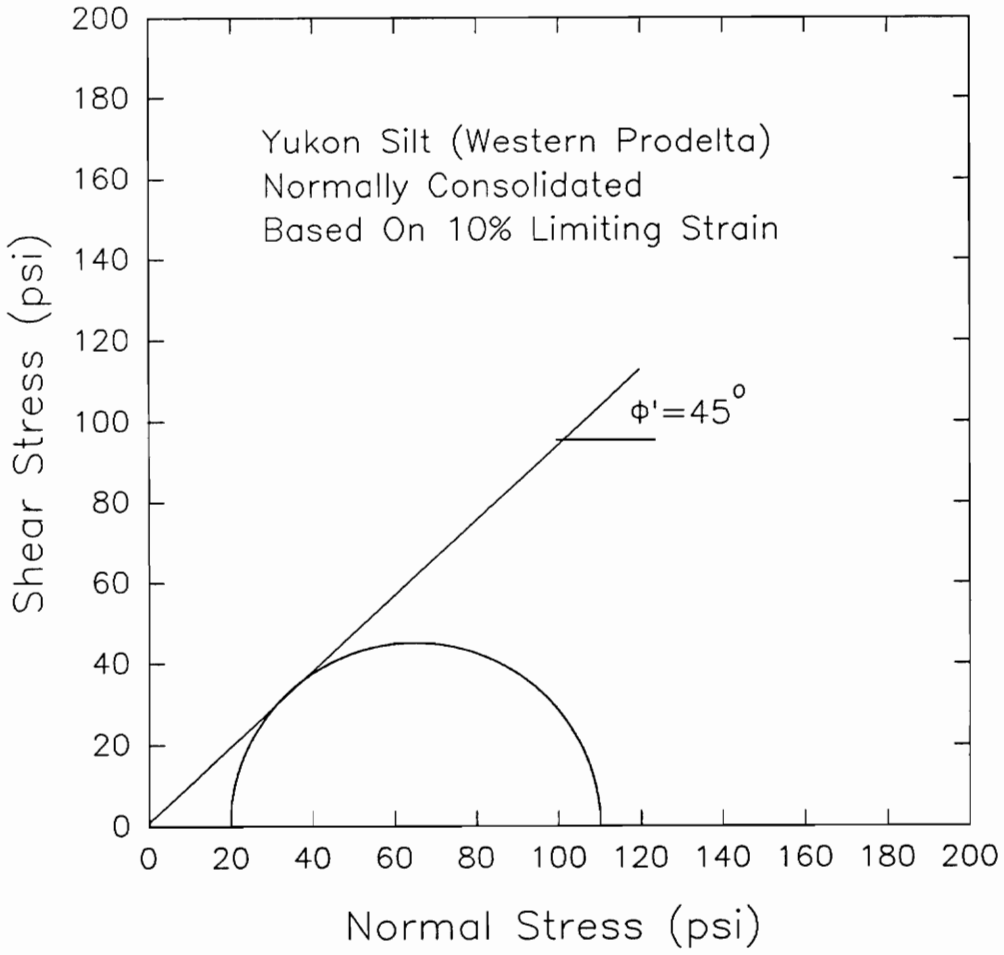

Figure 121 Effective Stress Mohr's Circle Measured For CU Triaxial Tests On Undisturbed Sample of Normally Consolidated Yukon Silt For Failure Based On 10% Limiting Strain (Western Prodelta)

Table 32 Values of ϕ' Determined For The Different Failure Criteria for Yukon Silt (Western Prodelta)

Failure Criteria	ϕ' (Degrees)	Average Strain To Failure (%)
u_{max}	41	3.5
Max $(\sigma_1-\sigma_3)$	N/A	N/A
Max (σ_1'/σ_3')	45	5.0
10% Limiting Strain	45	10
15% Limiting Strain	N/A	N/A
A-bar = 0	N/A	N/A

Figure 122 shows the relationship between the undrained shear strength and effective consolidation pressure for failure based on maximum pore pressure. The S_u/p ratio calculated is equal to 0.63.

Shown in Figure 123 is the determination of S_u/p based on maximum principal stress ratio. An S_u/p of 0.74 was measured for this failure criterion.

Using 10% limiting strain as failure criterion, the S_u/p calculated is equal to 1.10. This is shown in Figure 124.

Table 33 summarizes the S_u/p ratios determined for the different failure criteria. The lowest value of Su/p was obtained for failure based on maximum pore pressure.

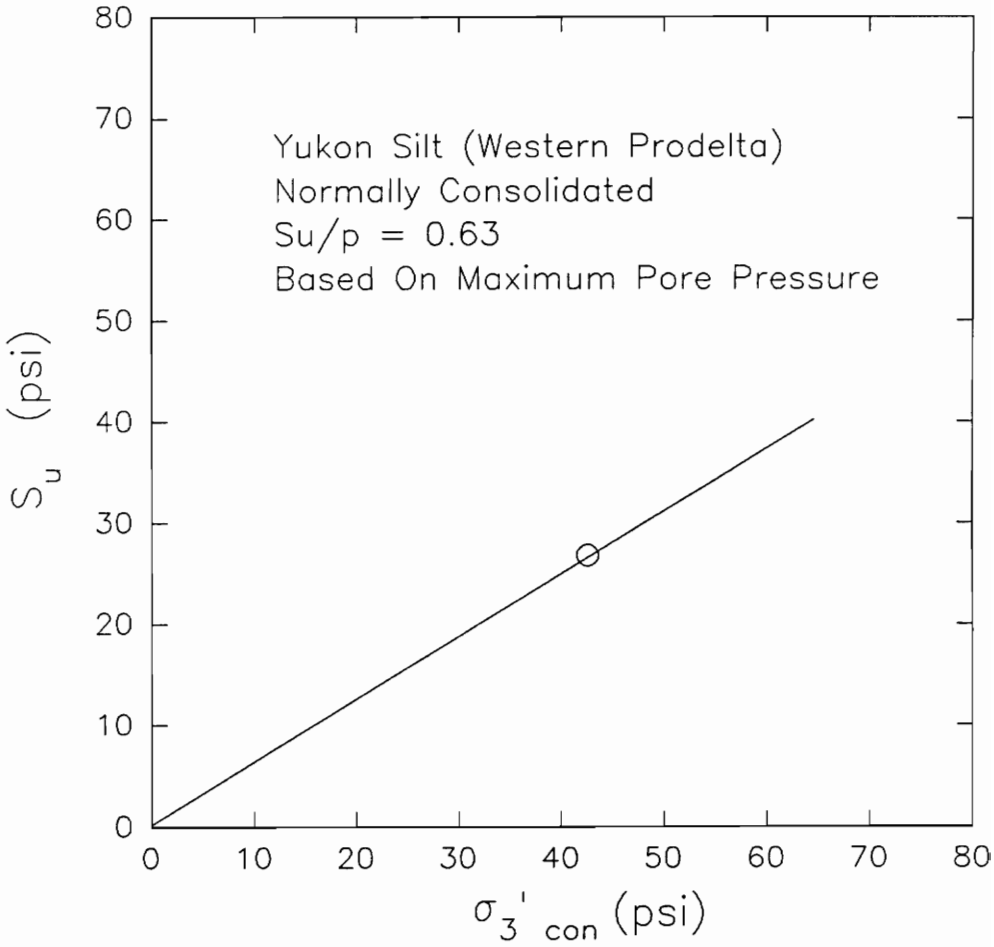

Figure 122 Undrained Shear Strength-Effective Consolidation Pressure Relationship Measured For CU Triaxial Test On Undisturbed Sample of Normally Consolidated Yukon Silt For Failure Based On Maximum Pore Pressure (Western Prodelta)

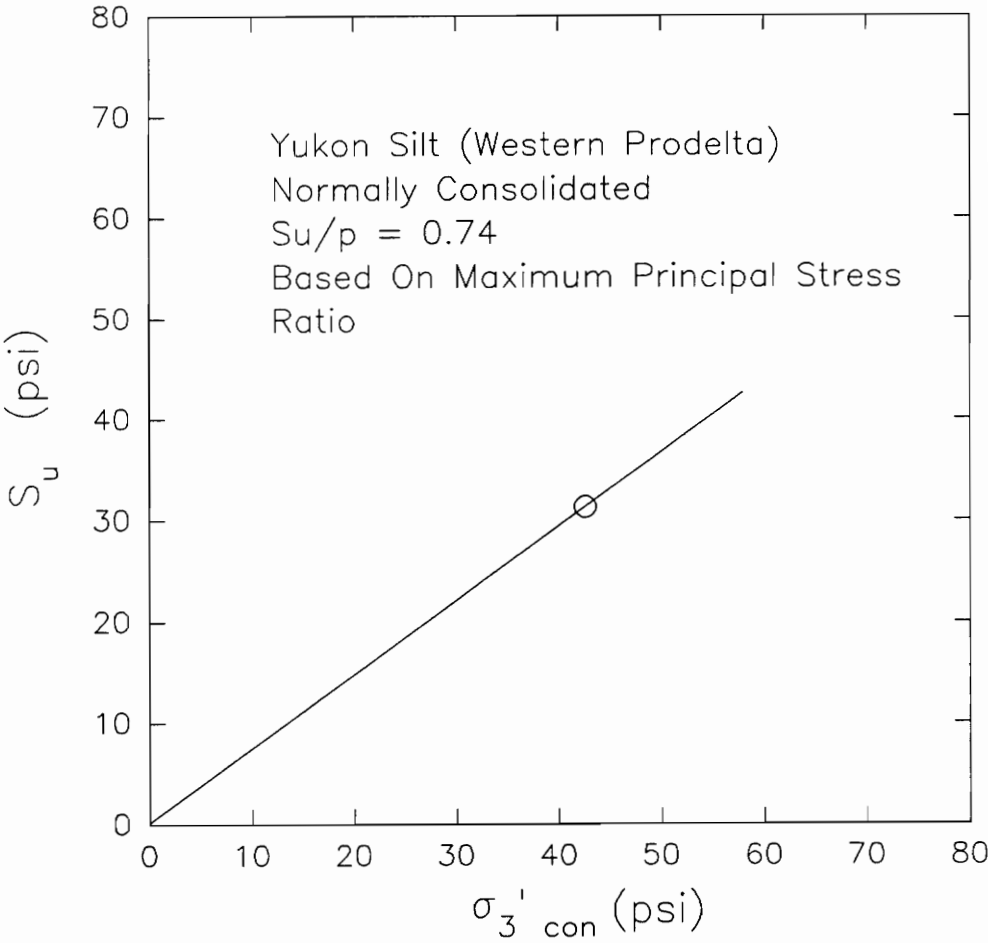

Figure 123 Undrained Shear Strength-Effective Consolidation Pressure Relationship Measured For CU Triaxial Test On Undisturbed Sample of Normally Consolidated Yukon Silt For Failure Based On Maximum Principal Stress Ratio (Western Prodelta)

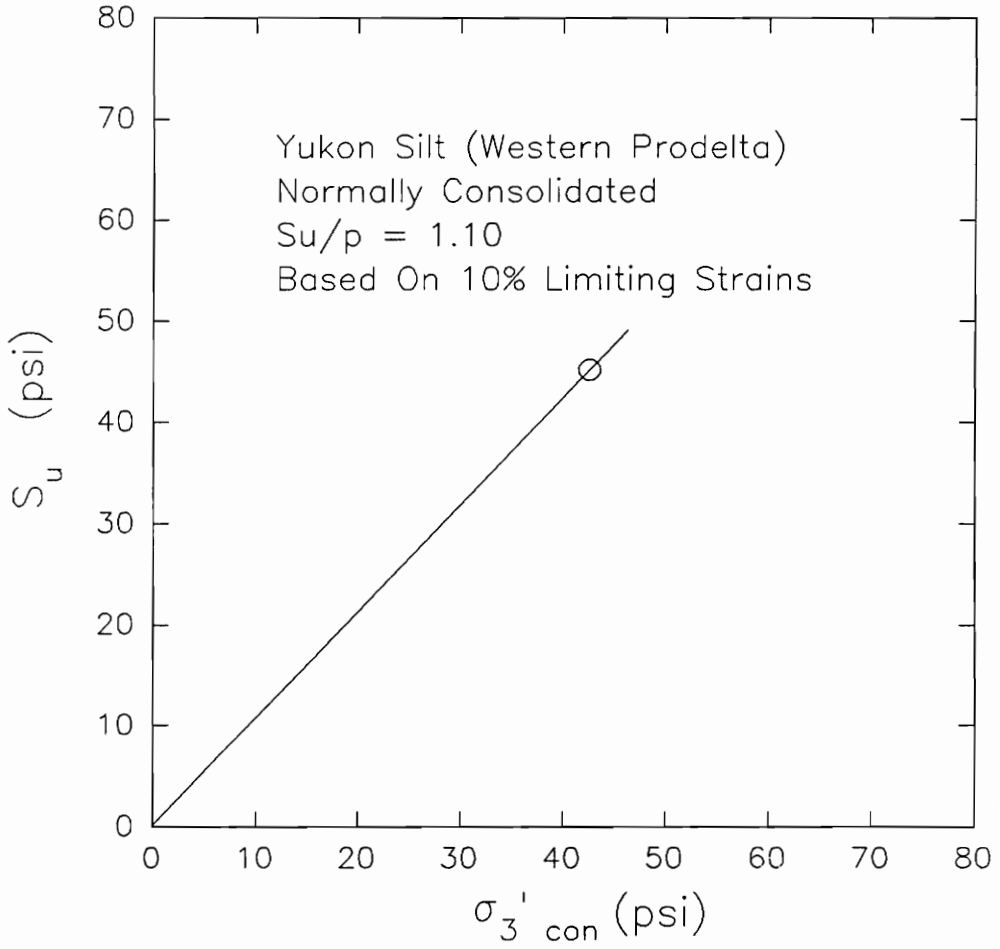

Figure 124 Undrained Shear Strength-Effective Consolidation Pressure Relationship Measured For CU Triaxial Test On Undisturbed Sample of Normally Consolidated Yukon Silt For Failure Based On 10% Limiting Strain (Western Prodelta)

Table 33 S_u/p Ratios Determined For The Different Failure Criteria for Yukon Silt (Western Prodelta)

Failure Criteria	S_u/p	Average Strain To Failure (%)
u_{max}	0.63	3.5
Max $(\sigma_1-\sigma_3)$	N/A	N/A
Max (σ_1'/σ_3')	0.74	5.0
10% Limiting Strain	1.10	10
15% Limiting Strain	N/A	N/A
A-bar = 0	N/A	N/A

Consolidated Undrained Triaxial Tests On Normally Consolidated Undisturbed Samples of Yukon Silt (Central Prodelta)

A series of CU triaxial tests were performed on undisturbed samples of Yukon silt. The samples were obtained from central prodelta. The effective consolidation pressures used for the test were 3.3 psi, 5.6 psi, 14.7 psi, 42.3 psi, 44.0 psi, and 50.0 psi.

Shown in Figure 125 are the deviator stress-strain relationships for the samples. Similar to the sample from western prodelta, the stress-strain diagrams had a rapid increase in the deviator stress at small range of strains. Three samples had a peak in the stress-strain diagrams at an average strain of 10%. Because of the dilative tendencies of the other specimens, the deviator stresses continued to increase with increasing strains. Failure did not correspond to peak deviator stress for these samples.

Figure 126 and 127 illustrate the minor effective stress-strain and principal stress ratio-strain relationships. The samples reached an average maximum principal stress ratio equal to 4.6 at an average strain of 5%.

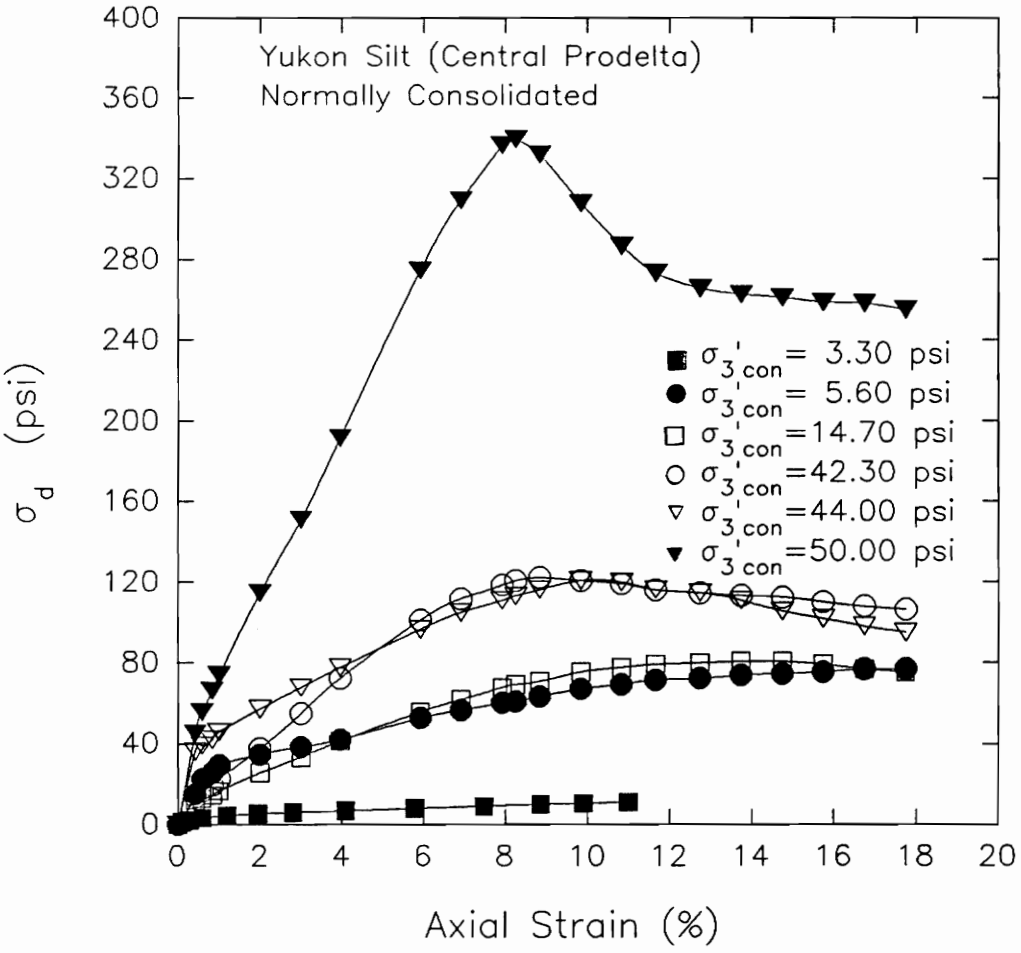

Figure 125 Deviator Stress-Strain Relationship Measured For CU Triaxial Tests On Undisturbed Samples of Yukon Silt (Central Prodelta)

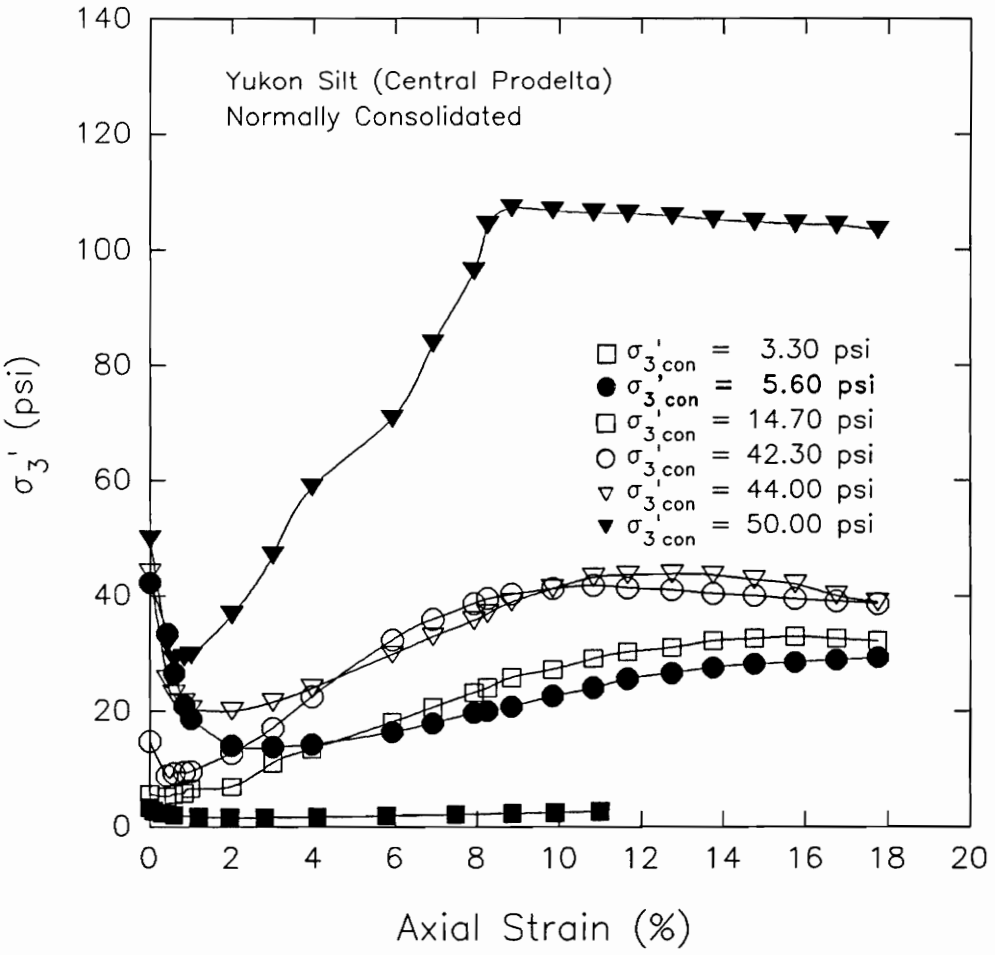

Figure 126 Minor Effective Stress-Strain Relationship Measured For CU Triaxial Tests On Undisturbed Samples of Yukon Silt (Central Prodelta)

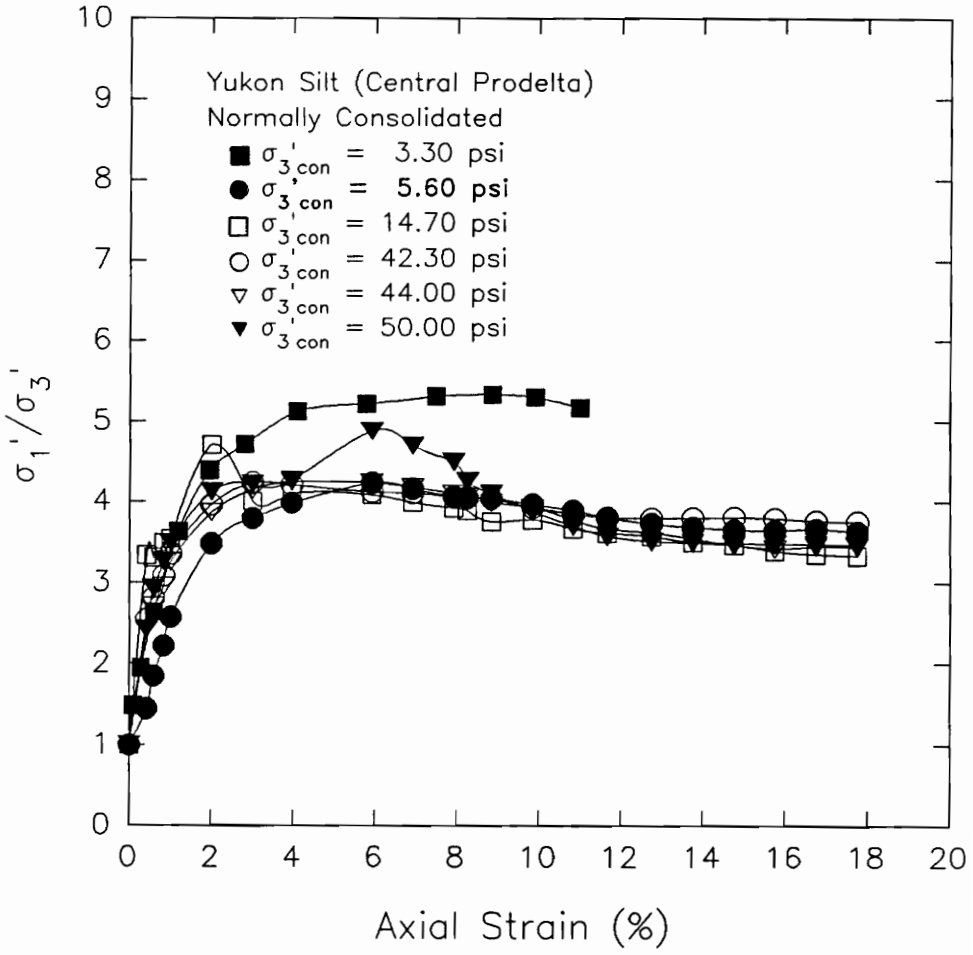

Figure 127 Principal Stress Ratio-Strain Relationship Measured For CU Triaxial Tests On Undisturbed Samples of Yukon Silt (Central Prodelta)

A-bar-strain and pore pressure strain relationships are shown in Figures 128 and 129. The pore pressures peaked at a strain of about 1%, then decreased continually as strains increased. The samples consolidated to 3.3 psi, 42.3 psi, and 44 psi had positive pore pressures throughout the tests.

Figure 130 shows the effective stress paths for the specimens. The behavior exhibited by the stress paths were to approach the K_f line at low strains and continued to climb the K_f as strains increased. The K_f line defined by the stress paths defines an α equal to 32°. This corresponds to an effective stress friction angle, ϕ', equal to 38°.

Effective Stress Interpretation of The CU Triaxial Tests On Normally Consolidated Undisturbed Samples of Yukon Silt (Central Prodelta)

The test results indicate that not all the different failure criteria could be applied for all the samples. The effective stress interpretation for these samples were done in the same manner as the previous silt samples.

Figure 131 shows the Mohr's circles for failure based on maximum pore pressure. The results show that

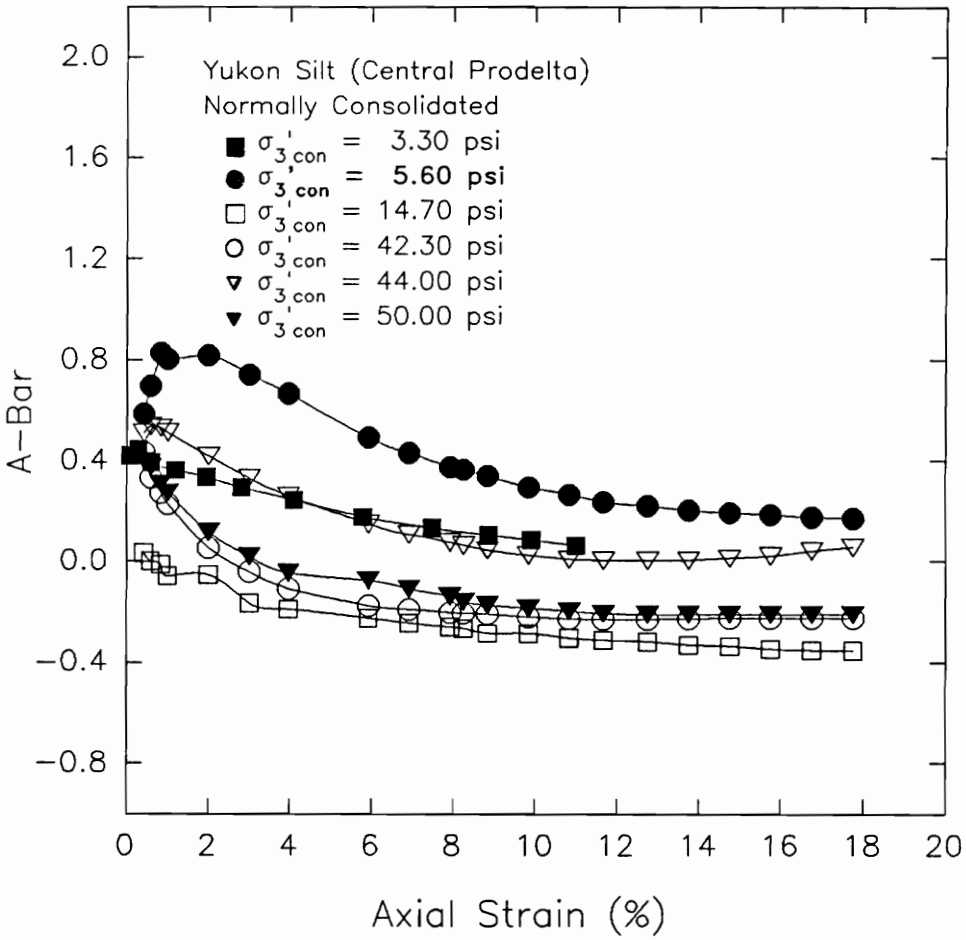

Figure 128 A-bar-Strain Relationship Measured For CU Triaxial Tests On Undisturbed Samples of Yukon Silt (Central Prodelta)

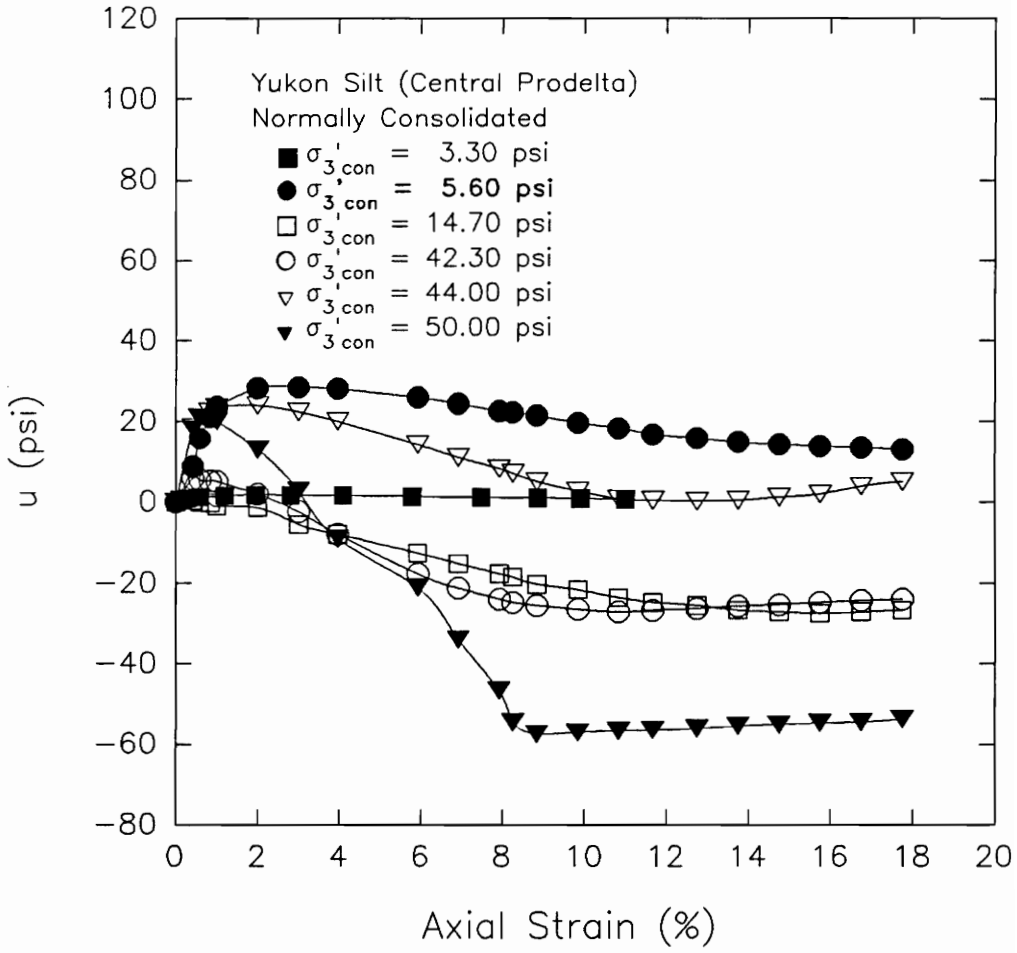

Figure 129 Pore Pressure-Strain Relationship Measured For CU Triaxial Tests On Undisturbed Samples of Yukon Silt (Central Prodelta)

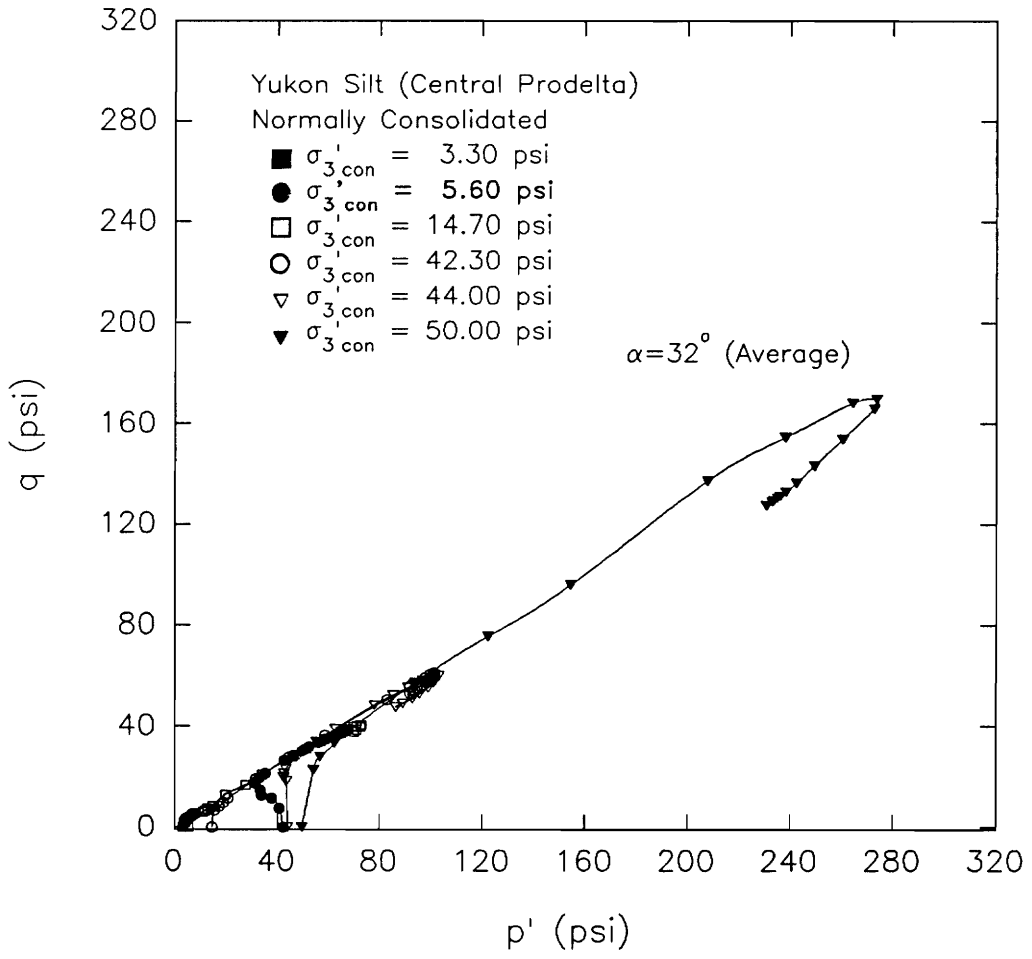

Figure 130 Effective Stress Paths Measured For CU Triaxial Tests On Undisturbed Samples of Yukon Silt (Central Prodelta)

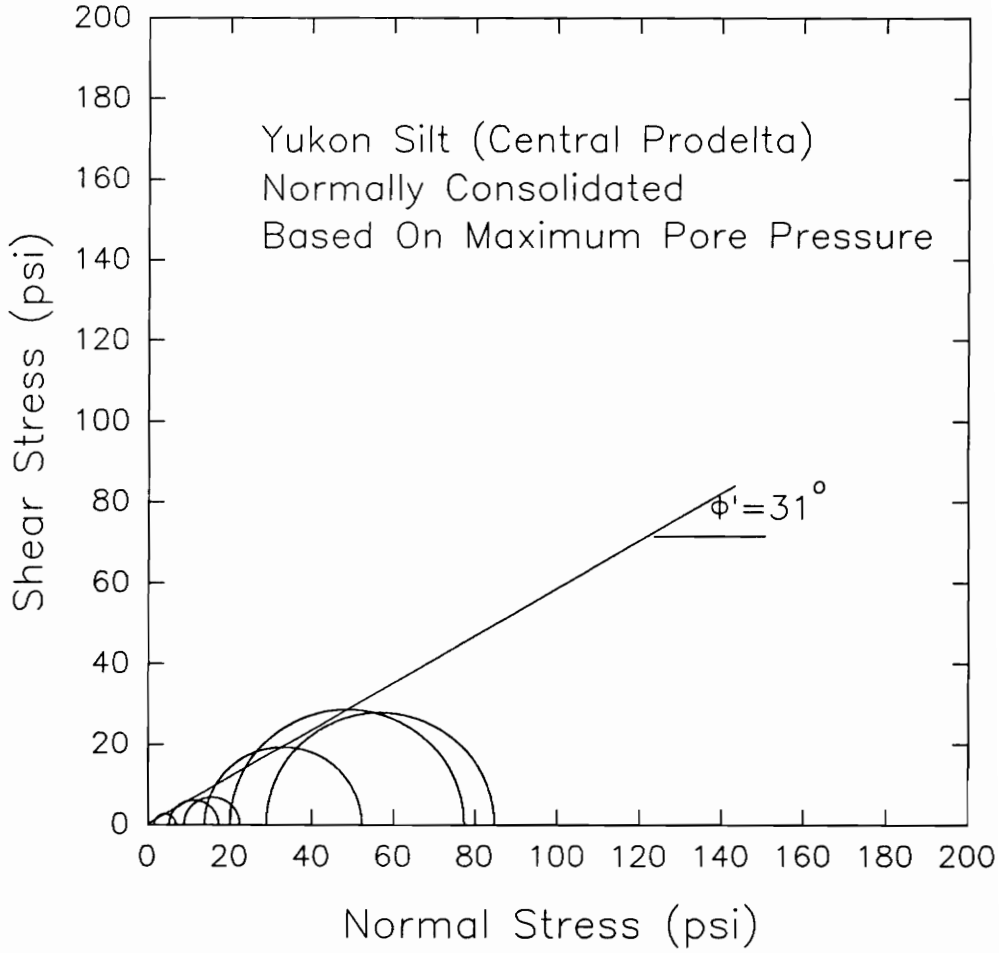

Figure 131 Effective Stress Mohr's Circles Measured For CU Triaxial Tests On Undisturbed Samples of Yukon Silt For Failure Based On Maximum Pore Pressure (Central Prodelta)

there was scatter in the data. With the effective cohesion intercept constrained to zero, the envelope gave an effective stress friction angle equal to 31°.

Figure 132 illustrates the Mohr's circles based on maximum deviator stress as failure criterion. The effective stress friction angle calculated is equal to 36°.

The Mohr's circles based on maximum principal stress ratio are shown in Figure 133. There was little scatter in the data. The effective stress friction angle measured for this failure criterion is equal to 37°.

Figures 134 and 135 illustrate the Mohr's circles using 10% and 15% limiting strains. A ϕ' equal to 35° was measured for both failure criteria.

An effective stress friction angle equal to 37° was measured using A-bar as failure criterion. The Mohr's circles are shown in Figure 136.

A summary of the effective stress friction angles for the different failure criteria is given in Table 34. Similar to the other silt samples, the lowest value of ϕ' was measured using maximum pore pressure as failure criterion. The ϕ' calculated from the other failure criteria ranged from 35° to 37°, which can be compared to a ϕ' equal to 38° obtained from the effective stress path.

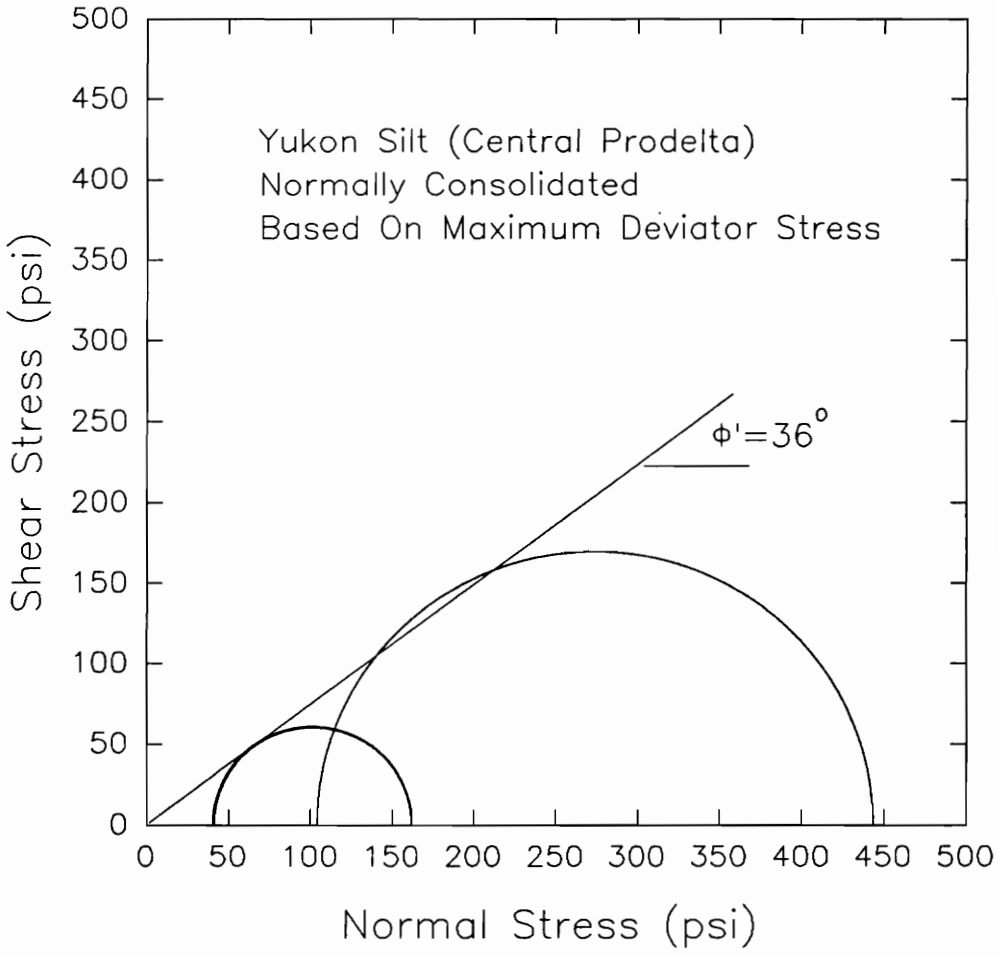

Figure 132 Effective Stress Mohr's Circles Measured For CU Triaxial Tests On Undisturbed Samples of Yukon Silt For Failure Based On Maximum Deviator Stress (Central Prodelta)

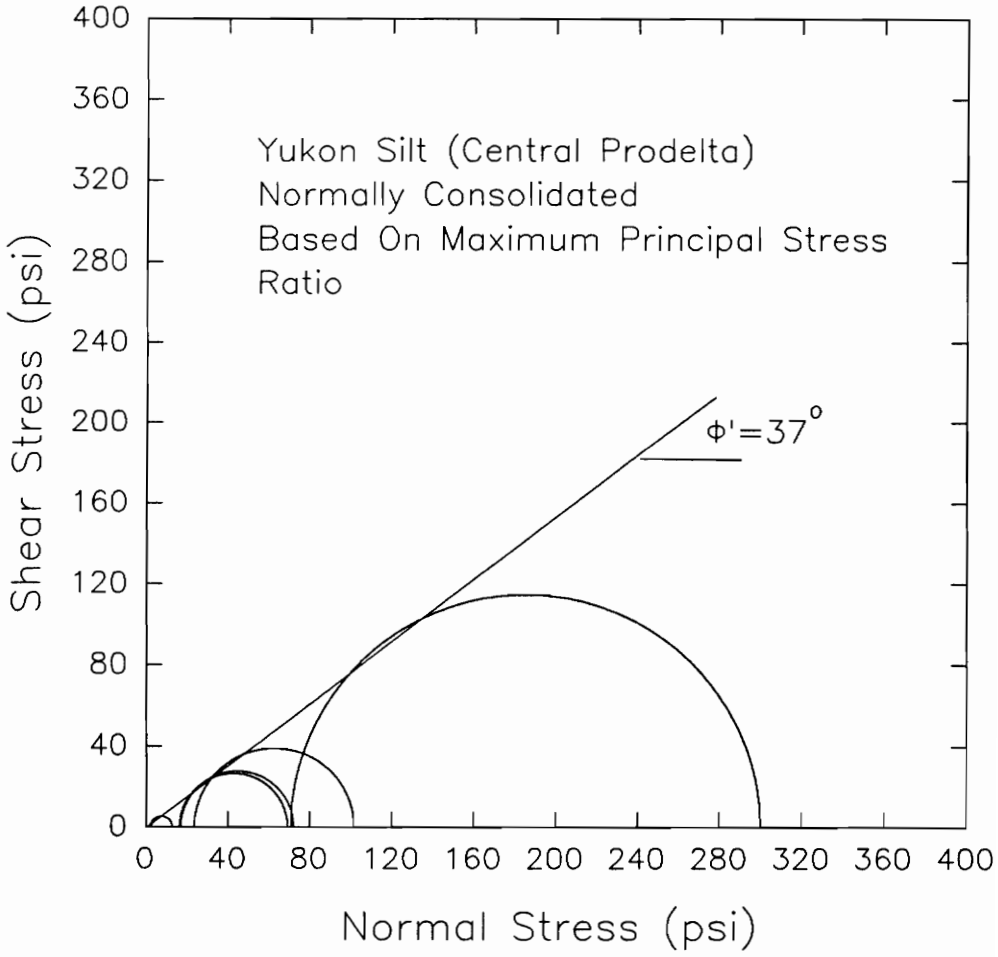

Figure 133 Effective Stress Mohr's Circles Measured For CU Triaxial Tests On Undisturbed Samples of Yukon Silt For Failure Based On Maximum Principal Stress Ratio (Central Prodelta)

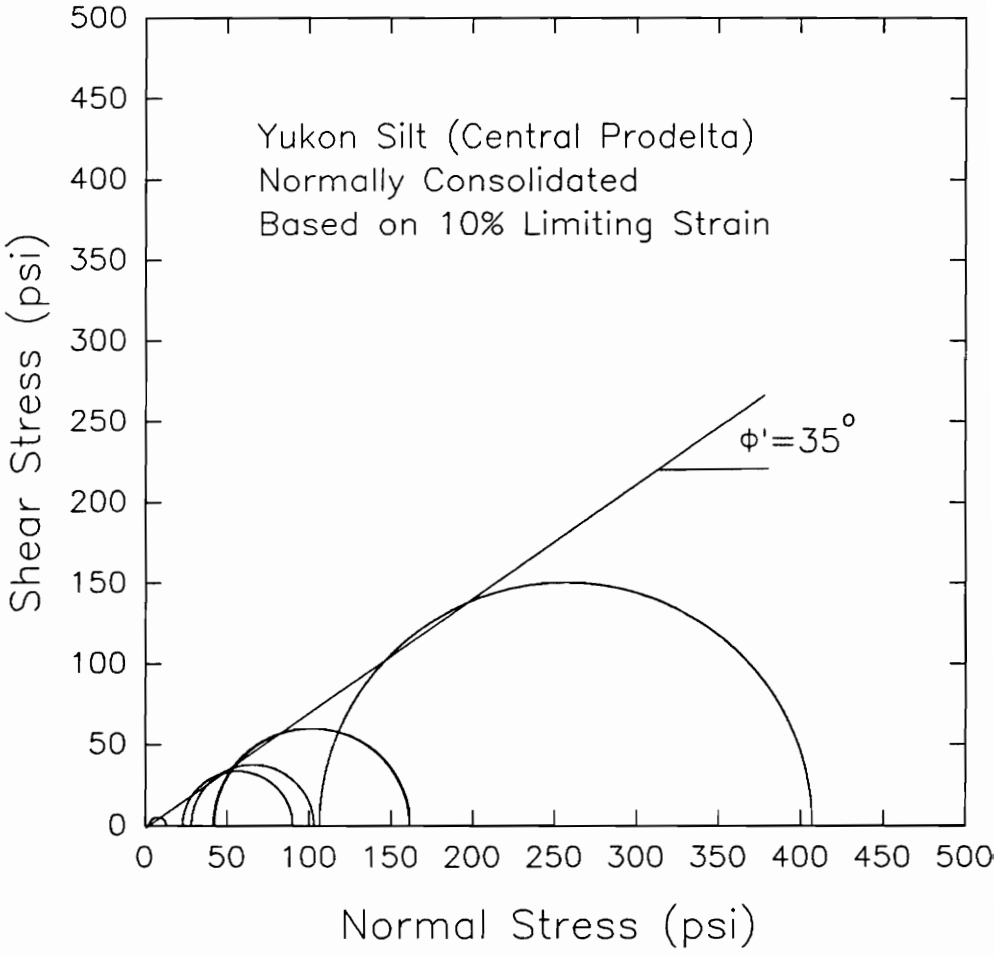

Figure 134 Effective Stress Mohr's Circles Measured For CU Triaxial Tests On Undisturbed Samples of Yukon Silt For Failure Based On 10% Limiting Strain (Central Prodelta)

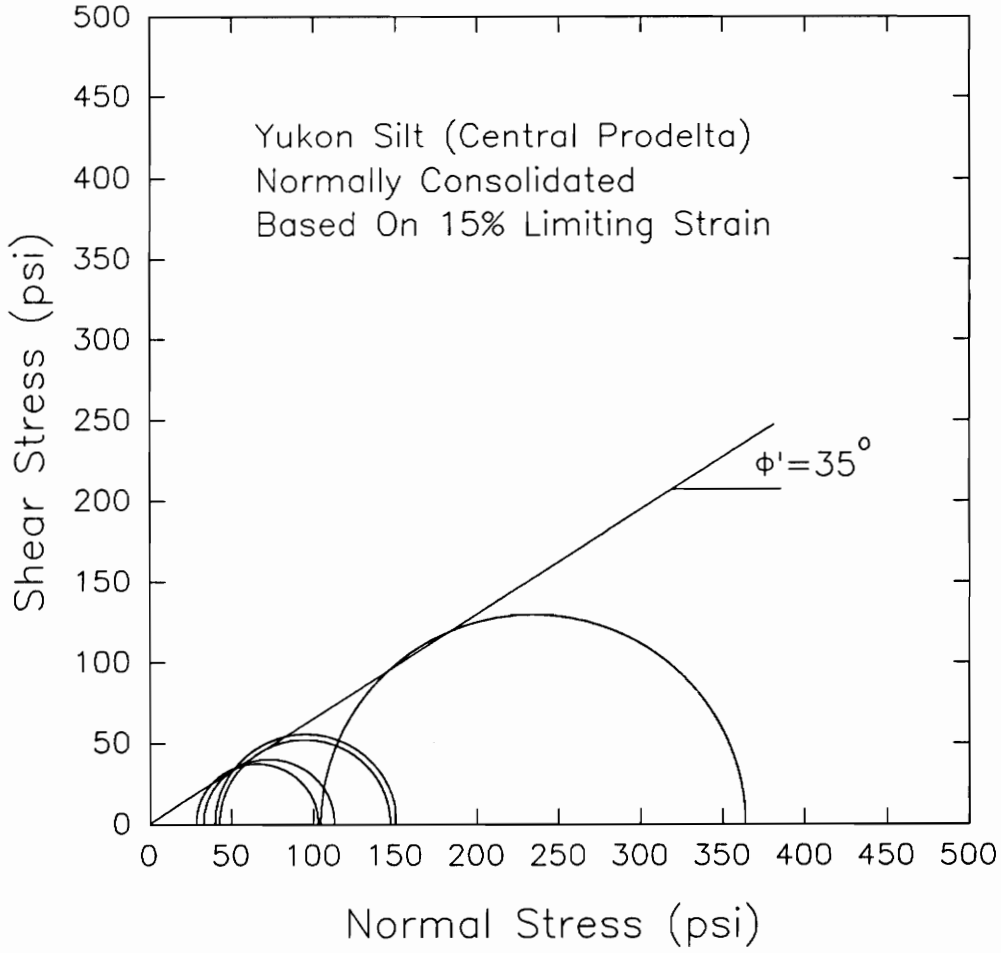

Figure 135 Effective Stress Mohr's Circles Measured For CU Triaxial Tests On Undisturbed Samples of Yukon Silt For Failure Based On 15% Limiting Strain (Central Prodelta)

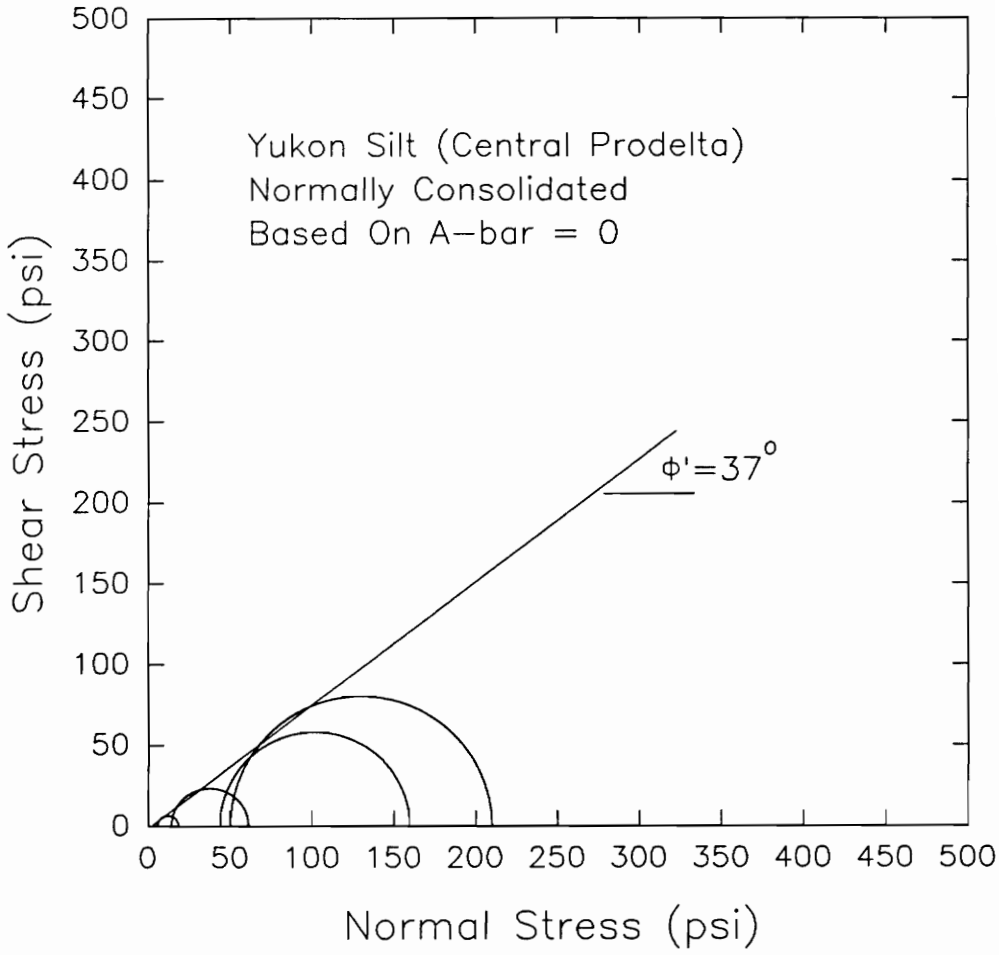

Figure 136 Effective Stress Mohr's Circles Measured For CU Triaxial Tests On Undisturbed Samples of Yukon Silt For Failure Based On A-bar = 0 (Central Prodelta)

Table 34 Effective Stress Friction Angles Measured For Different Failure Criteria For Yukon Silt (Central Prodelta)

Failure Criteria	ϕ' (Degrees)	Average Strain To Failure (%)
u_{max}	31	1%
Max.$(\sigma_1-\sigma_3)$	36	10%
Max.(σ_1'/σ_3')	37	5%
10% Limiting Strain	35	10%
15% Limiting Strain	35	15%
A-bar = 0	37	6%

Total Stress Interpretation of The CU Triaxial Tests On Normally Consolidated Samples of Yukon Silt (Central Prodelta)

The undrained strength ratios for these samples were determined in the same way as the sample obtained from western prodelta. Similar to the effective stress interpretation, not all the failure criteria could be applied to all the samples.

Figure 137 shows the relationships between the undrained shear strength and effective consolidation pressure for failure based on maximum pore pressure. The Su/p calculated is equal to 0.6.

An S_u/p equal to 2.7 was calculated using the maximum deviator stress as failure criterion. The data are plotted in Figure 138.

Shown in Figure 139 is the determination of S_u/p using the maximum principal stress ratio. The S_u/p measured for this failure criterion is equal to 1.5.

The data for failure based on 10% limiting strain are shown in Figure 140. The S_u/p ratio calculated is equal to 1.7.

Figure 141 illustrates the determination of the undrained strength ratio based on 15% limiting strain. An

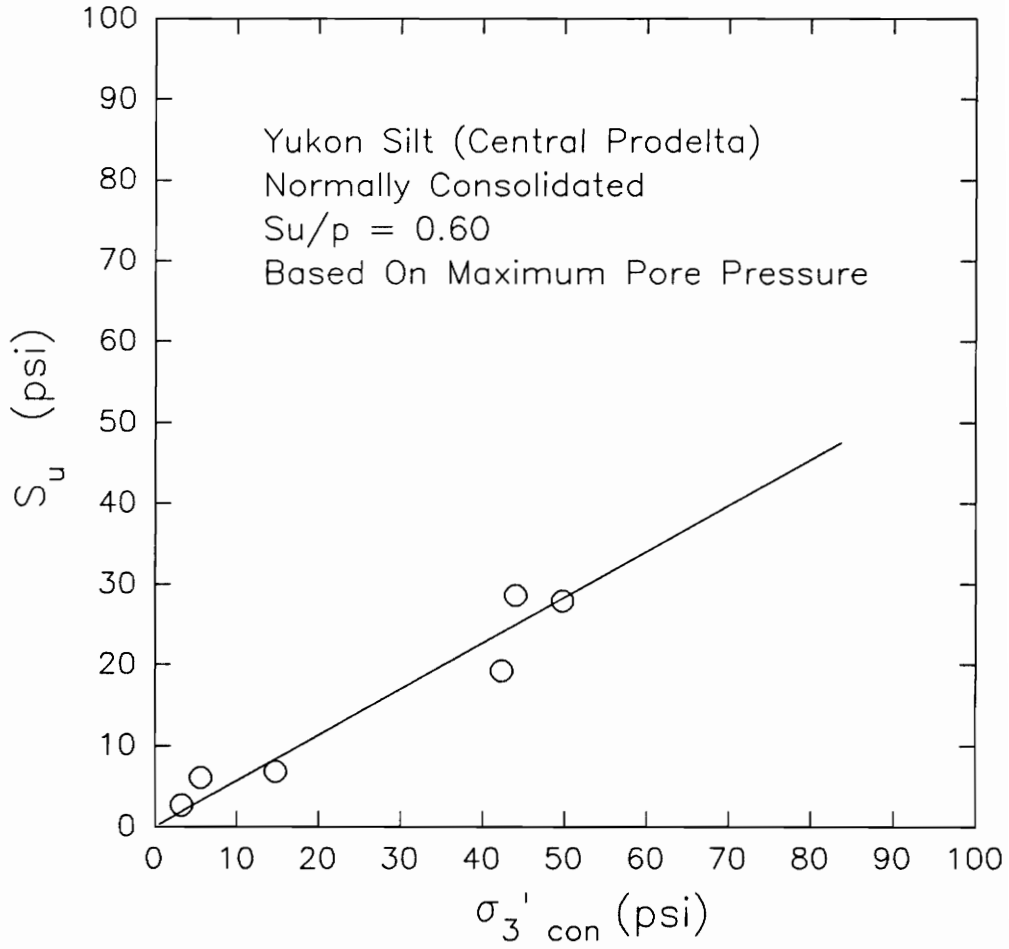

Figure 137 Undrained Shear Strength-Effective Consolidation Pressure Relationship Measured For CU Triaxial Tests On Undisturbed Samples of Yukon Silt For Failure Based On Maximum Pore Pressure (Central Prodelta)

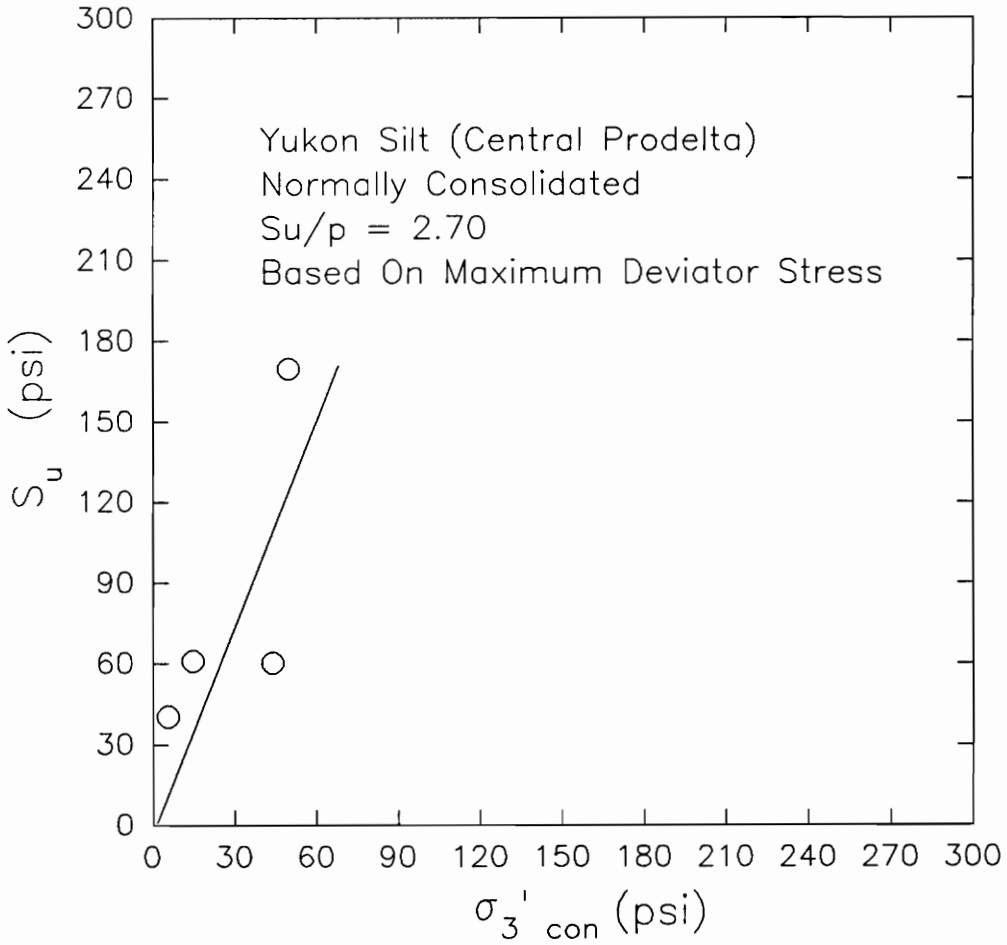

Figure 138 Undrained Shear Strength-Effective Consolidation Pressure Relationship Measured For CU Triaxial Tests On Undisturbed Samples of Yukon Silt For Failure Based On Maximum Deviator Stress (Central Prodelta)

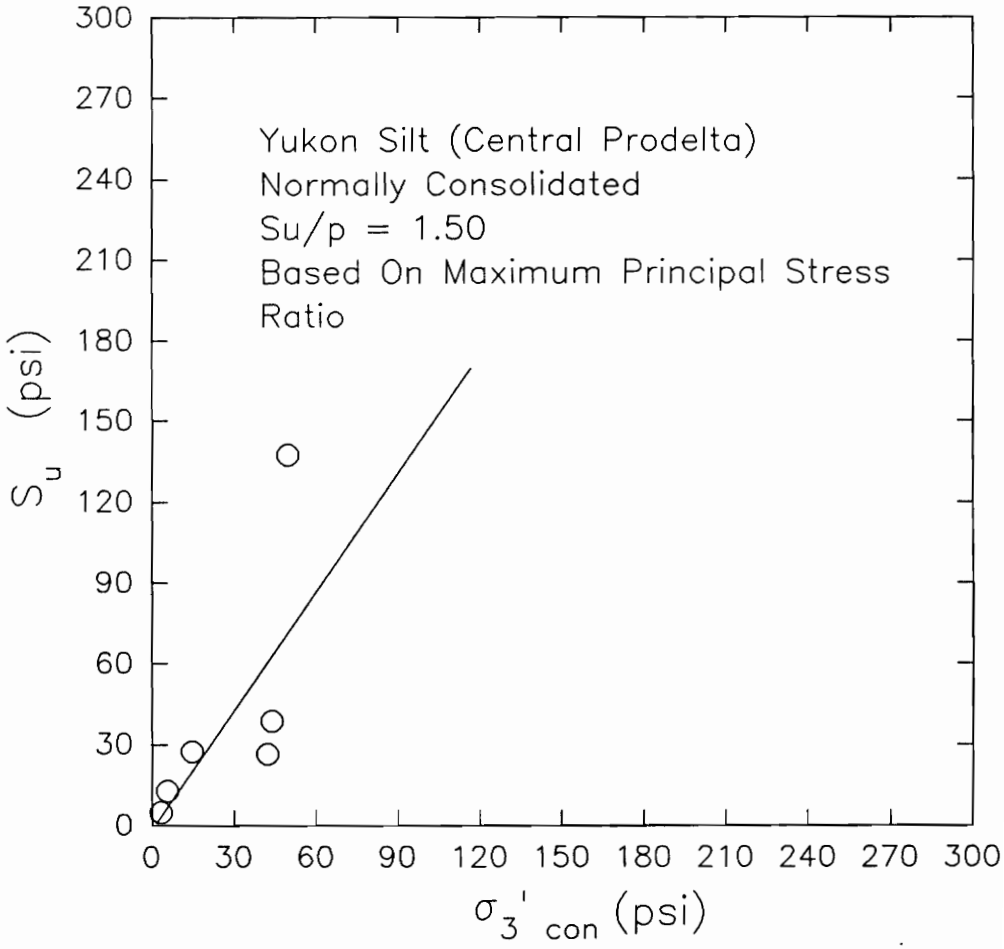

Figure 139 Undrained Shear Strength-Effective Consolidation Pressure Relationship Measured For CU Triaxial Tests On Undisturbed Samples of Yukon Silt For Failure Based On Maximum Principal Stress Ratio (Central Prodelta)

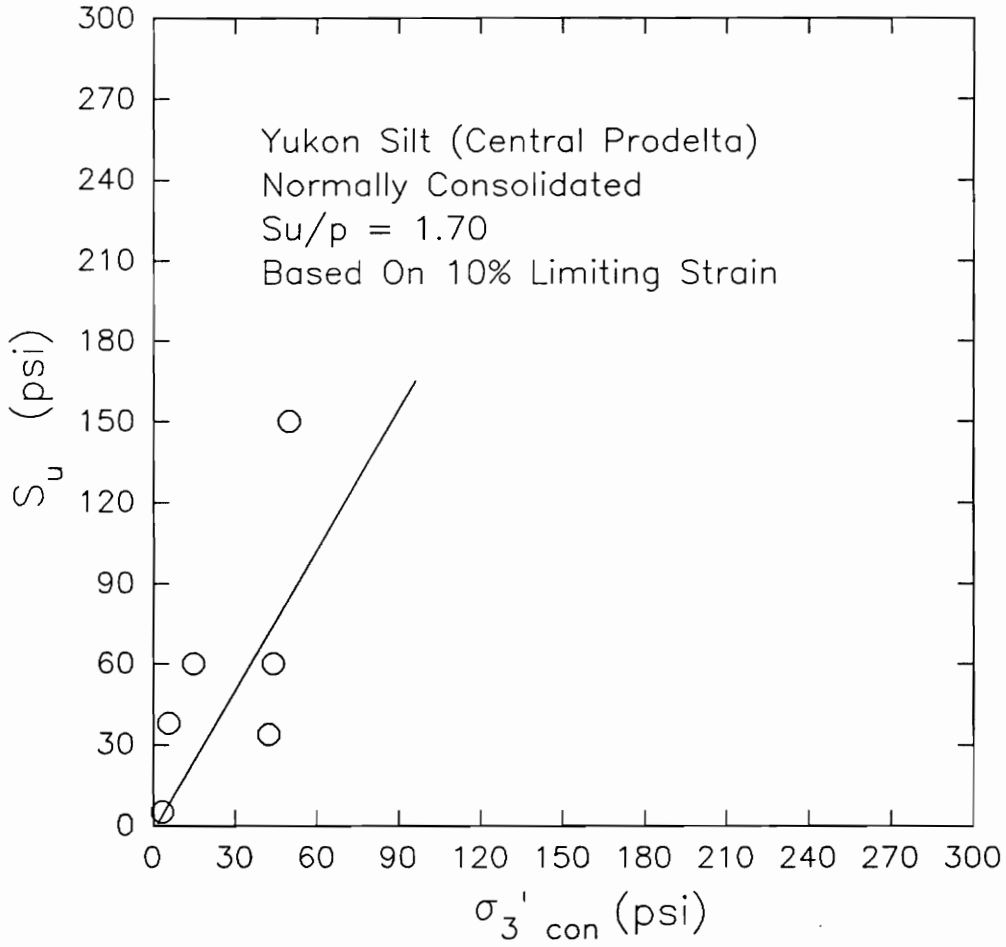

Figure 140 Undrained Shear Strength-Effective Consolidation Pressure Relationship Measured For CU Triaxial Tests On Undisturbed Samples of Yukon Silt For Failure Based On 10% Limiting Strain (Central Prodelta)

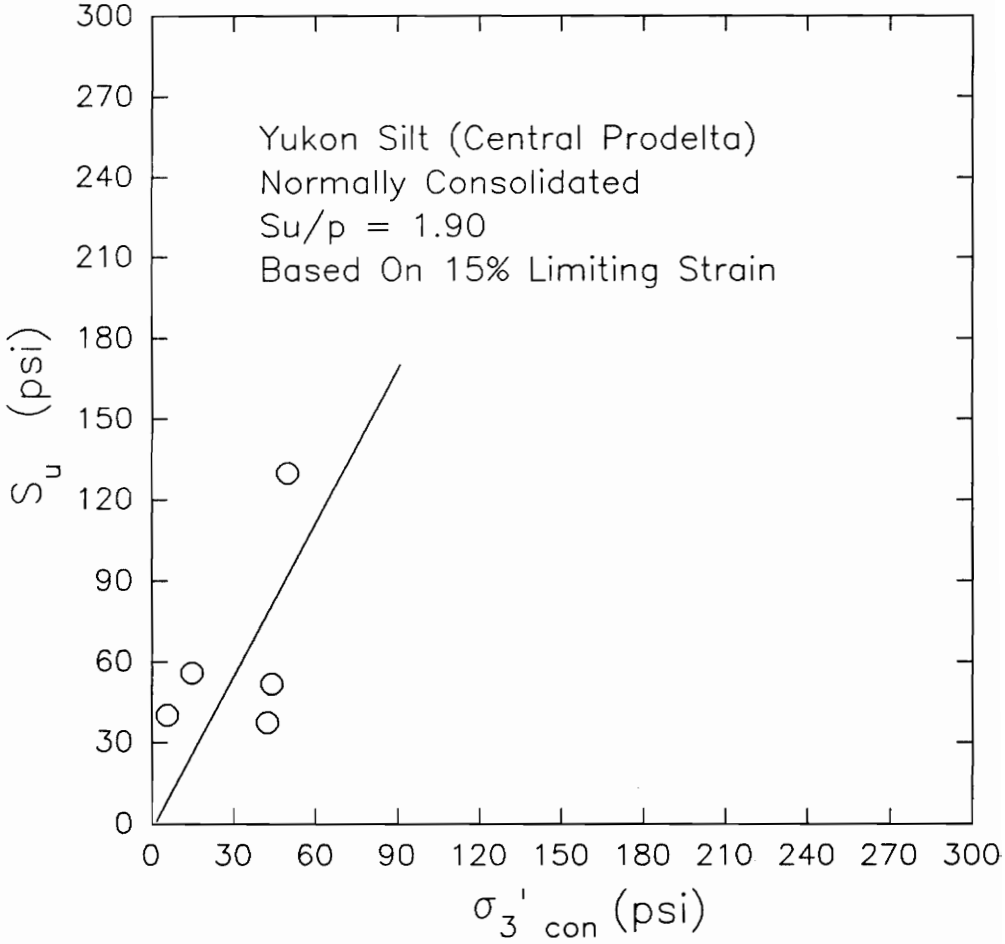

Figure 141 Undrained Shear Strength-Effective Consolidation Pressure Relationship Measured For CU Triaxial Tests On Undisturbed Samples of Yukon Silt For Failure Based On 15% Limiting Strain (Central Prodelta)

S_u/p equal to 1.9 was calculated using this failure criterion.

The data for failure based on A-bar=0 are plotted in Figure 142. The value of S_u/p is equal to 1.5.

Table 35 summarizes the S_u/p ratios for the different failure criteria. The lowest undrained strength ratio was determined using maximum pore pressure as failure criterion.

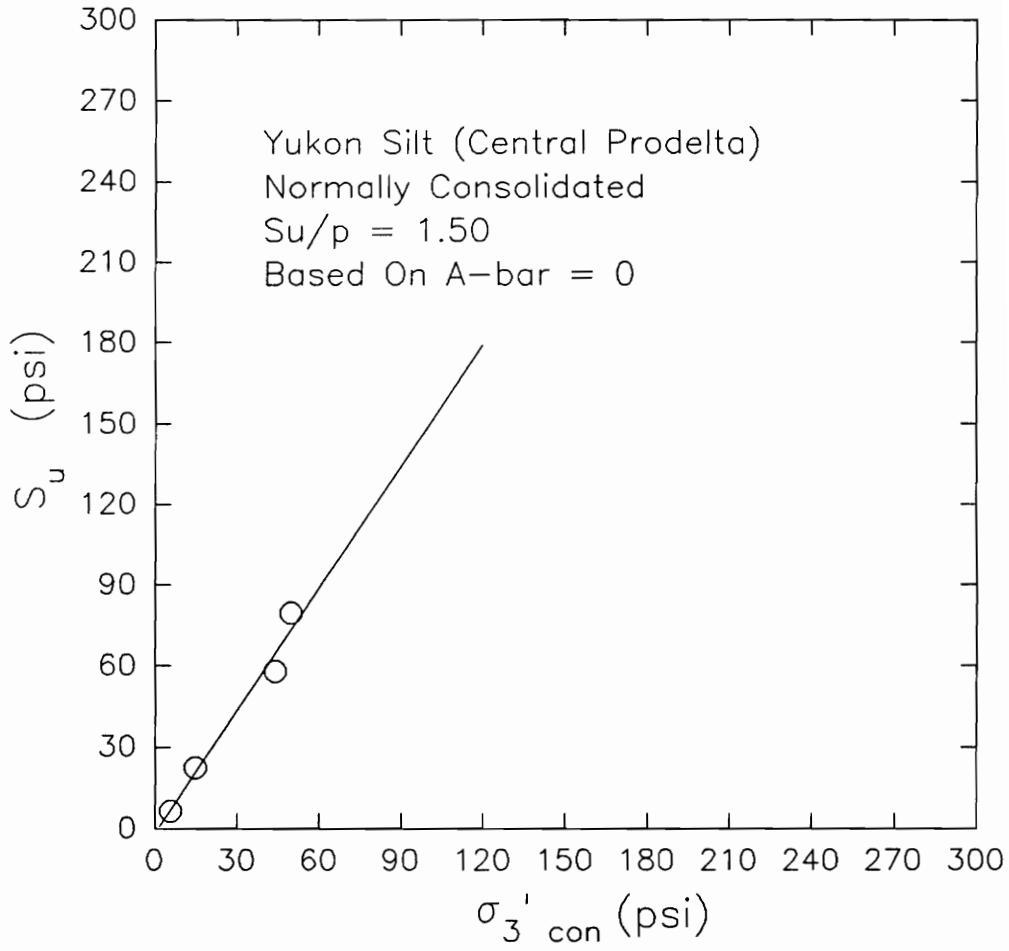

Figure 142 Undrained Shear Strength-Effective Consolidation Pressure Relationship Measured For CU Triaxial Tests On Undisturbed Samples of Yukon Silt For Failure Based On A-bar = 0 (Central Prodelta)

Table 35 S_u/p Ratios Measured For Different Failure Criteria For Yukon Silt (Central Prodelta)

Failure Criteria	S_u/p	Average Strain To Failure (%)
u_{max}	0.6	1%
Max.$(\sigma_1-\sigma_3)$	2.7	10%
Max.(σ_1'/σ_3')	1.5	5%
10% Limiting Strain	1.7	10%
15% Limiting Strain	1.9	15%
A-bar = 0	1.5	6

CHAPTER 5

ANALYSIS OF TEST RESULTS

Effects of Failure Criteria On The Values of The Effective Stress Friction Angles

Six different failure criteria were applied to the test results to evaluate the values of the effective stress friction angles. The results indicate that the choice of failure criteria influenced the values of ϕ' .

Defining failure based on maximum pore pressure, the ϕ' measured were much lower than determined using the other methods. Figure 143 illustrates the comparison of the effective stress friction angles measured for failure based on maximum pore pressure and maximum principal stress ratio. It can be seen that there is considerable amount of variation in the values of ϕ'. A difference as high as 6° can be measured from the two failure criteria.

The values of ϕ' measured from the different failure criteria, except u_{max}, showed small variations. Figure 144 illustrates the comparison of the ϕ' measured using maximum principal stress ratio and 10% limiting strain as failure criteria. The results indicate that the values of ϕ' are fairly consistent. A variation of ±1° could be measured from the two failure criteria, which could be attributed to scatter in the test results.

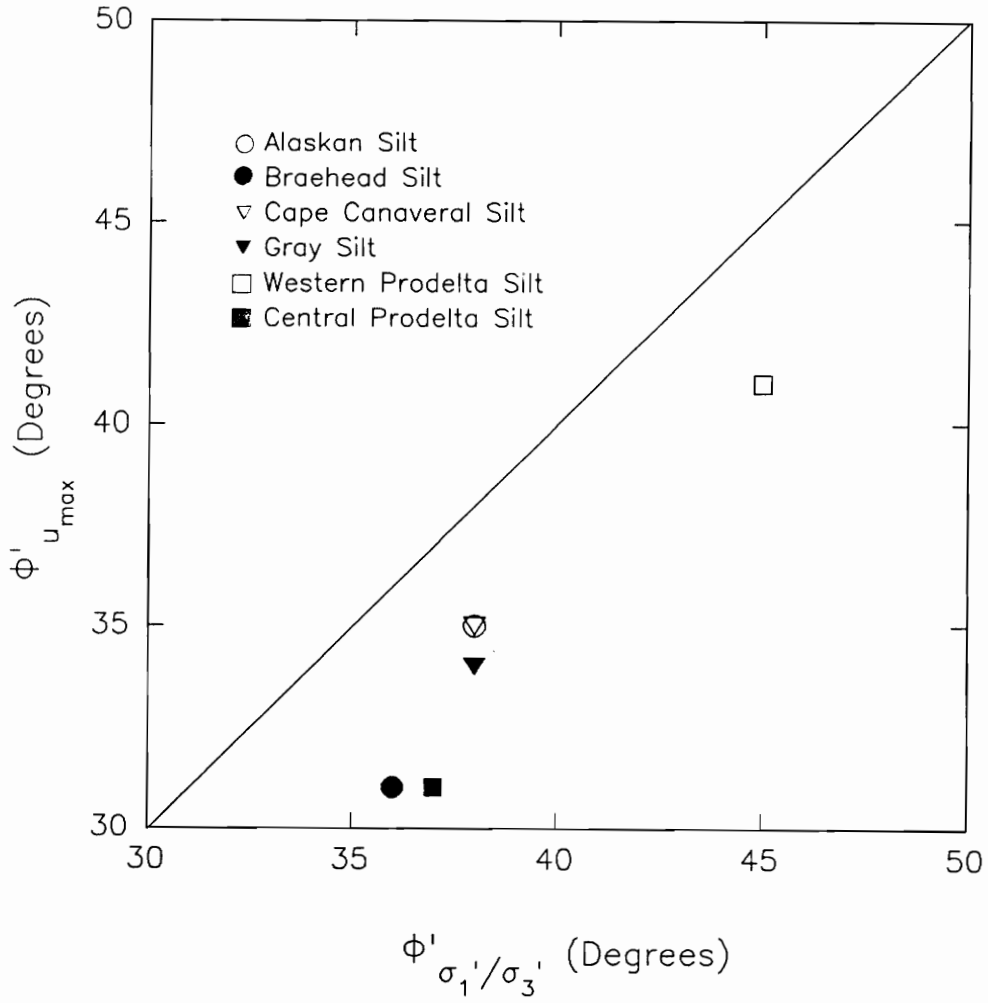

Figure 143 Comparison of the Effective Stress Friction Angles Measured For The Different Silt Samples For Failure Based On Maximum Principal Stress Ratio and Maximum Pore Pressure

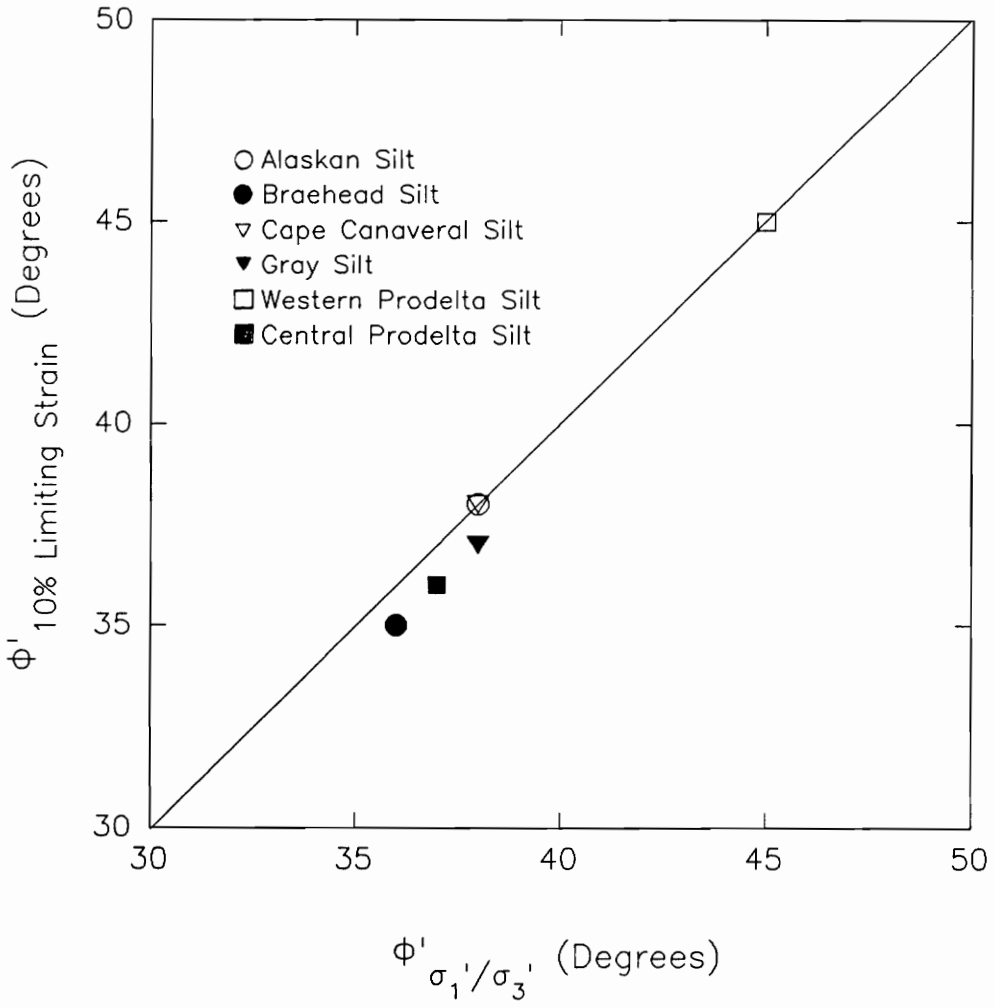

Figure 144 Comparison of the Effective Stress Friction Angles Measured For The Different Silt Samples For Failure Based On Maximum Principal Stress Ratio and 10% Limiting Strain

The conservative values of ϕ' based on maximum pore pressure could be explained by the dilative behavior of the specimens. The pore pressures during the tests increased only temporarily at small strains, then dropped as strains increased. The decrease in pore pressures increased the effective stresses, thus making the sample stronger at higher strains. This criteria also produced the smallest strains to failure. The maximum pore pressures were reached at strains ranging from 1% to 4%.

The consistency in the values of ϕ' using the different failure criteria, except u_{max}, could also be explained by the dilative behavior of the samples. The general trends of the effective stress paths were to approach the K_f line at small strains, then continued to climb the K_f line as strains increased. For soils with the effective cohesion intercept equal to zero, the maximum principal stress ratio corresponds closely to the condition where the stress path reached the K_f line. As shown in Table 36, the average strains to failure for maximum principal stress ratio were less than the average strains to failure for the other failure criteria. Since all the referenced silts behaved as c'=0 materials, then the p'-q coordinates of the different failure criteria, except u_{max}, are plotted on the K_f line. For this

Table 36 Average Strains To Failure Measured For CU Triaxial Tests For The Different Failure Criteria

Failure Criteria	u_{max}	σ_{dmax}	σ_1'/σ_3'	10%	15%	A=0
Alaskan Silt (ICU)	4%	20%	10%	10%	15%	N/A
Braehead Silt (CU)	2%	28%	7.5%	10%	15%	7.5%
Cape Canaveral Silt(CU)	1.7%	N/A	8.5%	10%	15%	16%
Gray Silt (CU)	3%	15%	5.5%	10%	15%	20%
Rhode Island Silt (CU)	3%	N/A	N/A	N/A	N/A	N/A
Yukon Silt						
Western Prodelta (CU)	3.5%	N/A	5%	10%	N/A	N/A
Central Prodelta (CU)	1%	10%	5%	10%	15%	6%

condition, the effective stress friction angle would be independent from the type of failure criteria.

These analyses can be well illustrated by the test results from Cape Canaveral silt. Figure 145 illustrates the effective stress path for the sample showing the points corresponding to the different failure criteria. The point represented by u_{max} was not yet on the K_f line, which is why the value of ϕ' calculated was 3° below the ϕ' measured from the other failure criteria. All other failure points are located on the K_f line.

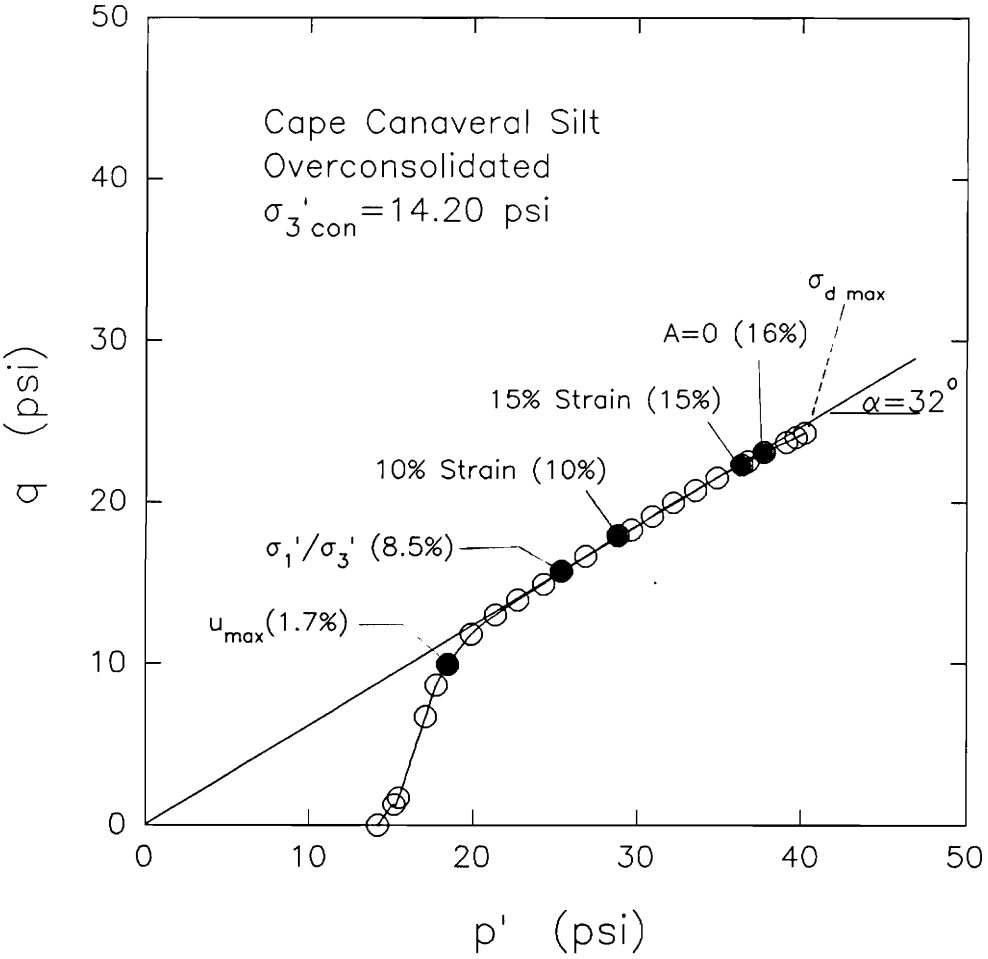

Figure 145 Effective Stress Path Measured For CU Triaxial Test On Cape Canaveral Silt

Effects of Failure Criteria On The Values of The Undrained Strength Ratios

Undrained shear strengths were evaluated using the CU and UU triaxial test results for the different silt samples. Due to the dilatant nature of the silt samples, a unique undrained shear strength could not be obtained. Six different failure criteria were used to determine the values of the undrained strength parameters, and comparisons were made using the undrained strength ratio, S_u/p. A summary of S_u/p ratios measured for the different specimens is given in Table 37.

For the normally consolidated Alaskan silt, the results from the CU and UU triaxial tests on the samples were used to evaluate the undrained strength ratios. Interpreting S_u/p from UU triaxial tests resulted to lower values of S_u/p as compared to the CU test results. From the CU triaxial tests, the undrained strength ratio calculated using maximum pore pressure was lower than the S_u/p ratios derived from the other failure criteria. For failure based on σ_{dmax}, the undrained strength ratio calculated was higher than the S_u/p for the other failure criteria because the average strain to failure for σ_{dmax} was greater than 15%. For normally consolidated clays, Skempton provided a correlation of S_u/p with the

Table 37 Values of S_u/p Ratios From CU And UU Triaxial Tests For The Different Failure Criteria

Failure Criteria	umax	σmax	σ1'/σ3'	10%	15%	A=0
Alaskan Silt (ICU)	0.62	0.9	0.81	0.81	0.88	N/A
Alaskan Silt (UU)	N/A	N/A	N/A	0.23	0.25	N/A
Braehead Silt (CU)	0.55	7.8	1.7	2.3	4.2	1.2
Brown Silt						
UD-85-4-9 (UU)	N/A	0.12	N/A	0.15	0.17	N/A
UD-85-4-11B (UU)	N/A	0.42	N/A	0.38	0.4	N/A
UD-100-S1-A (UU)	N/A	0.52	N/A	0.48	0.5	N/A
Cape Canaveral Silt(CU)	0.83	N/A	1.26	1.34	1.6	1.6
Gray Silt						
UD-85-2 (CU)	0.65	N/A	0.8	N/A	N/A	1.5
UD-101-S2-A (UU)	N/A	0.4	N/A	0.41	0.42	N/A
UD-100-S4-A1 (UU)	N/A	N/A	N/A	0.48	0.51	N/A
UD-101-S2-C2 (UU)	N/A	N/A	N/A	0.2	0.22	N/A
Rhode Island Silt (CU)	0.26	N/A	N/A	N/A	N/A	N/A
Yukon Silt						
Western Prodelta (CU)	0.63	N/A	0.74	1.1	N/A	N/A
Central Prodelta (CU)	0.6	2.7	1.5	1.7	1.9	1.5

plasticity index. Test results indicate that using Skempton's equation, the S_u/p calculated for the Alaskan silt was lower than measured.

The CU triaxial test results for Braehead silt showed scatter in the values of S_u/p. The lowest value of the undrained strength ratio was measured for failure based on maximum pore pressure. Since the sample failed at a strain of about 28%, σ_{dmax} gave the highest value of S_u/p, almost four times higher than the average value derived from other failure criteria. Although the sample was normally consolidated, Skempton's equation could not be applied to this specimen because the specimen was non-plastic.

The series of UU and CU triaxial tests for the overconsolidated brown silt and gray silt were used to evaluate the values of S_u/p. A considerable amount of scatter could be observed from the undrained strength ratios obtained from the UU triaxial tests. The CU tests gave higher values of S_u/p ratios than UU tests for all failure criteria. Based on the CU triaxial tests on gray silt, the S_u/p ratio obtained from u_{max} was lower than the values of S_u/p calculated from the other failure criteria. Interpretation based on σ_{dmax}, 10%, and 15% limiting strains were not applied because of the non-linear relationship between S_u and $\sigma_3'_{con}$. Similar to the

previous silt samples, there was difficulty in selecting a unique value of undrained shear strength because of the dilative behavior of the specimens. S_u/p was greatest for the failure criteria having the largest strain to failure.

For the overconsolidated Cape Canaveral silt, evaluating S_u/p ratio using σ_{dmax} was not possible because the sample did not show a peak deviator stress throughout the duration of the test. The lowest undrained shear strength was computed from u_{max} as failure criterion, which was almost half of the mean S_u/p determined from the other failure criteria. The results indicate that the values of S_u/p ratios increased with strain which made it difficult to define a unique undrained shear strength for the specimen.

The only failure criteria satisfied for the CU test on the normally consolidated Rhode Island silt was maximum pore pressure. Skempton's correlation of S_u/p with PI again leads to a conservative value of the undrained strength ratio.

The undrained strength ratios for the Yukon silt were evaluated using the CU triaxial test results on the samples. Due to the dilative behavior of the specimens, the values of S_u/p ratios increased with strain. Similar

to the other silt samples, maximum pore pressure as failure criterion gave the lowest value of S_u/p.

The test results from the different silt samples indicate that a unique undrained shear strength for a given silt sample could not be evaluated directly from both UU and CU triaxial tests. The choice of failure criteria influenced the values of the undrained strength ratios measured in CU triaxial tests. Because of the dilatant nature of the silt specimens, the strength increases with strain during shear.

UU triaxial tests resulted in lower values of S_u/p compared to CU tests results. The difference in the undrained strength parameters may be attributed to disturbance during sampling. Fleming (1985) conducted a study on the effect of disturbance on strengths of silt samples measured in the laboratory. The test results showed that the disturbance decreased the undisturbed strength of Alaskan silt by as much as 42%.

Skempton (1953) presented empirical correlations of undrained shear strength with Atterberg limits. Although the correlation proved to be useful for normally consolidated clays, the application to silts resulted in conservative values of S_u/p.

A more reliable method of evaluating undrained shear strength parameters is to determine how the undrained

shear strength is related to the changes in pore pressures (Torrey, 1982). The general trend of the stress paths is to approach the K_f line at small strains, then continue to climb the K_f line as strains increased.

Figure 146 shows a typical effective stress path for a dilative soil whose effective cohesion intercept is equal to zero. For a point on the stress path that is on the K_f line, the change in pore pressure and the applied deviator stress could be related to the α-angle of the K_f line, expressed as

$$\text{Tan } \alpha = \frac{\sigma_d/2}{\sigma_3{}'_{con} + \sigma_d/2 - \Delta u} \qquad (4)$$

Simplifying Eq.(4), it can be shown that

$$\frac{2\sigma_3{}'_{con}}{\sigma_d} = \frac{1 - \text{Tan } \alpha}{\text{Tan } \alpha} - \frac{2\Delta u}{\sigma_d} \qquad (5)$$

Since Tan α = sin ϕ' , $S_u/p = \sigma_d/2\sigma_3{}'_{con}$, and $A = \Delta u/\sigma_d$,

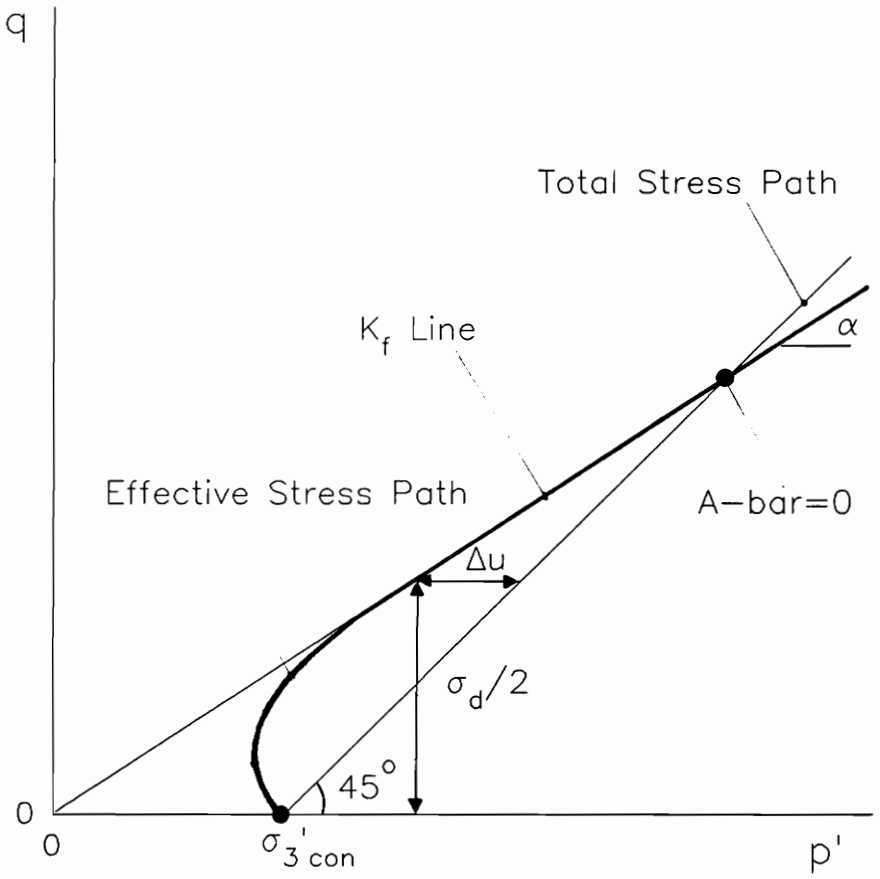

Figure 146 Typical Effective and Total Stress Paths For A Dilative Soil

Eq. (5) could be expressed as

$$S_u/p = \frac{\sin \phi'}{1 - (1 - 2A) \sin \phi'} \qquad (6)$$

Using Eq.(6) to evaluate the undrained shear strength parameters will reduce the scatter in the values of the undrained strength ratios because ϕ' could be defined well from the CU triaxial tests. Using the relationship between A-bar and strain, a value of A-bar could be selected in such a way that the shear strength does not correspond to a large amount of strain.

Possibility of Cavitation In UU Triaxial Tests

In UU triaxial tests on saturated soils, the angle of shearing resistance should be approximately equal to zero. However, when tests are conducted on dilative silts, a deviation from the $\phi = 0$ condition may occur in UU triaxial tests.

Brandon et al. (1990) presented a plot to determine the limiting undrained shear strength for soils that cavitate (Figure 1). If a silt sample cavitates in UU triaxial tests, the undrained shear strength for a given cell pressure should plot approximately on the contour defined by the effective stress friction angle.

Four samples of the Alaskan silt were tested in UU triaxial tests. All samples were saturated prior to shearing. The representative effective stress friction angle for these samples is equal to 38°. As shown in Figure 147, the undrained shear strengths plot well below the contour lines for the different values of ϕ'. Therefore, cavitation did not occur during the tests.

The values of the undrained shear strengths for sample UD-84-4-9 of brown silt are plotted in Figure 148. The effective stress friction angle for brown silt samples was not measured. Although the value of ϕ' for these samples is not known, it can be assumed that

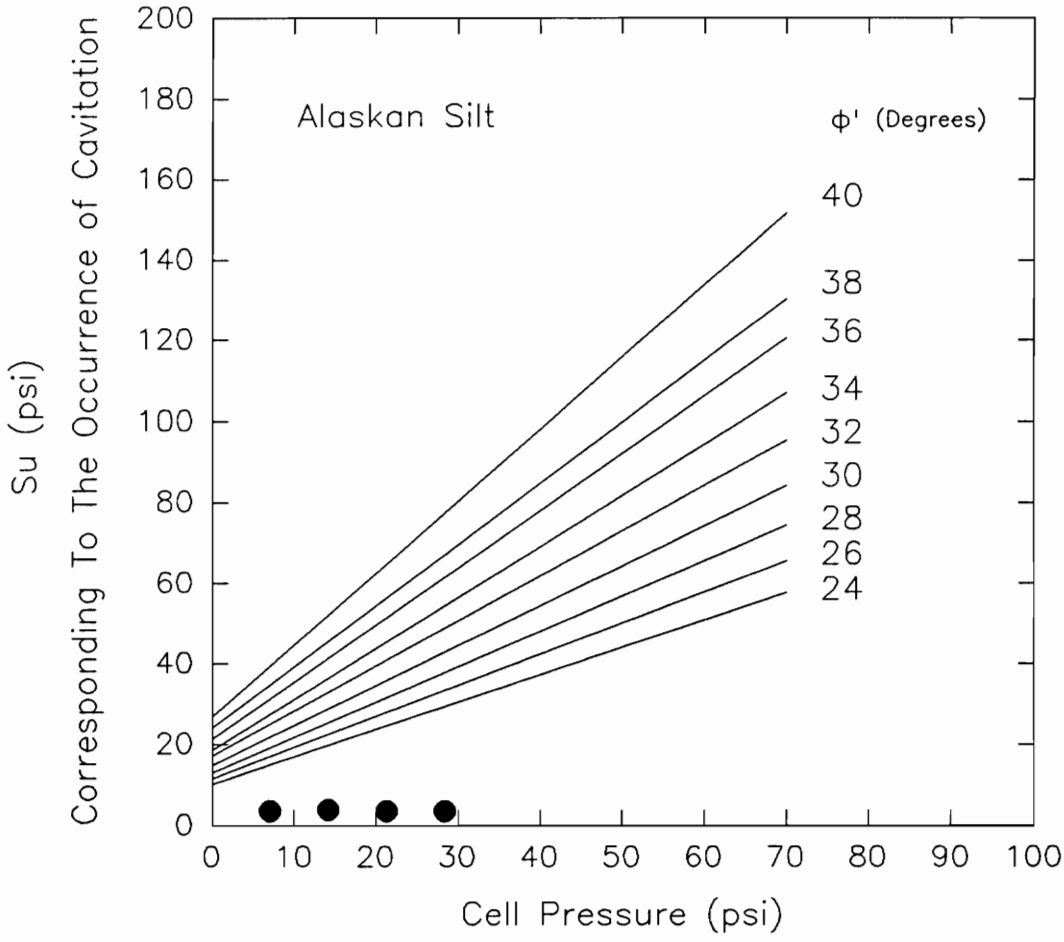

Figure 147 Undrained Shear Strengths Measured For UU Triaxial Tests On Alaskan Silt

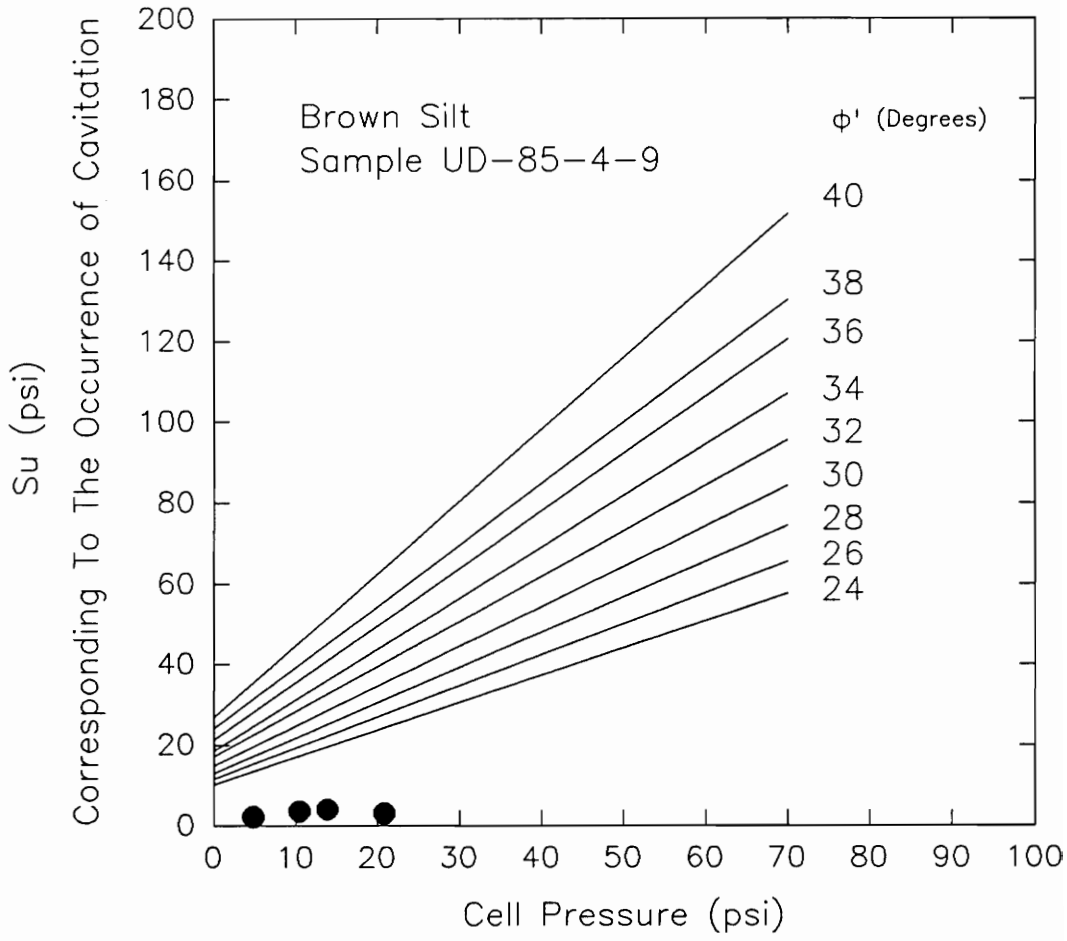

Figure 148 Undrained Shear Strengths Measured For UU Triaxial Tests On Brown Silt, West Williamson L.P.P. Pump Station (Sample UD-85-4-9)

cavitation did not influence their undrained shear strength because the data plot well beneath the contour lines.

Figures 149 and 150 show the data for samples UD-85-4-11B and UD-100-S1-A for brown silt. Similar to the previous sample, the plots indicate that cavitation did not affect the values of the undrained shear strengths.

For the gray silt samples, the effective stress friction angle measured from the CU triaxial tests is equal to 38°. The undrained shear strengths for samples UD-101-S2-A, UD-100-S4-A1, and UD-100-S2-C2 are plotted in Figures 151, 152, and 153. Since the data plot far below the contour line defined by the effective stress friction angle, it can be inferred that cavitation did not occur during the UU triaxial tests on the samples.

The occurrence of cavitation in UU triaxial tests could also be determined by calculating the value of the pore pressure at failure, u_f. A sample is said to have cavitated if the value of u_f decreased to -14.7 psi.

Shown in Figure 154 are the effective and total stress Mohr's circles for a triaxial test. The pore pressure at failure is defined as the difference between the maximum total stresses and maximum effective stresses, expressed as

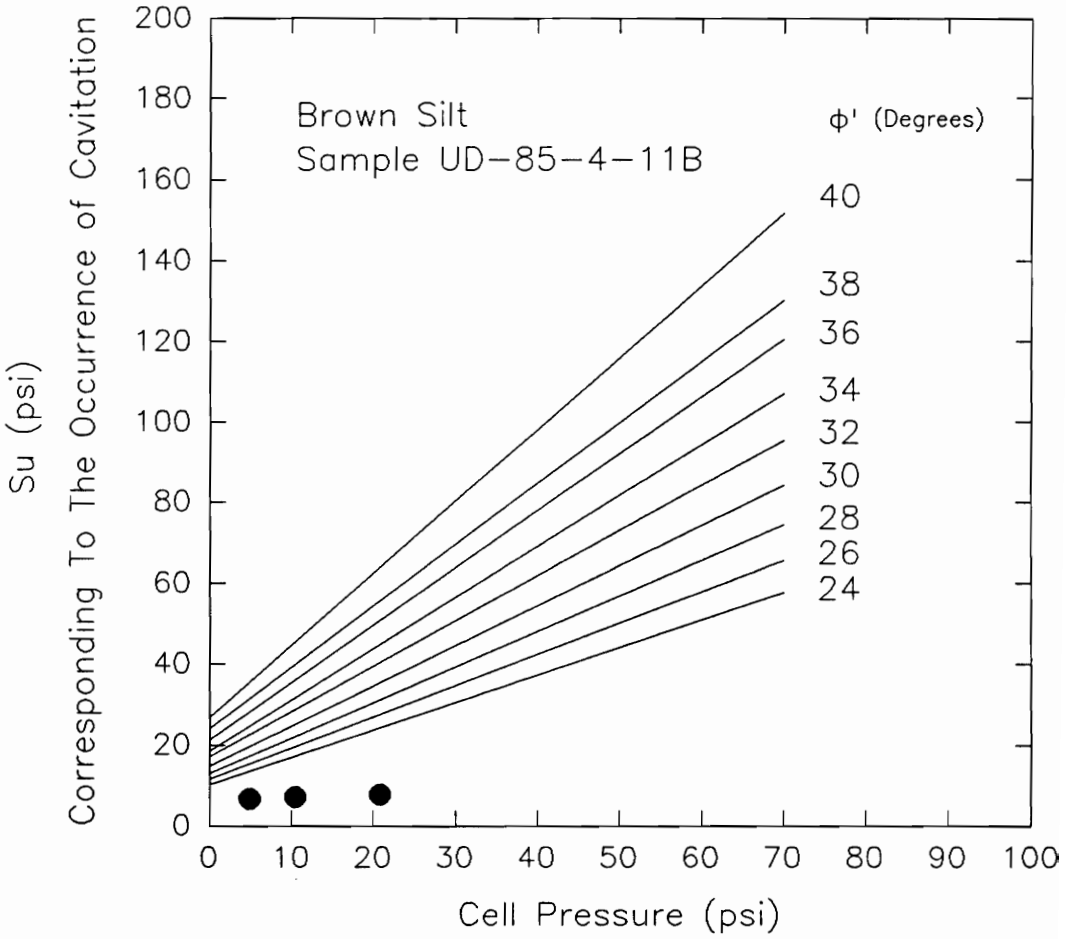

Figure 149 Undrained Shear Strength Measured For UU Triaxial Tests On Brown Silt, West Williamson L.P.P. Pump Station (Sample UD-85-4-11B)

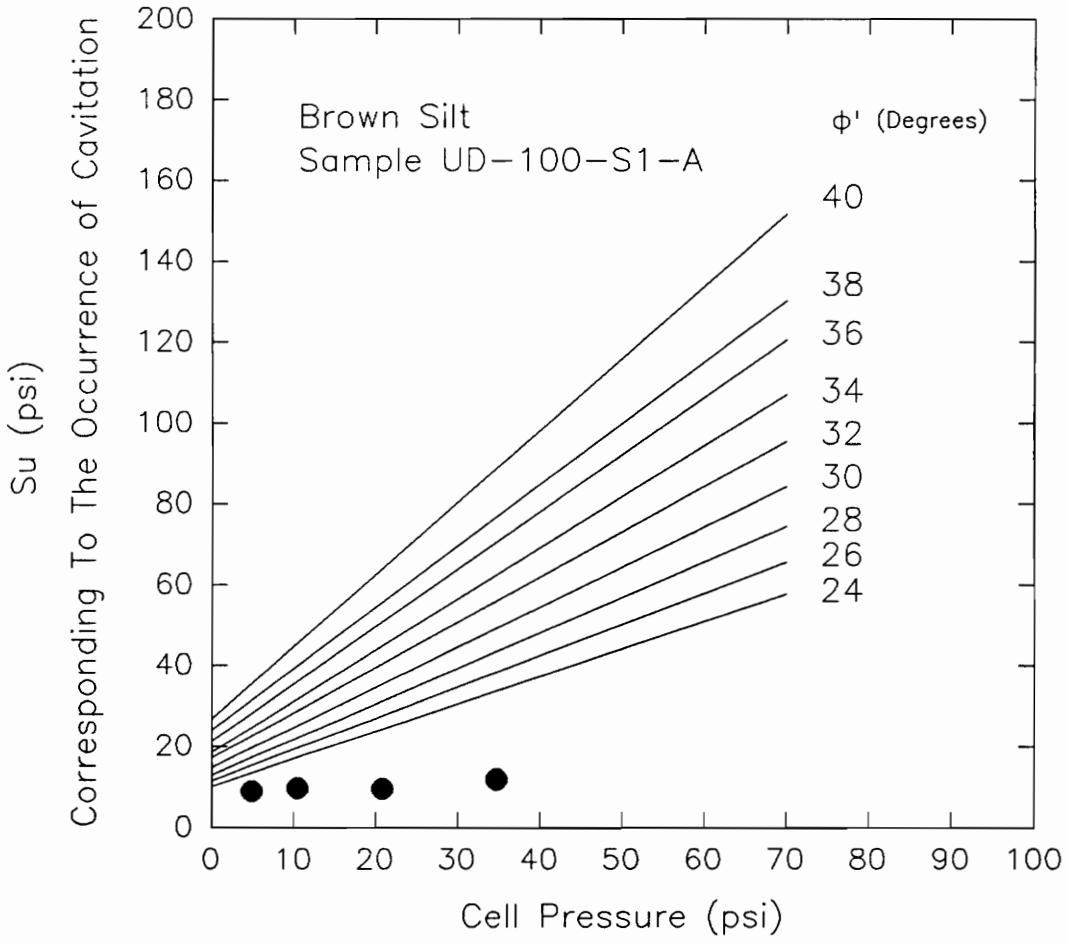

Figure 150 Undrained Shear Strength Measured For UU Triaxial Tests On Brown Silt, West Williamson L.P.P. Pump Station (Sample UD-100-S1-A)

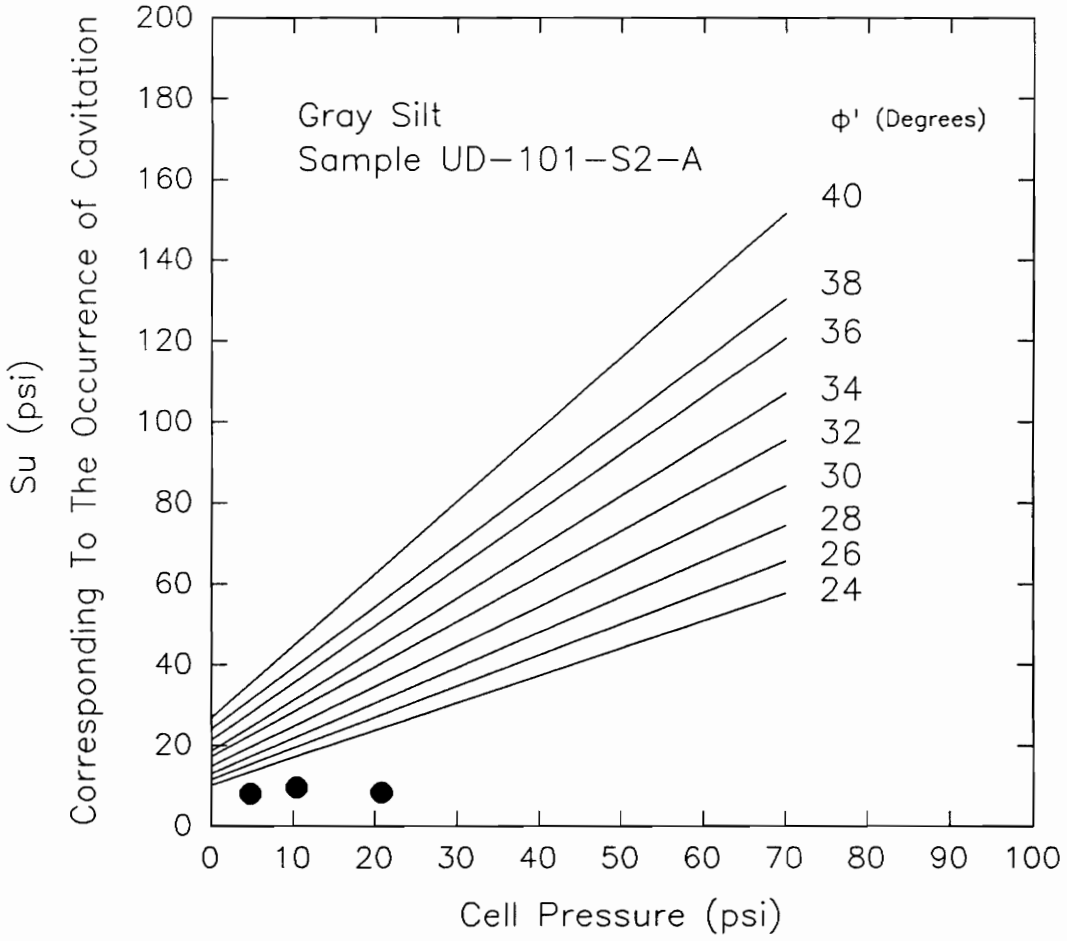

Figure 151 Undrained Shear Strength Measured For UU Triaxial Tests On Gray Silt, West Williamson L.P.P. Pump Station (Sample UD-101-S2-A)

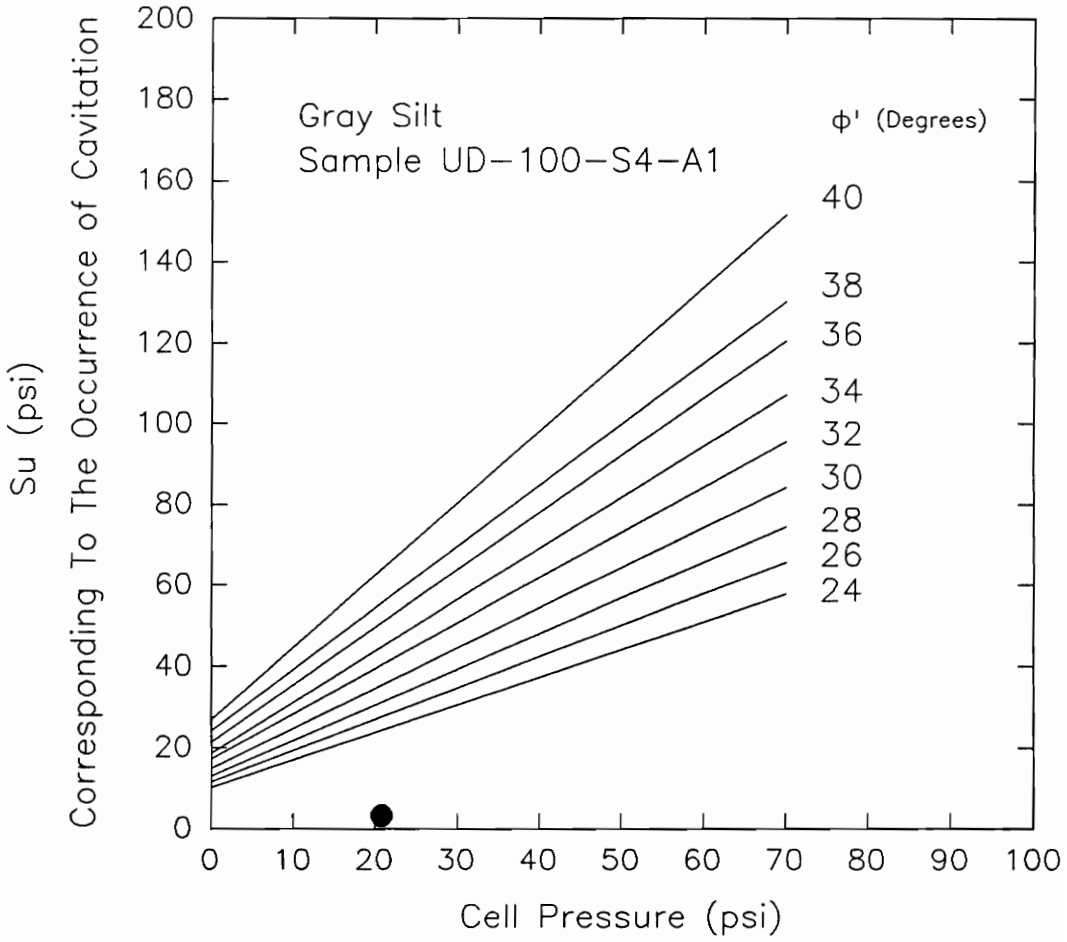

Figure 152 Undrained Shear Strength Measured For UU Triaxial Tests On Gray Silt, West Williamson L.P.P. Pump Station (Sample UD-100-S4-A1)

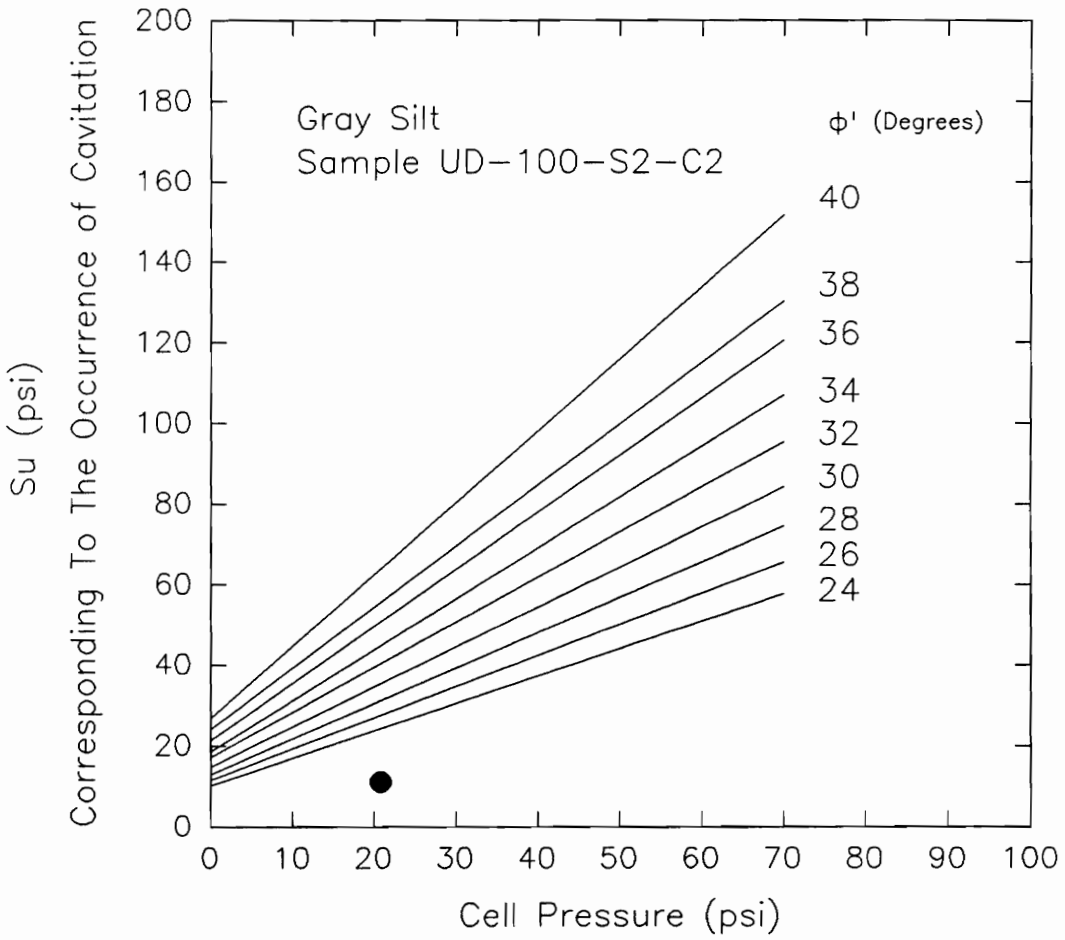

Figure 153 Undrained Shear Strength Measured For UU Triaxial Tests On Gray Silt, West Williamson L.P.P. Pump Station (Sample UD-100-S2-C2)

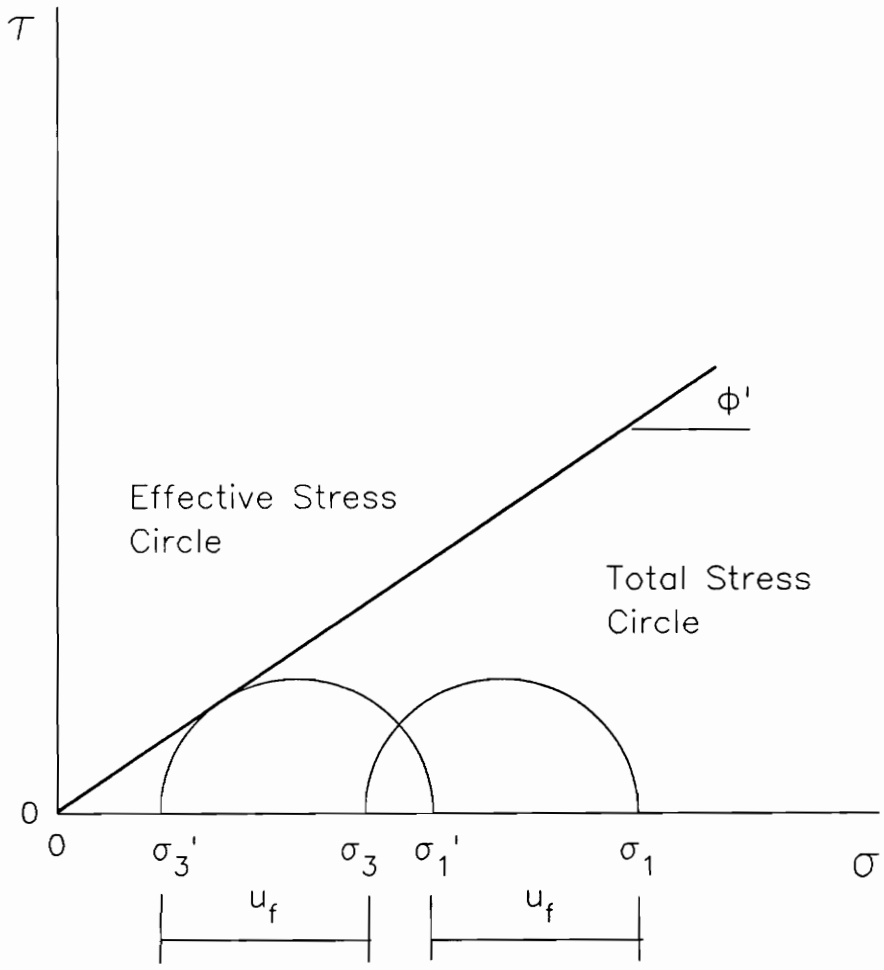

Figure 154 Effective Stress and Total Stress Mohr's Circles For A Triaxial Test

$$u_f = \sigma_1 - \sigma_1' \quad (7)$$

$$u_f = \sigma_3 - \sigma_3' \quad (8).$$

Considering the effective stress Mohr's circle, the relationship between the maximum effective stresses could be expressed by the equation

$$\sigma_1' = \sigma_3'[\tan^2(45° + \phi'/2)] \quad (9).$$

If Eq.(7) and Eq.(8) are substituted for Eq.(9), the pore pressure at failure could be expressed in terms of the maximum total stresses and effective stress friction angle by the equation

$$u_f = \frac{\sigma_1 - \sigma_3[\tan^2(45° + \phi'/2)]}{1 - \tan^2(45° + \phi'/2)} \quad (10).$$

Knowing the value of ϕ' from the CU triaxial tests, and the values of the maximum total stresses from UU triaxial tests, the occurrence of cavitation in UU tests can be checked by using Eq. (10).

Table 38 summarizes the pore pressures at failure for the UU triaxial tests on the different silt samples.

Based on the test results, it can be inferred that cavitation did not influence the values of the undrained shear strengths because the values of u_f calculated were all greater than -14.7 psi.

Table 38 Values of u_f Measured for The Unconsolidated Undrained Triaxial Tests On Different Silt Samples

Soil Sample	Cell Pressure (psi)	u_f (psi)
Alaskan silt	7.1	4.9
Alaskan silt	14.2	11.8
Alaskan silt	21.3	19.1
Alaskan silt	28.4	26.2
Gray silt		
UD-101-S2-A	4.8	-0.3
UD-101-S2-A	20.8	15.6
UD-101-S2-A	10.4	4.4
UD-101-S4-A1	20.8	18.8

CHAPTER 6

SUMMARY AND CONCLUSIONS

In the course of this research study, the results of tests conducted on different silt samples were investigated to determine the primary factors that control the strength parameters of silts. The silt samples investigated were:

1. Alaskan silt
2. Braehead silt
3. Brown and gray silt from West Virginia
4. Cape Canaveral silt
5. Rhode Island silt
6. Yukon silt

The effective stress friction angles were evaluated using the results from the CU triaxial tests. The UU triaxial test results were used to evaluate the undrained shear strengths of the specimens, and comparisons were made using the undrained strength ratio, S_u/p.

The results indicate that it is difficult to define failure for both UU and CU triaxial tests. Because of the dilatant nature of the specimens, the strength of the samples keeps increasing during shear. For this reason,

different failure criteria were utilized to evaluate the effective stress friction angles and the undrained shear strengths of the samples. These failure criteria were:

1. Maximum pore pressure
2. Maximum deviator stress
3. Maximum principal stress ratio
4. 10% limiting strain
5. 15% limiting strain
6. A-bar = 0
7. Reaching the K_f line

For CU triaxial tests, the choice of failure criteria influenced the values of the effective stress friction angles. Maximum pore pressure as failure criterion gave the lowest value of the effective stress friction angle. Using the different failure criteria, except u_{max}, the values of ϕ' measured for each silt specimen were fairly consistent.

The undrained shear strength parameters were evaluated using the CU and UU triaxial test results from the different silt samples. Similar to the calculation of ϕ', the value of S_u/p ratio depends on the failure criteria. The results show that a unique undrained shear strength could not be determined because the samples get stronger with increasing strain.

The values of S_u/p measured from the UU triaxial tests were lower than the undrained strength ratio derived from the CU triaxial tests. The difference in S_u/p may possibly be attributed to disturbance during sampling. Results indicate that the interpretation of the undrained shear strength using UU triaxial tests was hindered by the scatter in the values of S_u/p.

The values of the undrained strength ratio from the CU triaxial tests showed dependency on the type of failure criteria. Using maximum pore pressure as failure criterion, the undrained strength ratio resulted in lower values as compared to the S_u/p ratios measured from the other failure criteria. Results indicate that the value of the undrained shear strengths of the samples increased with increasing strain.

Skempton's correlation of S_u/p to plasticity index was used to estimate the undrained strength ratio of the normally consolidated samples. Although the correlation proves to be useful for normally consolidated clays, results were too conservative when applied to silt samples.

The test results show that the changes in pore pressure highly influences the load carrying capability of the samples. A reliable method of evaluating the undrained shear strength is to determine the relationship

between the undrained strength ratio and the changes in pore pressure. Brandon et al. (1982) presented an equation relating the undrained strength ratio, effective stress friction angle, and pore pressure parameter A-bar, expressed as

$$S_u/p = \frac{\sin \phi'}{1 - (1-2A) \sin \phi'}$$

Since there is a direct proportionality between changes in pore pressure and A-bar, the equation takes into account the effect of the changes in pore pressure. Scatter in the values of the undrained strength ratio could be minimized since the value of the effective stress friction angle could be defined well from the CU triaxial tests. Using the relationship between A-bar and strain, a value of A-bar should be selected in a way that the undrained shear strength does not correspond to large values of strains.

REFERENCES

Bishop, M. A., and Eldin G., "Undrained Triaxial Tests On Saturated Sands and Their Significance in the General Theory of Shear Strength", Geotechnique, Vol. II, 1950, pp. 13-32

Borgesson, L.; "Shear Strength of Inorganic Silty Soils", Proceedings of the 10th International Conference of Soil Mechanics and Foundation Engineering, Vol. 1 Stockholm 1981, pp. 567-572

Brandon, T. L., J. M. Duncan, J. T. Huffman, (1990), "Classification and Engineering Behavior of Silts", A report submitted to the U.S. Army Corps of Engineers, Lower Mississippi Valley Division, 144 p.

Duncan, J. M., Sehn, A.; "Investigation of the Cause of Failure of the Corrugated Metal Culvert at the West Williamson L.P.P. Pump Station, West Williamson West Virginia", A Report Prepared for the U.S. Army Corps of Engineers, Huntington District, 1987, 117 p.

Fleming, L.; "The Strength and Deformation Characteristics of Offshore California Silts", Thesis submitted to the University of California, Berkeley in partial fulfillment of the requirements for the degree of Doctor of Philosophy, 177 p.

Golder, H. Q., and Skempton, A. W., 1948, "The Angle of Shearing Resistance in Cohesive Soils for Tests at Constant Water Content", Proceedings, Second International Conference in Soil Mecahnics, pp. 185-192

Kondrad, J.M., M. Bozozuk and K.T. Law, "Study in In situ Testing Methods in Deltaic Silts", Proceedings of the 11th International Conference of Soil Mechanics and Foundation Engineering, Vol. 2, San Francisco, pp. 879-885.

Ladd, C. C., J.S. Weaver, J.T. Germaine, and D. P. Sauls, "Strength-Deformation Properties of Artic Silts", ASCE Specialty Conference, ARCTIC '85, San Francisco, 1985.

Nacci, V. A. and R. A. D'Andrea, "A Technique for the Preparation of Specimens of Loose Layered Silts", Soil Specimen Preparation for Laboratory Testing, ASTM STP 599, 1976, pp. 193-201.

Penman, A.D.M., "Shear Characteristics of a Saturated Silt Measured in Triaxial Compression", Geotechnique, Vol. III No. 8, Dec. 1953, pp. 312-328

Schultze, E. and Horn, A., "The Shear Strength of Silt", Proceedings, 6th International Conference of Soil Mechanics and Foundation Engineering, Vol. 1, Montreal, 1965, pp. 350-353.

Terzaghi, K. and R.B. Peck, Soil Mechanics in Engineering Practice, Second Ed., John Wiley and Sons, 1967, pp. 729

Torrey, V. H., "Laboratory Shear Strength of Dilative Silts", Report prepared for the Lower Mississippi Valley Division, U.S. Army Engineers Waterways Experiment Station, Vicksburg, MS, September 1982, 55 p.

Winters, W.J., "Liquefaction Potential of Sediment in the Northern Bering Sea", Strength Testing of Marine Sediments, ASTM STP 883, Philadelphia, 1985, pp. 454-472.

APPENDIX A

UNCONSOLIDATED UNDRAINED TESTS ON OVERCONSOLIDATED UNDISTURBED SAMPLES OF GRAY SILT

SAMPLE UD-101-S2-C2

SAMPLE UD-100-S4-A

PLOTS OF:

A. DEVIATOR STRESS-STRAIN RELATIONSHIPS

B. MOHR'S CIRCLES BASED ON MAXIMUM DEVIATOR STRESS

C. MOHR'S CIRCLES BASED ON 10% LIMITING STRAIN

D. MOHR'S CIRCLES BASED ON 15% LIMITING STRAIN

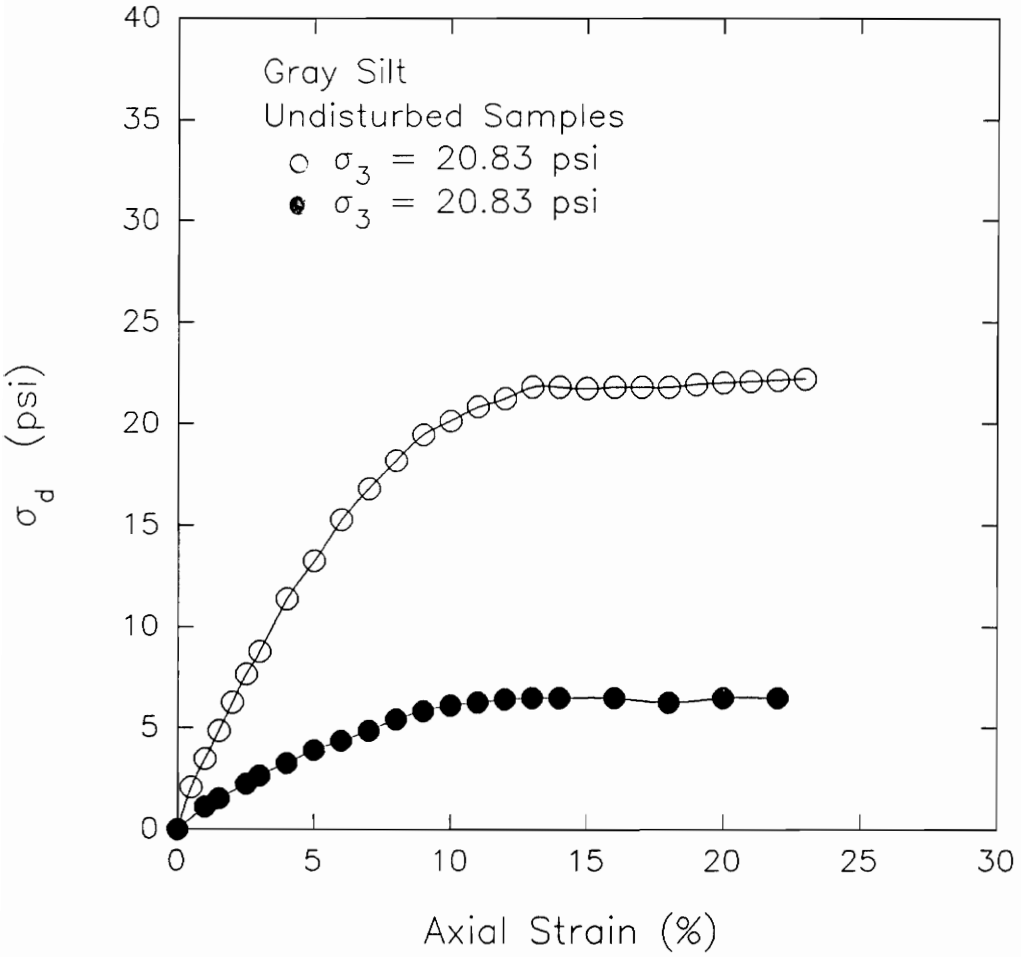

Deviator Stress-Strain Relationships For UU Triaxial Tests On Undisturbed Samples of Gray Silt, West Williamson L.P.P. Pumping Plant (Samples UD-101-S2-C2 and UD-100-S4-A1)

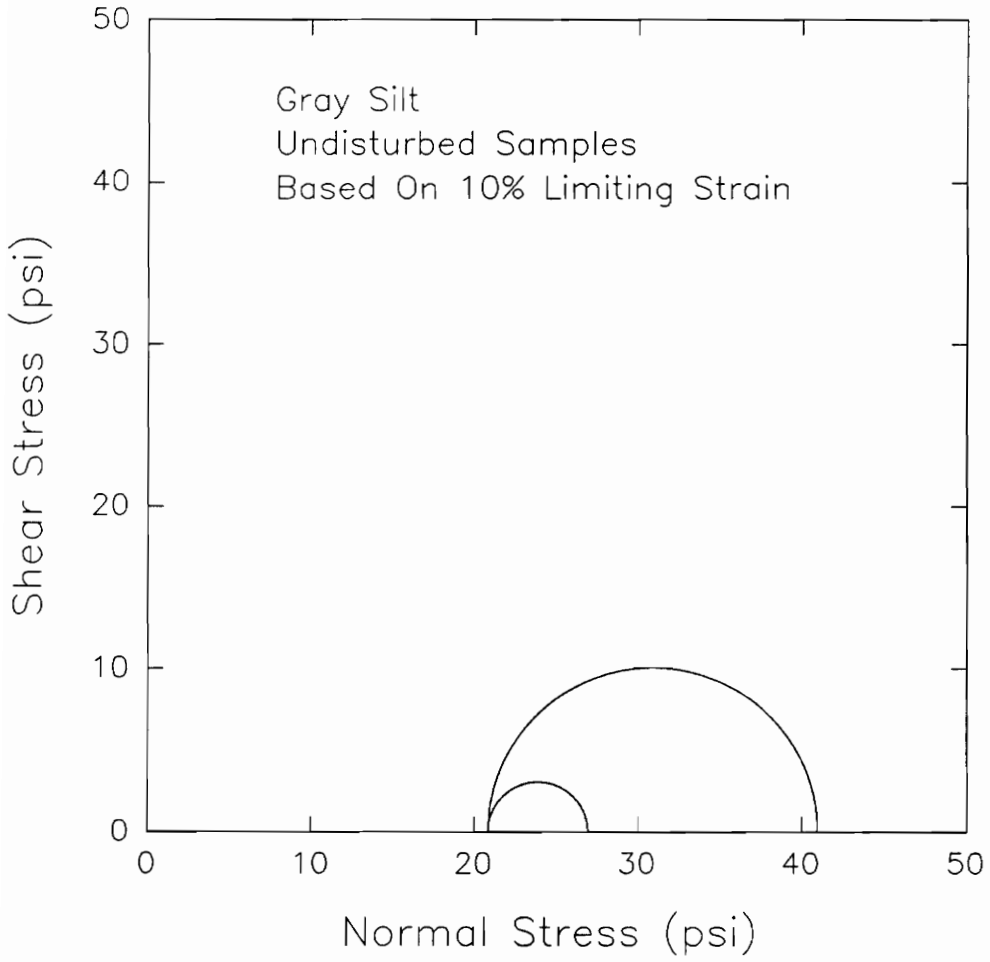

Mohr's Circles For UU Triaxial Tests On Undisturbed Samples of Gray Silt For Failure Based On 10% Limiting Strain, West Williamson L.P.P. Pumping Plant (Samples UD-101-S2-C2 and UD-100-S4-A1)

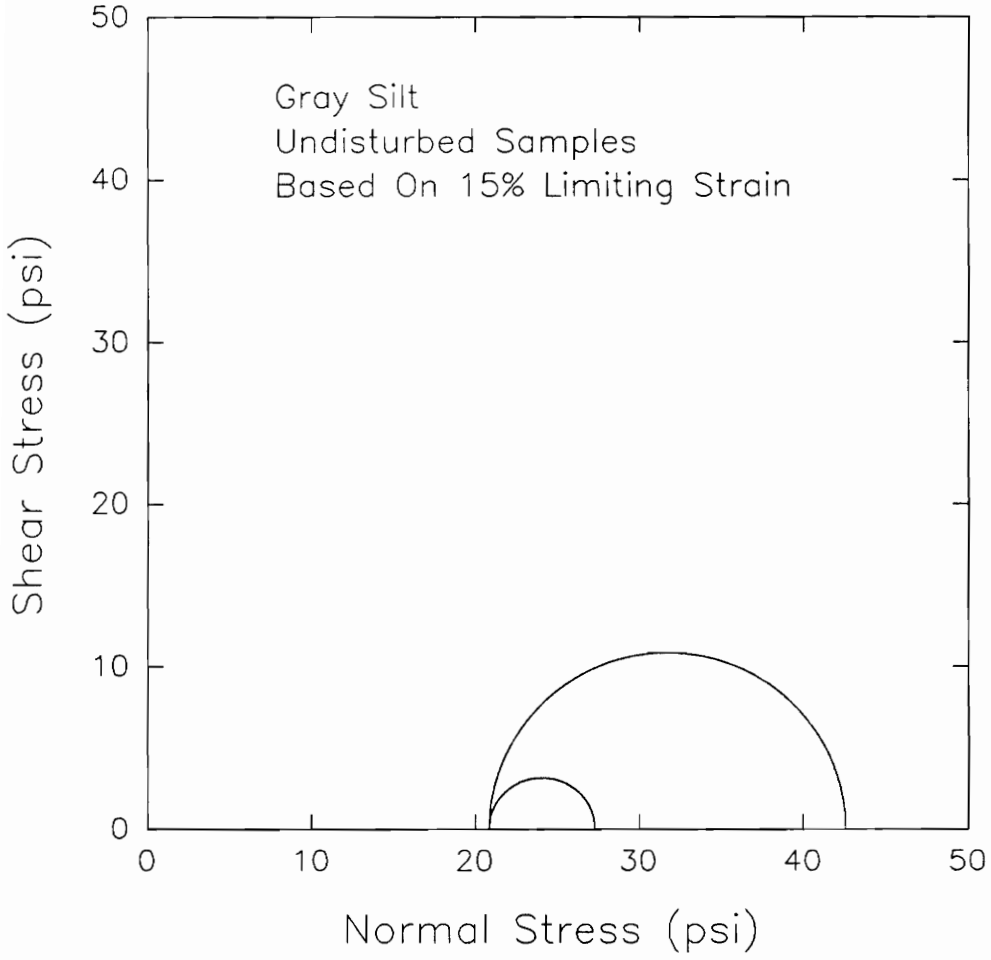

Mohr's Circles For UU Triaxial Tests On Undisturbed Samples of Gray Silt For Failure Based On 15% Limiting Strain, West Williamson L.P.P. Pumping Plant (Samples UD-101-S2-C2 and UD-100-S4-A1)

APPENDIX B

UNCONSOLIDATED UNDRAINED TESTS ON OVERCONSOLIDATED UNDISTURBED SAMPLES OF BROWN SILT

SAMPLE UD-85-4-11B

SAMPLE UD-100-S1-A

PLOTS OF:

A. DEVIATOR STRESS-STRAIN RELATIONSHIPS

B. MOHR'S CIRCLES BASED ON MAXIMUM DEVIATOR STRESS

C. MOHR'S CIRCLES BASED ON 10% LIMITING STRAIN

D. MOHR'S CIRCLES BASED ON 15% LIMITING STRAIN

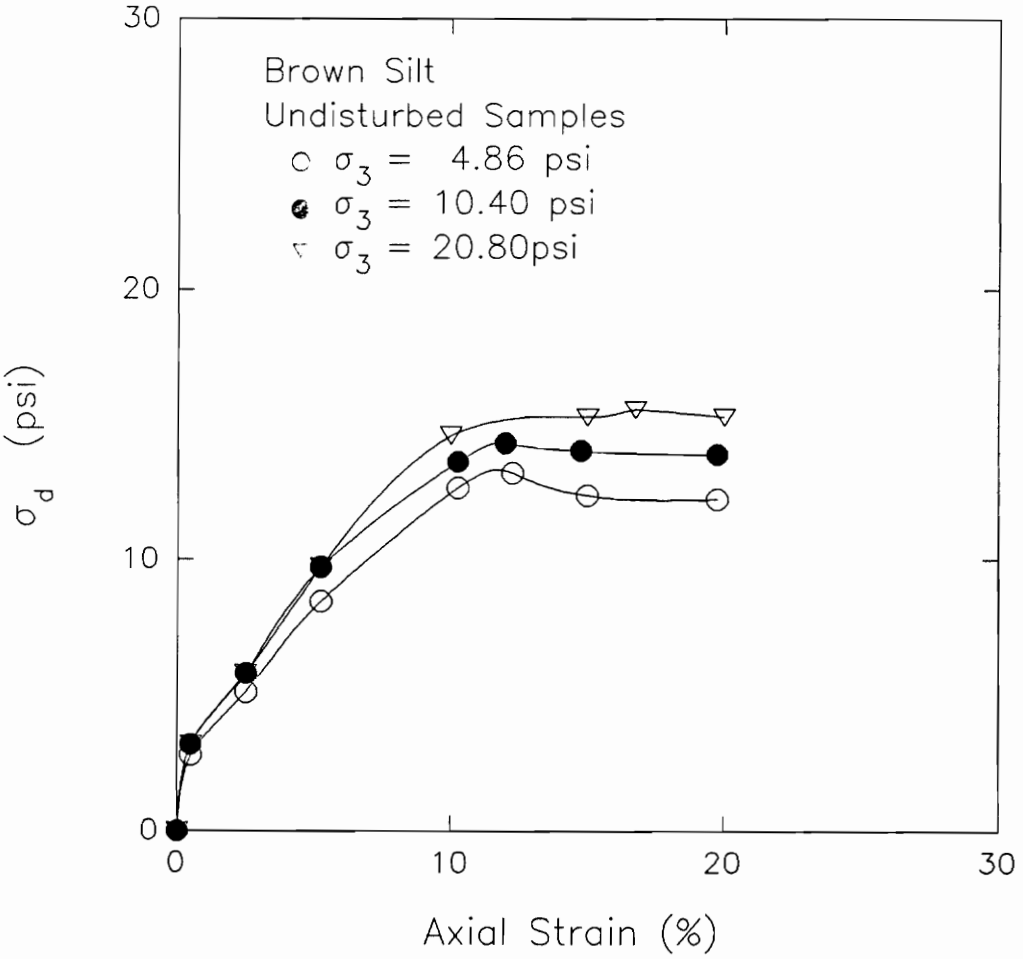

Deviator Stress-Strain Relationships For UU Triaxial Tests On Undisturbed Samples of Brown Silt, West Williamson L.P.P. Pumping Plant (Sample UD-85-4-11B)

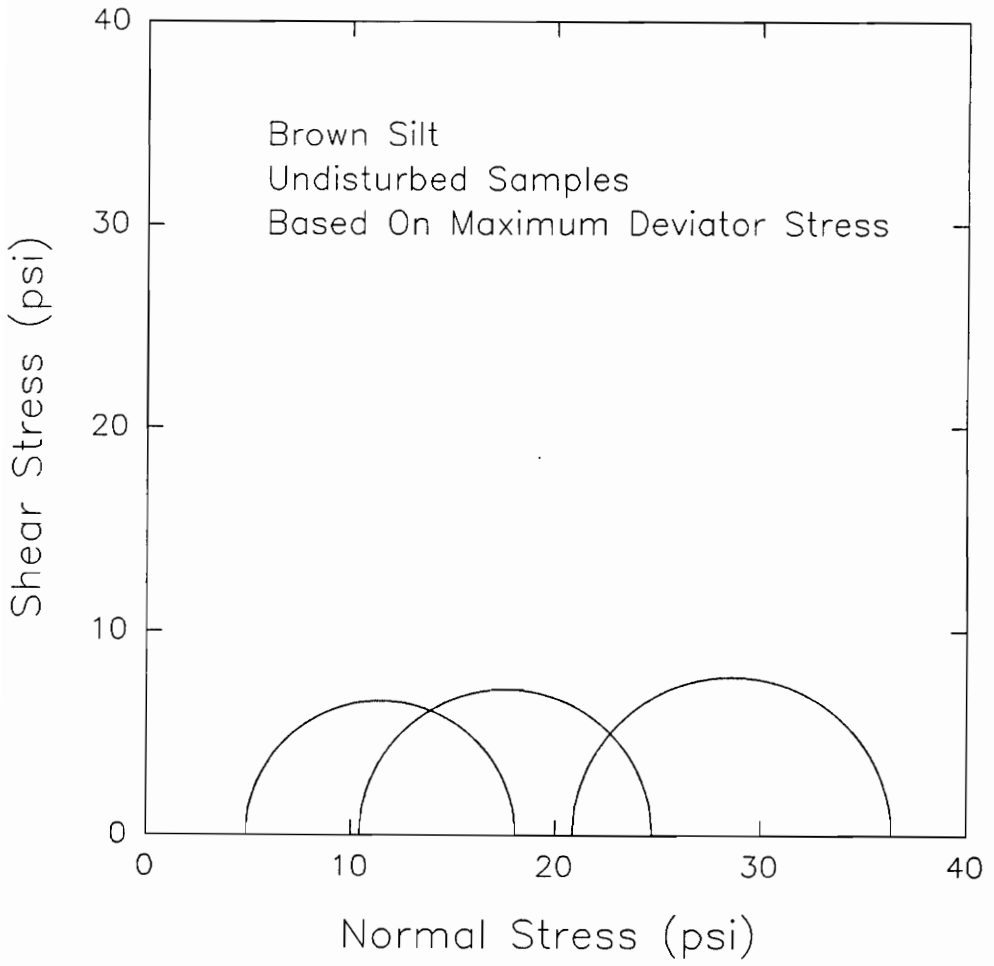

Mohr's Circles For UU Triaxial Tests On Undisturbed Samples of Brown Silt For Failure Based On Maximum Deviator Stress, West Williamson L.P.P. Pumping Plant (Sample UD-85-4-11B)

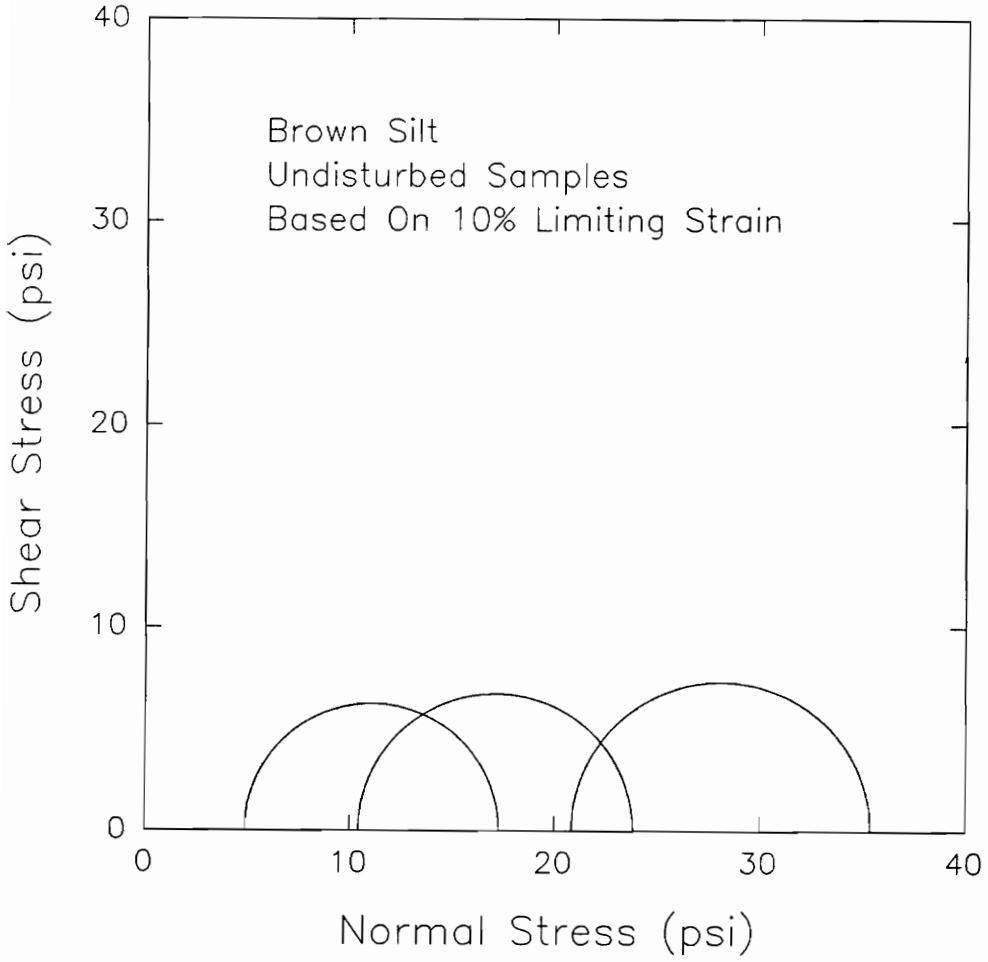

Mohr's Circles For UU Triaxial Tests On Undisturbed Samples of Brown Silt For Failure Based On 10% Limiting Strain, West Williamson L.P.P. Pumping Plant (Sample UD-85-4-11B)

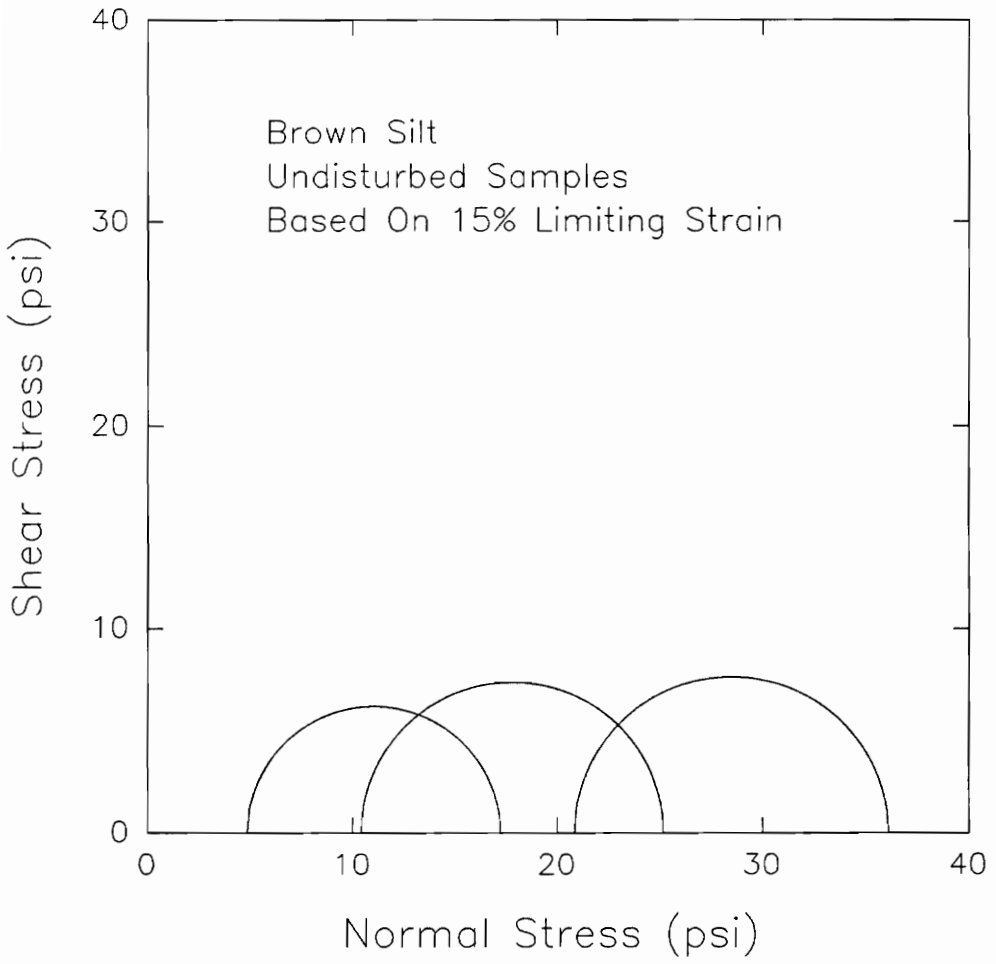

Mohr's Circles For UU Triaxial Tests On Undisturbed Samples of Brown Silt For Failure Based On 15% Limiting Strain, West Williamson L.P.P. Pumping Plant (Sample UD-85-4-11B)

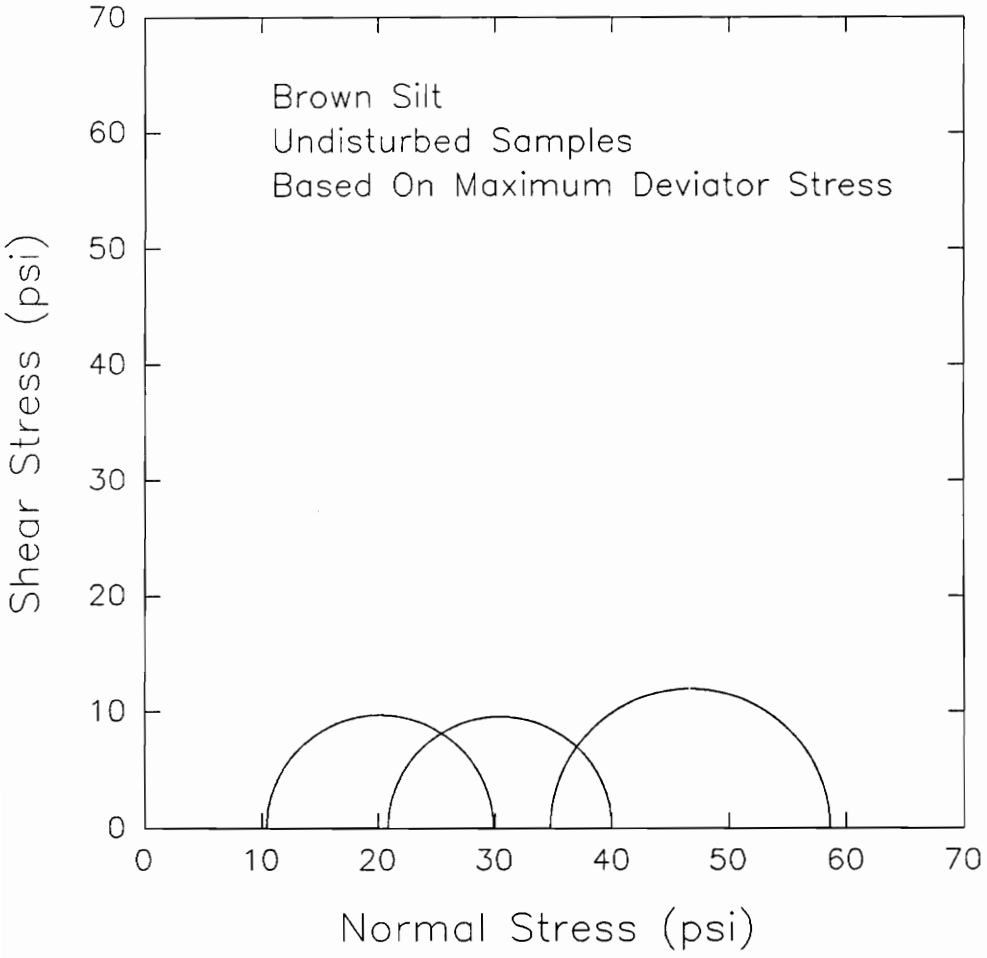

Mohr's Circles For UU Triaxial Tests On Undisturbed Samples of Brown Silt For Failure Based On Maximum Deviator Stress, West Williamson L.P.P. Pumping Plant (Sample UD-100-S1-A)

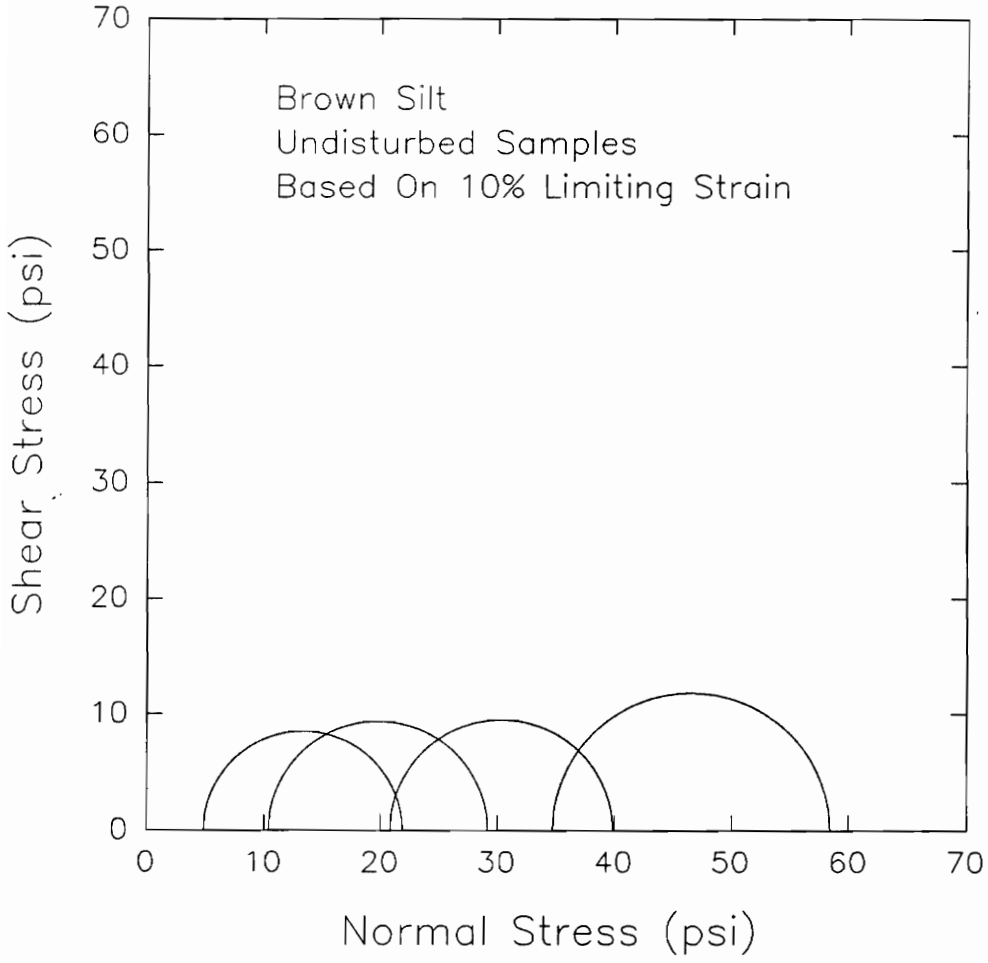

Mohr's Circles For UU Triaxial Tests On Undisturbed Samples of Brown Silt For Failure Based On 10% Limiting Strain, West Williamson L.P.P. Pumping Plant (Sample UD-100-S1-A)

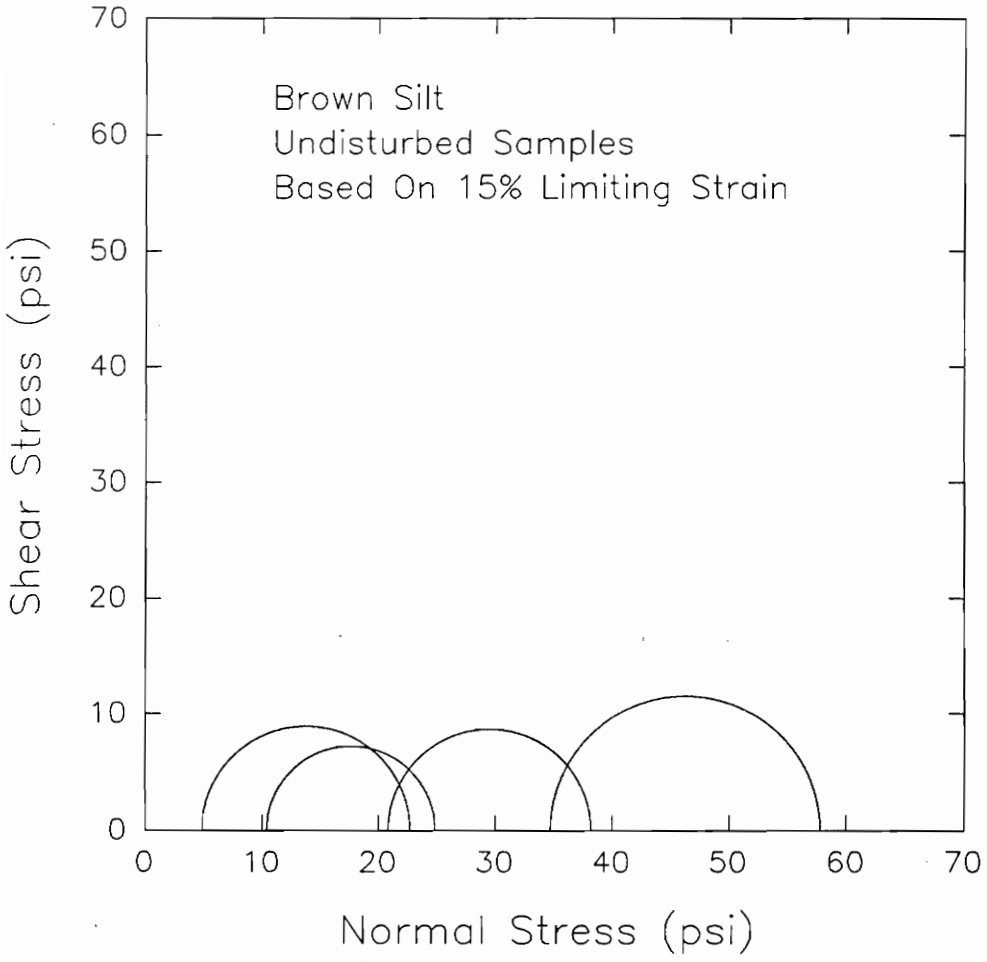

Mohr's Circles For UU Triaxial Tests On Undisturbed Samples of Brown Silt For Failure Based On 15% Limiting Strain, West Williamson L.P.P. Pumping Plant (Sample UD-100-S1-A)

VITA

Bonifacio I. dela Pena

Date of Birth :	May 14, 1960
Place of Birth :	Batangas, Philippines
Educational Attainment :	BS Civil Engineering
	Saint Louis University
	March, 1982
	Baguio City, Philippines
	MS Civil Engineering
	VPI and SU
	April, 1991
	Blacksburg, Virginia
	U.S.A.
Work Experience :	Professor/Soils Engr.
	Saint Louis University
	1982 to Present

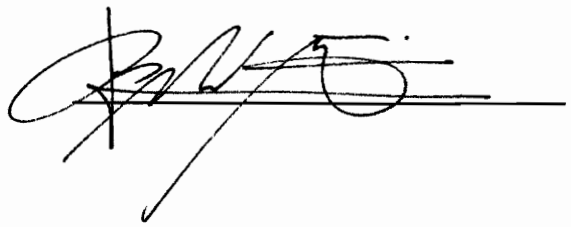

ABSTRACT

The purpose of this study is to investigate the primary factors which control the engineering behavior of silts. The methods of classifying silts at present do not provide much basis to infer how silts will behave in the field for design purposes.

In the course of this research study, series of UU and CU triaxial test results of different silt samples were gathered to investigate the factors that control the strength parameters of silts. Effective and total stress strength interpretation were done on the test results. The effective stress friction angle were evaluated using the CU triaxial test results. Undrained strength parameters were determined from the CU and UU triaxial test results, and comparison were performed using the undrained strength ratio S_u/p.

Silt samples which exhibit dilative behavior during undrained shear make it difficult to define failure. Because of this behavior, the test results were interpreted using different failure criteria to assess the effective stress friction angle and the undrained strength parameters.

Test results indicate that the effective stress friction angle can be evaluated using the CU triaxial test will little uncertainty.

The undrained shear strength of silt samples are influenced by the type of failure criteria. The results indicate that a unique undrained shear strength can not be determined because the samples get stronger with increasing strain. A reliable method of evaluating the undrained shear strength of silt samples is to determine the relationship between the undrained strength ratio and the changes in pore pressure.